AD-A151 766 MULTIPLE SCATTERING OF ELECTROMAGNETIC WAVES IN DISCRETE RANDOM MEDIA..(U) PENNSYLVANIA STATE UNIV UNIVERSITY PARK WAVE PROPAGATION LAB.. 1/3

UNCLASSIFIED V K VARADAN ET AL. 31 DEC 84 F/G 20/14 NL

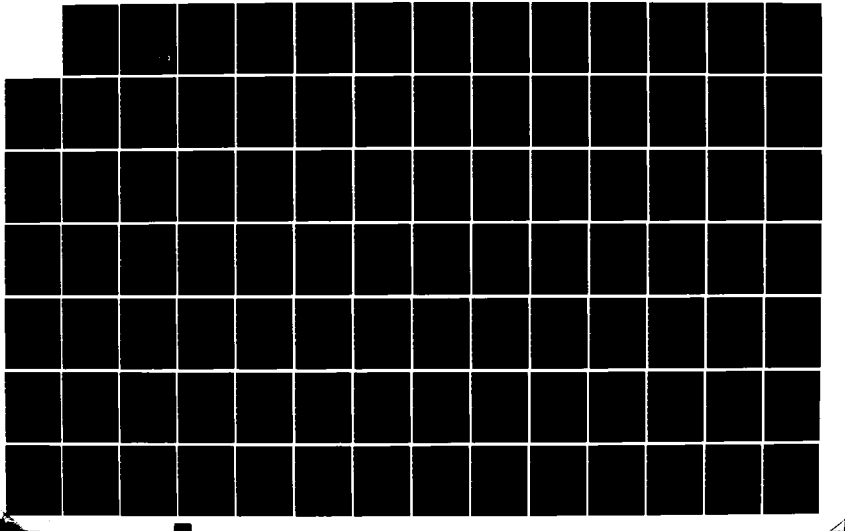

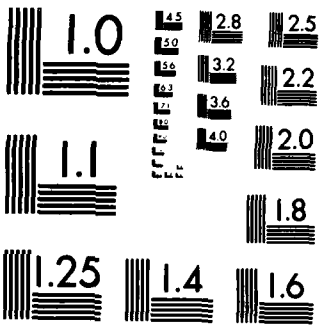

ARO 20846.16-GS

(2)

Wave Propagation Laboratory
The Pennsylvania State University

Multiple Scattering Of Electromagnetic Waves In Discrete Random Media

Final Report

Vijay K. Varadan and Vasundara V. Varadan

December 31, 1984

U.S. Army Research Office

Contract No: DAAG29-83-K-0097

Approved for Public Release
Distribution Unlimited

UNCLASSIFIED
SECURITY CLASSIFICATION OF THIS PAGE (When Data Entered)

REPORT DOCUMENTATION PAGE

A151 766

READ INSTRUCTIONS BEFORE COMPLETING FORM

1. REPORT NUMBER	2. GOVT ACCESSION NO. N/A; 3. RECIPIENT'S CATALOG NUMBER N/A
4. TITLE (and Subtitle) Multiple Scattering of electromagnetic waves in discrete random media	5. TYPE OF REPORT & PERIOD COVERED Final 1 July 1983 -31 October 1984; 6. PERFORMING ORG. REPORT NUMBER
7. AUTHOR(s) V. K. Varadan and V. V. Varadan	8. CONTRACT OR GRANT NUMBER(s) DAAG29 - 83 - K - 0097
9. PERFORMING ORGANIZATION NAME AND ADDRESS Wave Propagation Laboratory , 227 Hammond Bldg. Pennsylvania State University University Park, PA 16802	10. PROGRAM ELEMENT, PROJECT, TASK AREA & WORK UNIT NUMBERS
11. CONTROLLING OFFICE NAME AND ADDRESS U. S. Army Research Office Post Office Box 12211 Research Triangle Park, NC 27709	12. REPORT DATE December 31, 1984; 13. NUMBER OF PAGES 263
14. MONITORING AGENCY NAME & ADDRESS(if different from Controlling Office)	15. SECURITY CLASS. (of this report) Unclassified; 15a. DECLASSIFICATION/DOWNGRADING SCHEDULE

16. DISTRIBUTION STATEMENT (of this Report)

Approved for public release; distribution unlimited.

17. DISTRIBUTION STATEMENT (of the abstract entered in Block 20, if different from Report)

NA

18. SUPPLEMENTARY NOTES

The view, opinions, and/or findings contained in this report are those of the author(s) and should not be construed as an official Department of the Army position, policy, or decision, unless so designated by other documentation.

19. KEY WORDS (Continue on reverse side if necessary and identify by block number)

Multiple scattering, discrete random media, coherent and incoherent intensities phase velocity, attenuation, frequency dependence, Monte-Carlo pair-correlation function, T-matrix, hybrid T-matrix and reinforced orthogonalization schemes, lossy and lossless dielectric non-spherical scatterers of high aspect ratios, deeply corrugated rough surfaces, spatial stochastic system theory

20. ABSTRACT (Continue on reverse side if necessary and identify by block number)

The study of attenuation, dispersion and the intensity of electromagnetic waves in a discrete random medium was persued. The emphasis was on anisotropic effects induced by microstructure (nonspherical aligned scatterers); interpretation of the Quasi-Crystalline Approximation (QCA) as a partial summation of the multiple scattering series; a study of various methods of computing the pair- correlation function including Monte-Carlo techniques; a propagator model for wave propagation in random media based on Feynman diagrams and

DD FORM 1 JAN 73 1473 EDITION OF 1 NOV 65 IS OBSOLETE

UNCLASSIFIED
SECURITY CLASSIFICATION OF THIS PAGE (When Data Entered)

preliminary computations of the coherent and incoherent intensities which have also been compared with the experiments of Killey and Meeten; a spatial stochastic sytem model for wave propagation in random media and method of discontinuous stochastic field. A development that will be useful to the research on this project as well as the present one is the development of a QR-algorithm to obtain the T-matrix of scatterers with a high aspect ratio and deeply corrugated surfaces. Twelve Publications in refereed journals and three Chapters in Conference Proceedings have resulted from this support.

ORIGINATOR - SUPPLIED KEY WORDS INCLUDE:

FINAL REPORT

MULTIPLE SCATTERING OF ELECTROMAGNETIC WAVES IN DISCRETE RANDOM MEDIA

by

V.K. Varadan and V.V. Varadan

Wave Propagation Laboratory
The Pennsylvania State University
University Park, PA 16802

for the period

July 01, 1983 - October 31, 1984

U.S. Army Research Office

Research Triangle Park, NC 27709

Contract No. : DAAG29 - 83 - K - 0097

December 1984

SUMMARY

In this report, the effect of multiple scattering on coherent wave propagation in discrete random media has been investigated. The medium is modelled with a random distribution of spherical and non-spherical scatterers. In the recent past, we have been concerned with theoretical and numerical studies of electromagnetic wave propagation in discrete random media [1,2]. Of particular interest to us was the frequency dependence of the attenuation and the phase velocity of coherent waves as a function of volume fraction, size and shape of scatterers distributed in a host medium. We used a self-consistent multiple scattering theory wherein the response of a single scatterer was described by a T-matrix and several forms of the pair correlation function were used to take into account concentrations greater than 1%. Our results compared very favorably for a wide range of frequencies (ka from 3 to 84) and concentrations from 0 to 50% with the experiments of Ishimaru [3] and Killey and Meeten [4].

a) One of the objectives of the past year's efforts was to concentrate on anisotropic effects resulting from waves propagating at arbitrary angles to randomly distributed, aligned, pair-correlated, non-spherical scatterers[5]. Such problems have been studied by Twersky [6] wherein he has presented analytical results in the long-wavelength approximation. In Ref. 5, the similarity between Twersky's and our approaches is discussed. Although both formalisms are quite different, they result in the same dispersion equation. Our formulation is, however, more suited for numerical computations at higher frequencies. We have discussed this at some length in Ref. 7 wherein we have performed numerical computations of Twersky's equations for the acoustic case and compared it with computations for our equations. In Ref. 5,

the calculations performed are quite complicated since all values of the azimuthal index contribute in the expansion of coherent electromagnetic field in vector spherical functions. Our computed results [5] are in excellent agreement with those obtained by Twersky [6]. Average frequency dependent properties are also studied and presented. For comparison purposes, we have also investigated the electromagnetic wave propagation through randomly distributed and oriented scatterers by introducing the concept of a rotation matrix along with the T-matrix [8].

b) The close agreement between our theory and experiments, although very encouraging, calls for further research on specific issues such as (i) the range of validity of the Quasi-Crystalline Approximation (QCA) as well as corrections to it, and (ii) the generation of non-spherical two point correlation functions so that dense concentrations of non-spherical particles can be considered.

In order to determine the two point correlation functions for both spherical and non-spherical scatterers, we are developing a computer algorithm to solve the Percus - Yevick equations as well as Monte Carlo techniques [9]. In Ref. 9, two-dimensional Percus - Yevick equations are solved numerically with excellent comparisons with Monte Carlo calculations. For low concentrations, Twersky [10] has developed pair correlation functions purely based on geometry which agree with our computer generated values. In the Monte Carlo simulation, the computer is instructed to perform a series of small random displacements on the particles. If any displacement results in two "hard" particles overlapping, it is rejected; otherwise, it is accepted. The program is run for several million such displacements and an appro-

priate selection of the resulting data is utilized to evaluate averages. To implement this algorithm for a specific system one needs to define a "shape" which allows the computer to determine whether or not particle overlap has occurred. The implementation of the "physics" of the system and orientations of non-spherical particles is being pursued and the results will be reported in our future reports.

c) Secondly, our effort was also to have a clear physical understanding of QCA used by Twersky and us. The QCA is used to break the heirarchy of equations for the ensemble average of the field exciting a particular scatterer. As a result only a knowledge of the two particle correlation function is required. In a recent paper [11], we have shown what type of multiple scattering processes are included in the QCA and which ones are neglected. Explicit improvements to the QCA are also presented. We are currently implementing this improvement in our numerical algorithm. We have also performed some computations for various lossy and lossless dielectric scatterers to understand the effects of properties on wave attenuation,see Figs.1-8. We wish to continue this work further by studying the QCA and any corrections to it more closely so as to understand why it works as well as it does.

d) Thirdly, a general multiple scattering theory based on spatial stochastic system is developed to study wave propagation in discrete random media [12,13]. Using the concept of an "equivalent spatial stochastic system" and the joint probability distribution of scatterers, a general expression of the space correlation function and the intensity of the multiply scattered fields is established. The intensity calculations using this method compare with those of Twersky at long wavelengths. The method, however, seems to provide excellent comparison with experimental data [14].

e) A propagator model was developed to study coherent and incoherent intensities of electromagnetic wave propagation in discrete random media [4,15]. Lax's QCA with suitable averaging techniques and the T-matrix of a single scatterer have been employed in the analysis. Pair correlation functions generated by Monte Carlo simulation have been utilized in these computations. This model also provides a dispersion equation which is solved for both phase velocity and coherent attenuation as a function of frequency for various scatterer concentrations. Numerical results obtained show excellent agreement with the experimental measurements of Killey and Meeten [16]. This approach also shows excellent comparison with experimental data for scalar problems [17].

f) In addition, we have also developed a hybrid T-matrix method and a QR factorization scheme, which are ideally suited for scatterers of high aspect ratios [18-20]. These methods will enable us to study scattering by such objects as discs, long thin finite cylinders, etc. We have also developed a finite element algorithm for handling arbitrarily shaped inhomogeneous scatterers [21]. Recently, we have formulated an efficient scheme which overcomes the Rayleigh hypothesis in the application of the T-matrix approach for scattering by rough surfaces [22].

These additional efforts will eventually help us in applying our various multiple scattering approaches to compare with the actual field measurements for various kinds of debris.

Various publications resulting from our investigations are enclosed.

REFERENCES

1. V.N. Bringi, V.V. Varadan and V.K. Varadan, "The effects of pair correlation functions on coherent wave attenuation in discrete random media," IEEE Trans. Antennas and Propagation, AP-30, 805-808 (1982).

2. V.N. Bringi, V.K. Varadan and V.V. Varadan, "Coherent wave attenuation by a random distribution of particles," Radic Sci., 17, 946-952 (1982).

3. V.K. Varadan, V.N. Bringi, V.V. Varadan and A. Ishimaru, "Multiple scattering theory for waves in random media and comparison with experiments," Radio Sci., 18, 321-327 (1983).

4. V.K. Varadan and V.V. Varadan, "Progress in research on wave propagation and scattering in discrete random media using multiple scattering theory," CRDC Proc. Obscuration and Aerosol Res., to appear.

5. V.V. Varadan, Y. Ma and V.K. Varadan, "Frequency dependence of the attenuation of electromagnetic waves in media with anisotropy induced by microstructure," IEEE Trans. Antennas and Propagation, submitted (1984).

6. V. Twersky, "Coherent electromagnetic waves in pair-correlated random distributions of aligned scatterers," J. Math. Phys., 19, 215-230 (1978).

7. Y. Ma, V.K. Varadan and V.V. Varadan, "Application of Twersky's multiple scattering formalism to a dense suspension of elastic particles in water," J. Acoust. Soc. Am., 75, 335-339 (1984).

8. V.K. Varadan, Y. Ma and V.V. Varadan, "Coherent electromagnetic wave propagation through randomly distributed and oriented pair-correlated dielectric scatterers," Radio Sci., 19, 1445-1449 (1984).

9. Y. Ma, V.V. Varadan and V.K. Varadan, "Multiple scattering of waves from planar distributed particles," J. Appl. Phys., submitted (1984).

10. V. Twersky, "Multiple scattering of sound by correlated monolayers," J.Acoust. Soc. Am., 73, 68-84 (1983).

11. V.V. Varadan and V.K. Varadan, "The quasi-crystalline approximation and multiple scattering of waves in random media," IEEE Trans. Antennas and Propagation, submitted (1984).

12. K.C. Liu, V.V. Varadan and V.K. Varadan, "Multiple scattering of waves in discrete random media by method of spatial stochastic systems. I," J. Appl. Phys., submitted (1984).

13. K.C. Liu, V.V. Varadan and V.K. Varadan, "Multiple scattering of waves in discrete random media by method of spatial stochastic systems. II. Pair-correlated scatterers," J. Appl. Phys., submitted (1984).

14. K.C. Liu, V.V. Varadan and V.K. Varadan, "Wave scattering in random

media by method of discontinuous stochastic field," J. Acoust. Soc. Am., submitted (1984).

15. V.K. Varadan and V.V. Varadan, "A propagator model for multiple scattering and wave propagation in discrete random media," Radio Sci., submitted (1984).

16. A. Killey and G.H. Meeten, "Optical extinction and refraction of concentrated latex dispersions," J. Chem. Soc. Faraday Trans., 2, 587-599 (1981).

17. V.K. Varadan, V.V. Varadan and Y. Ma, "A propagator model for scattering of acoustic waves by bubbles in water," J. Acoust. Soc. Am., submitted (1984).

18. A. Lakhtakia, V.K. Varadan and V.V. Varadan, "Iterative extended boundary condition method for scattering by objects of high aspect ratios," J. Acoust. Soc. Am., 76, 906-912 (1984).

19. A. Lakhtakia, V.K. Varadan and V.V. Varadan, "Scattering by lossy dielectric nonspherical objects with nonvanishing magnetic susceptibility," J. Appl. Phys., 56, 3057-3060 (1984).

20. A. Lakhtakia, V.K. Varadan and V.V. Varadan, "Scattering by highly aspherical targets: EBCM coupled with reinforced orthogonalizations," Appl. Opt., 23, 3502-3504 (1984).

21. J.H. Su, V.V. Varadan and V.K. Varadan, "Finite element eigenfunction method (FEEM) for wave scattering by arbitrary 3-D axisymmetric scatterers," J. Appl. Mech., 51, 614-621 (1984).

22. A. Lakhtakia, V.K. Varadan and V.V. Varadan, "A T-matrix approach for EM scattering by a perfectly conducting periodic surface," Proc. IEEE, in press.

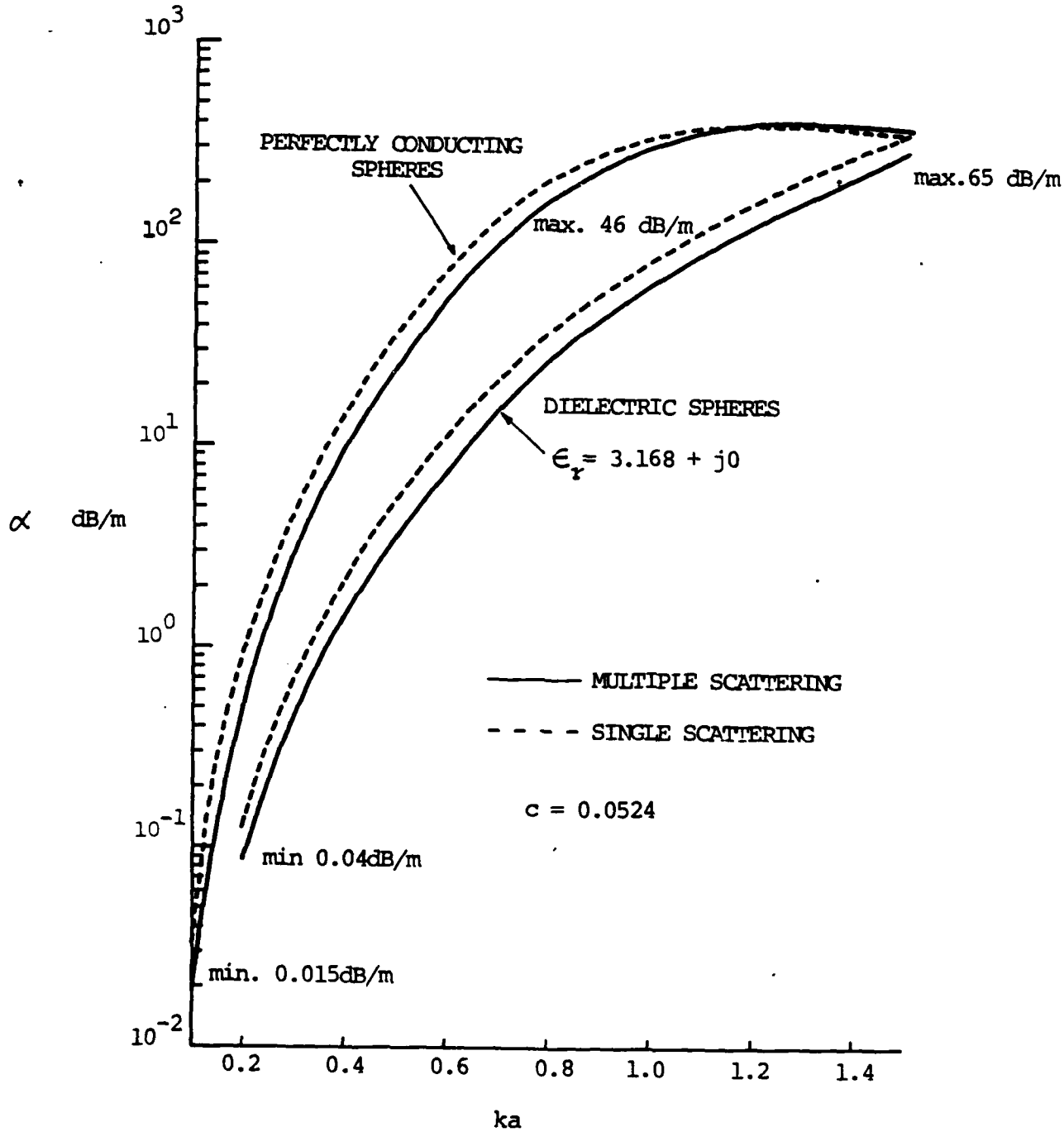

Figure 1. Coherent attenuation (dB/m) vs. nondimensional frequency.

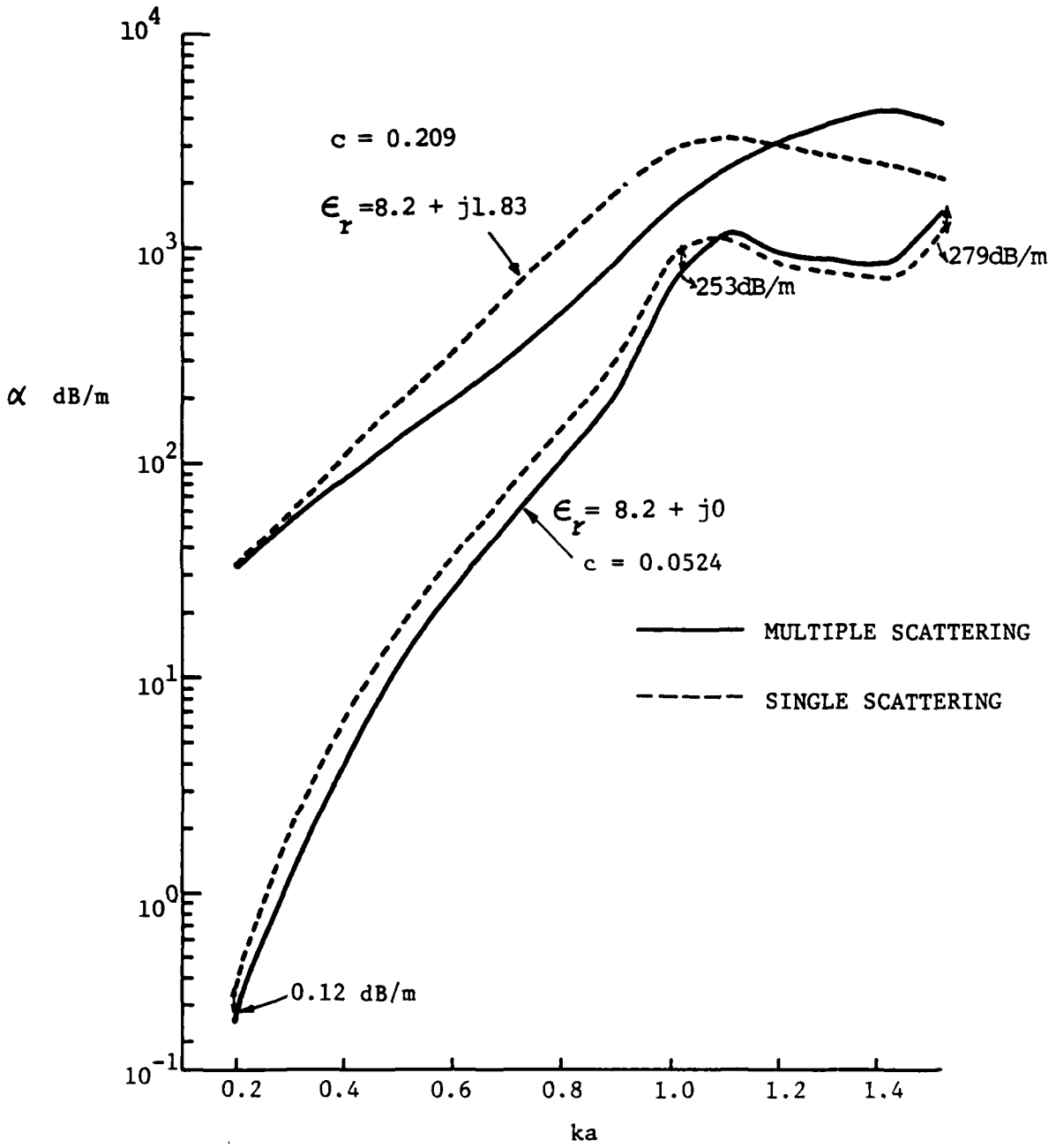

Figure 2. Coherent attenuation (dB/m) vs. nondimensional frequency

For identical scatterers, we obtain

$$\langle \alpha_n^i \rangle_i = 4\pi i^{\ell} \vec{A}_n(\hat{k}_o)\, e^{ik\hat{k}_o\cdot\vec{r}_i} + \sum_{j\neq i}\sum_{n'}\sum_{n''} T_{n'n''} \langle \alpha_{n''}^j \rangle_j \sigma_{n'n}(\vec{r}_i-\vec{r}_j)\, p(\vec{r}_j|\vec{r}_i)\, d\vec{r}_j \tag{8}$$

where $p(\vec{r}_j \mid \vec{r}_i)$ is the conditional probability distribution function and $\langle \alpha_n^i \rangle_i$ is the conditional expectation of α_n with the i-th scatterer located at $\vec{r}_i$.

The average exciting field is assumed to propagate with the wavenumber K of the effective medium. $K = K_1 + iK_2$ is a complex frequency dependent function unlike the wavenumber $k=\omega/c$ of the host medium. Thus,

$$\langle \alpha_n^i \rangle_i = X_n\, e^{iK\hat{k}_o\cdot\vec{r}_i} \tag{9}$$

when substituted into Eq. (8) permits us to evaluate a portion of the integral for impenetrable particles i.e., $p(\vec{r}_j \mid \vec{r}_i)=0$ if $|\vec{r}_i - \vec{r}_j| \leq 2a$ and $p(\vec{r}_j \mid \vec{r}_i) = \frac{1}{V}\, g(|\vec{r}_i - \vec{r}_j|)$ for $|\vec{r}_i - \vec{r}_j| > 2a$ where V is the large volume of the system such that $n_o = N/V$, the number density is finite. For details we refer to our earlier work in Ref. 9, the difference in this case being $\hat{k}_o \neq \hat{z}$.

If the scatterers are rotationally symmetric, then the T-matrices are diagonal in the azimuthal index, i.e. $m' = m''$. In this case we can assume without loss of generality that $\hat{k}_o$ is in the x-z plane since there is complete symmetry in the x-y plane. Further there is a very simple relationship between the dispersion equations that result for wave propagation with polarization parallel to the x-z plane and perpendicular to the x-z plane. For this case Eq. (9) when substituted into (8) results in the following equations for the coefficients $x_{1\ell m\sigma}$ and $x_{2\ell m\sigma}$:

where $\vec{r}_i$ denotes the center of the i-th scatterer, 'a' is the radius of the circumscribing sphere and

$$\begin{matrix}\text{Re}\\ \\ \text{Ou}\end{matrix} \quad \vec{\psi}_{1\ell m\sigma} = \nabla \times \left(\vec{r} \begin{matrix} j_\ell(kr) \\ \\ h_\ell^{(1)}(kr) \end{matrix} Y_{\ell m\sigma}(\theta,\phi)\right) \; ; \; \vec{\psi}_{2\ell m\sigma} = \frac{1}{k} \nabla \times \vec{\psi}_{1\ell m\sigma} \tag{5}$$

where j_ℓ and $h_\ell^{(1)}$ are Bessel and Hankel functions, $Y_{\ell m\sigma}$ are normalized spherical harmonics, $k=\omega/c$ is the wavenumber, $\ell \in [o,\infty]$ and $m \in [o,\ell]$, σ= even or odd.

Using the extended boundary condition method[5] we can derive a T-matrix to relate the unknown coefficients α and f as follows:

$$f^i_{\tau\ell m\sigma} = \sum_{\tau'\ell'm'\sigma} T^i_{\tau\ell m\sigma,\,\tau'\ell'm'\sigma'} \; \alpha^i_{\tau'\ell'm'\sigma'} \tag{6}$$

where T^i, the T-matrix of the i-th scatterer depends only on the frequency ω and the geometry and nature of the scatterer. It is independent of the direction of the incoming field and the observation point.

Substituting Eqs. (3), (4) and (6) in (2) and using the translation addition theorem for the vector spherical functions, we obtain

$$\alpha^i_n = 4\pi i^\ell \vec{A}_n(\hat{k}_o) \; e^{ik\hat{k}_o \cdot \vec{r}_i} + \sum_{j\neq i} \sum_{n'} \sum_{n''} \sigma_{n'n}(\vec{r}_i - \vec{r}_j) \; T^j_{n'n''} \; \alpha^j_{n''} \tag{7}$$

where the abbreviated index 'n' represents the set $\{\tau,\ell,m,\sigma\}$, $\vec{A}_n$ are vector spherical harmonics, $\vec{A}_1 = r\nabla Y_{\ell m\sigma}$ and $\vec{A}_2 = \vec{r}\times\vec{A}_1$ and $\sigma_{n'n}$ is the translation matrix[9].

A configurational average is performed in Eq. (7) over the random positions of the scatterers and the QCA is invoked in the usual manner[9].

presented for aligned spheroidal scatterers as a function of frequency, volume fraction of scatterers and the direction of propagation.

Wave Propagation in Media with Aligned Non-Spherical Scatterers

Consider an isotropic medium chacterized by a refractive index $\sqrt{\epsilon}$ in which aligned rotationally symmetric scatterers are randomly distributed. The rotational axis of symmetry is taken to be the z-axis. Although the formalism is applicable even if there is no rotational axes of symmetry, numerical results are presented only for spheroids. For the general case we refer to Twersky[1,2] for explicit, long wavelength results. Plane harmonic waves of frequency ω, propagate in the direction $\hat{k}_o(\alpha,\beta)$. If $\vec{U}^o$, $\vec{U}_i^e$ and $\vec{U}_i^s$ specify the incident field, the field exciting the i-th scatterer and the response to this field respectively, then self-consistency require that if there are N scatterers, the total field $\vec{U}^{tot}$ is given by

$$\vec{U}^{tot} = \vec{U}^o + \sum_i \vec{U}_i^s = \vec{U}_i^e + \vec{U}_i^s \tag{1}$$

or

$$\vec{U}_i^e = \vec{U}^o + \sum_{j\neq i} \vec{U}_j^s \tag{2}$$

The exciting and scattered field are expanded in a basis of vector spherical functions as follows:

$$\vec{U}_i^e(\vec{r}) = \sum_{\tau=1}^{2} \sum_{\ell m\sigma} \alpha_{\tau\ell m\sigma}^{i} \; Re\, \vec{\psi}_{\tau\ell m\sigma}(\vec{r}-\vec{r}_i) \quad ; \; |\vec{r}-\vec{r}_i| \leq 2a \tag{3}$$

$$\vec{U}_i^s(\vec{r}) = \sum_{\tau=1}^{2} \sum_{\ell m\sigma} f_{\tau\ell m\sigma}^{i} \; Ou\, \vec{\psi}_{\tau\ell m\sigma}(\vec{r}-\vec{r}_i) \quad ; \; |\vec{r}-\vec{r}_i| \geq 2a \tag{4}$$

INTRODUCTION

It is well known that in a medium with microstructure in the form of discrete random inhomogeneities, electromagnetic waves undergo attenuation as well as dispersion. If the inhomogeneities are either spherically symmetric or randomly oriented, the medium is macroscopically or on the average isotropic. The attenuation and phase velocity are independent of the direction of propagation. However, the medium can be effectively anisotropic if the scatterers are non-spherical and aligned. In this case the propagation characteristics of the medium are a function of the angle with respect to the axis of alignment (taken as the z-axis).

Such problems have been studied in detail by Twersky[1,2] for both acoustic and electromagnetic waves. He has presented analytical results for elliptical cylinders and ellipsoids in the long wavelength approximation including the effects of the pair correlation function. The formulation that we present is quite similar but is however more suited[3] for numerical computations at higher frequencies requiring smaller matrices to yield convergent results. The dispersion equation that we solve numerically is compared to that obtained by Twersky. Both treatments rely on the quasi-crystalline approximation (QCA) to break the heirarchy of equations for the ensemble average of the field exciting a particular scatterer. As a result only a knowledge of the two particle correlation function is required. In a recent report[4] we have shown what type of multiple scattering processes are included in the QCA and which ones are neglected. The response of a single scatterer to the field exciting it is characterized by a T-matrix. The T-matrix is numerically generated in a basis of vector spherical functions using Waterman's extended boundary condition method[5,6]. Earlier work using this general scheme was restricted to randomly oriented non-spherical scatterers or for wave propagation restricted to the alignment axis[8,9,10,11]. Numerical results are

FREQUENCY DEPENDENCE OF THE ATTENUATION OF ELECTROMAGNETIC WAVES IN MEDIA WITH ANISOTROPY INDUCED BY MICROSTRUCTURE

V. V. Varadan, Y. Ma and V. K. Varadan
Department of Engineering Science and Mechanics
The Pennsylvania State University
University Park, PA 16802

ABSTRACT

Electromagnetic wave propagation in a medium containing a random distribution of aligned, pair-correlated non-spherical scatterers is studied using the T-matrix to characterize the single scatterer response, the quasi-crystalline approximation and the two point pair correlation function. The resulting dispersion equation for the average medium is numerically solved as a function of frequency and the direction of propagation. Numerical results are presented for the attenuation of electromagnetic waves versus frequency, concentration and direction of propagation.

SCIENTIFIC PERSONNEL SUPPORTED BY THE PROJECT

1. K.C. Liu (Ph.D. expected by July '85)
2. Y. Ma
3. A. Lakhtakia

targets: EBCM coupled with reinforced orthogonalizations," Appl. Opt., 23, 3502-3504 (1984).

14. A. Lakhtakia, V.K. Varadan and V.V. Varadan, "A T-matrix approach for EM scattering by a perfectly conducting periodic surface," Proc. IEEE, to appear.

15. A. Lakhtakia, V.K. Varadan and V.V. Varadan, "On an improved T-matrix approach to study the scalar scattering of doubly periodic surfaces," Proceedings of the Second Army Conference on Applied Mathematics and Computing, F. Dressel (Ed.), to appear.

LIST OF MANUSCRPTS SUBMITTED OR PUBLISHED UNDER ARO SPONSORSHIP
DURING THE PERIOD

1. V.V. Varadan, Y. Ma and V.K. Varadan, "Frequency dependence of the attenuation of electromagnetic waves in media with anisotropy induced by microstructure," IEEE Trans. Antennas and Propagation, submitted.

2. V.K. Varadan, Y. Ma and V.V. Varadan, "Coherent electromagnetic wave propagation through randomly distributed and oriented pair-correlated dielectric scatterers," Radio Sci., 19, 1445-1449 (1984).

3. V.V. Varadan and V.K. Varadan, "The quasi-crystalline approximation and multiple scattering of waves in random media," IEEE Trans. Antennas and Propagation, submitted.

4. K.C. Liu, V.V. Varadan and V.K. Varadan, "Multiple scattering of waves in discrete random media by method of spatial stochastic systems. I," J. Appl. Phys., submitted.

5. K.C. Liu, V.V. Varadan and V.K. Varadan, "Multiple scattering of waves in discrete random media by method of spatial stochastic systems. II. Pair-correlated scatterers," J. Appl. Phys., submitted.

6. K.C. Liu, V.V. Varadan and V.K. Varadan, "Wave scattering in random media by method of discontinuous stochastic field," J. Acoust. Soc. Am., submitted.

7. V.K. Varadan and V.V. Varadan, "Progress in research on wave propagation and scattering in discrete random media using multiple scattering theory," CRDC Proc. Obscuration and Aerosol Res., to appear.

8. V.K. Varadan and V.V. Varadan, "A propagator model for multiple scattering and wave propagation in discrete random media," Radio Sci., submitted.

9. Y. Ma, V.K. Varadan and V.V. Varadan, "Multiple scattering of waves from planar distributed particles," J. Appl. Phys., submitted.

10. V.K. Varadan, V.V. Varadan and Y. Ma, "Wave propagation in composite media," ASME Special Publication on Impact and Wave Propagation in Composite Media, U. Yuceeoglu (Ed.), to appear.

11. A. Lakhtakia, V.K. Varadan and V.V. Varadan, "Iterative extended boundary condition method for scattering by objects of high aspect ratios," J. Acoust. Soc. Am., 76, 906-912 (1984).

12. A. Lakhtakia, V.K. Varadan and V.V. Varadan, "Scattering by lossy dielectric nonspherical objects with nonvanishing magnetic susceptibility," J. Appl. Phys., 56, 3057-3060 (1984).

13. A. Lakhtakia, V.K. Varadan and V.V. Varadan, "Scattering by highly aspherical

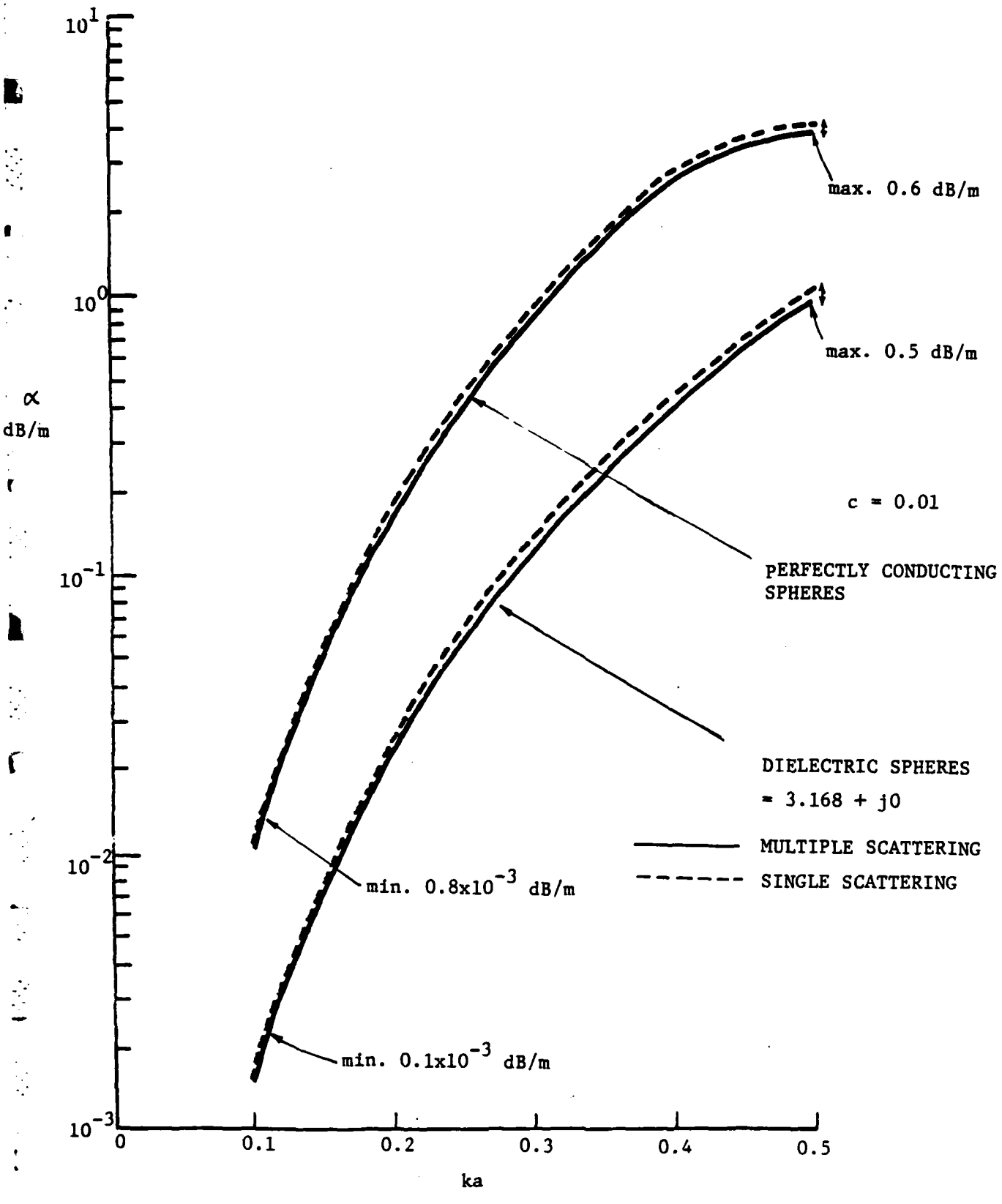

Fig.8 Coherent Attenuation (dB/m) vs. nondimensional frequency ka.

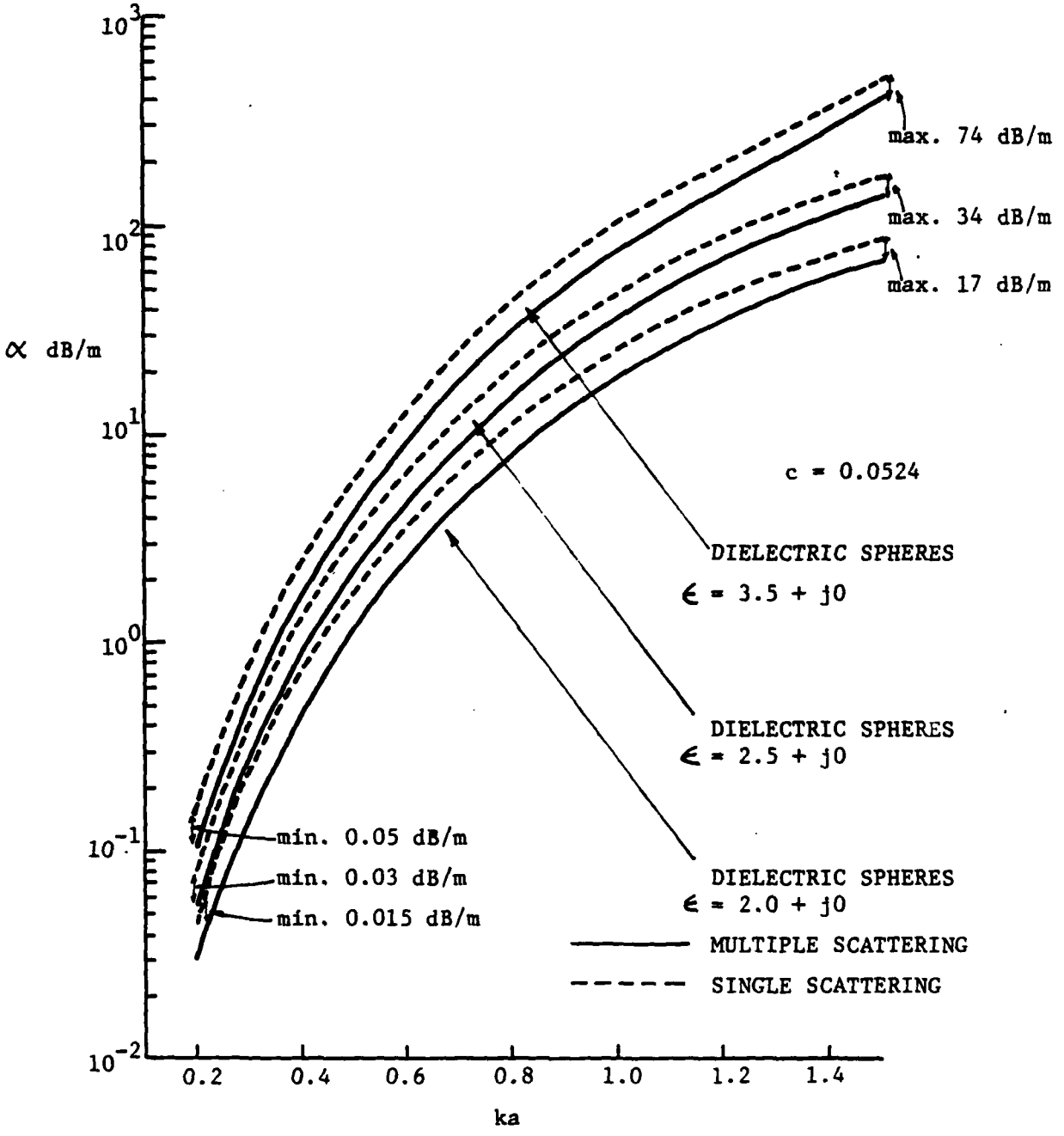

Fig.7 Coherent Attenuation (dB/m) vs. nondimensional frequency ka.

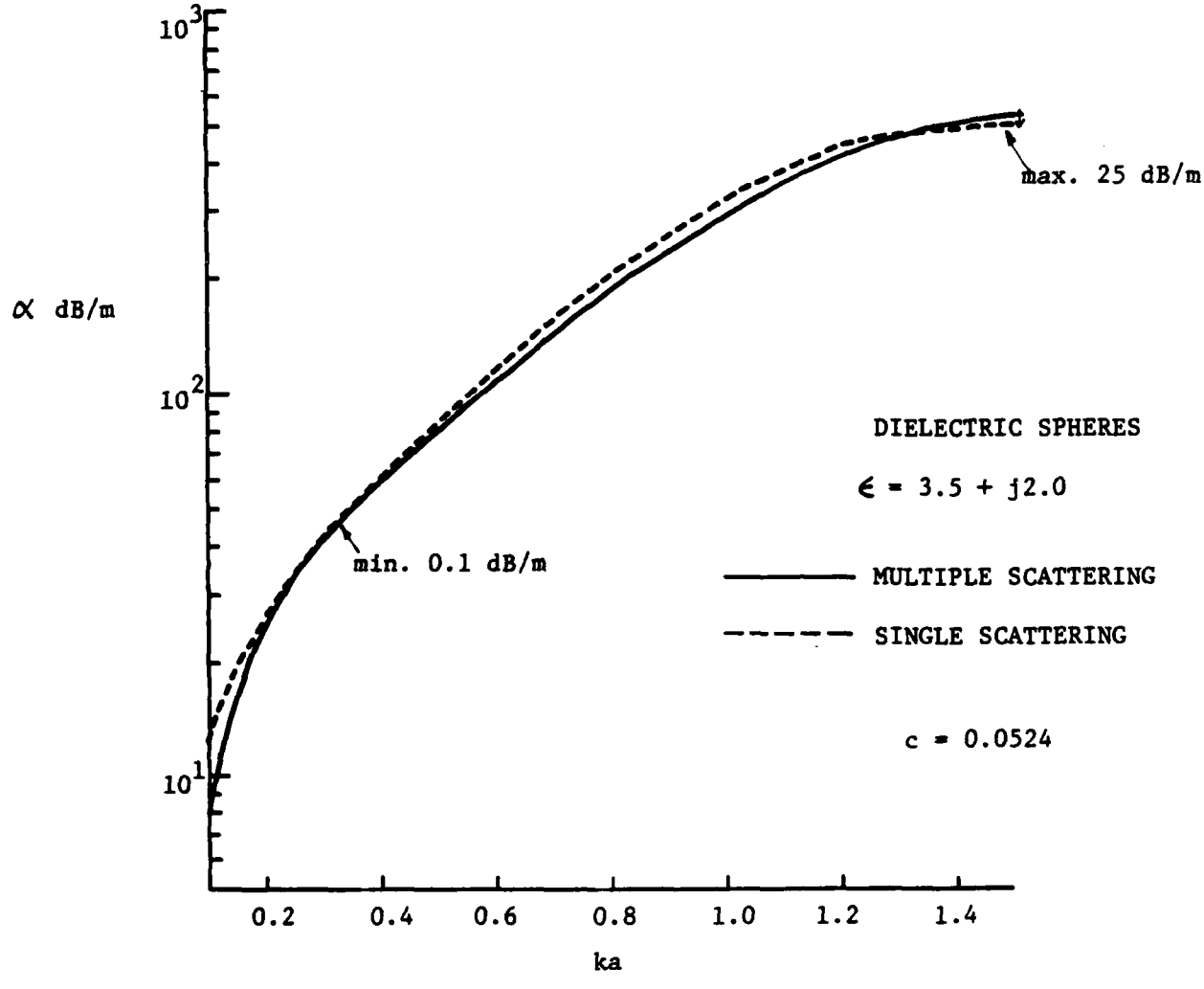

Fig.6 Coherent attenuation (dB/m) vs. nondimensional frequency ka.

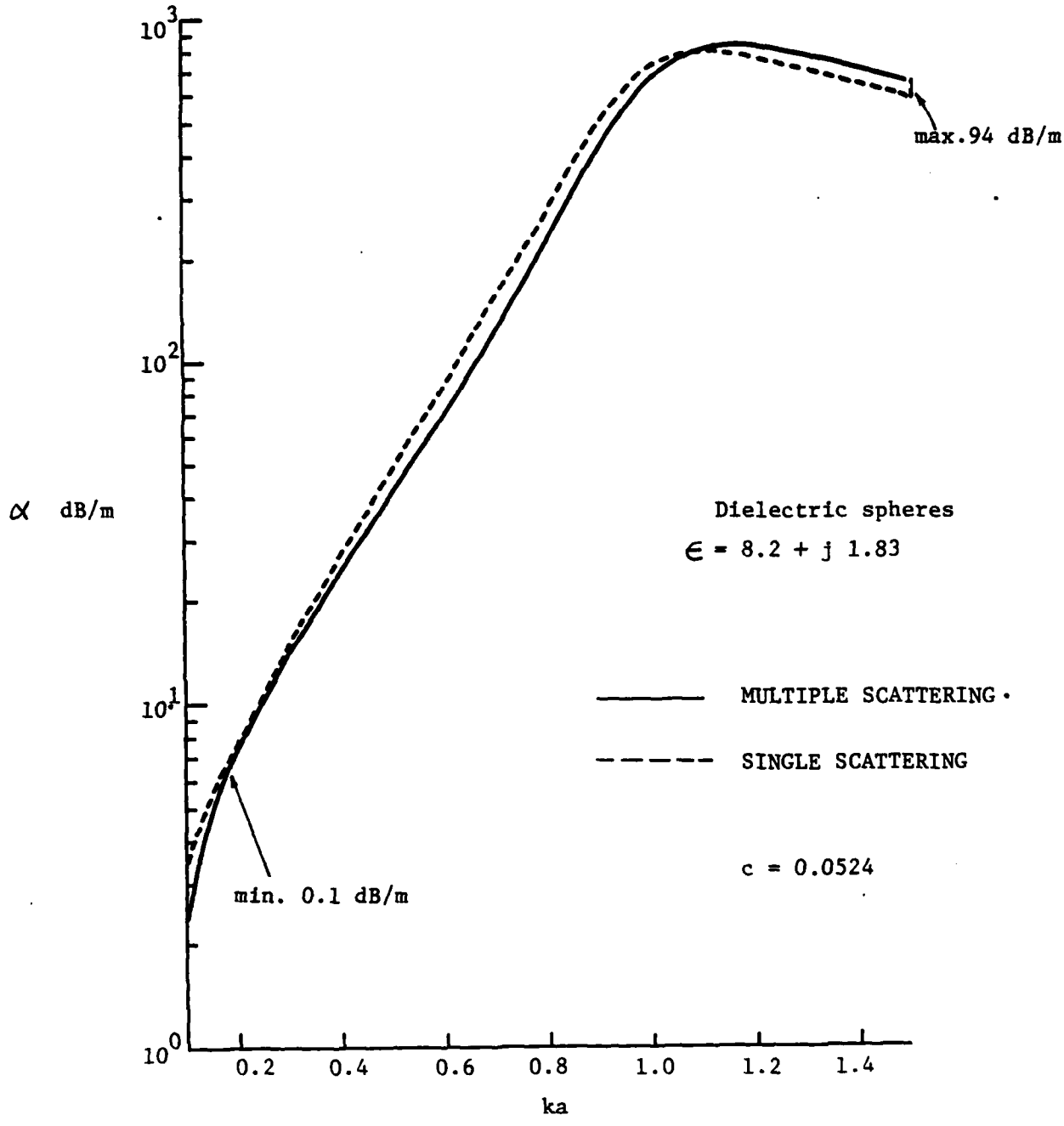

Fig.5 Coherent attenuation (dB/m) vs. nondimensional frequency ka

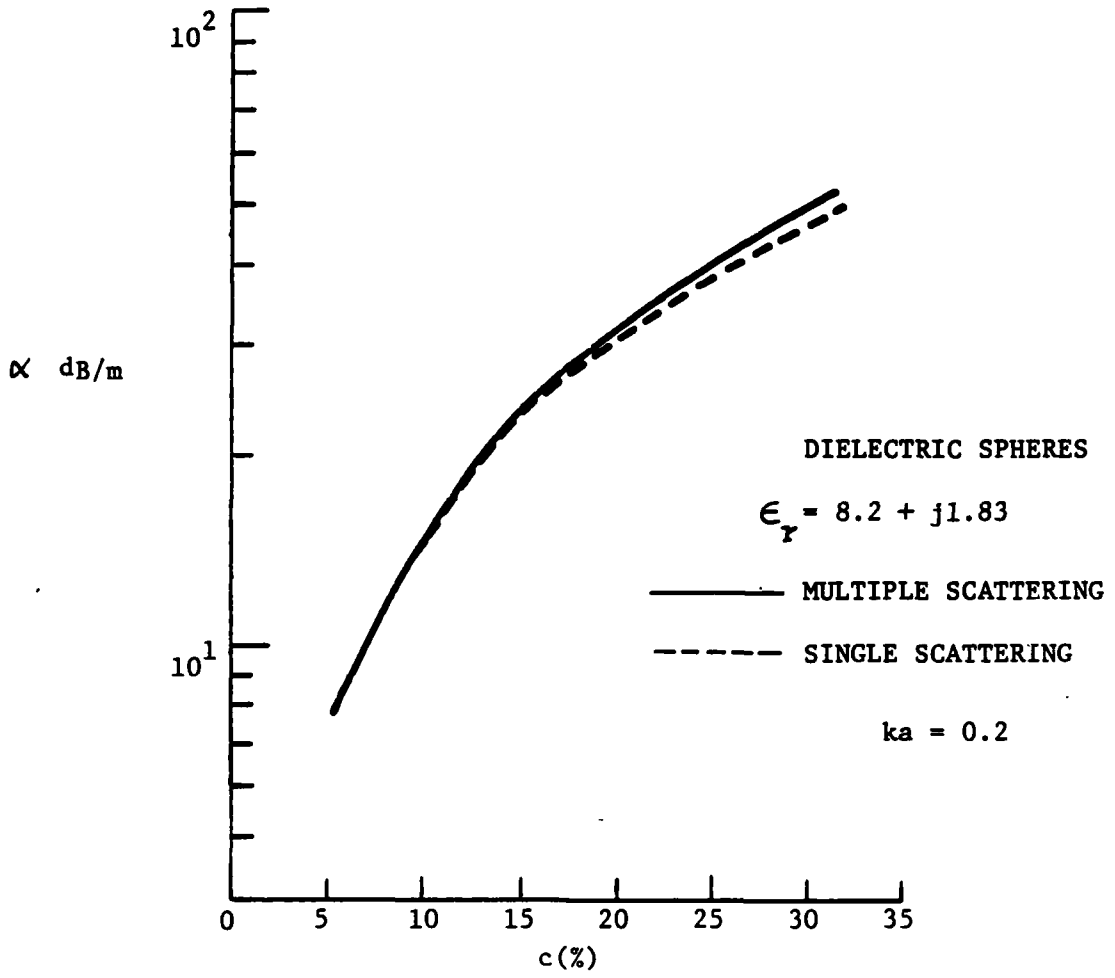

Figure 4. Coherent attenuation (dR/m) vs. concentration.

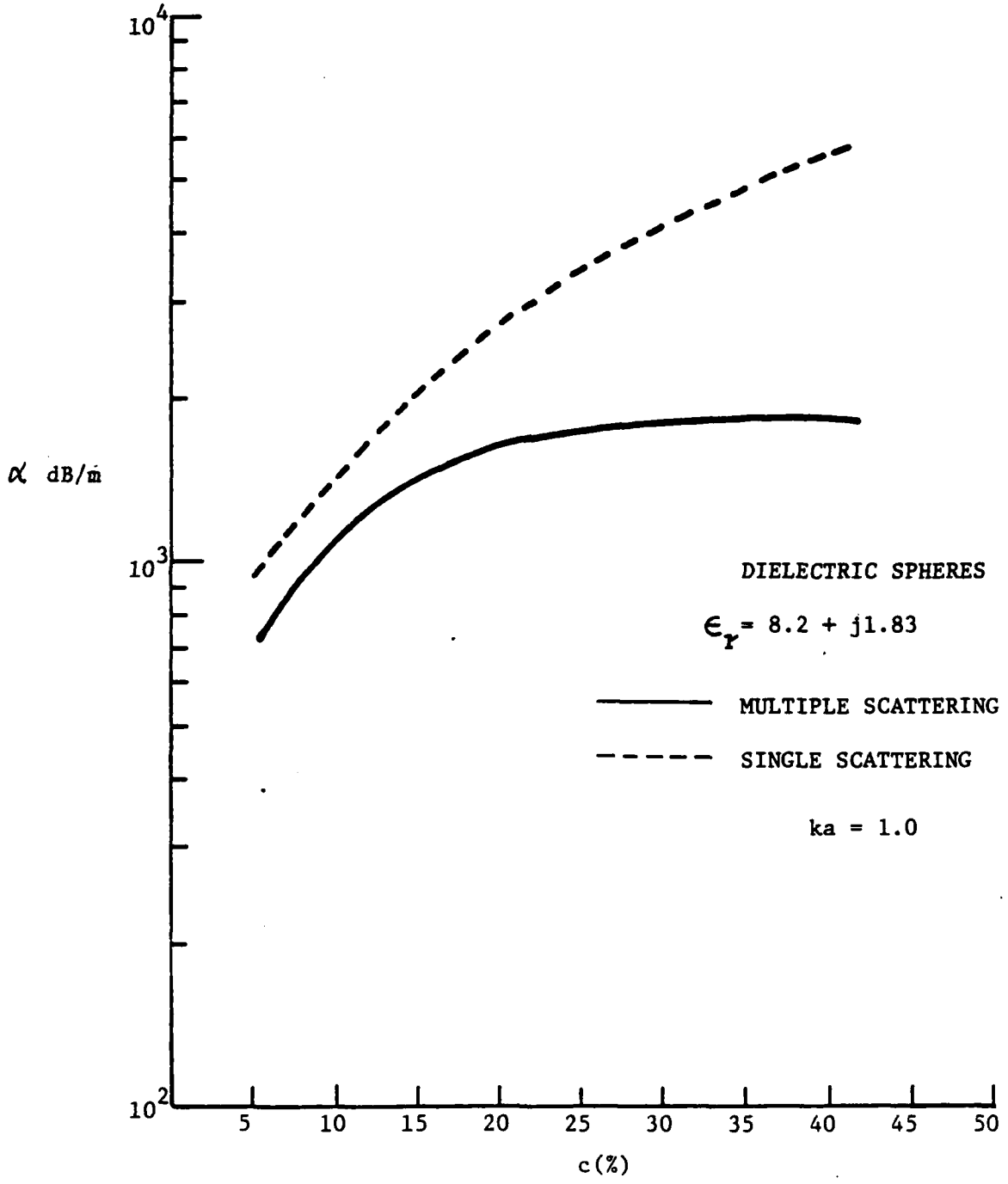

Figure 3. Coherent attenuation (dB/m) vs. concentration.

$$X_{1\ell mo} = n_o \sum_{\ell' m'} \sum_{\ell''} \sum_{\lambda=|\ell'-\ell|}^{\ell'+\ell} i^{\lambda} \Big[\Big\{ T^{m'}_{1\ell' o,\, 1\ell'' o}\; X^{m'}_{1\ell'' o} + T^{m'}_{1\ell' o,\, 2\ell'' e}\; X^{m'}_{2\ell'' e} \Big\}$$

$$\Big\{ B^{11,+}\; Y_{\lambda,\, m'-m,\, e}(\hat{k}_o)\; (-1)^m - B^{11,-}\; Y_{\lambda,\, m'+m,\, e}(\hat{k}_o) \Big\}$$

$$+ \Big\{ T^{m'}_{2\ell' e,\, 1\ell'' o}\; X^{m'}_{1\ell'' o} + T^{m'}_{2\ell' e,\, 2\ell'' e}\; X^{m'}_{2\ell'' e} \Big\} \tag{10a}$$

$$\Big\{ B^{21,+} Y_{\lambda,\, m'-m,\, e}(\hat{k}_o)(-1)^m - B^{21,-} Y_{\lambda,\, m'+m,\, e}(\hat{k}_o) \Big] \Big\{ \frac{16\pi a^2}{k^2 - K^2} (JH)_{\lambda} + 4\pi I_{\lambda} \Big\}$$

and

$$X_{2\ell me} = n_o \sum_{\ell' m'} \sum_{\ell''} \sum_{\lambda=|\ell'-\ell|}^{\ell'+\ell} i^{\lambda} \Big[\Big\{ T^{m'}_{1\ell' o,\, 1\ell'' o}\; X^{m'}_{1\ell'' o} + T^{m'}_{1\ell' o,\, 2\ell'' e}\; X^{m'}_{2\ell'' e} \Big\}$$

$$\Big\{ B^{12,+}\; Y_{\lambda,\, m'-m,\, e}(\hat{k}_o)\; (-1)^m - B^{12,-} Y_{\lambda,\, m'+m,\, e}(\hat{k}_o) \Big\}$$

$$+ \Big\{ T^{m'}_{2\ell' e,\, 1\ell'' o}\; X^{m'}_{1\ell'' o} + T^{m'}_{2\ell' e,\, 2\ell'' e}\; X^{m'}_{2\ell'' e} \Big\} \tag{10b}$$

$$\Big\{ B^{22,+}\; Y_{\lambda,\, m'-m,\, e}(\hat{k}_o)\; (-1)^m + B^{22,-} Y_{\lambda,\, m'+m,\, e}(\hat{k}_o) \Big\} \Big] \Big\{ \frac{16\pi a^2}{k^2 - K^2}\; (JH)_{\lambda} + 4\pi I_{\lambda} \Big\}$$

where

$$(JH)_{\lambda} = k\, j_{\lambda}(2Ka)\; h'_{\lambda}(2ka) - K\, j'_{\lambda}(2Ka)\; h_{\lambda}(2ka) \tag{11}$$

and

$$I_{\lambda} = \int_{2a}^{\infty} [\, g(x) - 1 \,]\; j_{\lambda}(Kx)\; h_{\lambda}(kx)\; x^2 dx \tag{12}$$

The four quantities $B^{11,\pm}$, $B^{22,\pm}$, $B^{12,\pm}$, $B^{21,\pm}$ are vestiges of the translation matrix after the angular and radial parts have been absorbed in the integration. Expressions for them may be found in terms of the Wigner coefficients and are given below

$$B^{11,\pm} = B^{22,\pm} = (-1)^{m'\pm m} \left(\pi \epsilon_m \epsilon_{m'} / 4 \epsilon_{m'\mp m} \right)^{1/2}$$

$$(-1)^{(\ell - \ell' + \lambda)/2} \left[\frac{(2\ell+1)(2\ell'+1)(2\lambda+1)}{\ell(\ell+1)\ \ell'(\ell'+1)} \right]^{1/2} \tag{13}$$

$$\begin{pmatrix} \ell' & \ell & \lambda \\ 0 & 0 & 0 \end{pmatrix} \begin{pmatrix} \ell' & \ell & \lambda \\ m' & \mp m & m \mp m' \end{pmatrix} \left[\ell'(\ell'+1) + \ell(\ell+1) - \lambda(\lambda+1) \right]$$

and

$$B^{12\pm} = B^{21\pm} = (-1)^{m'\pm m} \left(\pi \epsilon_m \epsilon_{m'} / 4 \epsilon_{m'\mp m} \right)^{1/2} \ i^{\ell - \ell' + \lambda + 1}$$

$$\left[\frac{(2\ell+1)(2\ell'+1)(2\lambda+1)}{\ell(\ell+1)\ \ell'(\ell'+1)} \right]^{1/2} \begin{pmatrix} \ell' & \ell & \lambda-1 \\ 0 & 0 & 0 \end{pmatrix} \begin{pmatrix} \ell' & \ell & \lambda \\ m' & \mp m & m \mp m' \end{pmatrix}$$

$$\left[\lambda^2 - (\ell' - \ell)^2 \right]^{1/2} \left[(\ell' + \ell + 1)^2 - \lambda^2 \right]^{1/2} \tag{14}$$

Equations (10a) and (10b) may be written in vector matrix notation in the form

$$X_i = M_{ij}\ X_j \tag{15}$$

The dispersion equation for the effective medium then becomes

$$\left| \delta_{ij} - M_{ij}(\omega, K, \hat{k}_o) \right| = 0 \tag{16}$$

where M_{ij} itself is an infinite matrix for each i,j. The determinantal equation must be solved numerically using suitable forms of the pair correlation function g(x), for given ω, $\hat{k}_o$, n_o and T. It is seen that the solution will

depend explicitly on the direction of wave propagation $\hat{k}_o$, rendering the medium effectively anisotropic.

Relationship to Twersky's Dispersion Equation

In a series of papers, Twersky[1,2] has derived the dispersion equation invoking the quasi-crystalline approximation and including the effects of pair correlation for both acoustic and electromagnetic wave propagation in pair correlated random distributions of aligned scatterers. For spherically symmetric statistics, i.e. requiring a spherical excluded volume even for non-spherical scatterers, we can show that the dispersion derived by Twersky[2] is identical to Eqs. (10a) and (10b) when the scattered field is written as an expansion in vector spherical harmonics.

In Ref. 2, Eq. (81), the dispersion equation for electromagnetic wave propagation in aligned, random distributions is given as

$$C_{nm} = -\sum_{\substack{ts\\ \mu\nu}} \left\{ \alpha_{n\nu}^{m\mu} \left[\mathcal{G}_1 \left(\begin{matrix} -\mu \\ \nu \end{matrix} \middle| \begin{matrix} t \\ s \end{matrix} \right) C_{st} - \mathcal{G}_2 \left(\begin{matrix} -\mu \\ \nu \end{matrix} \middle| \begin{matrix} t \\ s \end{matrix} \right) B_{st} \right] + \beta_{n\nu}^{m\mu} \left[\mathcal{G}_2 \left(\begin{matrix} -\mu \\ \nu \end{matrix} \middle| \begin{matrix} t \\ s \end{matrix} \right) C_{st} + \mathcal{G}_1 \left(\begin{matrix} -\mu \\ \nu \end{matrix} \middle| \begin{matrix} t \\ s \end{matrix} \right) B_{st} \right] \right\} \tag{17a}$$

and

$$B_{nm} = -\sum_{\substack{ts\\ \mu\nu}} \left\{ \gamma_{n\nu}^{m\mu} \left[\mathcal{G}_1 \left(\begin{matrix} -\mu \\ \nu \end{matrix} \middle| \begin{matrix} t \\ s \end{matrix} \right) C_{st} - \mathcal{G}_2 \left(\begin{matrix} -\mu \\ \nu \end{matrix} \middle| \begin{matrix} t \\ s \end{matrix} \right) B_{st} \right] + \delta_{n\nu}^{m\mu} \left[\mathcal{G}_2 \left(\begin{matrix} -\mu \\ \nu \end{matrix} \middle| \begin{matrix} t \\ s \end{matrix} \right) C_{st} + \mathcal{G}_1 \left(\begin{matrix} -\mu \\ \nu \end{matrix} \middle| \begin{matrix} t \\ s \end{matrix} \right) B_{st} \right] \right\} \tag{17b}$$

where in our notation

$$C_{nm} \rightarrow X_{1nm} \quad , \quad B_{nm} \rightarrow X_{2nm} \quad ; \quad n \in [0,\infty] \quad , \quad m \in [0,\infty]$$

are the scattered field coefficients,

$$\begin{bmatrix} \alpha_{n\nu}^{m\mu} & \beta_{n\nu}^{m\mu} \\ \gamma_{n\nu}^{m\mu} & \delta_{n\nu}^{m\mu} \end{bmatrix} \rightarrow \begin{bmatrix} T^{11} & T^{12} \\ T^{21} & T^{22} \end{bmatrix}$$

is the T-matrix of an individual scatterer and the two symbols $\mathscr{C}_1$ and $\mathscr{C}$ are related to the Fourier transform of the product of the pair correlation function and the translation matrix as in Eq. (8).

In the notation of the present paper and the abbreviated index notation we may write Twersky's equation, Eqs. (17a,b) in the form

$$\begin{pmatrix} X_1 \\ X_2 \end{pmatrix} = \begin{bmatrix} T^{11} & T^{12} \\ T^{21} & T^{22} \end{bmatrix} \begin{bmatrix} \mathscr{C}_1 & -\mathscr{C}_2 \\ \mathscr{C}_2 & \mathscr{C}_1 \end{bmatrix} \begin{bmatrix} X_1 \\ X_2 \end{bmatrix} \tag{18}$$

We note that Eqs. (10a,b) may be multiplied from the left by the T-matrix, so that the dispersion equation is in terms of the average scattered field coefficients rather than the exciting field. Then using $\langle f_n^i \rangle_{ij} \approx \langle f_n^i \rangle = X_{ne}^{iK\hat{k}_o \cdot \vec{r}_i}$ we can rewrite the dispersion equation in the form

$$X_n^i = a_n + n_o \sum_{n'n''} T_{nn'} \int \sigma_{n'n''}(\vec{r}_{ij})\, e^{iK\hat{k}_o \cdot \vec{r}_{ij}} X_{n''}^j \, g(|\vec{r}_{ij}|)\, d\vec{r}_j \, . \tag{19}$$

We further note that using the integral representation of the vector spherical functions the translation matrix can be written in the form

$$\sigma_{nn'}(k\vec{x}) = 2 \int_{C_\pm} d\hat{\gamma}\; \vec{A}_n(\hat{\gamma}) \cdot \vec{A}_{n'}(\hat{\gamma}) \left[i\,(1 - \delta_{\tau\tau'})(-1)^{\tau'} + \delta_{\tau\tau'} \right] e^{ik\hat{\gamma} \cdot \vec{x}} \tag{20}$$

where $c_{\pm}$ are the contours

Further $\vec{A}_n = \vec{A}_{\tau\ell m\sigma}$ are the vector spherical harmonics, $r\nabla Y_{\ell m\sigma}$ for $\tau=1$ and $-\vec{r}x\nabla Y_{\ell m\sigma}$ for $\tau=2$. Using the properties of the scalar products of vector spherical harmonics of the same argument as given for example by Twersky[2], Eq. (77), we can show that

$$\int \sigma_{nn'}(k\vec{x})\ e^{iK\hat{k}_0\cdot\vec{x}}\ g(|\vec{x}|)\ d\vec{x} = \begin{bmatrix} \mathfrak{C}_1 & -\mathfrak{C}_2 \\ \mathfrak{C}_2 & \mathfrak{C}_1 \end{bmatrix} \tag{21}$$

as defined in Eq. (80) of Ref.2 so that the dispersion equation derived here is identical to that of Twersky.

Results and Discussion

The dispersion equation (16) was programmed on an IBM 370. The main parts of the program consist of subroutines that a) generate the T-matrix for a given ω and shape of scatterer, b) set up the matrix $\delta_{ij} - M_{ij}$, c) special function programs d) determinant solver e) complex root finder based on Müellers Method and a main program that specifies the parameters ω, n_o, a, $\hat{k}_o$ and the shape and nature of the scatterer. The root finder returns the value of $K = K_1 + i\, K_2$ that renders $|\delta_{ij} - M_{ij}| = o$. This is then the complex, frequency dependent effective wavenumber of the medium. Although simple relations exist between the dispersion equations for parallel and perpendicular polarization, the resulting wavenumbers $K^{\parallel}$ and $K^{\perp}$ are in general different.

The truncation size of both T and M is varied till convergence is obtained. The computation is more time consuming than for the case when $\hat{k}_o = \hat{z}$ because an additional summation on the azimuthal index is involved i.e., the azimuthal modes are no longer uncoupled. This involves the storage of fairly large matrices. Typical computation times for an oblate spheroidal dielectric scatterer of aspect ratio 2:1 with $\epsilon_r^1 = 3.168$ and $\epsilon = 1$ for a given ω_1 n_o and $\hat{k}_o$ is 60 secs after the program has been tested for the correct matrix size.

We now present results in the form of plots of K_1, K_2 and $\langle\epsilon\rangle = \epsilon_R + i\, \epsilon_I$, the real and imaginary parts of the effective dielectric constant as a function of $k\,a = \omega\, a/c$, $\hat{k}_o$ $(\alpha, \beta = 0)$ and $c = n_o\, 4\pi\, a^3/3$ where 'a' is the semi-major axis of the oblate spheroid of aspect ratio 2:1, and 1.25:1. We recall that $\langle\epsilon\rangle = K^2/k^2$.

In Fig. 1, the phase velocity Re(k/K) is plotted as a function of frequency for both parallel and perpendicular polarization for $\alpha = 58.3°$ and $c = 0.21$. There is approximately 2% difference between the two cases except

at ka ~ 1.7 when a cross-over occurs. In Fig. 2, the attenuation given by Im (K/k) is plotted as a function of ka for both parallel and perpendicular polarization for $\alpha = 58.3°$ and c=0.21. There is approximately 2% difference between the two cases except at ka ~ 1.7 when a cross-over occurs. In Fig. 2, the attenuation given by Im (K/k) is plotted as a function of ka for both parallel and perpendicular polarization for $\alpha = 58.3°$ and c=0.21. Also included in the figure is the attenuation for α=0 and aspect ratio 1.25:1. In Figs. 3 and 4 the attenuation is plotted as a function of α varying from 0° to 90°. The attenuation is a slowly varying function of α and is maximum for α=0°. In Fig. 5, the attenuation and Re$\langle\varepsilon\rangle$ are plotted as a function of angle α for parallel polarization, c=0.052and ka=0.05 for an aspect ratio 1.25:1. In Fig. 6, the real part of $\langle\varepsilon\rangle$ is plotted as a function of frequency (ka) for several cases. The phase velocity for α=0° and a:b = 1.25:1 is significantly higher than the other three cases considered.

In Fig. 7, the complex plane plot of the effective dielectric constant is plotted for both parallel and perpendicular polarization for a/b = 2.0 and should be compared with Fig. 8 for a/b = 1.25. In Fig. 9, the complex plane plots of $\langle\varepsilon\rangle$ are shown for α=58.3° for parallel and perpendicular polarization. **Figure 10 shows the comparison of our results with those by other methods.**

In conclusion, we have demonstrated a scheme for computing the complex propagation characteristic's of a medium that is effectively anisotropic. Although, the effects are not dramatic, there is significant (measurable) difference between the results for parallel and perpendicular polarization. The effect of polarization is more significant than that of propagation direction. Finally we have also discussed how our dispersion equation for a medium with pair correlated aligned scatterers compares with Twersky's equation for the same system.

REFERENCES

1. V. Twersky, J. Math. Phys. 18 , 2468-2486 (1977).
2. V.Twersky, J. Math. Phys. 19 , 215-230 (1978).
3. Y. Ma, V.K. Varadan and V.V. Varadan, J. Acoust. Soc. Am., to appear.
4. V.V. Varadan and V.K. Varadan, to be published.
5. P.C. Waterman, Phys. Rev. D 3 , 825 (1971).
6. V.K. Varadan and V.V. Varadan eds., Acoustic, Electromagnetic and Elastic Wave Scattering - Focus on the T-Matrix Approach, Pergamon Press, New York (1980).
7. V.N. Bringi, V.V. Varadan and V.K. Varadan, Radio Science 17 , 946-952, (1982).
8. V.N. Bringi, V.K. Varadan and V.V. Varadan, IEEE Trans. AP-31 , 371-375 , (1983).
9. V.N. Bringi, T.A. Seliga, V.K. Varadan and V.V. Varadan in ' Multiple Scattering and Waves in Random Media ', P.L. Chow, W.E. Kohler and G.C. Papanicolaou eds., North Holland (1981).
10. V.K. Varadan, V.N. Bringi, V.V. Varadan and A. Ishimaru, Radio Science 18 , 321-327 , (1983).
11. V.V. Varadan, V.N. Bringi and V.K. Varadan in 'Macroscopic Properties of Disordered Media', R. Burridge, S. Childress and G.C. Papanicolaou eds., Springer-Verlag (1982).

ACKNOWLEDGEMENTS

This work was supported by the U.S. Army Research Office under Contract No: DAAG29-83-K-0097. Many helpful discussions with Dr. W.A.Flood and Dr. G.S. Brown are gratefully acknowledged.

FIGURE CAPTIONS

Fig. 1 Plot of phase velocity vercus normalized wavenumber for a distribution of aligned spheroids for wave propagation at $\alpha = 58.3^{\circ}$ for both parallel and perpendular polarization of the waves.

Fig. 2 Plot of attenuation versus normalized wavenumber for a distribution of aligned spheroids for wave propagation at $\alpha = 58.3^{\circ}$ and $\alpha = 0^{\circ}$.

Fig. 3 Plot of attenuation versus direction of wave propagation for aligned spheroids, parallel polarization.

Fig. 4 Plot of attenuation versus direction of wave propagation for aligned spheroids, perpendular polarization.

Fig. 5 Plot of attenuation and the real part of the dielectric constant of wave propagation in aligned spheroids.

Fig. 6 Plot of the real part of the dielectric constant versus normalized wavenumber for aligned and randomly oriented spheroids.

Fig. 7 Complex plane plot of the dielectric constant at different frequencies for aligned and randomly oriented spheroids.

Fig. 8 Complex plane plot of the dielectric constant at different frequencies for aligned spheroids.

Fig. 9 Complex plane plot of the dielectric constant at different frequencies for aligned spheroids.

Fig. 10 Comparison of our results with those by other methods at ka = 0.05

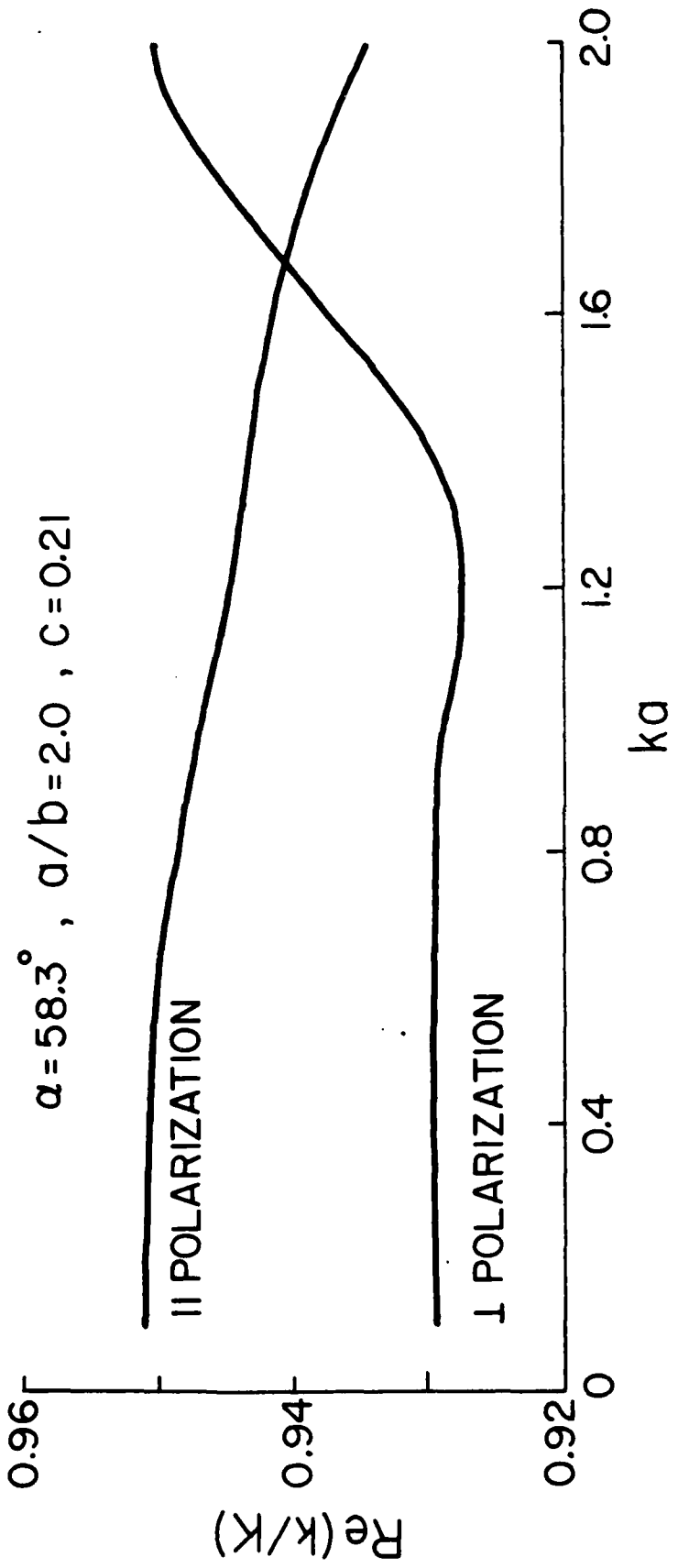
α=58.3°, a/b=2.0, c=0.21
II POLARIZATION
⊥ POLARIZATION
Re (k/K)
0.96
0.94
0.92
0
0.4
0.8
1.2
1.6
2.0
ka

Fig.1

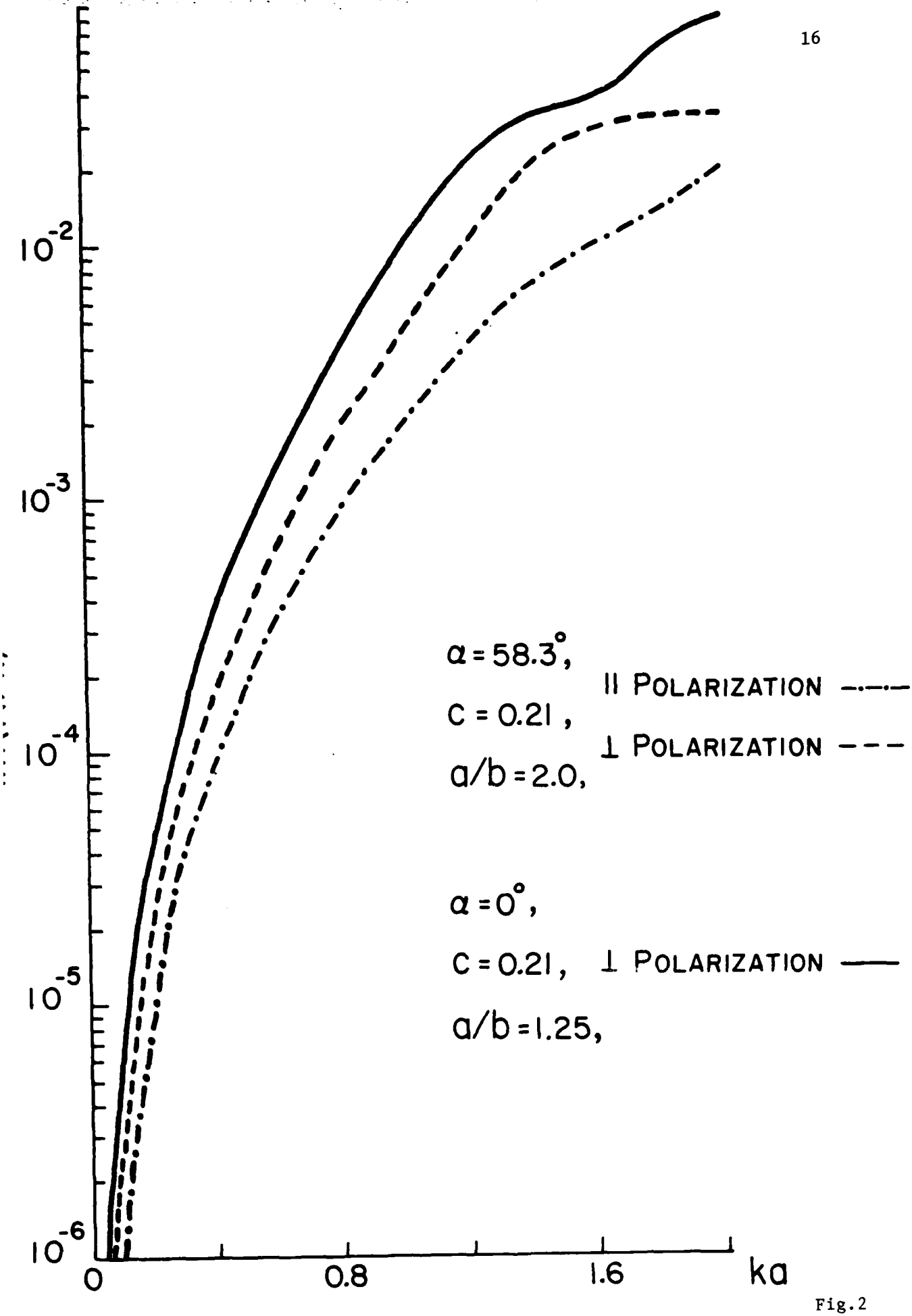
10^{-2}
10^{-3}
10^{-4}
10^{-5}
10^{-6}
0
0.8
1.6
ka
α = 58.3°,
c = 0.21,
a/b = 2.0,
II POLARIZATION
⊥ POLARIZATION
α = 0°,
c = 0.21,
a/b = 1.25,
⊥ POLARIZATION

Fig.2

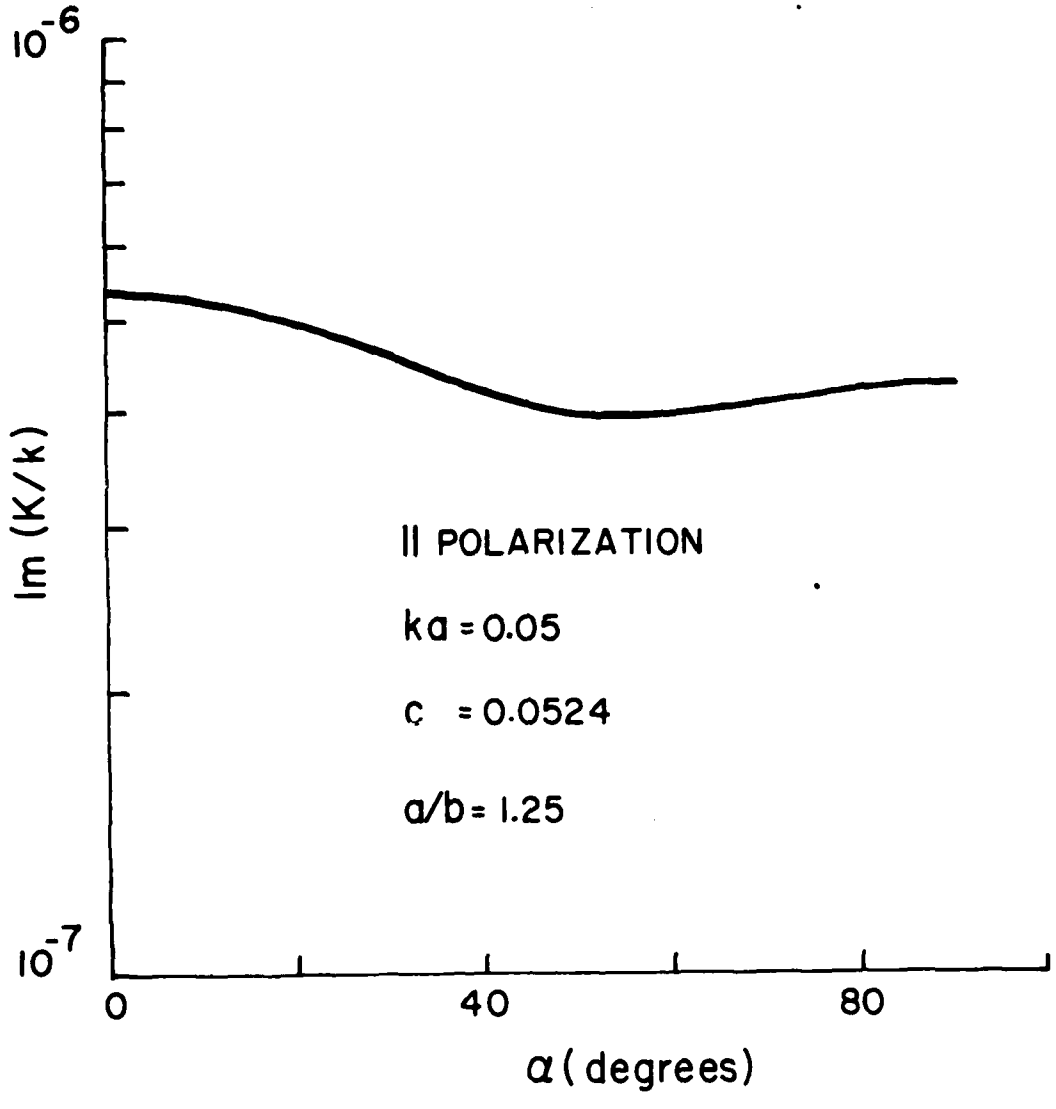
10^{-6}
10^{-7}
Im (K/k)
|| POLARIZATION
ka = 0.05
c = 0.0524
a/b = 1.25
0
40
80
α (degrees)

Fig. 3

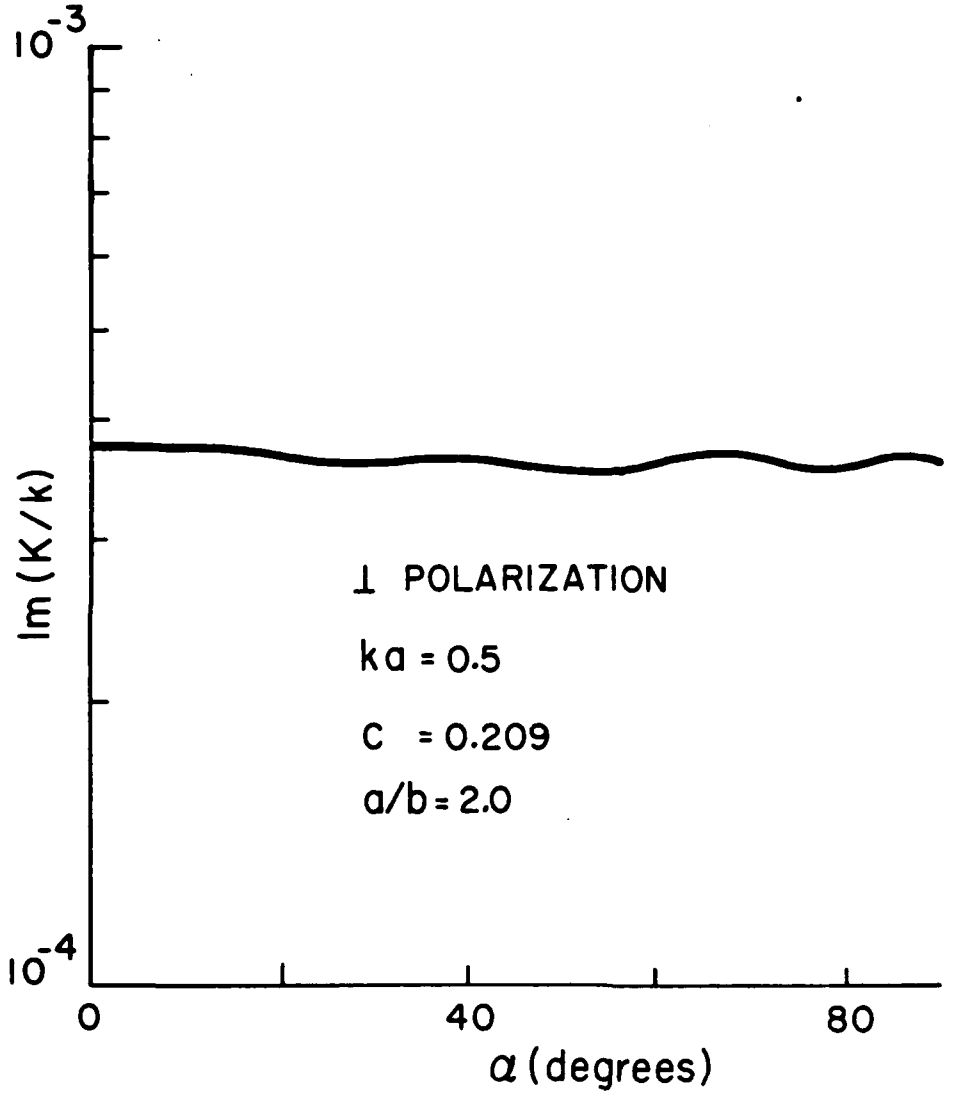

Fig.4

functions (Hankel functions) and functions regular at the origin (Bessel functions). We dispense with vector notation and the abbreviated index may denote $n \to \tau,\ell,m,\sigma$; $\tau = 1,2,3$; $\ell \in [o,\infty]$; $m \in [o,\ell]$. Thus the present discussion can apply equally well to acoustic (τ=1 only), electromagnetic (τ=2,3 only) or elastic (τ=1,2,3) wave propagation.

At a field point $\vec{r}$ in the host medium, the incident, scattered and exciting fields are expanded as follows,

$$u^{o}(\vec{r}) = \Sigma\ a_n\ \mathrm{Re}\ \psi_n(\vec{r}) \tag{3}$$

with for example

$$a_n = i^{-\ell}\ Y_{\ell m\sigma}(\hat{k}_o) \tag{4}$$

for plane acoustic waves propagating along $\hat{k}_o$ and $Y_{\ell m\sigma}$ are spherical harmonics;

$$u_i^{e}(\vec{r}) = \Sigma_n\ \alpha_n^{i}\ \mathrm{Re}\ \psi_n(\vec{r}-\vec{r}_i);\ |\vec{r}-\vec{r}_i| < 2a \tag{5}$$

and

$$u_i^{s}(\vec{r}) = \Sigma_n\ f_n^{i}\ \text{ou}\ \psi_n(\vec{r}-\vec{r}_i);\ |\vec{r}-\vec{r}_i| > 2a \tag{6}$$

where $\vec{r}_i$ denotes the center of the i-th scatterer, and 'a' is the radius of the sphere circumscribing any scatterer. The coefficients f_n^i and α_n^i are unknown but are however related via the T-matrix, which can be numerically calculated for scatterers of arbitrary shape using Waterman's extended boundary condition method.[18] Thus,

$$f_n^{i} = \Sigma_{n'}\ T_{nn'}\ \alpha_{n'}^{i} \tag{7}$$

where we have assumed that all scatterers are identical.

Substituting Eqs. (5) - (7) in (2) and using the translation-addition theorems for spherical wavefunctions and the orthogonality properties of spherical harmonics[13], we obtain

INTRODUCTION

Studies of wave propagation in discrete random media is of interest in acoustics, elastodynamics and electromagnetics and dates back to the studies of Rayleigh. In more recent times Foldy[2], Lax[1], Twersky[3-10], Vezzetti and Keller[11] and Bedeaux and Mazur[12] have made significant contributions to our understanding in this area. Computational techniques[13-17] that have been developed to solve the dispersion equation in dense random media at wavelengths comparable to scatterer size, are for the most part based on Refs. 1-12.

THE QUASI-CRYSTALLINE APPROXIMATION

Consider wave propagation in an infinite medium of volume $V \to \infty$ containing a random distribution of N scatterers, $N \to \infty$ such that $n_o = N/V$, the number density is finite. Plane harmonic waves of frequency ω propagate in the medium and undergo multiple scattering. Let u^{tot}, u^o, u_i^e and u_i^s denote respectively the total field, the incident field, the field exciting the i-th scatterer and the field scattered by the i-th scatterer. Then self consistency requires the following relationships between the fields.

$$u^{tot} = u^o + \sum_{i=1}^{N} u_i^s = u_i^e + u_i^s \tag{1}$$

and

$$u_i^e = u^o + \sum_{j \neq i}^{N} u_j^s \tag{2}$$

Although a general dispersion equation can be derived as in Twersky[5-7], in order to obtain explicit results for particular shapes of scatterers, one has to expand the exciting and scattered fields in a convenient set of basis functions, such as spherical wavefunctions. Let $\mathrm{Re}^{ou}\psi_n$ generally denote outgoing

THE QUASI-CRYSTALLINE APPROXIMATION AND MULTIPLE SCATTERING OF WAVES IN RANDOM MEDIA

Vasundara V. Varadan and Vijay K. Varadan

Department of Engineering Science and Mechanics
The Pennsylvania State University
University Park, PA 16802

ABSTRACT

The Quasi Crystalline Approximation (QCA) was first introduced by Lax[1] to break the infinite heirarchy of equations that results in studies of the coherent field in discrete random media. It simply states that the conditional average of a field with the position of one scatterer held fixed is equal to the conditional average with two scatterers held fixed i.e. $\langle\psi\rangle^{i}_{ij} = \langle\psi\rangle^{i}_{i}$. The QCA has met with great success[2] for a range of concentrations from sparse to dense and for long and intermediate wavelengths. In this paper, the QCA is interpreted as a partial resummation of the multiple scattering series that includes only two body correlations. An explicit expression is derived for the propagation in such a medium that yields the same dispersion equation as obtained using the QCA. Improvements to the QCA are suggested that still require only a knowledge of the two body correlation function.

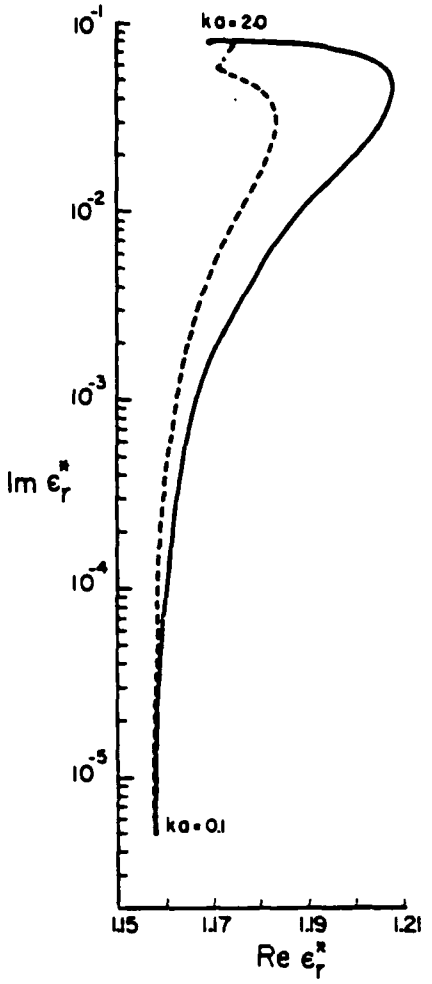

Fig. 4. Same as in Figure 3 for $a/b = 2.0$.

fact, the results of random orientation lie in between $\theta = 0°$ and 90°, and the same trend has been observed before by the authors in the elastic wave case [see *Varadan and Varadan*, 1980].

In Figures 3 and 4, average complex frequency dependent dielectric properties are presented for $c = 0.2$ for both aligned scatterers ($\theta = 0°$ for an incident wave with vertical polarization) and randomly oriented scatterers. The results indicate that the real part of dielectric constant (Re ϵ_r^*) is always less in the case of random orientation for the frequency range considered. At higher frequencies, there is a remarkable difference in the behavior of dielectric properties as depicted by Figures 3 and 4.

Acknowledgments. This work was supported by the U.S. Army Research Office under contract DAAG29-83-K-0097. Many helpful discussions with W. A. Flood, G. S. Brown and V. N. Bringi are gratefully acknowledged.

REFERENCES

Bringi, V. N., V. V. Varadan, and V. K. Varadan, The effects of pair correlation function on coherent wave attenuation in discrete random media, *IEEE Trans. Antennas Propag., AP-30*, 805–808, 1982*a*.

Bringi, V. N., V. K. Varadan, and V. V. Varadan, Coherent wave attenuation by a random distribution of particles, *Radio Sci., 17*, 946–952, 1982*b*.

Cruzan, O. R., Translational addition theorems for spherical vector wave equations, *Q. Appl. Math., 20*, 30–39, 1962.

Edmonds, A. R., *Angular Momentum in Quantum Mechanics*, Princeton University Press, Princeton, N. J., 1957.

Ishimaru, A., and Y. Kuga, Attenuation constant of coherent field in dense distribution of particles, *J. Opt. Soc. Am., 72*(10), 1317–1320, 1982.

Tsang, L., and J. A. Kong, Scattering of electromagnetic waves from a half space of densely distributed dielectric scatterers, *Radio Sci., 18*(6), 1260–1272, 1983.

Twersky, V., Coherent electromagnetic waves in pair-correlated random distributions of aligned scatterers, *J. Math. Phys., 19*, 215–230, 1978.

Twersky, V., Multiple scattering of sound by correlated monolayers, *J. Acoust. Soc. Am., 73*(1), 68–84, 1983.

Varadan, V. K., and V. V. Varadan (Eds.), *Acoustic, Electromagnetic and Elastic Wave Scattering—Focus on the T-Matrix Approach*, Pergamon, New York, 1980.

Varadan, V. K., and V. N. Bringi, and V. V. Varadan, Coherent electromagnetic wave propagation through randomly distributed dielectric scatterers, *Phys. Rev. D, 19*, 2480–2489, 1979.

Varadan, V. K., V. N. Bringi, V. V. Varadan, and A. Ishimaru, Multiple scattering theory for waves in discrete random media and comparison with experiments, *Radio Sci., 18*(3), 321–327, 1983.

Y. Ma, V. K. Varadan, and V. V. Varadan, Wave Propagation Laboratory, Department of Engineering Science and Mechanics, Pennsylvania State University, University Park, PA 16802.

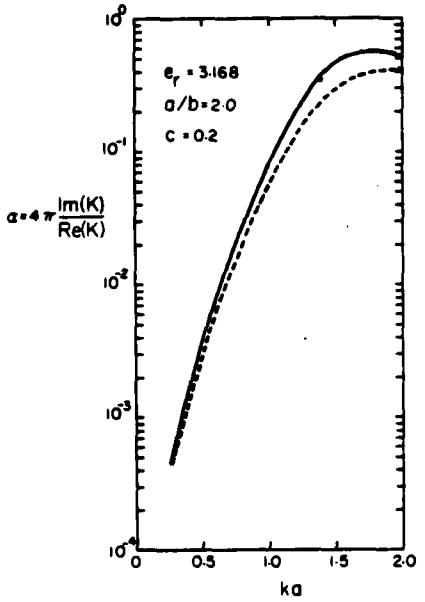

Fig. 2. Coherent attenuation vs. ka for spheroidal ice particles: solid lines parallel orientation, dashed line, random orientation; $a/b = 2.0$ (c is the effective spherical concentration).

differentiation with respect to the argument. The expressions for a and b occurring in (14) are related to the Wigner 3-j symbols and are given by *Cruzan* [1962]. Now the singular value of the coefficient matrix generated from (14) can be solved for the average propagation constant $K = K_1 + jK_2$. The real part K_1 is related to the phase velocity while the imaginary part K_2 is related to the coherent attenuation. Once K is known, one can also compute the normalized average complex dielectric constant as given by

$$\epsilon_r^* = \epsilon_r^{*\prime} + j\epsilon_r^{*\prime\prime} = (K/k)^2 \tag{16}$$

COMPUTATION

The procedure for computing coherent attenuation, phase velocity and average complex dielectric properties is similar to the one presented by *Varadan and Varadan* [1980]. For a given value of ka, the T-matrix of the scatterer is computed. A proper T-matrix size is chosen for a given ka to satisfy the unitary and symmetry properties. Retaining as many as 20 simultaneous equations for Y and Z in order to obtain proper convergence, we computed the complex determinant of the coefficient matrix corresponding to Y and Z of (14a) and (14b). The roots ($K = K_1 + iK_2$) of the resulting transcendental equation are obtained by Müller's complex root searching algorithm. We start from a low value of ka(=0.01) for which the values obtained from *Twersky* [1978] are used in our root searching algorithm. The values of ka are increased by small increments of the order of 0.05.

For illustration purposes, we have presented sample calculations only for concentration $c = 0.2$. The c refers to the effective spherical concentration; actual oblate spheroidal concentration equals to 0.1 for an aspect ratio $a/b = 2.0$. In Figures 1 and 2, the coherent attenuation is plotted as a function of ka for oblate spheroidal ice particles in free space with $a/b = 1.25$ and 2.0, respectively. The solid curve corresponds to that of aligned scatterers when the incident wave with vertical polarization is along the symmetry (minor) axis of the scatterer ($\theta = 0°$), while the dotted curve corresponds to that of randomly oriented scatterers. At higher frequencies, the results indicate that there is a significant difference in coherent attenuation between aligned and randomly oriented scatterers. For vertical polarizations, one could also perform computations when the wave is incident along symmetry (major) axes of aligned scatterers ($\theta = 90°$). The corresponding attenuation in this case is lower than that of the randomly oriented case. In

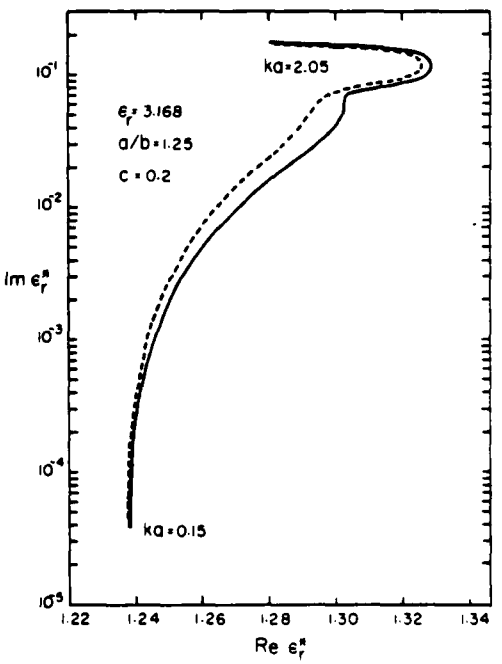

Fig. 3. Complex plane locus of the effective dielectric constant for a system of spheroidal ($a/b = 1.25$) ice particles: solid lines parallel orientation; dashed line, random orientation (c is the effective spherical concentration).

Thus, the actual concentration may be quite different from the effective spherical concentration for scatterers of large aspect ratio. For an exact calculation of a very dense system, assumption of spherical statistics for nonspherical particles may lead to considerable error. *Twersky* [1983] has considered nonspherical statistics for spheroidal scatterers in the sparse concentration limit. Extending this model to dense systems and numerically implementing it for high frequencies will be a problem of interest to the research community.

Performing the configurational averaging and invoking the quasi-crystalline approximation as outlined in *Twersky* [1978] and *Varadan et al.* [1979, 1980], we obtain the average scattered field coefficients as follows:

$$\begin{bmatrix} \langle B^i_{nm} \rangle_i \\ \langle C^i_{nm} \rangle_i \end{bmatrix} = \begin{bmatrix} \langle T^{11} \rangle & \langle T^{12} \rangle \\ \langle T^{21} \rangle & \langle T^{22} \rangle \end{bmatrix} \begin{bmatrix} \langle \psi^i_{n_1 m_1} \rangle \\ \langle \chi^i_{n_1 m_1} \rangle \end{bmatrix} \tag{10}$$

where

$$\langle \psi^i_{n_1 m_1} \rangle = \frac{2n_1 + 1}{n_1(n_1+1)} i^{n_1} \frac{e^{i\mathbf{k}\cdot\mathbf{r}_i}}{2i} [\delta_{m_1,1} + n_1(n_1+1)\delta_{m_1,-1}]$$
$$+ \frac{1}{V} \sum_{j=1}^{N}{}' \sum_{n_2=0}^{\infty} \sum_{m_2=-n_2}^{n_2} \int_{V'} [\langle B^j_{n_2 m_2} \rangle B^{n_2 m_2}_{n_1 m_1}(\mathbf{r}_i - \mathbf{r}_j)$$
$$+ \langle C^j_{n_2 m_2} \rangle C^{n_2 m_2}_{n_1 m_1}(\mathbf{r}_i - \mathbf{r}_j)] g(|\mathbf{r}_j - \mathbf{r}_i|)\, d\mathbf{r}_j \tag{11}$$

and

$$\langle \chi^i_{n_1 m_1} \rangle = \frac{2n_1 + 1}{n_1(n_1+1)} i^{n_1} \frac{e^{i\mathbf{k}\cdot\mathbf{r}_i}}{2i} [\delta_{m_1,1} + n_1(n_1+1)\delta_{m_1,-1}]$$
$$+ \frac{1}{V} \sum_{j=1}^{N}{}' \sum_{n_2=0}^{\infty} \sum_{m_2=-n_2}^{n_2} \int_{V'} [\langle B^j_{n_2 m_2} \rangle C^{n_2 m_2}_{n_1 m_1}(\mathbf{r}_i - \mathbf{r}_j)$$
$$+ \langle C^j_{n_2 m_2} \rangle B^{n_2 m_2}_{n_1 m_1}(\mathbf{r}_i - \mathbf{r}_j)] g(|\mathbf{r}_j - \mathbf{r}_i|)\, d\mathbf{r}_j \tag{12}$$

In (11) and (12), V' denotes the volume of the medium excluding a sphere of radius $2a$. For identical scatterers, $\sum_{j=1}^{N}{}' = N - 1$ and $4\pi(N-1)a^3/3V = c$, the volume concentration of "scatterers," provided N is large enough.

To find the average propagation constant K for the bulk medium, we assume a plane wave propagating with the effective wave number $\mathbf{K}$ in the incident wave direction with unknown amplitudes Y and Z:

$$\langle B^i_{nm} \rangle_i = Y_{nm} e^{i\mathbf{K}\cdot\mathbf{r}_i}$$
$$\langle C^i_{nm} \rangle_i = Z_{nm} e^{i\mathbf{K}\cdot\mathbf{r}_i} \tag{13}$$

Equation (13) is substituted into (10) and the extinction theorem can be invoked to cancel the incident wave term on the right-hand side of (11) and (12).

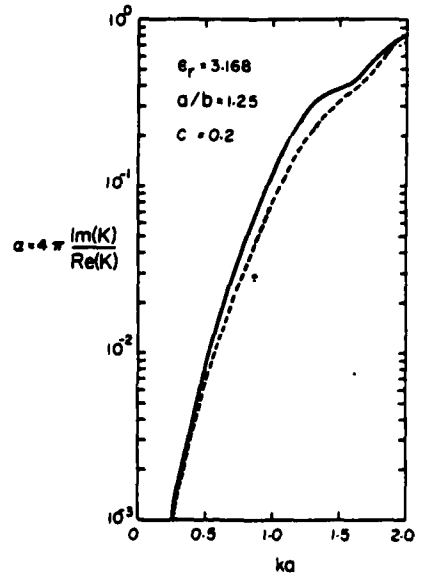

Fig. 1. Coherent attenuation vs. ka for spheroidal ice particles: solid line, parallel orientation; dashed lines random orientation; $a/b = 1.25$.

The resulting equations are

$$Y_{nm} = \sum_{q=|n_1-n_2|}^{n_1+n_2} \sum_{n_1=0}^{\infty} \sum_{n_2=0}^{\infty} \sum_{m_1=-n_1}^{n_1} \sum_{m_2=-n_2}^{n_2} (-1)^{m_2} i^{n_2-n_1} \delta_{m_1 m_2} (JH)_q$$
$$\cdot \{ Y_{n_2 m_2} [\langle T^{11} \rangle_{nm,n_1 m_1} a(n_2, n_1, q) a(m_2, n_2 | -m_1, n_1 | q)$$
$$- \langle T^{12} \rangle_{nm,n_1 m_1} b(n_2, n_1, q) a(m_2, n_2 | -m_1, n_1 | q, q-1)]$$
$$+ Z_{n_2 m_2} [\langle T^{12} \rangle_{nm,n_1 m_1} a(n_2, n_1, q) a(m_2, n_2 | -m_1, n_1 | q)$$
$$- \langle T^{11} \rangle_{nm,n_1 m_1} b(n_2, n_1, q) a(m_2, n_2 | -m_1, n_1 | q, q-1]\} \tag{14a}$$

and

$$Z_{nm} = \cdots \tag{14b}$$

where (14b) can be obtained from (14a) by replacing $\langle T^{11} \rangle$ and $\langle T^{12} \rangle$ by $\langle T^{21} \rangle$ and $\langle T^{22} \rangle$, respectively. The term $(JH)_q$ is given by

$$(JH)_q = \frac{6c}{(ka)^2 - (Ka)^2} [2ka\, j_q(2Ka) h'_q(2ka)$$
$$- 2Ka\, h_q(2ka) j'_q(2Ka)]$$
$$+ 24c \int_1^{\infty} x^2 [g(x) - 1] h_q(2kax) j_q(2Kax)\, dx \tag{15}$$

In (14) and (15), j_q and h_q are the spherical Bessel and Hankel functions, respectively, and the primes denote

we obtain, see *Varadan et al.* [1979] and *Varadan and Varadan* [1980],

$$b_n^{m(i)} = \frac{2n+1}{n(n+1)} i^n \frac{e^{i\mathbf{k}\cdot\mathbf{r}_i}}{2i} [\delta_{m,1} + n(n+1)\delta_{m,-1}] + \sum_{j=1}^{N}{}' \sum_{n_1=0}^{\infty} \sum_{m_1=-n_1}^{n_1} [B_{n_1}^{m_1(j)} B_{mn}^{m_1 n_1}(\mathbf{r}_i - \mathbf{r}_j) + C_{n_1}^{m_1(j)} C_{mn}^{m_1 n_1}(\mathbf{r}_i - \mathbf{r}_j)] \quad (2)$$

$$c_n^{m(i)} = \frac{2n+1}{n(n+1)} i^n \frac{e^{i\mathbf{k}\cdot\mathbf{r}_i}}{2i} [\delta_{m,1} + n(n+1)\delta_{m,-1}] + \sum_{j=1}^{N}{}' \sum_{n_1=0}^{\infty} \sum_{m_1=-n_1}^{n_1} [B_{n_1}^{m_1(j)} C_{mn}^{m_1 n_1}(\mathbf{r}_i - \mathbf{r}_j) + C_{n_1}^{m_1(j)} B_{mn}^{m_1 n_1}(\mathbf{r}_i - \mathbf{r}_j)] \quad (3)$$

where $\sum'$ denotes $j \neq i$, δ_{mn} is the Kronecker delta, and k is the wave number of the host medium. B and C are the scattered field coefficients, while b and c are the exciting field coefficients. The quantities $B_{mn}^{m_1 n_1}$ and $C_{mn}^{m_1 n_1}$ are the functions resulting from the translation theorem of the vector spherical functions.

We introduce next the T-matrix of a single scatterer which relates the scattered field expansion coefficients to the exciting field expansion coefficients as follows [*Varadan and Varadan*, 1980]:

$$\begin{pmatrix} B \\ C \end{pmatrix} = \begin{bmatrix} T^{11} & T^{12} \\ T^{21} & T^{22} \end{bmatrix} \begin{pmatrix} b \\ c \end{pmatrix} = (T) \begin{pmatrix} b \\ c \end{pmatrix}. \quad (4)$$

For aligned scatterers, if the T-matrix is computed with respect to xyz axes, then the T-matrix of all the N scatterers is the same. However, if the orientation of each scatterer with respect to the xyz axes is defined by the Euler angles α_i, β_i, γ_i, then the T-matrix of the ith scatterer is a function of the Euler angles and is defined by

$$T = D\hat{T}D^{-1} \quad (5)$$

Here, $\hat{T}$ is the T-matrix of a scatterer evaluated with respect to the set of coordinate axes natural to the scatterer (XYZ axes) and is independent of position and orientation (hence, the same for identical scatterers) and D is the rotation matrix given by *Edmonds* [1957], i.e.,

$$D_{mm'}^{n}(\alpha, \beta, \gamma) = e^{im\alpha} d_{m'n}^{n}(\beta) e^{im'\gamma} \quad (6)$$

where

$$d_{mm'}^{n}(\beta) = \left[\frac{(n+m)!(n-m)!}{(n+m')!(n-m')!}\right]^{1/2} \left(\cos\frac{\beta}{2}\right)^{m+m'} \left(\sin\frac{\beta}{2}\right)^{m-m'} P_{n-m}^{(n-m',m'+m)}(\cos\beta) \quad (7)$$

In (7), P is the Jacobi polynomial which can be expressed in terms of the associated Legendre polynomials [see *Edmonds*, 1957].

The T-matrix averaged over all possible orientations of the scatterer may then be written as

$$\langle T_{mm,m'm'} \rangle = \frac{1}{8\pi^2} \int_0^{2\pi} d\alpha \int_0^{2\pi} d\gamma \int_0^{\pi} d\beta \sin\beta \sum_{m_1,m_2} [D_{mm_1}^{n}(\alpha, \beta, \gamma) \hat{T}_{nm_1,n'm_2} (D^{-1})_{m_2m'}^{n'}(\alpha, \beta, \gamma)] = \frac{1}{2n+1} \hat{T}_{nm,n'm'} \delta_{nn'} \quad (8)$$

If (2) and (3) are multiplied by $\langle T \rangle$ from (8), we obtain a set of coupled equations for the scattered field expansion coefficients which are averaged over all possible orientations.

Thus, only the diagonal elements of the T-matrix of a nonspherical scatterer contribute to the average T-matrix. This has also been observed by *Twersky* [1978]. We note here that although the scatterers are nonspherical, because of their random orientations, the medium is effectively isotropic and is hence characterized by an isotropic dielectric tensor.

It remains now to perform an average over all possible positions. To this end, one can introduce a probability density function of finding the first scatterer at $\mathbf{r}_1$, the second scatterer at $\mathbf{r}_2$, and so forth by $p(\mathbf{r}_1, \mathbf{r}_2, \cdots, \mathbf{r}_N)$ which in turn may be expressed in terms of conditional probability, $p(\mathbf{r}_j | \mathbf{r}_i)$, of finding a scatterer at $\mathbf{r}_j$ if a scatterer is known to be at $\mathbf{r}_i$. The two point joint probability function $p(\mathbf{r}_j | \mathbf{r}_i)$ is in turn defined in terms of radial distribution function $g(|\mathbf{r}_j - \mathbf{r}_i|)$ as follows:

$$p(\mathbf{r}_j | \mathbf{r}_i) = \begin{cases} \frac{1}{V} g(|\mathbf{r}_j - \mathbf{r}_i|) & |\mathbf{r}_j - \mathbf{r}_i| \geq 2a \\ 0 & |\mathbf{r}_j - \mathbf{r}_i| < 2a \end{cases} \quad (9)$$

Here, V is the large but finite volume occupied by the scatterers and $2a$ is the largest dimension of the scatterer. Several models of $g(r)$ are available and are briefly outlined in *Varadan et al.* [1983]. The radial distribution functions obtained by using the self-consistent approximation which is a linear combination of the Percus-Yevick and Hypernetted Chain approximations seem to be good for a wide range of concentrations, and are also used in our computations here. It must be noted here, that our model assumes that although the particles are nonspherical with respect to an incident wave, statistically each particle is equivalent to a sphere of diameter equal to the largest diameter of the nonspherical particle.

Radio Science, Volume 19, Number 6, Pages 1445–1449, November–December 1984

Coherent electromagnetic wave propagation through randomly distributed and oriented pair-correlated dielectric scatterers

V. K. Varadan, Y. Ma, and V. V. Varadan

Wave Propagation Laboratory, Department of Engineering Science and Mechanics
Pennsylvania State University, University Park, Pennsylvania

(Received February 14, 1984; revised May 31, 1984; accepted May 31, 1984.)

Coherent attenuation of electromagnetic waves by randomly distributed and oriented pair-correlated dielectric scatterers is studied as a function of frequency and volume concentration of scatterers. Average frequency dependent dielectric properties are also studied. The results indicate that the attenuation and hence the effective properties differ considerably from those of aligned scatterers.

INTRODUCTION

In our earlier papers *Bringi et al.* [1982*a*, *b*], a multiple scattering formalism was given for the scattering and propagation of vector electromagnetic waves in a medium containing three-dimensional, identical, dielectric scatterers randomly distributed but having a single preferred orientation (aligned scatters). The extended integral equation or T-matrix method developed by Waterman (see for example *Varadan and Varadan* [1980]), in conjunction with suitable statistical averaging procedures and pair-correlation functions had been employed in such a study. Analytical dispersion relations were obtained at low frequencies in terms of the T-matrix of a single scatterer. At higher frequencies, numerical values of coherent attenuation and complex effective dielectric properties were presented for spheroidal scatterers for various concentrations when the incident wave propagated parallel to the minor axis of the scatterers. The computed results were found to be in good agreement with experimental findings of *Ishimaru and Kuga* [1982] as depicted in our paper [*Varadan et al.*, 1983]. We also cite the work of *Tsang and Kong* [1983] who have used exactly the same formalism for spherical scatterers.

In this paper, we extend the treatment to randomly oriented pair-correlated scatterers. For randomly distributed and oriented scatterers, two averages have to be performed, an ensemble average over the positions of the scatterers and the second an average on the T-matrix of a scatterer over orientations. Coherent attenuation is studied for dielectric scatterers in free space for different scatterer concentrations and range of frequencies. The results are compared with those obtained for aligned scatterers. At higher frequencies, the results indicate that there is a significant difference in phase velocity and attenuation between aligned and randomly oriented scatterers. Average frequency dependent properties are also presented in this study.

Paper number 4S0970.
0048-6604/84/004S-0970$08.00

OUTLINE OF THEORY

Consider an incident electromagnetic wave propagating along z direction in an infinite lossless, background (host) medium of ε_m, μ_0 containing a random distribution of identical randomly oriented N number of dielectric nonspherical scatterers of ε, μ_0 which are referred to a Cartesian coordinate system xyz. Let XYZ be the set of coordinate axes natural to the scatterer. For spheroidal scatterers, for example, the XYZ axes coincide with the symmetry axes of the spheroid.

The total electric field at any point in the host medium is the sum of incident field and the fields scattered by all the scatterers. The field that excites a given scatterer, (say, the ith scatterer), $\mathbf{E}_i^e$, however, is the incident field, $\mathbf{E}^{inc}$, plus the fields scattered from all the other scatterers, $\mathbf{E}_j^s$:

$$\mathbf{E}_i^e(\mathbf{r}) = \mathbf{E}^{inc}(\mathbf{r}) + \sum_{j \neq i}^{N} \mathbf{E}_j^s(\mathbf{r} - \mathbf{r}_j) \tag{1}$$

where $\mathbf{r}$ and $\mathbf{r}_j$ are position vectors of the observation point and the center of the jth scatterer, respectively. Expanding all the fields in terms of vector spherical functions as a basis and employing the translation theorem and the orthogonality of the basis functions,

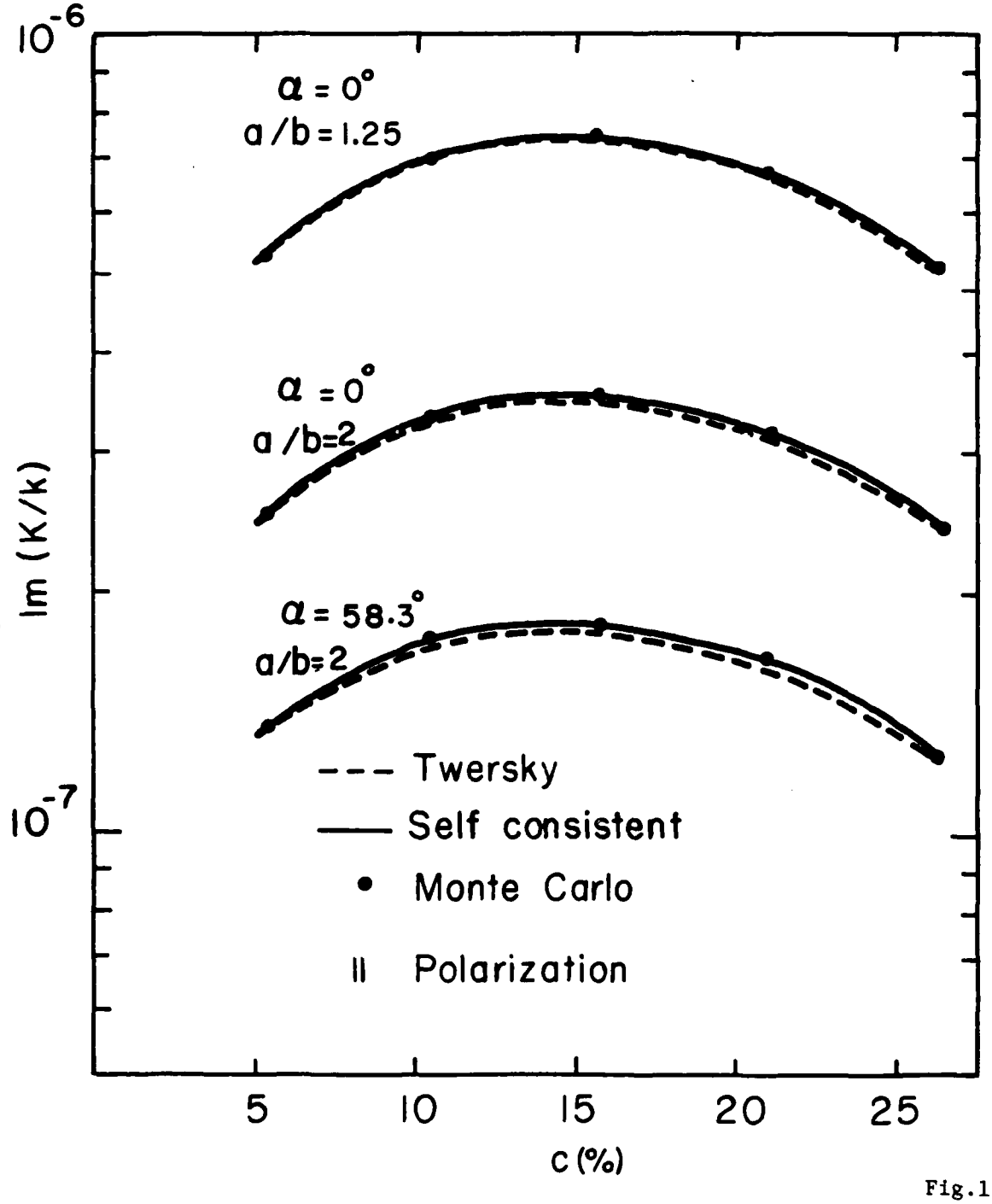
10^{-6}
10^{-7}
Im (K/k)
α = 0°
a/b = 1.25
α = 0°
a/b=2
α = 58.3°
a/b=2
--- Twersky
—— Self consistent
• Monte Carlo
II Polarization
5
10
15
20
25
c (%)

Fig.10

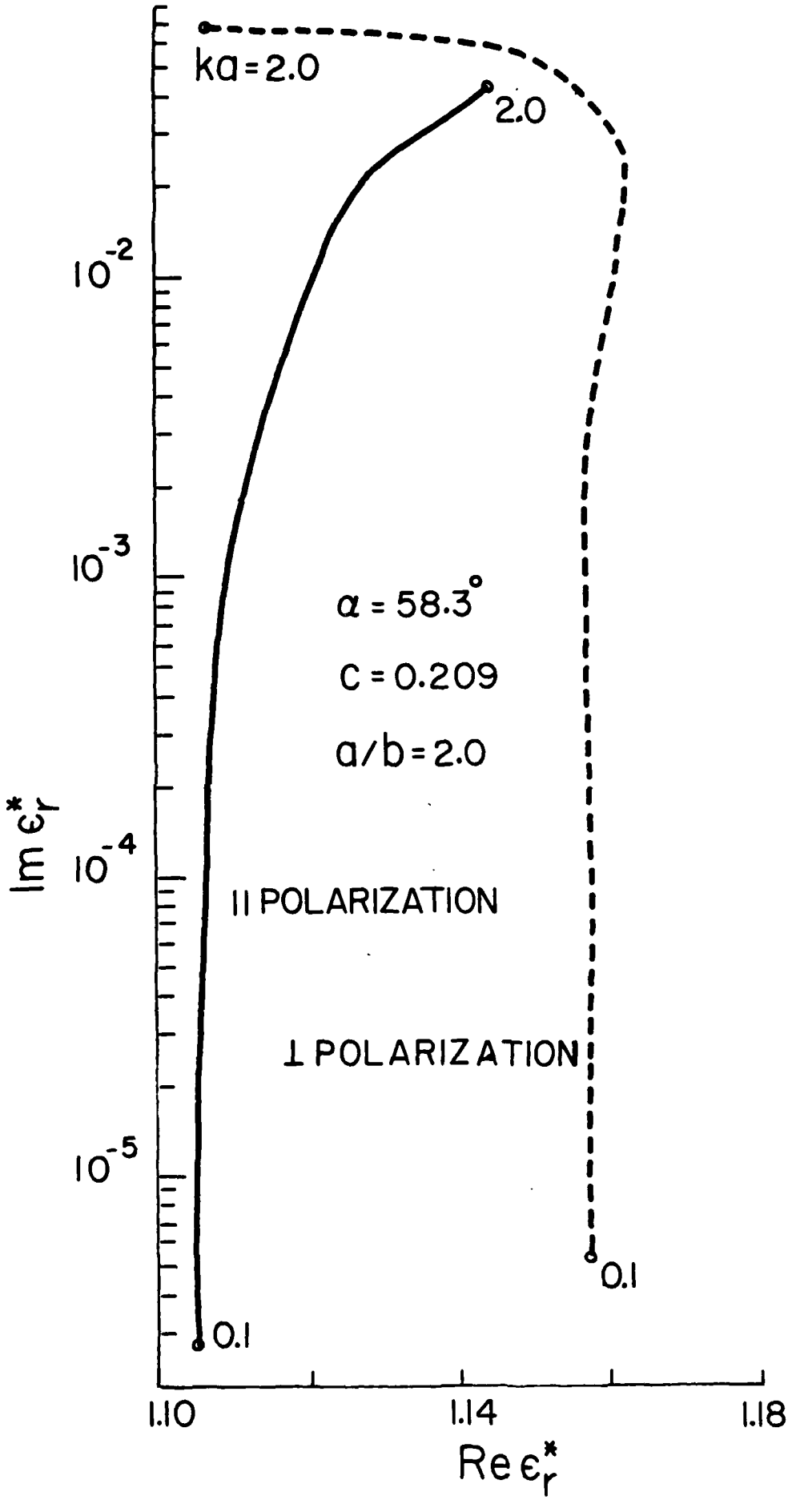
ka=2.0
2.0
10^{-2}
10^{-3}
10^{-4}
10^{-5}
$\alpha = 58.3^{\circ}$
c = 0.209
a/b = 2.0
II POLARIZATION
⊥ POLARIZATION
0.1
0.1
1.10
1.14
1.18
$\mathrm{Im}\,\epsilon_r^*$
$\mathrm{Re}\,\epsilon_r^*$

Fig.9

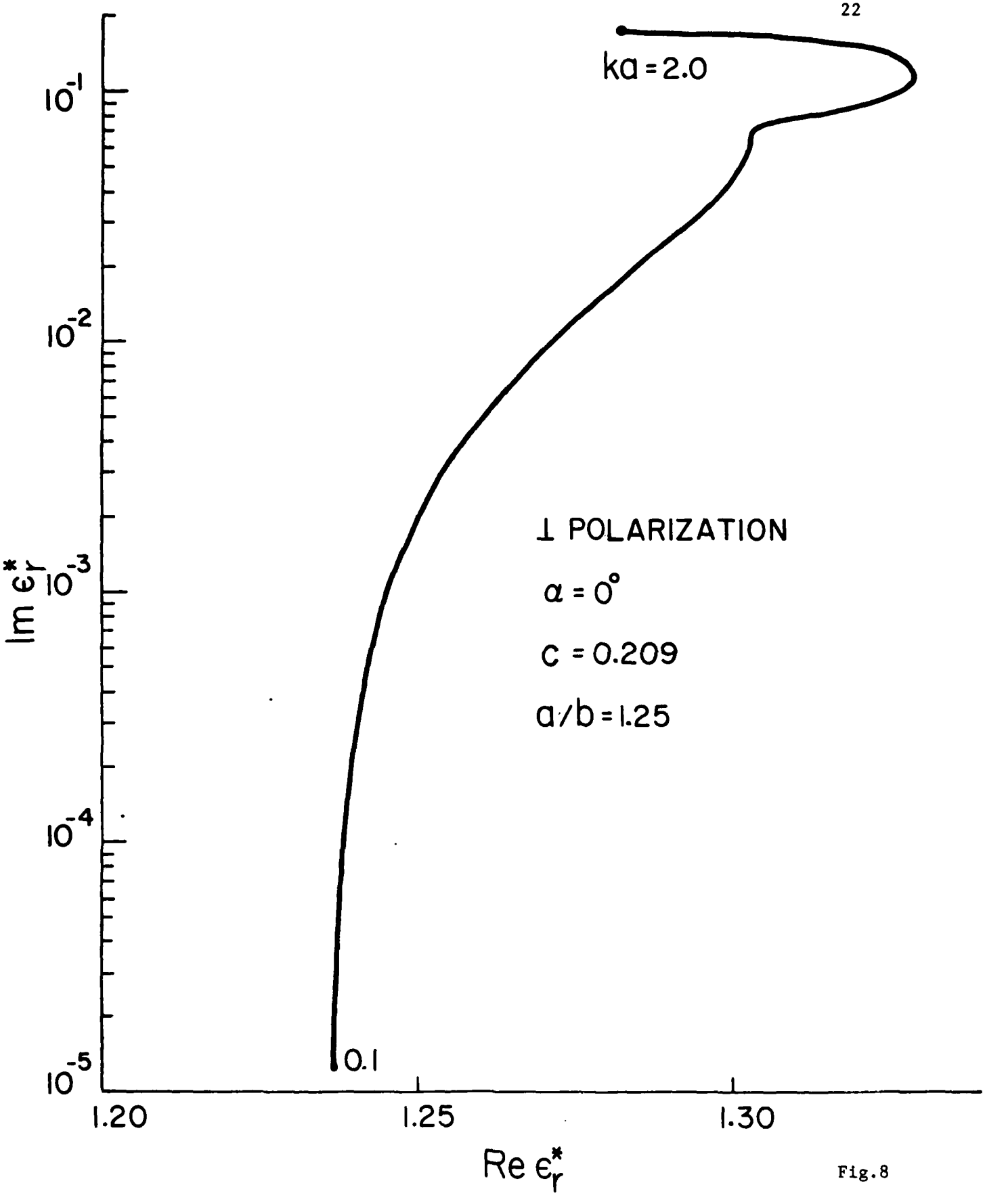
ka = 2.0
0.1
⊥ POLARIZATION
α = 0°
c = 0.209
a/b = 1.25
10^{-1}
10^{-2}
10^{-3}
10^{-4}
10^{-5}
Im ϵ_r^*
1.20
1.25
1.30
Re ϵ_r^*

Fig.8

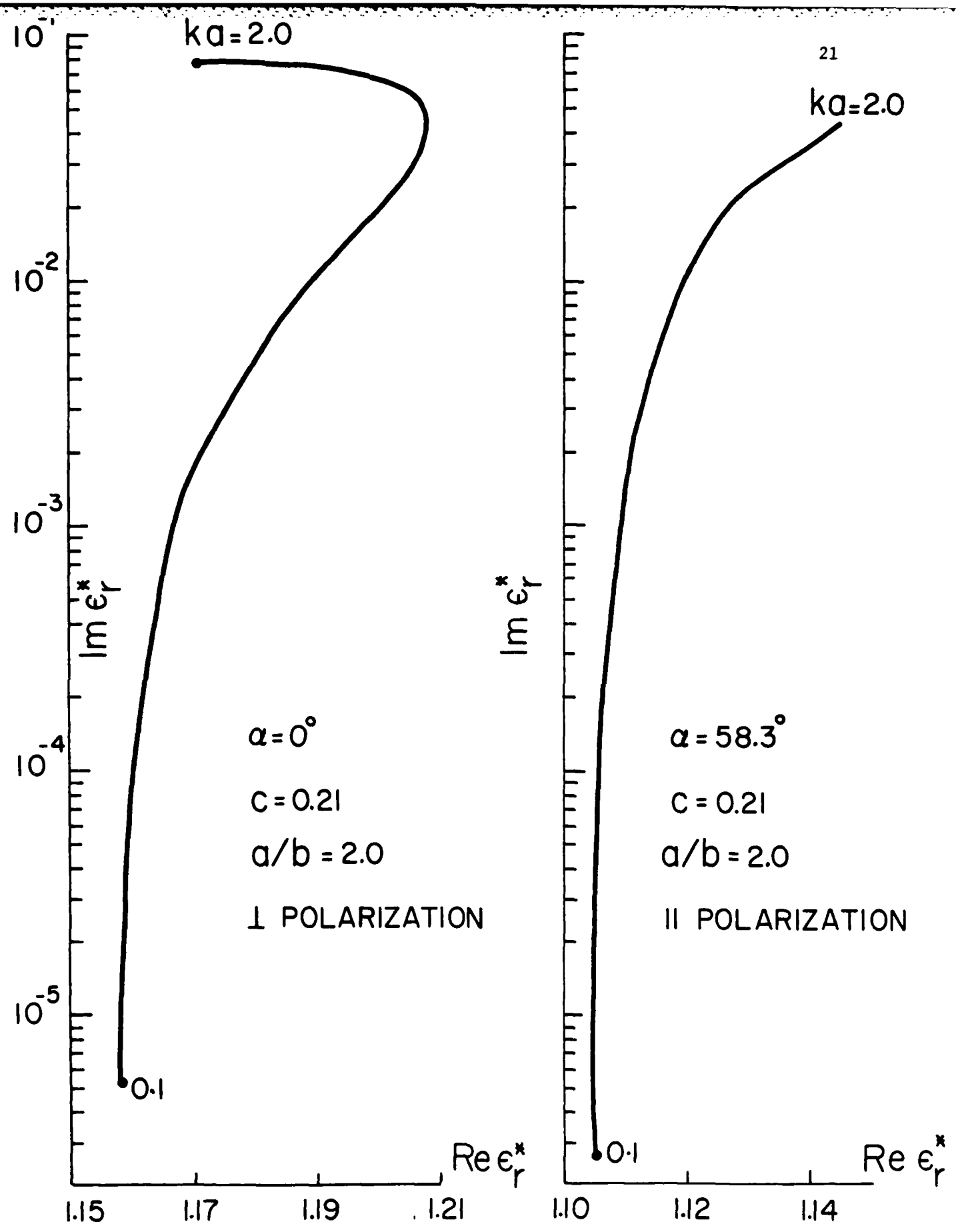
ka=2.0
10^{-1}
10^{-2}
10^{-3}
10^{-4}
10^{-5}
Im ϵ_r^*
α = 0°
c = 0.21
a/b = 2.0
⊥ POLARIZATION
0.1
Re ϵ_r^*
1.15
1.17
1.19
1.21
ka=2.0
Im ϵ_r^*
α = 58.3°
c = 0.21
a/b = 2.0
II POLARIZATION
0.1
Re ϵ_r^*
1.10
1.12
1.14

Fig.7

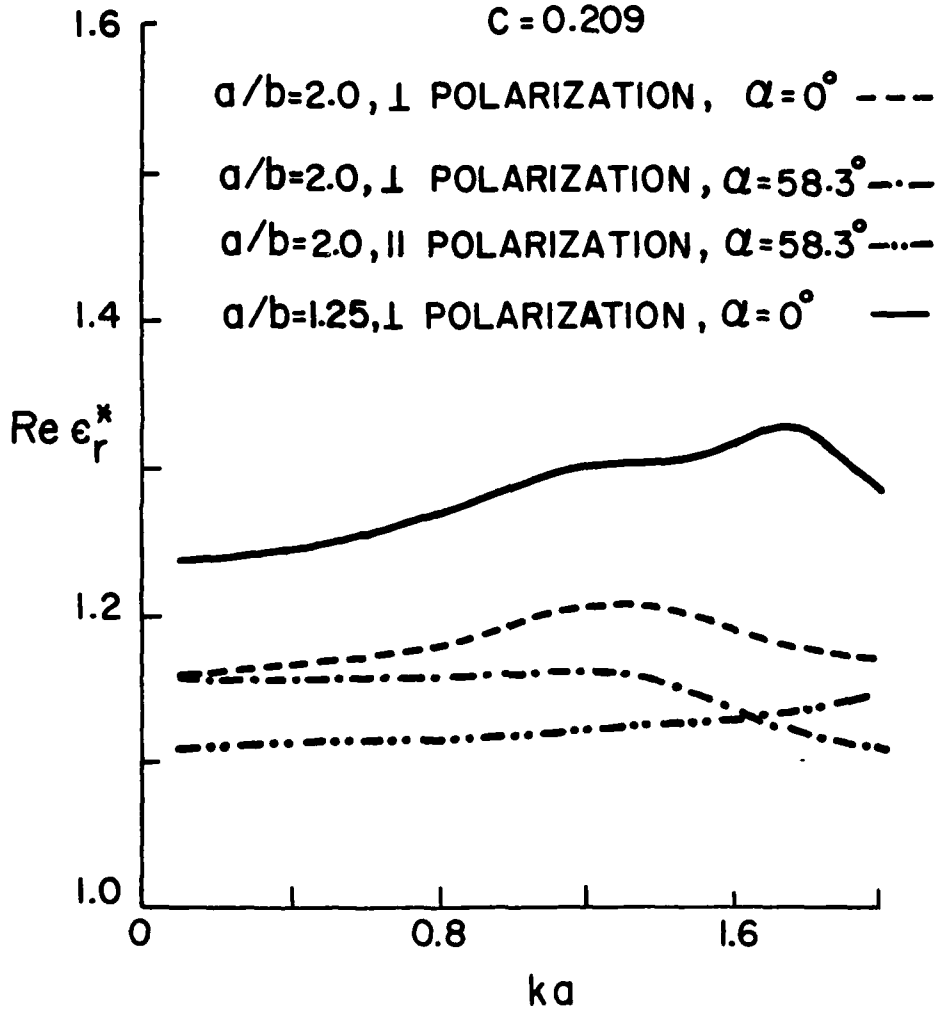
C = 0.209
a/b=2.0, ⊥ POLARIZATION, α=0°
a/b=2.0, ⊥ POLARIZATION, α=58.3°
a/b=2.0, II POLARIZATION, α=58.3°
a/b=1.25, ⊥ POLARIZATION, α=0°
Re ε*r
1.6
1.4
1.2
1.0
0
0.8
1.6
ka

Fig.6

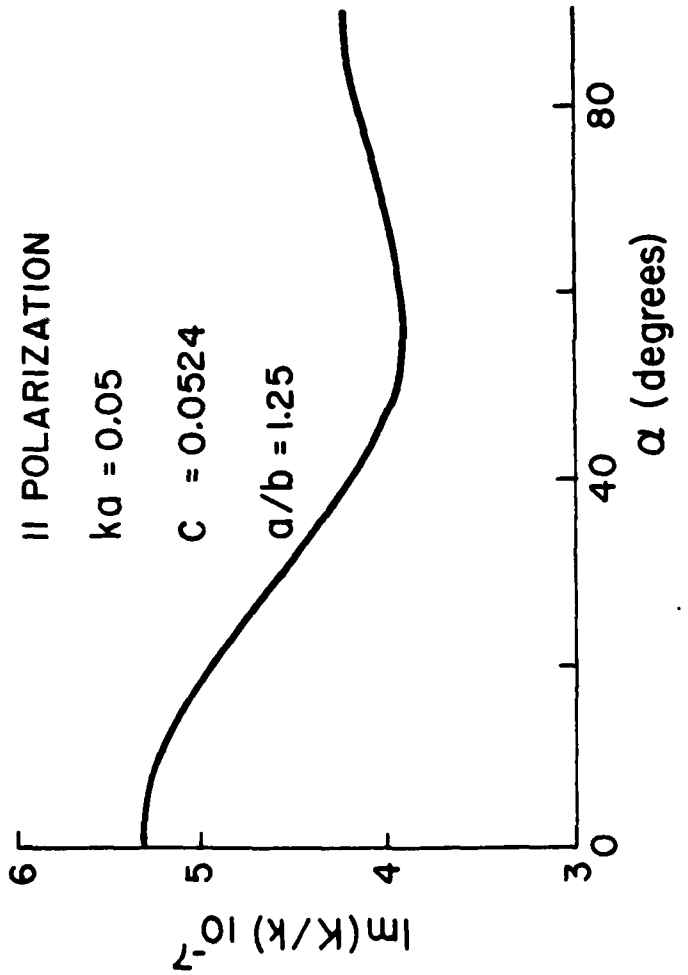
II POLARIZATION
ka = 0.05
c = 0.0524
a/b = 1.25
Im(K/k) 10^-7
6
5
4
3
0
40
80
α (degrees)

Fig.5

$$\alpha_n^i = a_n^i + \sum_{j\neq i} \sum_{n'} \sum_{n''} \sigma_{nn'}(\vec{r}_j - \vec{r}_i) \quad T_{n'n''}\alpha_{n''}^j \tag{8}$$

where

$$ou\psi_n(\vec{r}-\vec{r}_j) = \sum_{n'} \sigma^t_{nn'}(\vec{r}_j-\vec{r}_i) \quad Re\psi_{n'}(\vec{r}-\vec{r}_i) \tag{9}$$

and $\sigma_{nn'}$ is the translation matrix for spherical wavefunctions.

Equation (8) is averaged over the positions of the scatterers to yield an equation of the form

$$\langle\alpha_n^i\rangle_i = a_n^i + \sum_{j\neq i} \sum_{n'} \sum_{n''} T_{n'n''} \int \sigma_{nn'}(\vec{r}_j-\vec{r}_i) \langle\alpha_{n''}^j\rangle_{ij} \, p(\vec{r}_j \mid \vec{r}_i) d\vec{r}_j \tag{10}$$

where

$$a_n^i = a_n \, e^{ik\hat{k}_o\cdot\vec{r}_i},$$

$p(\vec{r}_j \mid \vec{r}_i)$ is the conditional probability distribution and $\langle\alpha_{n''}^j\rangle_{ij}$ is the conditional average of $\alpha_{n''}^j$ with the positions of both the i-th and j-th scatterers held fixed.

It is obvious that Eq. (10) results in an infinite heirarchy because $\langle\alpha_{n''}^j\rangle_{ij}$ is related to $\langle\alpha_n^k\rangle_{ijk}$ and so on. The QCA first invoked by Lax[2] and also independently by Twersky[3] simply states that

$$\langle\alpha_{n''}^j\rangle_{ij} \approx \langle\alpha_{n''}^j\rangle_j \tag{11}$$

i.e., the conditional expectation of α_n^j is independent of the position of the i-th scatterer. This would be an exact statement if the system was perfectly crystalline, because, in this case the position of every scatterer in the system is fixed and the neighborhood of every scatterer is the same. Twersky[3] has commented on the connection between the QCA and partial sums of the multiple scattering series. The QCA neglects back and forth scattering between a fixed pair of scatterers, thus in any term of the multiple scattering series, each scatterer appears only once and only two scatterers participate in a given scattering process, i.e. this would require only a knowledge of

two body correlations. In the next section we make this more clear by a diagrammatic representation of the multiple scattering series.

Substituting Eq. (11) in (10) and noting that

$$p(\vec{r}_j \mid \vec{r}_i)\begin{cases} = 0\,; \mid \vec{r}_j-\vec{r}_i \mid < 2a \\ = \frac{1}{V}\, g(\mid \vec{r}_{ij} \mid)\,; \mid \vec{r}_j-\vec{r}_i \mid = \mid \vec{r}_{ij} \mid \geq 2a \end{cases} \tag{12}$$

we obtain

$$\langle \alpha_n^i \rangle_i = a_n^i + n_o\, T_{n'n''} \int_{V-v} \sigma_{nn'}(\vec{r}_{ij}) \langle \alpha_{n''}^j \rangle_j \; g(\mid \vec{r}_{ij} \mid)\, d\vec{r}_j \tag{13}$$

In Eq. (12), $g(x)$ is the radial distribution function assuming spherically symmetric statistics even for non spherical particles, i.e. the exclusion volume of the impenetrable particles is assumed to be spherical. In Eq. (13), the summation convention is used, and if the particles are identical $\Sigma_j' = N-1 \approx N$ when N is large and v is the exclusion volume equal to $4\pi(2a)^3/3$.

We now assume that the average field in the medium is a plane wave propagating in the direction $\hat{k}_o$ of the original plane wave in the host medium, however, the average field propagates in an effective or average medium which is homogeneous and characterized by an effective propagation constant $K = K_1 + iK_2$ which is complex and frequency dependent. Thus

$$\langle \alpha_n^i \rangle_i = X_n\, e^{iK\hat{k}_o \cdot \vec{r}_i} \tag{14}$$

and Eq. (13) can hence be written as

$$\begin{aligned} X_n e^{iK\hat{k}_o \cdot \vec{r}_i} = A_n e^{ik\hat{k}_o \cdot \vec{r}_i} + n_o T_{n'n''} X_{n''} e^{iK\hat{k}_o \cdot \vec{r}_i} \{ & \int_{V-v} \sigma_{nn'}(\vec{r}_{ij}) e^{iK\hat{k}_o \cdot \vec{r}_{ji}} d\vec{r}_j \\ & + X_n \int_{V-v} \sigma_{nn'}(\vec{r}_{ij}) e^{iK\hat{k}_o \cdot \vec{r}_{ji}} [g(\mid \vec{r}_{ij} \mid)-1]\, d\vec{r}_j \} \end{aligned} \tag{15}$$

The second term on the RHS of Eq. (15) can be converted into a surface integral using the divergence theorem and surface integral on S_∞, which defines the boundary of the system, cancels the incident wave term on the RHS of Eq. (15). Thus Eq. (15) simplifies to

$$X_n = n_o T_{n'n''} X_{n''} \sum_{\lambda=|\ell-\ell'|}^{\ell+\ell'} D_{nn'}(\lambda)[2kaj_\lambda(2Ka)h'_\lambda(2ka)-2Kaj'_\lambda(2Ka)h_\lambda(2ka)]$$
$$+ \int_{V-v} [g(x)-1]j_\lambda(Kx)\, h_\lambda(kx)x^2 dx \qquad (16)$$

where $D_{nn'}(\lambda)$ is the vestige of the translation matrix after the spatial and angular parts have been absorbed in the integration. Different expressions result depending on whether we are discussing acoustic, electromagnetic or elastic wave propagation. Equation (16) can be rewritten as

$$(\delta_{nn'} - M_{nn'})\, X_{n'} = 0 \qquad (17)$$

The dispersion equation for the effective medium is then simply

$$|\, \delta_{nn'} - M_{nn'} \,|(k,K,n_o,v,T,g) = 0 \qquad (18)$$

which depends on $k=\omega/c$, the effective wavenumber K, the number density n_o, the exclusion volume v, the T-matrix or the scatterer characteristics and a model for the radial distribution function. By assuming values for all variables but K, the determinantal equation can be solved numerically to yield the value of the effective propagation constant.

MULTIPLE SCATTERING SERIES

If we substitute Eqs. (8) in (5) and then(1) and iterate we obtain the following:

$$u^{tot}(\vec{r})=u^{o}(\vec{r})+\sum_{i} ou\psi_{n}(\vec{r}-\vec{r}_{i})T_{nn'}a^{i}_{n'} + \sum_{ij}{}' \Sigma' ou\psi_{n}(\vec{r}-\vec{r}_{i})T_{nn'}\sigma_{n'n''}(\vec{r}_{ij})T_{n''n'''}a^{j}_{n'''}$$

$$+ \sum_{ij\ k}{}' \Sigma' \Sigma' ou\psi_{n}(\vec{r}-\vec{r}_{i})T_{nn'} - - - - + - - - - \qquad (19)$$

Equation (19 can be averaged over the positions of the particles to yield

$$\langle u^{tot}(\vec{r})\rangle = u^{o}(\vec{r}) + \sum_{i} T_{nn'} \int ou\psi_{n}(\vec{r}-\vec{r}_{i})a^{i}_{n}p(\vec{r}_{i})d\vec{r}_{i}$$

$$+ \sum_{ij}{}' \Sigma' T_{nn'}T_{n''n'''} \int ou\psi_{n}(\vec{r}-\vec{r}_{i})\sigma_{n'n''}(\vec{r}_{ij})\, a^{j}_{n''}\, p(\vec{r}_{i})\, p(\vec{r}_{j}\,|\,\vec{r}_{i})d\vec{r}_{j}d\vec{r}_{i} \qquad (20)$$

$$+ - - - -$$

We note that Eq. (20) involves all orders of joint probability functions. Each term in Eq. (20) represents beginning with the second term, scattering from one inhomogeneity, at a time scattering from two inhomogeneities at a time etc. We note that sums of the form $\sum_{ij\ k}{}' \Sigma' \Sigma'$ involve the selection of three particles at a time from N particles, the prime on $\sum_{j}{}'$ indicates $j \neq i$, Σ' indicates $k \neq j$ but $k = i$ is permitted, i.e. particle 'i' can participate in the 3 body process more than once. Thus the three body process can include any number of scattering in any order between the three objects.

Equation (20) can be rewritten in a different manner, defining the T-matrix of 2, 3, 4 etc. particle configurations. Denoting by T(2), T(3), T(4), etc. the T-matrix of 2, 3, 4 particle configurations we get

$$\langle u^{tot}(\vec{r})\rangle = u^{o}(r) + N\int ou\psi(\vec{r}-\vec{r}')\ T(1)\,a'\,p(\vec{r}_1)d\vec{r}_1$$

$$+ \frac{N(N-1)}{2}\int ou\psi(\vec{r}-\vec{r}')\ T\ (2)\ a'\ p(1,2)d\vec{r}_1 d\vec{r}_2 \qquad (21)$$

$$+ \frac{N(N-1)(N-2)}{3!}\int ou\psi(\vec{r}-\vec{r}')T\ (3)a'p(1,2,3)d\vec{r}_1 d\vec{r}_2 d\vec{r}_3$$

$$+ - - - -$$

where r' denotes the common origin for the multiple object configuration p(1,2,3...) are joint probability functions. We must note that in Eq. (21), the T-matrices must be included under the integral sign unlike Eq. (20) because T(2), T(3) etc. depend explicitly upon the relative position of the particles.

To solve Eq. (20) or (21) is a formidable task and it is not surprising that the QCA was introduced at an early stage by Lax[1] and Twersky[3]. To show the connection between Eq. (20) and Eq. (16) we now place some severe restrictions on the allowed multiple scattering processes. First of all we require that each particle can contribute only once to any term of the multiple scattering series. Further we do not permit any back and forth scattering between a pair of scatterers. Finally only two body correlations are permitted so that the restricted form of Eq. (20) can be represented diagrammatically as

$\langle u^{tot}(\vec{r})\rangle = u^{o}(\vec{r}) +$ 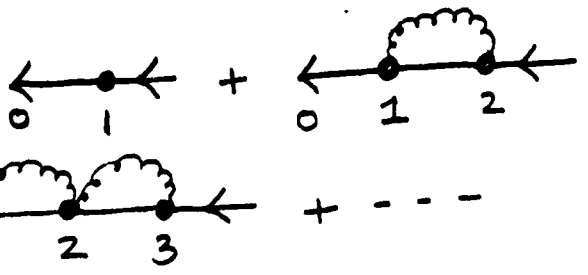

(22)

where ← denotes the incident plane wave, • denotes a scatterer,  denotes scattering from particle 2 to particle 1,  denotes the correlation

between the positions of particles 1 and 2 and finally $\overset{0}{\bullet}\!\!\leftarrow\!\!\overset{1}{\bullet}$ denotes the propagation from particle 1 to the observation point $\vec{r}$. In equation (22) $\bullet\!\leftarrow$ will be replaced by a_n, each $\bullet\!\!<$ will be replaced by $T\sigma T$ where σ the translation matrix accounts for the propagation of waves from one scatterer to another and $\overset{1}{\bullet}\!\frown\!\overset{2}{\bullet}$ will be replaced by p(1,2). Hence the explicit form of Eq. (22) is then

$$\begin{aligned}
\langle u^{tot}(\vec{r})\rangle &= u^{o}(\vec{r}) + N\int ou\psi(r-r_1)Ta^{1}p(r_1)d\vec{r}_1 \\
&+ N^2\int ou\psi(r-r_1)T\sigma(r_{12})Ta^{2}p(1,2)dr_1dr_2 \\
&+ N^3\int ou\psi(r-r_1)T\sigma(r_{12})p(1,2)T\sigma(r_{23})p(2,3) \\
&\qquad Ta^{3}\,dr_1dr_2dr_3 \qquad (23) \\
&+ N^4\int ou\psi(r-r_1)T\sigma(r_{12})p(1,2)T\sigma(r_{23})p(2,3)T \\
&\qquad \sigma(r_{34})p(3,4)Ta^{4}dr_1..dr_4 \\
&+ - - -
\end{aligned}$$

In Eq. (23), we have removed the restrictions in sums like $\sum_{ij}\sum'_{k}\Sigma'$ etc. by noting that p(1,2) is automatically zero if $r_2=r_1$. Any inaccuracies introduced by this procedure becomes smaller as $N \to \infty$. For spherical statistics, we note that

$$p(r_1)=\frac{1}{V}\,; \quad p(1,2) = p(r_1,r_2) = \frac{1}{V}\,g(|r_1-r_2|)$$

We now introduce spatial fourier transforms of the translation matrix and the radial distribution functions and denote them by $\bar{\sigma}(k)$ and $\bar{g}(k)$ respectively. Using the convolution theorem, Eq. (23) can be simplified to

$$\langle u^{tot}(r)\rangle = u^{o}(r)+n_{o}\int ou\psi(\vec{r}-\vec{r}_{1})T\{1 + n_{o}\overline{\sigma g(\vec{K})}\ T+n_{o}^{2}\overline{\sigma g(\vec{K})}T\overline{\sigma g(\vec{K})}T \tag{24}$$

$$+ n_{o}^{3}\overline{\sigma g(\vec{K})}T\overline{\sigma g(\vec{K})}T\overline{\sigma g(\vec{K})}T \ + - - - \} \ e^{iK\hat{k}_{o}\cdot(\vec{r}_{1}-\vec{r}_{2})}a^{2}d\vec{K}d\vec{r}_{1}d\vec{r}_{2}$$

where

$$\overline{\sigma g(\vec{K})} = \int \sigma(\vec{x})g(|\vec{x}|)e^{i\vec{K}\cdot\vec{x}}d\vec{x} \tag{25}$$

The terms on the RHS of Eq. (24) can be summed formally and we can rewrite Eq. (24) as

$$\langle u^{tot}(\vec{r})\rangle = u^{o}(\vec{r}) + ou\psi_{n}(\vec{r}-\vec{r}_{1})T_{nn'} \tag{26}$$

$$n_{o}\int \{1-n_{o}\overline{\sigma g}(\vec{K})T\}^{-1} \ e^{i\vec{K}\cdot(\vec{r}_{1}-\vec{r}_{2})}a_{n''}^{2}\,d\vec{K}d\vec{r}_{1}d\vec{r}_{2}$$

This new form of the average field can be interpreted as an incident plane wave propagating through an effective medium of propagation constant K and propagator $\{1-\overline{\sigma g}T\}^{-1}$ undergoing scattering from a particle at r_1 and then propagating to the observation point r with the wavenumber of the host medium. In Eq. (26) we note that

$$e^{iK\cdot(\vec{r}_{1}-\vec{r}_{2})}a_{n''}^{2} = e^{i\vec{K}\cdot\vec{r}_{1}}a_{n''}$$

so that if

$$\{1 - n_{o}\overline{\sigma g}T\}^{-1}(\vec{K}) = \bar{H}(\vec{K}) \tag{27}$$

then

$$\langle u^{tot}(\vec{r})\rangle = u^{o} + n_{o}\int ou\psi_{n}(\vec{r}-\vec{r}')\ T_{nn'}\bar{H}_{n'n''}(\vec{r}'')a_{n''}d\vec{r}'$$

The dispersion equation in the model medium are given by the zeroes of $\bar{H}$ (K) which yields the effective propagation constant of the medium. We recall that the propagator in the host medium has a Fourier transform of the form $1/(k^2-\omega^2/c^2)$ which has a pole at $k=\omega/c$. The poles of the new propagator

are then determined by the roots of the determinantal equation

$$| 1-n_o\overline{\sigma g}\ (K)T | = 0. \tag{28}$$

We observe that Eq. (28) and Eq. (18) are identical since

$$M_{nn'}(k,K,n_o,\ v,\ T,\ g) = n_o\ \overline{\sigma_{nn''}g}(K)\ T_{n''n'} \tag{29}$$

Thus the QCA is exactly equivalent to summing the class of multiple scattering diagrams denoted in Eq. (22). This has also been qualitatively discussed by Twersky[3]. We can now proceed to improve the QCA. Since we are somewhat limited in our knowledge of the higher order correlation functions at the moment we will restrict ourselves to improvements that do not require knowledge of higher order correlations.

We start with Eq. (21), which is a multiple scattering series written in terms of the T-matrix of clusters of particles which are then averaged over the positions and relative spacing of the particles in the cluster. We begin by noting that T(2), the T-matrix of a two particle configuration depends only on the relative position of the two particles and takes the form, (see Peterson and Strom[18])

$$T(2) = \mathrm{Re}[\sigma(\vec{\rho}_1)]\{T[1 - \sigma\ (\vec{\rho}_2-\vec{\rho}_1)T\sigma(\vec{\rho}_1-\vec{\rho}_2)T]^{-1}[1+\sigma(\vec{\rho}_2-\vec{\rho}_1)T\mathrm{Re}(\sigma(\vec{\rho}_1-\vec{\rho}_2))]$$

$$\mathrm{Re}(\sigma(-\vec{\rho}_1)) \ +\ \{1\leftrightarrow 2\} \tag{30}$$

where the second term is obtained by interchanging $\vec{\rho}_1$ and $\vec{\rho}_2$, $\vec{\rho}_1$, $\vec{\rho}_2$ are the positions of the two particles relative to a common origin which is located at $\vec{r}'$ i.e., $\vec{r}_i = \vec{r}' + \vec{\rho}_i$, i = 1, 2.

Terms of the form $(1-\sigma T\sigma T)^{-1}$ denote repeated back and forth scattering between particles 1 and 2. In addition to other more complicated terms,

these 'ping-pong' terms are explicitly neglected by the QCA. The QCA can be improved by including these terms in the multiple scattering series. The price is not too great to pay since only a knowledge of two particle correlations is still required.

The 3-body T-matrix must be simplified as follows:

$$T(3) = T(1,2,3) = T(1,2)\, T(2,3) \tag{31}$$

We note that we have neglected terms of the form T(1,3) since particles 1 and 3 would appear out of order in the chain and hence prevent us from summing the series using convolution techniques. The 3-body joint probability function is approximated as follows:

$$p(1,2,3) \approx p(1)p(2|1)p(3|2) \tag{32}$$

which we note is different from Kirkwood's superposition approximation for the 3-body correlation function.

Using Eqs. (31) and (32) and similar approximations for the higher order terms, Eq. (21) can be written as

$$\begin{aligned}\langle u^{tot}(\vec{r}_o)\rangle &= u^o + N\int ou\psi(0,1)Ta'p(1)dr_1 \\ &+N^2\int ou\psi(0,1)T\ \sigma(1,2)T\ [1-\sigma(2,1)T\ \sigma(1,2)T]^{-1}\ p(1)\ a^2\ p(2|1)\ dr_1 dr_2 \\ &+N^3\int ou\psi(0,1)T\ \sigma(1,2)T\ [1-\sigma(2,1)T\ \sigma(1,2)T]^{-1}\ \sigma(2,3)T \\ &\qquad [1-\sigma(3,2)T\sigma(2,3)T]^{-1}\ a^3\ p(1)\ p(2|1)\ p(3|2)\ dr_1\ dr_2\ dr_3 \\ &+ - - - - -\end{aligned} \tag{33}$$

Let

$$T(1,2) = \sigma(1,2)T\ [1-\sigma(2,1)T\sigma(1,2)T]^{-1}$$

which is a function of $\vec{r}_1$ $\vec{r}_2$ only.

We denote by

$$n_o\ \overline{T(1,2)\ g(2|1)}\ (k) = N\int T(1,2)p(2|1)e^{i\vec{k}\cdot(\vec{r}_1-\vec{r}_2)}\, d(\vec{r}_2-\vec{r}_1) \tag{34}$$

then

$$\langle u^{tot}(\vec{r}\bullet)\rangle = u^{o} + \int ou\psi(0,1)T\,[1 - n_{o}\overline{T(1,2)g}]^{-1}(K) \qquad (35)$$
$$e^{i\vec{k}\bullet(\vec{r}_1-\vec{r}_2)}\ a^2 d\vec{r}_1\ d\vec{r}_2\ d\vec{K}$$

The major difference between Eq. (26) and Eq. (35) is that $\sigma(1,2)T$ has been replaced by $\sigma(1,2)T[1-\sigma(2,1)T\sigma(1,2)T]^{-1}$. The hole correction integral is not as simple as before since a complicated matrix inverse also enters the integrand. The propagation constant for this improved version of the effective medium are determined by the zeroes of

$$|\ 1 - n_{o}\overline{T(1,2)g}(k)\ | = 0 \qquad (36)$$

CONCLUSION

In this paper we have shown that the QCA is a partial resummation of the multiple scattering series that omits back and forth scattering between fixed pairs of scatterers. An expression for the propagation in such a medium is derived whose poles are the same as those obtained by solving the roots of the determinental equations obtained invoking the QCA.

The difference between Eq. (28) and Eq. (36) can only be tested by actual computation of the effective wave-number for a given system. The QCA has already met with much success in explaining the experimentally measured attenuation of electromagnetic waves for a distribution of latex spheres in water for concentration up to 40% and wavelengths comparable to scatterer size. It may be reasonably asked if any improvements can be achieved by including additional multiple scattering processes as in Eq. (36). A logical way to answer this before implementing improvements on the QCA in the multiple scattering algorithm is to study electromagnetic scattering from a fixed pair of scatterers as a function of frequency varying the distance between the scatterers and the material properties of the scatterers with respect to the host. This will give us important insight as to the importance of such processes in wave propagation in random media.

Acknowledgement: This work was supported by the Army Research Office under Contract No. DAAG29-83-K-0097.

REFERENCES

1. M. Lax, "Multiple Scattering of Waves II. The Effective Field in Dense Systems", Phys. Rev. 85, p. 621-629, (1952).

2. L. L. Foldy, "The Multiple Scattering of Waves", Phys. Rev. 67, p. 107-119, (1945).

3. V. Twersky, "On Propagation in Random Media of Discrete Scatterers", Proc. Sympos. Appl. Math., 16, p. 84-116 (Providence, R.I., Amer. Math. Society, 1964).

4. V. Twersky, "Multiple Scattering by Arbitrary Configurations in Three Dimensions", J. Math. Phys. 3, p. 83-91, (1962).

5. V. Twersky, "Multiple Scattering of Electromagnetic Waves by Arbitrary Configurations", J. Math. Phys. 8, p. 589-610, (1967).

6. V. Twersky, "Coherent Scalar Field in Pair-correlated Random Distributions of Aligned Scatterers", J. Math. Phys. 18, p. 2468-2486, (1977).

7. V. Twersky, "Coherent Electromagnetic Waves in Pair-correlated Random Distributions of Aligned Scatterers", J. Math. Phys. 19, p. 215-230, (1978).

8. V. Twersky, "Constraint on the Compound Depolarization Factor of Aligned Ellipsoids", J. Math. Phys. 19, p. 2576-2578, (1978).

9. V. Twersky, "Scattering Theory and Diagnostic Applications" in "Multiple Scattering and Waves in Random Media" edited by P. L. Chow, W. E. Kohler and G. C. Papanicolaou, North Holland, p. 267-285, (1981).

10. V. Twersky, "Propagation and Attenuation in Composite Media" in "Macroscopic Properties of Disordered Media" edited by R. Burridge, S. Childress and G. C. Papanicolaou, Spring-Verlag, p. 258-271, (1982).

11. D. J. Vezzetti and J. B. Keller, "Refractive Index, Attenuation, Dielectric Constant and Permeability for Waves in a Polarizable Medium", J. Math. Phys. 8, p. 1861-1870, (1967).

12. D. Bedeaux and P. Mazur, "On the Critical Behaviour of the Dielectric Constant for a Nonpolar Fluid", Physics 67, p. 23-54, (1973).

13. V. N. Bringi, T. A. Seliga, V. K. Varadan and V. V. Varadan, "Bulk Propagation Characteristics of Discrete Random Media" in "Multiple Scattering and Waves in Random Media" edited by P. L. Chow, W. E. Kohler and G. C. Papanicolaou, North-Holland, p. 43-75, (1981).

14. V. V. Varadan, V. N. Bringi and V. K. Varadan, "Frequency Dependent Dielectric Constants of Discrete Random Media" in "Macroscopic Properties of Disordered Media" edited by R. Burridge, S. Childress and G. C. Papanicolaou, Springer-Verlag, p. 272-284, (1982).

15. V. N. Bringi, V. V. Varadan and V. K. Varadan, "Coherent Wave Attenuation by a Random Distribution of Particles", Radio Science, 17, p. 946-952, (1982).

16. V. N. Bringi, V. K. Varadan and V. V. Varadan, "Average Dielectric Properties of Discrete Random Media Using Multiple Scattering Theory", IEEE Trans. AP-31, p. 371-375, (1983).

17. V. K. Varadan, V. N. Bringi, V. V. Varadan and A. Ishimaru, "Multiple Scattering Theory for Waves in Discrete Random Media and Comparison with Experiments", Radio Science 18, p. 321-327, (1983).

18. B. Peterson and S. Strom, "T-Matrix for Electromagnetic Scattering from an Arbitrary Number of Scatterers with Continuously Varying Electromagnetic Properties", Phys. Rev. D 8, p. 3661, (1973).

MULTIPLE SCATTERING OF WAVES IN DISCRETE RANDOM MEDIA BY METHOD OF SPATIAL STOCHASTIC SYSTEMS

K. C. Liu, V. V. Varadan, and V. K. Varadan

Department of Engineering Sciences and Mechanics
and Graduate Program in Acoustics
The Pennsylvania State University
University Park, PA 16802

pace Cross Correlation Function of Successive Scattered Fields

ross Correlation

Consider two sequences of scatterers $\{j_1,j_2,\ldots,j_m\}$ and $\{k_1,k_2,\ldots,k_n\}$, hich do not overlap each other, and do not repeat in each series, i.e. no ny pair among $j_1,\ldots j_m,k_1,\ldots,k_n$ is equal. The space cross correlation unction of the successive scattered fields $p_{j1\cdots jm}(4)$ and $p_{kl\ldots kn}(r)$ s defined by

$$K^{k_1\ldots k_n}_{j_1\cdots j_m}(r_1,r_2) = \mathcal{E}\{\rho_{j_1\ldots j_m}(r_1)\rho_{k_1\ldots k_n}(r_2)\} \tag{5.1}$$

here $\mathcal{E}$ is the mathematic expectation operator.

Let $S_{j_1},S_{j_2},\ldots,S_{j_m}$ be the regions occupied by $j_1^{th},j_2^{th},\ldots,j_m$ catterers with mass center at origin, respectively. Thenwith rather high ccuracy we can make the following approximation

$$\psi(\rho_{j_1}+r') = \psi(\rho_{j_1})e^{-ik(\rho_{j_1})\,r'}\,,\quad \rho\, r'\varepsilon\, S_{j_1} \tag{5.3}$$

$$\Gamma(\rho_{j_{i+1}}-\rho_{j_i}+r_i',\, k_i,\, \theta_{j_i}) = \Gamma(\rho_{j_{i+1}}-\rho_{j_i},k_i,\theta_{j_i})e^{-ik\frac{\rho_{j1+1}-\rho_{ji}}{|\rho_{ji+1}-\rho_{ji}|}\,r_i'}$$

$$r_i'\,\varepsilon\, S_{j_{i+1}},\quad i=1,2,\ldots,m. \tag{5.4}$$

Then (3.15) can be simplified to

$$P_{j_1\cdots j_m}(r_m) = \psi(\rho_{j_1})\,\Gamma(\rho_{i_2}-\rho_{i_1},k(\rho_{j_1}),\theta_{j_1})\,\Gamma(\rho_{j_3}-\rho_{j_2},\, k\frac{\rho_{j2}-\rho_{j1}}{|\rho_{j_2}-\rho_{j_1}|},\,\theta_{j_2})$$

$$\Gamma(\rho_{i_4}-\rho_{j_3},k\frac{\rho_{j3}-\rho_{j2}}{|\rho_{j3}-\rho_{j2}|}\,,\,\theta_{j_3})\ldots\Gamma(\rho_{j_m}-\rho_{j_{m-1}},\,k\frac{\rho_{jm-1}-\rho_{jm-2}}{|\rho_{j_{m-1}}-\rho_{jm-2}|},\,\theta_{j_{m-1}}) \tag{5.5}$$

$$\Gamma(r_m-\rho_{jm},\,k\frac{\rho_{jm}-\rho_{jm-1}}{|\rho_{jm}-\rho_{jm-1}|}\,,\,\theta_{jm})$$

If we note that

$$\bigcap_{k=1}^{n-i} D^c_{\rho_{i+k}}(\theta_i,\theta_{i+k}) = R_3 \qquad \text{when } i=n. \tag{4.20}$$

Figure 7 shows the case of i=n-3. The shaded area denotes the region

$$\bigcap_{k=1}^{n-i} D^c_{\rho_{i+k}}(\theta_i,\theta_{i+k})$$

It can be proved that if any one of the following conditions

1 $\sigma_m << a$, where σ_m is the maximum deviation of the surface of each scatterer with a spherical surface, which encloses the same volume as a single scatterer, a is the radius of this sphere.

2 $V\gamma_m << 1$, where V is the volume of a single scatterer, $\gamma_m = \max\{\gamma(\rho), \rho \varepsilon R_3\}$~

3 $\sigma_\theta << 11$, where σ is the standard deviation of random vector θ_j:

$$\sigma_\theta = [\mathcal{E}\{|\theta_j - \mathcal{E}[\theta_j]|^2\}]^{1/2} \tag{4.21}$$

is satisfied, then (4.19) can be simplified to

$$f(\rho_1,\ldots,\rho_n, \theta_1,\ldots,\theta_n) = \prod_{i=1}^{n} f_\theta(\theta_i) \frac{\gamma(\rho_i)}{N-(n-i)} X(\rho_i, \bigcap_{k=1}^{n-i} \overline{D}^c_{\rho_{i+k}}), \tag{4.22}$$

where $\overline{D}_{\rho_{i+k}}$ is the mathematical expectation of $D\rho_{i+k}(\theta_i, \theta_{i+k})$ as defined by a similar expression as (4.14). The conditions 1, 2 and 3 mean that respectively:

1. the shape of each scatterer closes to sphere,
2. the scatterers in space are not very dense, and
3. all the scatterers have about the same orientation.

It should be noticed that, equation (4.22) holds as long as only one of these conditions is satisfied. It, however, does not require all of them are satisfied.

Again, as in Part II[2], it can be proved that

$$f_{n-2}(\rho_{n-2}|\rho_{n-1},\rho_n,\theta_{n-2},\theta_{n-1},\theta_n)$$

$$= \begin{cases} \dfrac{\gamma(\rho_{n-2})}{N-2}, & \rho_{n-2} \in [D_{\rho_{n-1}}(\theta_{n-2},\theta_{n-1}) \cup D_{\rho_n}(\theta_{n-2},\theta_n)]^c \\ 0 & \rho_{n-2} \in D_{\rho_{n-1}}(\theta_{n-2},\theta_{n-1}) \cup D_{\rho_n}(\theta_{n-2}\ \theta_n), \end{cases} \tag{4.15}$$

or

$$f_{n-2}(\rho_{n-2}|\rho_{n-1},\rho_n,\theta_{n-2},\theta_{n-1},\theta_n)$$

$$= \frac{\gamma(\rho_{n-2})}{N-2} X\ (\rho_{n-1},\ D^c_{\rho_{n-1}}(\theta_{n-2},\theta_{n-1})\ \ D_{\rho_n}(\theta_{n-2},\theta_n)), \tag{4.16}$$

and, even more generally

$$f_i(\rho_i|\rho_{i+1},\ldots,\rho_n,\theta_i,\theta_{i+1},\ldots,\theta_n)$$

$$= \frac{\gamma(\rho_i)}{N-(n-i)} X\ (\rho_i, \bigcap_{k=1}^{n-i} D^c_{\rho_{i+k}}(\theta_i,\theta_{i+k})) \tag{4.17}$$

$$i=1,\ 2,\ \ldots,\ n-1$$

Therefore, (4.4) becomes

$$f(\rho_1,\ldots,\rho_n,\theta_1,\ldots,\theta_n)$$

$$= \left[\prod_{i=1}^{n} f_\theta(\theta_i)\right] \cdot \left[\prod_{i=1}^{n-1} \frac{\gamma(\rho_i)}{N-(n-i)} X\ (\rho_i, \bigcap_{k=1}^{n-i} D^c_{\rho_{i+k}}(\theta_i,\theta_{i+k}))\right] \frac{\gamma(\rho_n)}{N} \tag{4.18}$$

and (4.18) can also be written as

$$f(\rho_1,\ldots,\rho_n,\ \theta_1,\ldots,\ \theta_n) = \prod_{i=1}^{n} f_\theta(\theta_i) \frac{\gamma(\rho_i)}{N-(n-i)} X(\rho_i, \bigcap_{k=1}^{n-i} D^c_{\rho_{i+k}}(\theta_i,\theta_{i+k})) \tag{4.19}$$

$\theta_{n-1} - \theta_n$, i.e. on the relative orientation of these two scatterers.

$D^c_{\rho n}$ is the complement set of $D_{\rho n}$, i.e.

$$D^c_{\rho n}(\theta_{n-1}, \theta_n) = R/D_{\rho n}(\theta_{n-1}, \theta_n) , \tag{4.7}$$

In terms of the characteristic function of set D_ρ then let

$$X(\rho_{n-1}, D_{\rho n}(\theta_{n-1}, \theta_n) = \begin{cases} 1, \ \rho_{n-1} \in D_{\rho n}(\theta_{n-1}, \theta_n), \\ 0, \ \rho_{n-1} \in D_{\rho n}(\theta_{n-1}, \theta_n), \end{cases} \tag{4.8}$$

and (4.6) can be expressed as

$$f_{n-1}(\rho_{n-1}|\rho_n, \theta_{n-1}, \theta_n) = \frac{\gamma(\rho_{n-1})}{N-1} X(\rho_{n-1}, D^c_{\rho n}(\theta_{n-1}, \theta_n)) \tag{4.9}$$

We define

$$f_{n-1}(\rho_{n-1}|\rho_n) = \iint_{\Theta} f_{n-1}(\rho_{n-1}|\rho_n, \theta_{n-1}, \theta_n) f_\theta(\theta_{n-1}) f_\theta(\theta_n) d\theta_{n-1} d\theta_n \tag{4.10}$$

and by substituting (4.9) in (4.10), we obtain

$$f_{n-1}(\rho_{n-1}|\rho_n) = \frac{\gamma(\rho_{n-1})}{N-1} X(\rho_{n-1}, D^c_n), \tag{4.11}$$

where

$$X(\rho_{n-1}, D^c_n) = \iint_{\Theta} X(\rho_{n-1}, D^c_{\rho n}(\theta_{n-1}, \theta_n)) f_\theta(\theta_{n-1}) f_\theta(\theta_n) d\theta_{n-1} d\theta_n \tag{4.12}$$

Further, by means of the relation

$$X(\rho, D) = 1 - X(\rho, D^c) \tag{4.13}$$

(D can be any set) and using the properties of probability distribution density, from (4.2) we get

$$X(\rho_{n-1}, D_{\rho n}) = \iint_{\Theta} X(\rho_{n-1}, D_{\rho n}(\theta_{n-1}, \theta_n)) f_\theta(\theta_{n-1}) f_\theta(\theta_n) d\theta_{n-1} d\theta_n \tag{4.14}$$

This shows that the region $D_{\rho n}$ is the mathematical expectation of the region $D_{\rho n}(\theta_{n-1}, \theta_n)$,

$$f_n(\vec{\rho}_n) = \frac{\nu(\vec{\rho}_n)}{N} , \quad \vec{\rho}_n \in R_3 , \tag{4.3}$$

where $\nu(\rho)$ is the mathematical expectation (or mean value) of the volume density of the mass centers (representative points) of scatterer (or number of representative points[2] in unit volume) and N is the total number of scatterers.

Strictly speaking, when the shape of each scatterer is not spherical, the mass center positions $\rho_{j1},\ldots, \rho_n$ are not independent of the orientation angles $\theta_{j1},\ldots, \theta_{jn}$, and (4.2) should be replaced by

$$\begin{aligned} f(\rho_1,\ldots, \rho_n, \theta_1,\ldots, \theta_n) &= f_\rho(\rho_1,\ldots, \rho_n|\theta_1,\ldots, \theta_n)\, f_\theta(\theta_1,\ldots, \theta_n) \\ &= f_1(\rho_1|\rho_2,\ldots, \rho_n, \theta_1,\ldots, \theta_n)\, f_2(\rho_2|\rho_3\ldots, \rho_n, \theta_2,\ldots,\theta_n) \\ &\cdot f_3(\rho_3|\rho_4,\ldots,\rho_n, \theta_3,\ldots,\theta_n)\ldots f_{n-1}(\rho_{n-1}|\rho_n, \theta_{n-1}, \theta_n)\, f_n(\rho_n) \\ &\cdot f_\theta(\theta_1)\, f_\theta(\theta_2)\ldots f_\theta(\theta_n), \end{aligned} \tag{4.4}$$

and from the assumption 1 mentioned above

$$f_n(\rho_n|\theta_n) = f_n(\rho_n) \tag{4.5}$$

Expression (4.4) is the more general expression when the assumption 2 has been removed, or only under the assumptions 1 and 3. The following derivation will be done also under only assumption 1 and 3.

By following the procedures used in Part II[2], it can be proved that

$$f_{n-1}(\rho_{n-1}|\rho_n, \theta_{n-1}, \theta_n) = \begin{cases} \dfrac{\nu(\rho_{n-1})}{N-1} , & \rho_{n-1} \in D^c_{\rho_n}(\theta_{n-1}, \theta_n) \\ 0 & \rho_{n-1} \in D_{\rho_n}(\theta_{n-1}, \theta_n) \end{cases} \tag{4.6}$$

where $D_{\rho_n}(\theta_{n-1}, \theta_n)$ is the region enclosed by the locus of the mass center of scatter $(\rho_{n-1}, \theta_{n-1})$ which is just tangent with the scatterer (ρ_n, θ_n), as shown in Figure 6. Obviously this region D_{ρ_n} depends on the orientation angles θ_{n-1} and θ_n. The shape of $D_\rho(\theta_{n-1})$ depends only on the vector difference

Multi-Demensional Joint Probability Distribution of Scatterers

In order to calculate the correlation function and intensity of multiple scattered field, the expression of multi-dimensional joint probability distribution function or density of random vectors $\vec{\rho}_{j1}$, $\vec{\rho}_{j2},\ldots,$ $\vec{\rho}_{jn}$ and θ_{j1}, $\theta_{j2},\ldots,$ θ_{jn}, $(\vec{\rho}_1,\ldots,\vec{\rho}_n, \theta_1,\ldots,\theta_n)$ is needed. In this paper, we assume

1 The orientation and the mass center position for each scatterer are mutually independent, (in unconditional distribution).

2 The orientation of each scatterer is also independent of the mass center position of other scatterers.

3 The orientation angles θ_{j1}, $\theta_{j2},\ldots,$ θ_{jn} of any n scatterers from N scatterer are jointly independent, and have the same probability distribution.

From these assumptions, $f(\vec{\rho}_1,\ldots,\vec{\rho}_n, \theta_1,\ldots,\theta_n)$ can be written as

$$f(\vec{\rho}_1,\ldots,\vec{\rho}_n, \theta_1,\ldots,\theta_n) = f_\rho(\rho_1,\ldots,\rho_n)\, f_\theta(\theta_1)\, f_\theta(\theta_2)\ldots f_\theta(\theta_n) \qquad (4.1)$$

where $f_\rho(\vec{\rho}_1,\ldots,\vec{\rho}_n)$ is the joint probability distribution density of $\vec{\rho}_{j1}$, $\vec{\rho}_{j2},\ldots,$ $\vec{\rho}_{jn}$, and $f_\theta(\theta)$ is the probability distribution density of θ_{j1} (or θ_{j2}, or $\theta_{j3},\ldots$).

$f_\rho(\vec{\rho}_1,\ldots,\vec{\rho}_n)$ can be expressed in terms of the conditional probability densities as

$$f_\rho(\vec{\rho}_1,\ldots,\vec{\rho}_n) = f_1(\vec{\rho}_1|\vec{\rho}_2,\ldots,\vec{\rho}_n)\, f_2(\vec{\rho}_2|\vec{\rho}_3,\ldots,\vec{\rho}_n)\, f_3(\vec{\rho}_3|\vec{\rho}_4,\ldots,\vec{\rho}_n)$$
$$\ldots f_{n-1}(\vec{\rho}_{n-1}|\vec{\rho}_n)\, f_n(\vec{\rho}_n) \qquad (4.2)$$

where $f_1(\vec{\rho}_1|\,\vec{\rho}_2,\ldots,\vec{\rho}_n)$ is the conditional probability density of $\vec{\rho}_{j1}$ under the condition $\vec{\rho}_{j2} = \vec{\rho}_2$, $\vec{\rho}_{j3} = \vec{\rho}_3,\ldots,$ and $\vec{\rho}_{jn} = \vec{\rho}_n$. f_2, $f_3,\ldots,$ f_{n-1} denote similarly. $f_n(\vec{\rho}_n)$ is the unconditional probability distribution density of $\vec{\rho}_{jn}$. By using the methods employed in Part II[2], it can be easily proved that

The expressions (3.15) and (3.16) are the general expressions of the successive scattered field, in terms of the incident wave ψ and the scattering functions g, of each single scatterer, g is called the unit impulse response functions, Γ is called wave-vector response. All of them are similar to the Green's function. The function $\rho_{j1\ldots jm}(\vec{r})$ is called the successive field of the scatters $j_1, j_2, \ldots, j_m$.

Finally, considering scatterers j, to j_m, we obtain

$$p_{j1\ldots j_m}(\vec{r}_m) = \overbrace{\int_{R_3} \cdots \int}^{m} \psi(\vec{\rho}_{j1}+\vec{r}')g(\vec{\rho}_{j2}-\vec{\rho}_{j1}+\vec{r}_1', \vec{r}', \theta_{j1})g(\vec{\rho}_{j3}-\vec{\rho}_{j2}+\vec{r}_2', \vec{r}_1', \theta_{j2})$$

$$\ldots g(\vec{\rho}_{j_m}-\vec{\rho}_{j_{m-1}}+\vec{r}_{m-1}', \vec{r}_{m-2}', \theta_{j_{m-1}})g(\vec{r}_m - \vec{\rho}_{j_m}, \vec{r}_{m-1}', \theta_{j_m})\, d\vec{r}'\, d\vec{r}_1' \ldots d\vec{r}_{m-1}' \tag{3.15}$$

or

$$p_{j1\ldots j_m}(\vec{\rho}_{j_m} + \vec{r}''_{m-1}) = p_{j1\ldots j_m}(\vec{r}_m) =$$

$$\overbrace{\int_{R_3} \cdots \int}^{m} \psi(\vec{\rho}_{j1}+\vec{r}')g(\vec{r}'', \vec{r}', \theta_{j1})g(\vec{r}_1'', \vec{r}_1', \theta_{j2})g(\vec{r}_2'', \vec{r}_2', \theta_{j3})$$

$$\ldots g(\vec{r}''_{m-2}, \vec{r}'_{m-2}, \theta_{j_{m-1}})g(\vec{r}_m-\vec{\rho}_{j_m}, \vec{r}'_{m-1}, \theta_{j_m})\, d\vec{r}'\, d\vec{r}_1' \ldots d\vec{r}_{m-1}' \tag{3.16}$$

where (see Figure 5)

$$\vec{r}_i = \vec{\rho}_{j_i} + \vec{r}''_{i-1}, \quad \text{or} \quad \vec{r}''_{i-1} = \vec{r}_2 - \vec{\rho}_{j_i}$$

$$\vec{r}_{i-1} = \vec{\rho}_{j_i} + \vec{r}'_{i-1} \quad \text{or} \quad \vec{r}'_{i-1} = \vec{r}_{i-1} - \vec{\rho}_{j2},$$

$$\vec{r}''_{i-1} = \vec{\rho}_{j_{i+1}} - \vec{\rho}_{j_i} + \vec{r}'_i, \quad i = 1, 2, \ldots, m. \tag{3.17}$$

Let

$$\Gamma(\vec{r}'', \vec{k}, \theta) = \int_{R_3} g(\vec{r}'', \vec{r}', \theta)\, e^{-i\vec{k}\cdot\vec{r}'}\, d\vec{r}', \tag{3.18}$$

Then

$$g(\vec{r}'', \vec{r}', \theta) = \frac{1}{(2\pi)^3} \int_{K_3} \Gamma(\vec{r}'', \vec{k}, \theta)\, e^{+i\vec{k}\cdot\vec{r}'}\, d\vec{k}, \tag{3.19}$$

or

$$p_{j1}(\vec{\rho}_{j1} + \vec{r}'') = \int_{R_3} \psi(\vec{\rho}_{j1} + \vec{r}')g(\vec{r}'', \vec{r}', \theta_{j1})\, d\vec{r}' \tag{3.8}$$

Similarly, or the j_2^{th} scatterer with orientation angle θ_{j2}, and mass center of which is located at P_{j2}, when incident wave is $\rho_{j1}(\vec{r})$, the scattered wave $\rho_{j1j2}(\vec{r})$ can be expressed as

$$p_{j1j2}(\vec{r}_2) = \int p_{j1}(\vec{\rho}_{j2} + \vec{r}_1')g(\vec{r}_2 - \vec{\rho}_{j2}, \vec{r}_1', \theta_{j2})\, d\vec{r}_1' \tag{3.9}$$

or

$$p_{j1j2}(\vec{\rho}_{j2} + \vec{r}_1'') = \int_{R_3} p_{j1}(\vec{\rho}_{j2} + \vec{r}_1')g(\vec{r}_1'', \vec{r}_1', \theta_{j2})\, d\vec{r}_1' \tag{3.10}$$

Substituting (3.7), (3.8) into (3.9) and (3.10) respectively, we have (note that $\vec{\rho}_{j1} + \vec{r}'' = \vec{\rho}_{j2} + \vec{r}'_1$)

$$p_{j1j2}(\vec{r}_2) = \iint_{R_3} \psi(\vec{\rho}_{j1} + \vec{r}')g(\vec{\rho}_{j2} - \vec{\rho}_{j1} + \vec{r}_1', \vec{r}', \theta_{j1})g(\vec{r}_2 - \vec{\rho}_{j2}, \vec{r}_1', \theta_{j2})d\vec{r}'d\vec{r}_1' \tag{3.11}$$

or

$$p_{j1j2}(\vec{\rho}_{j2} + \vec{r}_1'') = \iint_{R_3} \psi(\vec{\rho}_{j1} + \vec{r}')g(\vec{r}'', \vec{r}', \theta_{j1})g(\vec{r}_1'', \vec{r}_1', \theta_{j2})\, d\vec{r}'d\vec{r}_1' \tag{3.12}$$

Similarly, if a third scatterer, i.e., the j_3^{th} one, is now added in this analysis, then

$$p_{j1j2j3}(\vec{r}_3) = \iiint_{R_3} \psi(\vec{\rho}_{j1} + \vec{r}')g(\vec{\rho}_{j2} - \vec{\rho}_{j1} + \vec{r}_1', \vec{r}', \theta_{j1})g(\vec{\rho}_{j3} - \vec{\rho}_{j2} + \vec{r}_2', \vec{r}_1', \theta_{j2}) \cdot g(\vec{r}_3 - \vec{\rho}_{j3}, \vec{r}_2', \theta_{j3})\, d\vec{r}'\, d\vec{r}_1'\, d\vec{r}_2' \tag{3.13}$$

and

$$p_{j1j2j3}(\vec{\rho}_{j3} + \vec{r}_2'') = \iiint_{R_3} \psi(\vec{\rho}_{j1} + \vec{r}')g(\vec{r}'', \vec{r}', \theta_{j1})g(\vec{r}_1'', \vec{r}_1', \theta_{j2}) \cdot g(\vec{r}_2'', \vec{r}_2', \theta_{j3})\, d\vec{r}'\, d\vec{r}_1'\, d\vec{r}_2' \tag{3.14}$$

3. Successive Scattering Formula

Suppose the j_i^{th} scatterer is located as in Figure 4. Its mass center is at $\vec{\rho}_{ji}$, and its orientation angle is

$$\theta_{ji} = (\theta_1, \theta_2, \theta_3).$$

Then the unit impulse response of its equivalent system can be expressed as $g(\vec{r}_1, \vec{r}, \vec{\rho}_{j1}, \theta_{j1})$ and the scattered wave $p_{j1}(\vec{r})$, when the incident wave is $\psi(\vec{r})$ (suppressing $e^{i\omega t}$), can be expressed from (2.1) as

$$p_{j1}(\vec{r}_1) = \int_{R_3} \psi(\vec{r})\, g(\vec{r}_1, \vec{r}, \vec{\rho}_{j1}, \theta_{j1})\, d\vec{r} \tag{3.1}$$

Let

$$\vec{r}' = \vec{r} - \vec{\rho}_{j1}, \quad \vec{r}'' = \vec{r}_1 - \vec{\rho}_{j1} \tag{3.2}$$

Then

$$\vec{r} = \vec{\rho}_{j1} + \vec{r}', \quad \vec{r}_1 = \vec{\rho}_{ji} + \vec{r}'', \quad d\vec{r} = d\vec{r}' \tag{3.3}$$

and (3.1) becomes

$$p_{j1}(\vec{\rho}_{j1} + \vec{r}'') = \int_{R_3} \psi(\vec{\rho}_{j1} + \vec{r}')\, g(\vec{\rho}_{j1} + \vec{r}'', \vec{\rho}_{j1} + \vec{r}', \vec{\rho}_{j1}, \theta_{j1})\, d\vec{r}' \tag{3.4}$$

Obviously,

$$g(\vec{\rho} + \vec{r}'', \vec{\rho} + \vec{r}', \vec{\rho}, \theta) = g(\vec{r}'', \vec{r}', \theta) \tag{3.5}$$

$$g(\vec{r}'', \vec{r}', 0) = g(\vec{r}'', \vec{r}') \tag{3.6}$$

so that (3.4) becomes

$$p_{j1}(\vec{r}_1) = \int_{R_3} \psi(\vec{\rho}_{j1} + \vec{r}')\, g(\vec{r}_1 - \vec{\rho}_{j1}, \vec{r}', \theta_{j1})\, d\vec{r}' \tag{3.7}$$

It should be noticed that: 1) this "equivalence" is only for the scattered field outside the scatterer, and 2) the "equivalent scatterer" and the "equivalent spatial stochastic system" do not really exist. They are only for the convenience of calculation.

$\Gamma(r,k)$ can be called wave-vector response function of the scatterer or of the system, and from (2.3),

$$g(r,r_o) = \frac{1}{(2\pi)^3} \int_{K_3} \Gamma(\vec{r},\vec{k}) e^{-i\vec{k}\cdot\vec{r}_o}\, d\vec{k} \tag{2.4}$$

where K_3 is the 3-dimensional wave-vector space, and $d\vec{k}$ is the volume element in it.

in Figure 2. When this scatterer is immobile and the incident wave is a monochromatic plane wave with unit amplitude and wave-vector k, the scattered wave, can be expressed as $p(\vec{r},\vec{k})e^{i\omega t}$, where $p(\vec{r},\vec{k})$ is complex amplitude of the scattered wave and can be expressed in terms of a scattering matrix.

Consider another "imaginary scatterer" or a "spatial stochastic system" with the following properties: 1) It is totally transparent to the incident wave, and incident wave can penetrate it without damping, 2) it has the same shape as the real scatterer mentioned above. When the incident wave is $\delta(\vec{r}-\vec{r}_o)e^{i\omega t}$, the scattered wave can be expressed as $g(\vec{r},\vec{r}_o)e^{i\omega t}$, and when the incident wave is any monochromatic wave $s(\vec{r})e^{i\omega t}$ (not necessarily plane wave), the scattered wave (output of this system) can be expressed as

$$p(\vec{r}) = \int_{R_3} s(\vec{r}_o)g(\vec{r},\vec{r}_o)d\vec{r}_o, \tag{2.1}$$

where $g(\vec{r},\vec{r}_o)$ is the unit impulse response function of the first kind[1] of the system, and R_3 is the real 3-dimensional space. The factor $e^{i\omega t}$ will be omitted from now on. When s(r) is a uniform plane monochromatic wave with unit amplitude and wave-vector,

$$s(\vec{r}) = e^{i\vec{k}\cdot\vec{r}}, \tag{2.2}$$

the scattered wave can be expressed, from (2.1), as

$$p(\vec{r}) = \int_{R_3} e^{i\vec{k}\cdot\vec{r}}\, g(\vec{r},\vec{r}_o)d\vec{r}_o = \Gamma(\vec{r},\vec{k}). \tag{2.3}$$

If $\Gamma(\vec{r},\vec{k})$ is just equal to the $p(\vec{r},\vec{k})$ mentioned above, then this imaginary scatterer is called the "equivalent scatterer" of the original scatterer, and this spatial stochastic system is called the "equivalent spatial stochastic system" of this original scatterer.

1. Introduction

The problem of multiple scattering of discrete scatterers randomly distributed in space appears frequently in various applications and has been treated by many authors in various ways, for example, Varadan and Varadan[4-8] and Twersky.[9-11]

In this paper, this problem will be treated based on the general theory of spatial stochastic systems,[1-3] and the general multiple scattering theory.[2,3] We consider the following problem: scatterers of any shape and size randomly distributed (not necessarily uniformly in some region) in space. All the scatterers have the same shape, same size and the same scattering property individually and are motionless. The orientation of scatterers is also not necessarily uniformly distributed. Therefore they also can be in the same orientation when orientation angle distribution is S-function. The total number of scatterers can be finite or infinite. The region occupied by the scatterers can be bounded or unbounded, or the whole 3-dimensional real space R_3, see Figure 1. The incident monochromatic wave $\psi(\vec{r})e^{i\omega t}$ can have an arbitrarily shaped wave-front. We are going to find out the multiple scattered field $p(\vec{r})e^{i\omega t}$ and its space correlation function and intensity in the whole space, (except inside each scatterer) inside as well as outside the region in which the scatterers are distributed.

For more complex media involving, for example, several kinds of scatterers, we can use the system decomposition method (mutual feedback connection case) and solve it in terms of the results obtained in this paper.

2. Equivalent Spatial Stochastic System

Consider a single scatterer having a given shape and known scattering properties, and establish a coordinate system at its center of mass, as shown

Abstract

In this paper, a multiple scattering theory based on spatial stochastic system is presented to study wave propagation in discrete random media. Using the concept of an "equivalent spactial stochastic system" and the derivation of the expressions for the joint probability distribution of scatterers and the successive scattered fields, a general expression of the space correlation function and the intensity of multiple scattered field is established. This expression shows that as long as the scattering characteristics of each constituent scatterer excited by a plane monochromatic wave are known along with the volume distribution density of the scatterers, the space correlation function and the intensity of the field multiply scattered by the scatterer distribution excited by an arbitrary monochromatic wave can be calculated rather simply.

where $k = \frac{\omega}{c}$ is the wave number of incident wave.

From (5.5) and (4.22), the space cross correlation function of the successive scattered field can be expressed as

$$K^{k_1 \cdots k_n}_{j_1 \cdots j_m}(r_1, r_2) = \overbrace{\int \cdots \int}^{m+n}_{R_3} \overbrace{\int \cdots \int}^{m+n}_{\Theta} \psi^*(\rho_1)\psi(\rho_i)\, \Gamma^*(\rho_2-\rho_1, k(\rho_1), \theta_1)$$

$$\Gamma^*(\rho_3-\rho_2, k\frac{\rho_2-\rho_1}{|\rho_2-\rho_1|}, \theta_2) \cdots \Gamma^*(\rho_m-\rho_{m-1}, k\frac{\rho_{m-1}-\rho_{m-2}}{|\rho_{m-i}-\rho_{m-2}|}, \theta_{m-1})$$

$$\Gamma^*(r_1-\rho_m, k\frac{\rho_m-\rho_{m-1}}{|\rho_m-\rho_{m-1}|}, \theta_m)\, \Gamma(\rho'_2-\rho'_1, k(\rho_i), \theta_i)\, \Gamma(\rho'_3-\rho'_2, k\frac{\rho'_2-\rho'_1}{|\rho'_2-\rho'_1|}, \theta'_2) \cdots$$

$$\Gamma(\rho'_n-\rho'_{n-1}, k\frac{\rho'_{n-1}-\rho'_{n-2}}{|\rho'_{n-1}-\rho'_{n-2}|}, \theta'_{n-1})\, \Gamma(r_2-\rho'_n, k\frac{\rho'_n-\rho'_{n-1}}{|\rho'_n-\rho'_{n-1}|}, \theta'_n)$$

$$\cdot \prod_{i=1}^{m+n} f_\theta(\theta_i)\, \frac{\gamma(\rho_i)}{N-(m+n-i)}\, X(\rho_i, \bigcap_{k=1}^{m+n-i} \bar{D}^c_{\rho_{i+k}}) \cdot$$

$$\cdot d\rho_1 \cdots d\rho_m\, d\rho'_1 \cdots d\rho'_n\, d\theta_1 \cdots d\theta_m d\theta_i \cdots d\theta'_n \qquad (5.6)$$

where

$$\rho_{m+1}=\rho'_i,\ \rho_{m+2}=\rho'_i, \ldots, \rho_{m+n}=\rho'_n$$

$$\theta_{m+1}=\theta'_i,\ \theta_{m+2}=\theta'_2, \ldots, \rho_{m+n}=\rho'_n \cdot$$

Let $$\Phi(r,k)=\int_{\Theta} \Gamma(r,k,\theta) f_\theta(\theta)\, d\theta\ , \qquad (5.7)$$

and is called the "average wave-vector response function" of a single scatterer with respect to its random orientation. Then (5.6) becomes

$$K^{k_1\cdots k_n}_{j_1\cdots j_m}(r_1,r_2)=\overbrace{\int\cdots\int}^{m+n}_{R_3}\psi^*(\rho_1)\psi(\rho_i)\Phi^*(\rho_2-\rho_1,\ k(\rho_1))$$

$$\Phi^*(\rho_3-\rho_2,k\frac{\rho_2-\rho_1}{|\rho_2-\rho_1|})\ \cdots\ \overset{*}{\Phi}(\rho_m-\rho_{m-1},\ k\frac{\rho_{m-1}-\rho_{m-2}}{|\rho_{m-1}-\rho_{m-2}|})$$

$$\Phi^*(r_1-\rho_m,\ k\frac{\rho_m-\rho_{m-1}}{|\rho_m-\rho_{m-1}|})\ \Phi(\rho_i-\rho_i,\ k(\rho_i))\ \Phi\ (\rho_3'-\rho'_2,\ k\frac{\rho_2'-\rho_1'}{|\rho_2'-\rho_1'|})\ .$$

$$\ldots\Phi(\rho_n'-\rho_{n-1}',\ k\frac{\rho'_{n-1}-\rho'_{n-2}}{|\rho'_{n-1}-\rho'_{n-2}|})\ \Phi\ (r_2-\rho_n',\ k\frac{\rho_n'-\rho'_{n-1}}{|\rho'_n-\rho'_{n-1}|}$$

$$\prod_{i=1}^{m+n}\frac{\gamma(\rho_i)}{N-(m+n-i)}\ X\ (\rho_i,\ \bigcap_{k=1}^{m+n-i}\bar{D}^c_{\rho_{i+k}})\ d\rho_1\ldots d\rho_m\ d\rho_i\ldots d\rho_n' \quad . \tag{5.8}$$

Let

$$I_1=\int_{R_3}\psi(\rho_i)\Phi(\rho_2-\rho_i,\ k(\rho_1))\ \Phi\ (\rho_3-\rho_2,\ k\frac{\rho_2-\rho_1}{|\rho_2-\rho_1|})\ \frac{\gamma(\rho_1)}{N-(m+n-1)} \quad . \tag{5.9}$$

$$\cdot X\ (\rho_1,\ \bigcap_{k=1}^{m+n-1}\bar{D}^c_{\rho_{1+k}})\ d\rho_1\ ,$$

By means of DeMorgan's Law and the properties of the characteristic function of sets, it is easy to show that

$$X(\rho_1,\ \bigcap_{k=1}^{m+n-1}\bar{D}^c_{\rho_{k+1}})=1-X(\rho_1,\ [\bigcap_{k=1}^{m+n-1}\bar{D}^c_{\rho_{k+1}}]^c)$$

$$=1-X(p_1,\ \bigcup_{k=1}^{m+n-1}\bar{D}_{\rho_{k+1}})$$

$$= 1 - \sum_{k=1}^{m+n-1} X(\rho_1, \bar{D}_{\rho_{k+1}}) + \sum_{k=1}^{m+n-1} \sum_{\substack{\ell=1 \\ k\neq\ell}}^{m+n-1} X(\rho_1, \bar{D}_{\rho_{k+1}} \cap \bar{D}_{\rho_{\ell+1}})$$

$$- \sum_{\substack{k=1 \\ k\neq\ell,\ \ell\neq q,\ q\neq k}}^{m+n-1} \sum_{\ell=1}^{m+n-1} \sum_{q=1}^{m+n-1} X(\rho_1, \bar{D}_{\rho_{k+1}} \cap \bar{D}_{\rho_{\ell+1}} \cap \bar{D}_{\rho_{q+1}}) + \ldots \quad . \tag{5.10}$$

Substituting (5.10) in (5.9), we have

$$I_1 = I_1^{(0)} - I_1^{(1)} + I_1^{(2)} - I_1^{(3)} + \ldots = \sum_{n=0}^{\infty} (-1)^n I_1^{(n)} \tag{5.11}$$

where

$$I_1^{(0)} = \int_{R_3} \psi^*(\rho_1)\ \Phi^*(\rho_2-\rho_1,\ k(\rho_1))\ \Phi^*(\rho_3-\rho_2,\ k\frac{\rho_2-\rho_1}{|\rho_2-\rho_1|})\ \frac{\gamma(\rho_1)}{N-(m+n-1}\ d\rho_1 \tag{5.12}$$

$$I_1^{(1)} = \frac{1}{N-(m+n-1)} \sum_{k=1}^{m+n-1} \int_{R_3} \psi^*(\rho_1)\ \Phi^*(\rho_2-\rho_1, k(\rho_1))\ \Phi^*(\rho_3-\rho_2, k\frac{\rho_2-\rho_1}{|\rho_2-\rho_1|}) \tag{5.13}$$

$$\cdot\gamma(\rho_1)\ X(\rho_1, \bar{D}_{\rho_{k+1}})\ d\rho_1$$

$$I_1^{(2)} = \frac{1}{N-(m+n-1)} \sum_{k=1}^{m+n-1} \sum_{l=1}^{m+n-1} \int_{R_3} \psi^*(\rho_1)\ \Phi^*(\rho_2-\rho_1, k(\rho_1))\ \Phi^*(\rho_3-\rho_2, k\frac{\rho_2-\rho_1}{|\rho_2-\rho_1|})$$

$$\cdot\gamma(\rho)\ X(\rho_1, \bar{D}_{\rho_{k+1}} \cap \bar{D}_{\rho_{l+1}})\ d\rho_1 \tag{5.14}$$

$I_1^{(3)}$ = ... (similar and omited)

Let $\rho_2 - \rho_1 = u_1$, then $\rho_1 = \rho_2 - u$, and (5.12) and (5.13) transform to the following expressions respectively:

$$I_1^{(0)} = \frac{1}{N-(m+n-1)} \int_{R_3} \psi^*(\rho_2-u_1)\ \phi^*(u_1, k(\rho_2-u_1))\ \Phi^*(\rho_3-\rho_2, k\frac{u_1}{|u_1|})\ \gamma(\rho_2-u_1)\ du_1 \tag{5.15}$$

Since the function $\Phi(u,k)$ rapidly attenuates with u and its "effective domain", $k(\ )$ and $\gamma(\ )$ can be treated as constants, we let

$$\psi(\rho_2-u_1) = \psi(\rho_2)e^{ik(\rho_2).u_1},\ \psi^*(\rho_2-u_1)=\psi^*(\rho_2)e^{ik(\rho_2)-u_1} \qquad (5.16)$$

and (5.15) becomes

$$I_1^{(0)}=\frac{1}{N-(m+n-1)}\psi^*(\rho_2)\gamma(\rho_2)\int_{R_3}\Phi^*(u_1,k(\rho_2))\Phi^*(\rho_3-\rho_2,k\frac{u_1}{|u_1|})e^{-ik(\rho_2).u_1}du_1 \qquad (5.17)$$

It can be shown that, in the summation of (5.13), only the first term plays the main rule, and the summation of other terms is much smaller than the first term and can be neglected. Thus,

$$I_1^{(1)}=\frac{1}{N-(m+n-1)}\int_{\bar{D}_{\rho_2}}\psi^*(\rho_1)\Phi^*(\rho_2-\rho_1,k(\rho_1))\Phi^*(\rho_3-\rho_2,k\frac{\rho_2-\rho_1}{|\rho_2-\rho_1|})\gamma(\rho_1)d\rho_1 \qquad (5.18)$$

By similar reasons as it was used in the drivations of (5.17), (5.18) becomes

$$I_1^{(1)}=\frac{1}{N-(m+n-1)}\psi^*(\rho_2)\gamma(\rho_2)\int_{\bar{D}_0}\Phi^*(u_1,k(\rho_2))\Phi^*(\rho_1-\rho_2,k\frac{u_1}{|u_1|})e^{-ik(\rho_2).u_1}du_1 \qquad (5.19)$$

Now, it can be shown that the series (5.11) converges rapidly and

$$\Big|\sum_{n=2}^{\infty}(-1)^n I_1^{(n)}\Big| << |I_1^{(0)}-I_1^{(1)}| \qquad (5.20)$$

Therefore, from (5.17), (5.19), taking $I_1=I_1^{(0)}-I_1^{(1)}$, we have

$$I_1=\frac{1}{N-(m+n-1)}\psi^*(\rho_2)\gamma(\rho)\int_{R_3\setminus\bar{D}_0}\Phi^*(u_1,k(\rho_2))\Phi^*(\rho_3-\rho_2,k\frac{u_1}{|u_1|})e^{-ik(\rho_2).u_1}du_1 \qquad (5.21)$$

Let

$$\Phi_2^*(\rho_3-\rho_2,k(\rho_2)=\int_{R_3\setminus\bar{D}_0}\Phi^*(u_1,k(\rho_2))\Phi^*(\rho_3-\rho_2,k\frac{u_1}{|u_1|})e^{-ik(\rho_2).u_1}du_1 \qquad (5.22)$$

Then (5.21) becomes

$$I_1 = \frac{1}{N-(m+n-1)} \psi^*(\rho_2)\gamma(\rho_2)\Phi_2^*(\rho_3-\rho_2, k(\rho_2)). \tag{5.23}$$

Next, let

$$I_2 = \int_{R_3} I_1 \, \Phi^*(\rho_4-\rho_3, k\frac{\rho_3-\rho_2}{|\rho_3-\rho_2|}) \frac{\gamma(\rho_2)}{N-(m+n-2)} X(\rho_2, \bigcap_{k=1}^{m+n-2} \bar{D}^c_{\rho_{k+2}}) d\rho_2 \tag{5.24}$$

Substituting (5.23) into (5.24), by the similar steps as above, we obtain

$$I_2 = \frac{1}{N-(m+n-1)} \cdot \frac{1}{N-(m+n-2)} \gamma^*(\rho_3)\gamma^2(\rho_3)\Phi_3^*(\rho_4-\rho_3, k(\rho_3)) \tag{5.25}$$

where

$$\Phi_3(\rho_4-\rho_3, k(\rho_3)) = \int_{R_3 \setminus \bar{D}_{\rho_0}} \Phi_2(u_2, k(\rho_3))\Phi(\rho_4-\rho_3, k\frac{u_2}{|u_2|}) e^{ik(\rho_3).u_2} du_2 \tag{5.26}$$

Similarly

$$I_3 = \frac{1}{N-(m+n-1)} \cdot \frac{1}{N-(m+n-2)} \cdot \frac{1}{N-(m+n-3)} \psi^*(\rho_4)\gamma^3(\rho_4)\Phi_4^*(\rho_5-\rho_4, k(\rho_4)) \tag{5.27}$$

where

$$\Phi_4(\rho_5-\rho_4, k(\rho_4)) = \int_{R_3 \setminus \bar{D}_{\rho 0}} \Phi_3(u_3, k(\rho_4))\Phi(\rho_5-\rho_4, k\frac{u_3}{|u_3|}) e^{ik(\rho_4).u_3} du_3 \tag{5.28}$$

Continuing this,

$$I_{m-2} = \left[\prod_{k=1}^{m-2} \frac{1}{N-(m+n-k)} \right] \psi^*(\rho_{m-1}\gamma^{m-1}(\rho_{m-1})\Phi_{m-1}^*(\rho_m-\rho_{m-1}, k(\rho_{m-1})), \tag{5.29}$$

where

$$\Phi_{m-1}(\rho_m-\rho_{m-1},k(\rho_m))=\int_{R_3\,\bar{D}_{\rho 0}} \Phi_{m-2}(u_{m-2}(u_{m-2},k(\rho_{m-1}))\Phi(\rho_m-\rho_{m-1},k\frac{u_{m-2}}{|u_{m-2}|})e^{ik(\rho_{m-1}).u_{m-2}}$$

$$du_{m-2} \tag{5.30}$$

However, the derivations of I_{m-1} and I_m will be slightly different.

$$I_{m-1}=\int_{R_3} I_{m-2}\,\Phi^*(r_1-\rho_m,k\frac{\rho_m-\rho_{m-1}}{|\rho_m-\rho_{m-1}|})\,\frac{\gamma(\rho_{m-1})}{N-(m+n-(m-1))}\,X(\rho_{m-1},\bigcap_{k=1}^{n+1}\bar{D}^c_{\rho_{k+m-1}})d\rho_{m-1} \tag{5.31}$$

Substituting (5.29) into (5.31), similarly, one has

$$I_{m-1}=\Big[\prod_{k=1}^{m-1}\frac{1}{N-(m+n-k)}\Big]\,\psi^*(\rho_m)\gamma^{m-1}(\rho_m)\Phi_m^*(r_1-\rho_m,k(\rho_m)), \tag{5.32}$$

where

$$\Phi_m(r_1-\rho_m,(k(\rho_m))=\int_{R_3\setminus\bar{D}_{\rho m}} \Phi_{m-1}(u_{m-1},k(\rho_m))\Phi(r_1-\rho_m,k\frac{u_{m-1}}{|u_{m-1}|})e^{ik(\rho_m).u_{m-1}}du_{m-1} \tag{5.33}$$

$$I_m=\int_{R_3} I_{m-1}\,\frac{\gamma(\rho_m)}{N-(\Delta+n-\Delta)}\,X(\rho_m,\bigcap_{k=1}^{n}\bar{D}^c_{\rho_{k+m}})\,d\rho_m \tag{5.34}$$

Substituting (5.32) into (5.34), in view of the fact that the field point r_1 is not inside any scatterer, we get

$$I_m=\prod_{k=1}^{m}\frac{1}{N-(m+n-k)}\int_{R_3}\psi^*(\rho_m)\gamma^m(\rho_m)\Phi_m^*(r_1-\rho_m,k(\rho_m))d\rho_m. \tag{5.35}$$

Next, we proceed the later half part of the integration in (5.8), similarly.

Let

$$I_1 = \int_{R_3} \psi(\rho_1)\Phi(\rho_2'-\rho_1', k(\rho_1'))\Phi(\rho_3'-\rho_2', k\frac{\rho_2'-\rho_1'}{|\rho_2'-\rho_1'|}) \frac{\gamma(\rho_i)}{N-(n-1)} X(\rho_1', \bigcap_{k-1}^{n-1} \bar{D}^c_{\rho'_{k+1}}) d\rho_i, \quad (5.36)$$

so that finally we get an expression similar to (5.23):

$$I_i = \frac{1}{N-(n-1)} \psi(\rho_2')\gamma(\rho_2')\Phi_2(\rho_3'-\rho_2', k(\rho_2')) \quad (5.37)$$

$$I_2' = \frac{1}{N-(n-1)} \cdot \frac{1}{N-(n-2)} \psi(\rho_3')\gamma^2(\rho_3')\Phi_3(\rho_4'-\rho_3', k(\rho_3')), \quad (5.38)$$

$$I_{n-2}' = \prod_{k=1}^{n-2} \frac{1}{N-(n-k)} \psi(\rho_{n-1}')\gamma^{n-2}(\rho_{n-1}')\Phi_{n-1}(\rho_n'-\rho_{n-1}', k(\rho_{n-1})), \quad (5.39)$$

$$I_{n-1}' = \prod_{k=1}^{n-1} \frac{1}{N-(n-k)} \psi(\rho_n')\gamma^{n-1}(\rho_n')\Phi_n(r_2-\rho_n', k(\rho_n')), \quad (5.40)$$

$$I_n' = \prod_{k=1}^{n} \frac{1}{N-(n-k)} \int_{R_3} \psi(\rho_n')\gamma^n(\rho_n')\Phi_n(r_2-\rho_n', k(\rho_n'))d\rho_n' . \quad (5.41)$$

By means of (5.35) and (5.36), (5.8) becomes

$$K^{k\ldots k_n}_{j_1\cdots j_m}(r_1, r_2) = \prod_{k=1}^{m+n} \frac{1}{N-(m+n-k)} \cdot$$

$$\int_{R_3} \psi^*(\rho_m)\gamma^m(\rho_m)\Phi_m^*(r_1-\rho_m, k(\rho_m))d\rho_m \cdot \quad (5.42)$$

$$\int_{R_3} \psi(\rho_n')\gamma^n(\rho_n')\Phi_n(r_2-\rho_n', k(\rho_n'))d\rho_n' ,$$

for

$$\{j_1, j_2, \ldots,\} \quad \{k_1, k_2, \ldots, k_n\} = \emptyset$$

Auto-Correlation

When the two sequences $\{j_1,\ldots, j_m\}$ and $\{k_1,\ldots,k_n\}$ are completely conincident with each other, i.e. m=n and $j_1 = k_1$, $j_2 = k_2$, ..., $j_m = k_m$, the cross correlation function $K^{k_1\cdots k_n}_{j_1\cdots j_m}(r_1,r_2)$ becomes the auto-correlation function of $p_{j1\cdots j_m}(r)$ defined as

$$K_{j_1\cdots j_m}(r_1,r_2) = \xi\{p_{j_1\cdots j_m}(r_1)\ p_{j_1\cdots j_m}(r_2)\}. \tag{5.43}$$

Substituting (5.5) into (5.43) and using (4.22), we get $K_{j_1\cdots j_m}(r_1,r_2)$

$$= \xi\{|\psi(\rho_{ji})|^2|\ \Gamma(\rho_{j_2}-\rho_{j_1}, k(\rho_{j_1}),\ \theta_{j_1})|^2\ |\Gamma(\rho_{j_3}-\rho_{j_2}, k\frac{\rho_{j_2}-\rho_{j_1}}{|\rho_{j_2}-\rho_{j_1}|}\ \theta_{j_2})|^2$$

$$\left|\Gamma(\rho_{j_4}-\rho_{j_3},\ k\frac{\rho_{j3}-\rho_{j2}}{|\rho_{j_3}-\rho_{j2}|}\ \theta_{j_3})\right|^2\ldots|\Gamma(\rho_{j_m}-\rho_{j_{m-1}}, k\frac{\rho_{j_{m-1}}-\rho_{j_{m-2}}}{|\rho_{j_{m-1}}-\rho_{j_{m-2}}|}\theta_{j_{m-1}})\Big|^2$$

$$\Gamma(r_1-\rho_m,\ k\frac{\rho_{j_m}-\rho_{j_{m-1}}}{|\rho_{j_m}-\rho_{j_{m-1}}|},\ \theta_{j_m})\ \Gamma(r_2-\rho_m,\ k\frac{\rho_{j_m}-\rho_{j_{m-1}}}{|\rho_{j_m}-\rho_{j_{m-1}}|}\ \theta_{j_m})\}$$

$$= \int_{R_3}^{m}\cdots\int\ \int_{\Theta}^{m}\cdots\int\ \psi(\rho_1)^2|\Gamma(\rho_2-\rho_1,\ k(\rho_1),\ \theta_1)|^2|\Gamma(\rho_3-\rho_2,\ k\frac{\rho_2-\rho_1}{|\rho_2-\rho_1|},\ \theta_2)|^2.$$

$$\left|\Gamma(\rho_4-\rho_3,\ k\frac{\rho_3-\rho_2}{|\rho_3-\rho_2|},\ \theta_3)\right|^2\ldots|\Gamma(\rho_m-\rho_{m-1},\ k\frac{\rho_{m-1}-\rho_{m-2}}{|\rho_{m-1}-\rho_{m-2}|},\ \theta_{m-1})|^2.$$

$$\Gamma^*(r_1-\rho_m,\ k\frac{\rho_m-\rho_{m-1}}{|\rho_m-\rho_{m-1}|},\ \theta_m)\ \Gamma(r_2-\rho_m,\ k\frac{\rho_m-\rho_{m-1}}{|\rho_m-\rho_{m-1}|},\ \theta_m).$$

$$\prod_{i=1}^{m} f_\theta(\theta_i)\ \frac{\gamma(\rho_i)}{N-(m-i)}\ X\ (\rho_i,\ \bigcap_{k=1}^{m-i}\bar{D}^c_{\rho_{i+k}})\ d\rho_1\ldots d_{\rho m}\ d\theta_1\ldots d\theta_m \tag{5.44}$$

Let

$$\Psi(r,k)= \int_{\Theta} |\Gamma(r,k,\theta)|^2 f_\theta(\theta)d\theta \ , \tag{5.45}$$

$$\Psi_c(r_1,r_2,k) = \int_{\Theta} \Gamma^*(r_1,k,\theta)\ \Gamma(r_2,k,\theta) f_\theta(\theta)d\theta \tag{5.46}$$

Then (5.44) becomes

$$K_{j_1\ldots j_m}(r_1,r_2) = \int_{R_3}^{m}\cdots\int |\psi^2(\rho_1)|^2 \Psi(\rho_2-\rho_1, k(\rho_1))\Psi(\rho_3-\rho_2, k\frac{\rho_2-\rho_1}{|\rho_2-\rho_1|}) \cdot$$

$$\cdot\ \Psi(\rho_4-\rho_3,\ k\ \frac{\rho_3-\rho_2}{|\rho_3-\rho_2|}) \ \ldots\ \Psi(\rho_m-\rho_{m-1},\ k\ \frac{\rho_{m-1}-\rho_{m-2}}{|\rho_{m-1}-\rho_{m-2}|}) \tag{5.47}$$

$$\cdot\ \Psi_c(r_1-\rho_m,\ r_2-\rho_m,\ k\ \frac{\rho_m-\rho_{m-1}}{|\rho_m-\rho_{m-1}|}) \prod_{i=1}^{m} \frac{\gamma(\rho_i)}{N-(m-i)} X(\rho_i, \bigcap_{k=1}^{m-i} D^{-c}_{\rho_{i+k}\ 1})d\rho \ldots d\rho_m$$

Following derivations of Section 5.1, let

$$J_1 = \int_{R_3} |\psi(\rho_1)|^2 \Psi(\rho_2-\rho_1,\ k(\rho_1))\ \Psi\ (\rho_3-\rho_2,\ k\ \frac{\rho_2-\rho_1}{|\rho_2-\rho_1|})\ \frac{\gamma(\rho_1)}{N-(m-1)} \tag{5.48}$$

$$\cdot\ X(\rho_1, \bigcap_{k=1}^{m-1} D^{-c}_{\rho_{k+1}})\ d\rho_1$$

Comparing (5.48) with (5.9), one can see that they have the same form, and the only difference is that the ψ, Φ m+n in (5.9) become $|\psi|^2$, Ψ, m in (5.48), respectively. Seeing that the function Φ (u,k) attenuates with u even faster thanfunction Φ (u,k) does, and from (5.16),

$$|\psi\ (\rho_2-u_1)|^2 = |\psi\ (\rho_2)|^2 e^{i2k(\rho_2).u_1}|^2 = |\psi(\rho_2)|^2 \tag{5.49}$$

where u is in the "effective domain" of (u,k), finally, we get

$$J_1 = \frac{1}{N-(m-1)}|\psi(\rho_2)|^2\gamma(\rho_2)\int_{R_3\setminus\bar{D}_0}\Psi(u_1,k(\rho_2))\ \Psi\ (\rho_3-\rho_2,k\frac{u_1}{|u_1|})\ du_1 \tag{5.50}$$

Let

$$\Psi_2(\rho_3-\rho_2,\ k(\rho_2)) = \int_{R_3\setminus\bar{D}_0}\Psi(u_1,k(\rho_2))\Psi(\rho_3-\rho_2,\ k\frac{u_1}{|u_1|})e^{i2k(\rho_2).u_1}du_1. \tag{5.51}$$

Then

$$J_1 = \frac{1}{N-(m-1)}|\psi(\rho_2)|^2\gamma(\rho_2)\ \Psi_2(\rho_3-\rho_2,\ k(\rho_2)) \tag{5.52}$$

Similarly, let

$$J_2 = \int_{R_3} J_1\ \Psi\Big(\rho_4-\rho_3,\ k\frac{\rho_3-\rho_2}{|\rho_3-\rho_2|}\Big)\ \frac{\gamma(\rho_2)}{N-(m-2)}\ X(\rho_2,\bigcap_{n=1}^{m-2}\bar{D}^c_{\rho_{k+1}})\ d\rho_2 \tag{5.53}$$

Then

$$J_2 = \frac{1}{N-(m-1)}\cdot\frac{1}{N-(m-2)}|\psi(\rho_3)|^2\gamma^2(\rho_3)\Psi_3(\rho_4-\rho_3,\ k(\rho_3)) \tag{5.54}$$

where

$$\Psi_3(\rho_4-\rho_3,\ k(\rho_3)) = \int_{R_3\setminus\bar{D}_0}\Psi_2(u_2,k(\rho_3))\Psi(\rho_4-\rho_3,\ k\frac{u_2}{|u_2|})\ du_2 \tag{5.55}$$

Going on in this way, finally, let

$$J_{m-2} = \int_{R_3} J_{m-3}\ \Psi(\rho_m-\rho_{m-1},\ k\frac{\rho_{m-1}-\rho_{m-2}}{|\rho_{m-1}-\rho_{m-2}|})\ \frac{\gamma(\rho_{m-2})}{N-(m-2)}$$

$$\cdot\ X(\rho_{m-2},\bigcap_{k=1}^{2}\bar{D}^c_{\rho_{k+m-2}})\ d\rho_{m-2}\ , \tag{5.56}$$

$$J_{m-2} = \prod_{k=1}^{m-2} \frac{1}{N-(m-k)} \; |\psi(\rho_{m-1})|^2 \gamma^{m-2}(\rho_{m-1}) \Psi_{m-1}(\rho_m - \rho_{m-1},\, k(\rho_{m-1})), \quad (5.57)$$

where

$$\Psi_{m-1}(\rho_m - \rho_{m-1},\, k(\rho_{m-1})) = \int_{R_3 \setminus \bar{D}_0} \Psi_{m-2}(u_{m-2}, k(\rho_{m-1}))\, \Psi\left(\rho_m - \rho_{m-1}, k \frac{u_{m-2}}{|u_{m-2}|}\right) du_{m-2} \quad (5.58)$$

Let

$$J_{m-1} = \int_{R_3} J_{m-2}\, \Psi_c\left(r_1 - \rho_m,\, r_2 - \rho_m,\, k \frac{\rho_m - \rho_{m-1}}{|\rho_m - \rho_{m-1}|}\right) \frac{\gamma(\rho_{m-1})}{N-1}\, X(\rho_{m-1}, \bar{D}^c_{\rho_m})\, d\rho_{m-1}, \quad (5.59)$$

Then

$$J_{m-1} = \left[\prod_{k=1}^{m-1} \frac{1}{N-(m-k)}\right] |\psi(\rho_m)|^2 \gamma^{m-1}(\rho_m) \Psi(r_1 - \rho_m, r_2 - \rho_m,\, k(\rho_m)), \quad (5.60)$$

where

$$\Psi_{mc}(r_1 - \rho_m, r_2 - \rho_m,\, k(\rho_m)) = \int_{R_3 \setminus \bar{D}_0} \Psi_{m-1}(u_{m-1},\, k(\rho_m))$$

$$\Psi_c\left(r_1 - \rho_m,\, r_2 - \rho_m,\, k \frac{u_{m-1}}{|u_{m-1}|}\right) du_{m-1} \quad (5.61)$$

Finally,

$$K_{j_1 \cdots j_m}(r_1, r_2) = J_m = \int_{R_3} J_{m-1} \frac{\gamma(\rho_m)}{N}\, d\rho_m \quad (5.62)$$

$$K_{j_1 \cdots j_m}(r_1, r_2) = K^{j_1 \cdots j_m}_{j_1 \cdots j_m}(r_1, r_2) \quad (5.63)$$

$$= \prod_{k=1}^{m} \frac{1}{N-(m-k)} \int_{R_3} |\psi^2(\rho_m)|^2 \gamma^m(\rho_m) \Psi_{mc}(r_1 - \rho_m, r_2 - \rho_m, k(\rho_m))\, d\rho_m$$

pace Correlation Function of Multiple Scattered Field

By means of the system decomposition method in the spatial stochastic ystem theory [1], it can be proved that the space correlation function of he multiple scattered field p(r)

$$K_\rho(r_1, r_2) = \mathcal{E}\{\rho^*(r_1)\rho(r_2)\} \tag{6.1}$$

an be expressed in terms of the space cross correlation function of the uccessive scattered field as

$$K_\rho(r_1,r_2)=\sum_{m=1}^{\infty}\sum_{n=1}^{\infty}\sum_{j=1}^{N}\cdots\sum_{j_m=1}^{N}\sum_{k_1=1}^{N}\cdots\sum_{k_n=1}^{N} K^{k_1\ldots k_n}_{j_1\ldots j_m}(r_1,r_2).$$

$$j_i\neq j_{i-1},\ i=2,\ldots,m,\ k_\ell\neq k_{\ell-1},\ \ell=2,\ldots,n. \tag{6.2}$$

This is a general relation. Here the set $\{j_1, j_2, \ldots, j_m\}$ and the set $\{k_1, k_2, \ldots, k_n\}$ can overlap with each other, i.e. the intercept $\{k_1, \ldots k_n\}$ $\{j_1, \ldots, j_n\}$ is not necessarily to empty set; and inside the set $\{j_1, \ldots, j_m\}$, the elements can be the same, or can be repeated any number of times, provided that all the pairs of a'jacent elements are all different; and so does the set $\{k_1, \ldots, k_n\}$.

Now let us divide $K_p(r_1, r_2)$ into three parts:

$$K_\rho(r_1,r_2)=K_\rho^{(a)}(r_1,r_2)+K_\rho^{(b)}(r_1,r_2)+K_\rho^{(c)}(r_1,r_2), \tag{6.3}$$

where $K_\rho^{(a)}(r_1,r_2)$ denotes that part, which consists those terms in the summation (6.2), where the sequence $\{j_1, \ldots, j_m\}$ and sequence $\{k_1, \ldots, k_n\}$ do not overlap at all, or do not have any common element as shown in Figure 9, i.e.

$$K_\rho^{(a)}(r_1,r_2)=\sum_{m=1}^{\infty}\sum_{n=1}^{\infty}\sum_{j=1}^{N}\cdots\sum_{j_m=1}^{N}\sum_{k_1=1}^{N}\cdots\sum_{k_n=1}^{N} K^{k_1\ldots k_n}_{j_1\ldots j_m}(r_1,r_2)$$

$$j_i \neq j_{i-1}, i=2, \ldots, m_i \quad k_\ell \neq k_{\ell-1}, \ell=2,\ldots,n \tag{6.4}$$

$$\{j_1,\ldots,j_m\} \quad \{k_1,\ldots,k_n\} = \emptyset .$$

$K_p^{(c)}(r_1,r_2)$ denotes that part, which consists of those terms, where the sequence $\{j_1,\ldots,j_m\}$ and sequence $\{k_1\ldots,k_n\}$ completely coincide with each other, as shown in Figure 10.

$$K_p^{(c)}(r_1,r_2) = \sum_{m=1}^{\infty} \sum_{n=1}^{\infty} \sum_{j_1=1}^{N} \cdots \sum_{j_m=1}^{N} \sum_{k_1=1}^{N} \cdots \sum_{k_n=1}^{N} K_{j_1\ldots j_m}^{k_1\ldots k_n}(r_1,r_2)$$

$$j_i \neq j_{i-1} \quad i=2, \ldots, m, \; k_{\ell \neq} k_{\ell-1}, \; \ell=2,\ldots,n$$

$$m=n, \; j_i=k_i, \; i=1,2,\ldots m.$$

$$= \sum_{m=1}^{\infty} \sum_{j_1=1}^{N} \cdots \sum_{j_m=1}^{N} K_{j_1\ldots j_m}^{j_1\ldots j_m}(r_1,r_2) \tag{6.5}$$

$$j_1 \neq j_{i-1}, \quad i=2, \ldots, m$$

The part $K_p^{(b)}(r_1 r_2)$ denotes the sum of those terms, in which, the sequence $j_1,\ldots, j_m\}$ and $\{k_1 m \ldots, k_n\}$ are partially overlapping. In the next part of this paper, it will be shown that this part $k_p^{(b)}(r_1, r_2)$ can be neglected and the error of this neglect will be estimated.

erivation of $k_p(a)\ (r_1, r_2)$

In the derivation of $k_p(a)\ (r_1, r_2)$, we neglect the contribution of hose terms, where $\{i_1, \ldots, j_m\}$ or $\{k_1, \ldots, k_n\}$ have repeat element, ust as Twersky did [11]. [The correctness of this neglect has been shown y Twersky.] Thus, from (6.4), we have

$$K_p^{(a)}(r_1,r_2) = \sum_{m=1}^{N} \sum_{n=1}^{N-m} N(N-1)(N-2)\ldots (N-m+1)(N-m)(N-m-1)\ldots(N-m0(n01)].$$

$$\cdot K_{j_1\ldots j_m}^{k_1\ldots k_m}(r_1,r_2)$$

$$= \sum_{m=1}^{N} \sum_{n=1}^{N-m} \{ \prod_{k=1}^{m+n} [N-(m+n-k)]\} K_{j_1\ldots j_m}^{k_1\ldots k_n}(r_1,r_2),$$

or

$$K_p^{(a)}(r_1,r_2) = \sum_{m=1}^{N} \sum_{n=1}^{N-m} \int_{R_3} \Psi^*(\rho) \gamma^m(\rho)\Phi_m^*(r_1-\rho,k(\rho))d\rho$$

$$\cdot \int_{R_3} \Psi(\rho')\gamma^n(\rho')\Phi_n(r_2-\rho',k(\rho'))d\rho' \qquad (6.6)$$

when N >> 1, the upper limits of the summation in (6.6) can be replaced be infinity, and (6.6) becomes

$$K_\rho^{(a)}(r_1,r_2) = \sum_{m=1}^{\infty} \sum_{n=1}^{\infty} \int_{R_3} \psi^*(\rho)\gamma^m(\rho)\Phi_m^*(r_1-\rho,k(\rho))d\rho$$

$$\cdot \int_{R_3} \psi(\rho')\gamma^n(\rho')\Phi_n(r_2-\rho',\ k(p'))d\rho' \qquad (6.7)$$

This is the required general expression of the first term of the space correlation function of the multiple scattered field when the incident field is a monochromatic wave $\psi(r)$. Clearly, the evaluations of the function Φ_m, Φ_n will be the main problems in finding $k_p\ (r_1, r_2)$. Now we are going to proceed with this calculation.

AD-A151 766 MULTIPLE SCATTERING OF ELECTROMAGNETIC WAVES IN DISCRETE RANDOM MEDIA..(U) PENNSYLVANIA STATE UNIV UNIVERSITY PARK WAVE PROPAGATION LAB.. 2/3

UNCLASSIFIED V K VARADAN ET AL. 31 DEC 84 F/G 20/14 NL

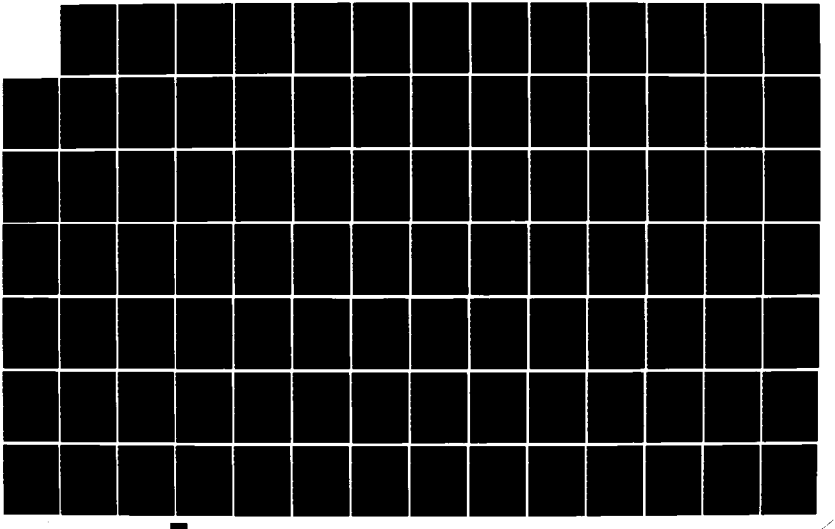

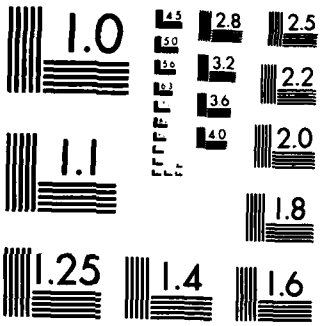

Because throughout this paper, the frequency of the incident wave is fixed, the function $\Phi(u, k(\rho))$ can be defined in another form $\Phi(u, n(\rho))$ or simply $\Phi(u, n)$, where $n(\rho)$ is the unit vector in the direction of $k(\rho)$. Thus, (5.22) can be changed to

$$\Phi_2(u_2,n(\rho_2)) = \int_{R_3\setminus\bar{D}_0} \Phi(u_1,n(\rho_2))\Phi(u_2, \frac{u_1}{|u_1|}\, e^{i\frac{w}{c}\, n(\rho_2)\cdot u_1}\, du. \tag{6.6}$$

Research shows that, for a single scatterer with any shape and for any incident frequency, the function $\Phi(u,n)$ is always separable, (far field approximation) i.e. $\Phi(u,n)$ can be written as the form

$$\Phi(u_1,n) = W(u_1)\Lambda(n_1,n) \tag{6.7}$$

where $u_1 = |u_1|$, and $n_1 = u_1/|u_1|$ is a unit vector. Substituting (6.7)' into (6.6)', and using $du_1 = u_1^2\, d\Omega_{n_1} du_1$, where $d\Omega$ is the solid angle element (see Figure 10), we get

$$\begin{aligned}\Phi_2(u_2,n(\rho_2)) &= \int_{\Omega} \int_{E(\vec{n}_1)} W(u_1)\Lambda(n_1,n(\rho_2))W(u_2)\Lambda(n_2,n_1) \\ &\qquad , e^{i\frac{\omega}{c}n(\rho_2)\cdot n_1 u_1}\, u_1\, d\Omega_{n_1} du_1 \\ &= W(u_2) \int_{\Omega} \Lambda(n_1,n(\rho_2))\Lambda(n_2,n_1) \\ &\quad \cdot \Big[\int_{E(\vec{n}_1)} W(u_1)\, u_1^2\, e^{i\frac{\omega}{c}n(\rho_2).n_1 u_1} du_1 \Big]\, d\Omega_{n_1}\end{aligned} \tag{6.8}$$

where Ω is the whole solid angle space, $E(n)$ is the set, which consists of those points in the direction of n_1 and outside the region D_o. The integral limit $\int_{E(n)}$ usually can be replaced by the simpler form $\int_{R(n)}$ if every half radial line has only one intersection point with the surface of region D_o.

Obviously, the integral in the square brackets in (6.9) is a function of n_1 and $n(\rho_2)$, and is independent of u_1. Therefore, let

$$U(n_1,n(\rho_2)) = \int_{E(n_1)} W(u_1)\, u_1^2\, e^{i\frac{\omega}{c}n(\rho_2).n_1 u_1}\, du_1 \tag{6.9}$$

and (6.8) becomes

$$\Phi_2(u_2,n(\rho_2)) = W(u_2)\Lambda_2(n_2,n(\rho_2)), \tag{6.10}$$

where

$$\Lambda_2(n_2,n) = \int_{\Omega} \Lambda(n_1,n)U(n_1,n)\Lambda(n_2,n_1)\, d\Omega_{n_1}, \tag{6.11}$$

or

$$\Lambda_2(n_2,n) = \int_{\Omega} \Lambda_1(n_1,n)\Lambda(n_2,n_1)\, d\Omega_n, = (\Lambda_1 *_\theta \Lambda)(n_2,n) \tag{6.12}$$

if we let

$$\Lambda_1(n_1,n) = \Lambda(n_1,n)\ U(n_1,n). \tag{6.13}$$

If the integral in (6.12) is called "angular convolution of Λ_1 and Λ, and denoted by symbol $*_\theta$, then (6.12) can be written as

$$\Lambda_2 = \Lambda_1 *_\theta \Lambda = (\Lambda U) *_\theta \Lambda \tag{6.14}$$

Substituting (6.7) and (6.10) into (6.14), using the similar steps, finally, we get

$$\Phi_3(u_3,n(\rho_3)) = W(u_3)\Lambda_3(n_3,n(\rho_3)), \tag{6.15}$$

where

$$\Lambda_3(n_3,n) = \int_{\Omega} \Lambda_2(n_2,n)U(n_2,n)\Lambda(n_3,n_2)\, d\Omega_{n_2} \tag{6.16}$$

$$= [(\Lambda_2 U) *_\theta \Lambda](n_3,n),$$

or

$$\Lambda_3 = (\Lambda_2 U)*_\theta \Lambda, \tag{6.17}$$

$$\Lambda_3 = \{[(\Lambda U)*_\theta \Lambda]U\}*_\theta \Lambda, \tag{6.18}$$

Similarly, it can be proved that

$$\Phi_4(u_4, n(\rho_4)) = W(u_4)\Lambda_4(n_4, n) \tag{6.19}$$

and

$$\Lambda_4 = (\{[(\{\Lambda U\}*_\theta \Lambda)U]*_\theta \Lambda\}U)*\Lambda \tag{6.20}$$

going on in the same way, until m, we get

$$\Phi_m(u_m, n) = W(u_m)\Lambda_m(n_m, n), \tag{6.21}$$

and

$$\Lambda_m(n_m, n) = \int_\Omega \Lambda_{m-1}(n_{m-1}, n)U(n_{m-1}, n)\Lambda(n_m, n_{m-1})d\Omega n_{m-1}, \tag{6.22}$$

$$\Lambda_m = (\cdots(\Lambda U)*_\theta \Lambda)U)*_\theta \Lambda)\cdots U)*_\theta \Lambda \tag{6.23}$$

Let us define a linear operator L such that

$$L\, f = (fU)*_\theta \Lambda \tag{6.24}$$

Then

$$\Lambda_m = L \cdots L\, \Lambda = L^{m-1}\Lambda \tag{6.25}$$

In the separation expression of Φ, (6.7), $W(u_1)$ is called attenuation function, and $\Lambda\ (n_1, n)$ to be dimensionless and normalized, that is

$$\int_\Omega \Lambda(n_1, n)d\Omega n_1 = 1 \tag{6.26}$$

Now let

$$A = \int_{R_0} |W(u_1)| u_1^2 \, du_1 \tag{6.27}$$

Then from (6.9),

$$|U(n_1,n)| \leq A, \ \forall \ n_1, \ n\epsilon\Omega$$

Define

$$U_0(n_1,n) = \frac{1}{A} \int_{E(n_1)} W(u_1) u_1^2 \, e^{i\frac{\omega}{c} n,n_1 u_1} \, du_1 \tag{6.28}$$

then

$$U_0(n_1,n) = \frac{1}{A} U(n_1,n) \quad U(n_1 n) = A U_0(n_1,n) \tag{6.29}$$

Then $U_0(n_1,n)$ is dimensionless and

$$|U_0(n_1,n)| \leq | \quad \forall \ n,n\epsilon\Omega \tag{6.30}$$

We define another linear operator $\mathcal{L}_0$ such that

$$\mathcal{L}_0 f = (U_0 f) *_\theta \Lambda \tag{6.31}$$

Then

$$\mathcal{L} f = A \mathcal{L}_0 f \tag{6.32}$$

$$\Lambda_m = A^{m-1} \, {}^{m-1}_{0}\Lambda \tag{6.33}$$

$$\Phi_m(u_m,n(\rho_m)) = A^{m-1} W(u_m) (\mathcal{L}_0^{m-1}\Lambda)(n_m,n(\rho_m)) \tag{6.34}$$

With the help of (6.26) and (6.30), from (6.12), (6.13), (6.16), (6.22) and (6.33), it can be proved that

$$\int_\Omega \Lambda_2(n_2 n) d\Omega_{n_2} \leq A, \quad \forall \ n \ \epsilon\Omega, \tag{6.35}$$

$$\int_{\Omega} \Lambda_3(n_3,n)\,d\Omega_{n_3} \leq A^2, \quad \forall\ n\in\Omega, \tag{6.36}$$

$$\int_{\Omega} \Lambda_m(n_{m_1} n)\,d\Omega_{n_m} \leq A^{m-1} \quad \forall\ n\in\Omega \tag{6.37}$$

Therefore

$$\int_{\Omega} (\mathcal{L}_0^{m-1}\Lambda)(n_{m_1} n)\,d\Omega_{n_m} \leq 1 \quad , \quad \forall\ n\in\Omega \tag{6.38}$$

This shows that, $\mathcal{L}_0^m$ is a bounded operator when $m\to\infty$, and the norm $\mathcal{L}_0^{m-1}\Lambda$ is also bounded. On the other hand, convolution always expands the domain of the function and makes it more uniform and flat. Successive convolution always makes a function more and more uniform and finally makes it tend to a constant. Therefore, it is reasonable to regard $\mathcal{L}_0^{m-1}\Lambda$ as a constant

$$\lim_{m\to\infty} \mathcal{L}_0^{m-1}\Lambda = a \ , \tag{6.39}$$

and (6.34) becomes

$$\lim_{m\to\infty} \Phi_m(u_m, n(\rho)) = a\, A^{m-1}\, W(u_m). \tag{6.40}$$

Applying (6.34) to (6.5), finally, we get

$$K_p^{(a)}(r_1,r_2) = \sum_{m=1}^{\infty}\sum_{n=1}^{\infty} \int_{R_3} \psi^*(\rho) A^{m-1} W^*(|n-\rho|)(\mathcal{L}_0^{m-1}\Lambda)^*\left(\frac{n-\rho}{|n-\rho|}\, n(\rho)\right) d\rho$$

$$\int_{R_3} \psi(\rho')\nu^n(\rho') A^{n-1} W(|r_2-\rho'|)(\mathcal{L}_0^{n-1}\Lambda)\left(\frac{r_2-\rho'}{|r_2-\rho'|}\ ,\ n(\rho')\right) d\rho' \tag{6.41}$$

This is the final required result. From this expression, it is easy to see that, the convergence of this infinite series mainly depends on the attenuation function W(u) of each single scatterer and the volume density function $\nu(\rho)$ of the scatterers in view of the convergence of $\mathcal{L}_o^m\Lambda$ and the expression (6.27) of A.

Derivation of $k_p^{(c)}(r_1, r_2)$ and $k_p(r_1, r_2)$

In deriving $k_p^{(c)}(r_1, r_2)$, and also neglect the contribution of those terms, where $\{j_1, \ldots, j_m\}$ has repeat elements. Then from (6.5),

$$K_p^{(c)}(r_1, r_2) = \sum_{m=1}^{N} N(N-1)(N-2)\ldots(N-(m-1))\, K_{j_1\ldots j_m}(r_1, r_2)$$
$$= \sum_{m=1}^{N} \{ \prod_{k=1}^{m} [N-(m-k)] \}\, K_{j_1\ldots j_m}(r_1, r_2). \tag{6.44}$$

Substituting (5.63) into (6.44), changing N into ∞ in the upper limit of summation for sufficient charge N, we have

$$K_p^{(c)}(r_1, r_2) = \sum_{m=1}^{\infty} \int_{R_3} |\psi(\rho)|^2 \gamma^m(\rho) \Psi_{mc}(r_1-\rho, r_2-\rho, k(\rho))\, d\rho \tag{6.45}$$

Because in this paper, only monochromatic waves are considered, so the variable k can be replaced by the unit vector $n = k/k$ in the function $\Gamma(u_1, k, \theta)$. Usually $\Gamma(u_1, n\ \theta)$ is separable, i.e. one can set

$$\Gamma(u_1, n, \theta) = W(u_1)\, \Lambda_\theta(n_1, n, \theta), \tag{6.46}$$

where $\Lambda_\theta(n_1, n, \theta)$ is dimensionless and normalized and $n_1 = u_1/u$, $u_1 = u_1$ Substituting (6.46) into (5.45) and (5.46), one has

$$\Psi(u_1, n) = |W(u_1)|^2\, L(n_1, n), \tag{6.47}$$

$$\Psi_c(u_1, u_2, n) = W^*(u_1)\, W(u_2)\, K_\Lambda(n_1, n_2, n), \tag{6.48}$$

where

$$L(n_1, n) = \int_\Theta |\Lambda_\theta(n_1, n, \theta)|^2 f_\theta(\theta)\, d\theta, \tag{6.49}$$

$$K_\Lambda(n_1, n_2, n) = \int_\Theta \Lambda_\theta^*(n_1, n, \theta)\, \Lambda(n_2, n, \theta)\, f_\theta(\theta)\, d\theta \tag{6.50}$$

From (5.7) and (6.7)', we have

$$\Lambda(n_1, n) = \int_\theta \Lambda_\theta(n_1, n, \theta)\, f_\theta(\theta)\, d\theta \tag{6.51}$$

Applying (6.47) to (5.51), one has

$$\Psi_2(u_2,\ n(\rho_2)) = \int_\Omega \int_{E(\ )} |W(u_1)|^2\ L(n_1, n(\rho_2)\, |W(u_2)|^2\ L(n_2,\ n_1)$$

$$u_1^2\ d\Omega n_1\ du_1 = |W(u_2)|^2 \int_\Omega L(n_1,\ n(\rho_2))\ L(n_2,\ n_1).$$

$$\cdot \left[\int_{E(n_1)} |W(u_1)|^2\ u_1^2\ du_1\right] d\Omega n_1 \qquad (6.52)$$

Let

$$V(n_1) = \int_{E(n_1)} |W(u_1)|^2\ u_1^2\ du_1 \qquad (6.53)$$

The (6.52) becomes

$$\Psi_2(u_2,\ n(\rho_2)) = |W(u_2)|^2\ L_2(n_2,\ n(\rho_2)) \qquad (6.54)$$

where

$$L_2(n_2,\ n) = \int_\Omega L(n_1,\ n)\ V(n_1)\ L(n_2,\ n_1)\ d\Omega n_1 \qquad (6.55)$$

Let

$$L_1(n_1, n) = L(n_1,\ n)\ V\ (n_1). \qquad (6.56)$$

Then (6.57)

$$L_2(n_2,\ n) = \int_\Omega L_1(n_1,\ n)\ L(n_2,\ n_1)\ d\Omega n = (L_1\ *_\theta\ L)(n_2,\ n),$$

and

$$L_2 = L_1\ *_\theta\ L = (LV)\ *_\theta\ L$$

By the similar way, with Section 6.1, one can get

$$\Psi_3(u_3,\ n(\rho_3)) = |W(u_3)|^2\ L_3(n_3,\ n(\rho_3)) \qquad (6.58)$$

where

$$L_3(n_3,\ n) = \int_\Omega L_2(n_2,\ n)\ V(n_2)\ L(n_3,\ n_2)\ d\Omega n_2 \qquad (6.59)$$

and

$$L_3 = (L_2 V) *_\theta L = \{[(LV) *_\theta L] V\} *_\theta L \tag{6.60}$$

Going on in this way, finally, we get

$$\Psi_{m-1}(u_{m-1}, n(\rho_{m-1}) = |W(u_{m-1})|^2 L_{m-1}(n_{m-1}, n(\rho_{m-1})), \tag{6.61}$$

where

$$L_{m-1}(n_{m-1}, n) = \int_\Omega L_{m-2}(n_{m-2}, n) V(n_{m-2}) L(n_{m-1}, n_{m-2}) d\Omega n_{m-2} \tag{6.62}$$

and

$$L_{m-1} = (\underbrace{\cdots(LV) *_\theta L) V) *_\theta L) \cdots V}_{m-1}) *_\theta L \tag{6.63}$$

Define a linear operator $\mathcal{M}$ as

$$\mathcal{M} f = (Vf) *_\theta L \tag{6.64}$$

then

$$L_{m-1} = \underbrace{\mathcal{M} \cdots \mathcal{M}}_{m-2} L = \mathcal{M}^{m-2} L \tag{6.65}$$

Substituting (6.61) and (6.48) into (5.61), we have

$$\begin{aligned}
&\Psi_{mc}(u'_m, u''_m, n(\rho_m)) \\
&= \int_\Omega \int_{E(n_{m-1})} |W^2(u_{m-1})|^2 L_{m-1}(n_{m-1}, n(\rho_m)) W^*(u'_m) W(u''_m) \\
&\quad K_\Lambda(n'_m, n''_m, n_{m-1}) e^{i2\frac{\omega}{c} n(\rho_m) n_{m-1} u_{m-1}} u^2_{m-1} d\Omega n_{m-1} \cdot du_{m-1} \\
&= W^*(u'_m) W(u''_m) \int_\Omega L_{m-1}(n_{m-1}, n(\rho_m)) V(n_{m-1})) \cdot K_\Lambda(n'_m, n''_m, n_{m-1}) d\Omega n_{m-1}
\end{aligned} \tag{6.66}$$

Let

$$\begin{aligned}
L_k(n', n', n) &= \int_\Omega L_{m-1}(n_{m-1}, n) V(n_{m-1},) \cdot K_\Lambda(n', n'', n_{m-1}) d\Omega n_{m-1} \\
&= [(L_{m-1} V) *'_\theta K_\Lambda] (n', n', n)
\end{aligned} \tag{6.67}$$

Then

$$\Psi_{mc}\ (u_m', u_m'', n(\rho_m)) = W^*(u_m')\ W(u_m'')\ L_k\ (n_m', n_m'', n(\rho_m)), \tag{6.68}$$

$$L_k = [(M^{m-2}L)V] *_\theta' K_\Lambda \tag{6.69}$$

Here $*_\theta'$ is called angular convolution of the second kind, and defined as

$$(\varphi_1 *_\theta' \varphi_2)\ (n', n'', n) = \int_\Omega \varphi_1(n_1, n)\ \varphi_2(n', n'', n_1)\ d\Omega n_1 \tag{6.70}$$

Applying (6.68) and (6.69) to (6.45), using (6.3), (6.14) and the analysis about $K_p^{(b)}(r_1, r_2)$ we get the final result:

$$K_p(r_1, r_2) = \sum_{m=1}^{\infty} \int_{R_3} |\psi(\rho)|^2 \gamma^m(\rho)\ W^*\ (|r_1-\rho|)\ W\ (|r_2-\rho|)$$

$$.\{[\mathcal{M}^{m-2}L)V] *_\theta' K_\Lambda\}\ (\frac{r_1-\rho}{|r_1-\rho|}\ ,\ \frac{r_2-\rho}{|r_2-\rho|}\ ,\ n(\rho))\ d\rho + M_r^*\ (r_1)\ M_r(r_2) \tag{6.71}$$

where

$$M_r(r) = \sum_{m=1}^{\infty} \int_{R_3} \psi(\rho)\gamma^m(\rho)A^{n-1}W(|r-\rho|)(L_0^{n-1}\ \Lambda)(\frac{r-\rho}{|r-\rho|}\ ,\ n(\rho))\ d\rho \tag{6.72}$$

If we define normalized attenuation function $W_o(u)$ and normalized V function as

$$W_0(u) = \frac{1}{A}\ W(u)\ ,\quad V_0(n_1) = \frac{1}{A^2}\ V(n_1), \tag{6.73}$$

and normalized linear operator M_0 as

$$\mathcal{M}_0 f = (V_0 f) *_\theta L \tag{6.74}$$

then

$$V_0(n_1, n) = \int_{E(n_1)} |W_0(u_1)|^2 u_1^2\ du_1 \tag{6.74}$$

$$\mathcal{M} = A\,\mathcal{M}_0 \tag{6.75}$$

and (6.71) and (6.72) become

$$K_p(r_1, r_2) = \sum_{m=1}^{\infty} A^{2m} \int_{R_3} |\psi(\rho)|^2 \gamma^m(\rho)\, W_0^*(|r_1-\rho|) W_0(|r_2-\rho|$$

$$\cdot\{[(\mathcal{M}_0^{m-2} L) V_0] *_\theta' K_\Lambda\}\left(\frac{n-\rho}{|n-\rho|}, \frac{r_2-\rho}{|r_2-\rho|}, n(\rho)\right) d\rho + M_p^*(n) M_p(r_2) \qquad (6.76)$$

where

$$M_p(r) = \sum_{m=1}^{\infty} A \int_R \psi(\rho)\gamma^m(\rho) W_0(|r-\rho|)\, (\mathcal{L}_0^{n-1}\Lambda)\left(\frac{r-\rho}{|r-\rho|}, n(\rho)\right) d\rho \qquad (6.77)$$

It can be proved that $M_p(r)$ is just the mathematical expectation of random field p(r), ie

$$M_p(r) = \mathcal{E}\{p(r)\} \qquad (6.78)$$

Setting $r_1 = r_2 = r$ in (6.76), we get the general expression of entensity of multiple scattered field defined by

$$M_p^{(2)}(r) = \mathcal{E}\{p^2(r)\} = K_p(r,r) \qquad (6.79)$$

Seeing that

$$K_\Lambda(n_1, n_1, n) = L(n_1, n) , \qquad (6.80)$$

We get

$$M_p^{(2)}(r) = \sum_{m=1}^{\infty} A^{2m} \int_{R_3} |\psi(\rho)|^2 \gamma^m(\rho) |W_0(|r-\rho|)|^2$$

$$\cdot(\mathcal{M}_0^{m-1} L)\left(\frac{r-\rho}{|r-\rho|}, n(\rho)\right) d\rho + |M_p(r)|^2 \qquad (6.81)$$

Expressions (6.76), (6.81) and(6.77) are the general expression of the space correlation function, intensity and mathematical expectation of multiple scattered field p(r) (complex amplitude) respectively.

We can prove that the linear operator $\mathcal{M}_0^m$ is also bounded as $m \to \infty$, and

$$\lim_{m\to\infty} \mathcal{M}_0^m L = b,$$

b is a constant, which is independent of n_1 and n. Therefore, the convergence of the summation in (6.76) and (6.81) mainly depends on the density function $\gamma(\rho)$ and the constant A (which is just similar or proportional to the so called "scattering cross section").

Conclusion

The general expressions of the space correlation function, intensity and mathematical expectation of the (complex amplitude of) multiply scattered field caused by randomly distributed scatterers of any shape, any volume density distribution and any orientation distribution, excited by an arbitrary monochromatic incident wave are obtained and shown in (6.76), (6.81) and 6.77) respectively. These expressions in their series form show the dependence of the space correlation function, intensity and mathematical expectation of multiply scattered field on all of the following factors:

1. the complex amplitude of incident wave $\psi(r)$,
2. the volume distribution density of scatterers $\nu(r)$,
3. the constant A defined in (6.27) and (6.46), which denotes the scattering cross section of each scatterer and the total attenuation,
4. the directivity function Λ_θ (n_1, n, θ) [see (6.46)] through Λ (n_1, n) [see (6.51)], L (n_1, n) [see (6.49)] k_Λ (n_1, n_2, n) [see (6.50)], and the linear operators $\mathcal{L}_o$ and $\mathcal{M}_o$ defined by (6.74), (6.73), (6.53), (6.31), (6.29) and (6.9), and finally
5. the attenuation function $W_o(u)$ defined by (6.73) and (6.46),

where the angular convolution operation $*_\theta$ and $*'_\theta$ are defined by (6.57) and (6.70) respectively. As long as these factors are given, the space correlation function, intensity and mathematical expectation of the multiple scattered field can be calculated through a single summation, a single volume integration and a successive convolution operation.

The space correlation function, the intensity and the mathematical expectation of the multiply scattered field strongly depend on i) the volume density function $\gamma(r)$ of scatterers and ii) the constants A (including the

1. INTRODUCTION

At any point in a random medium, the total wave fields can be considered as a sum of two components, viz, a coherent or an average wave and an incoherent component due to change in scatterer positions and states from configuration to configuration. The averages of the square of magnitude of the coherent and incoherent fields are called the coherent and incoherent intensities, respectively. For a plane wave incident on a medium containing a random distribution of scatterers, the coherent intensity attenuates due to scattering and absorption. Incoherent scattering effects introduce 'noise' into the system and cause fluctuations in the coherent amplitude and phase. In many practical applications, it is important to assess the incoherent scattered intensity relative to the total intensity in order to relate theoretical and experimental results. Propagation of the coherent wave is generally expressed in terms of a bulk propagation coefficient characterizing the scatterer filled medium[1-6]. Incoherent effects are usually determined by solving 'approximate' integral equations or by solving special forms of the radiative transfer equations.[7] Such formulations are generally valid under conditions of sparse concentrations and for weak multiple scattering for either Rayleigh scatterers or large scatterers which scatter primarily in the forward direction. To overcome such limitations, a propagator model has been presented for studying both coherent and incoherent intensities in Ref. 8. Lax's quasi-crystalline approximation (QCA) with suitable averaging techniques and the T-matrix of a single scatterer has been employed in the analysis. Pair correlation functions generated by Monte-Carlo simulation have been used in the computation.

ABSTRACT

This paper treats discrete scatterers randomly distributed in a host medium as a random medium with discontinuous property. First, the wave equation with random discontinuous coefficient is reduced to a random integral equation of Fredholm type and its solution is obtained in terms of Neumann series. Then, the expressions of the mean value, mean square value and the space correlation function of the scattered field are obtained in terms of the space correlation function or space spectrum of the random field $\beta(\vec{r},\omega)$ which depends on the properties, shape, size and concentration of scatterers and the properties of the surrounding medium For spherical scatterers, the space correlation function is obtained, and the mean square value of the scattered field is expressed as a function of concentration of scatterers. The results obtained by the present theory are compared with some available experimental results.

WAVE SCATTERING IN RANDOM MEDIA BY METHOD OF DISCONTINUOUS STOCHASTIC FIELD

by

K. C. Liu, V. V. Varadan and V. K. Varadan
Wave Propagation Lab
Department of Engineering Science and Mechanics
The Pennsylvania State University, University Park, PA 16802

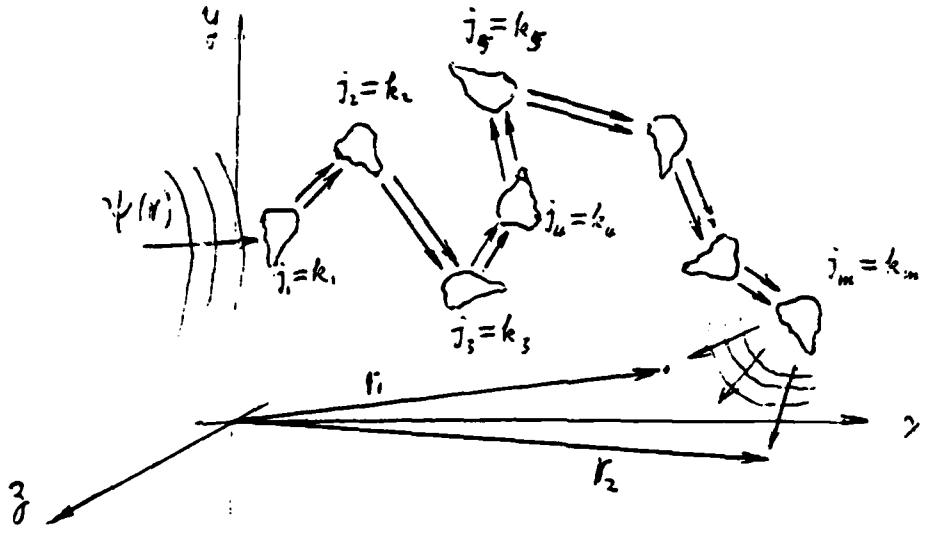

Figure 10. completed overlaped two paths of successive scattering

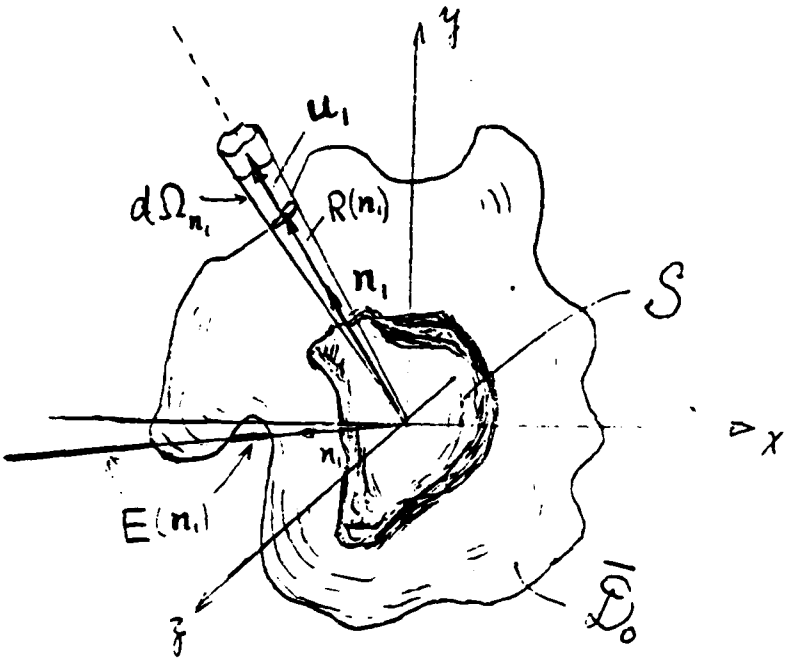

Figure 11. Relationship of domain S, domain $\bar{\Omega}_0$, set $E(n_1)$, vectors u_1 on n_1

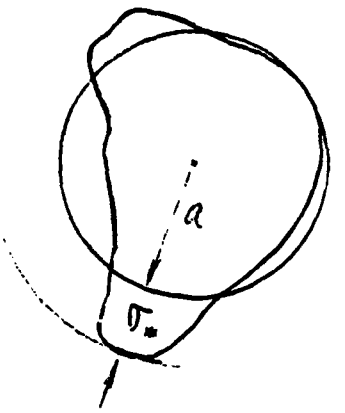

Figure 8. Comparison of a scatterer with arbitrary ~~shape~~ shape with a sphere of same volume, ~~and~~

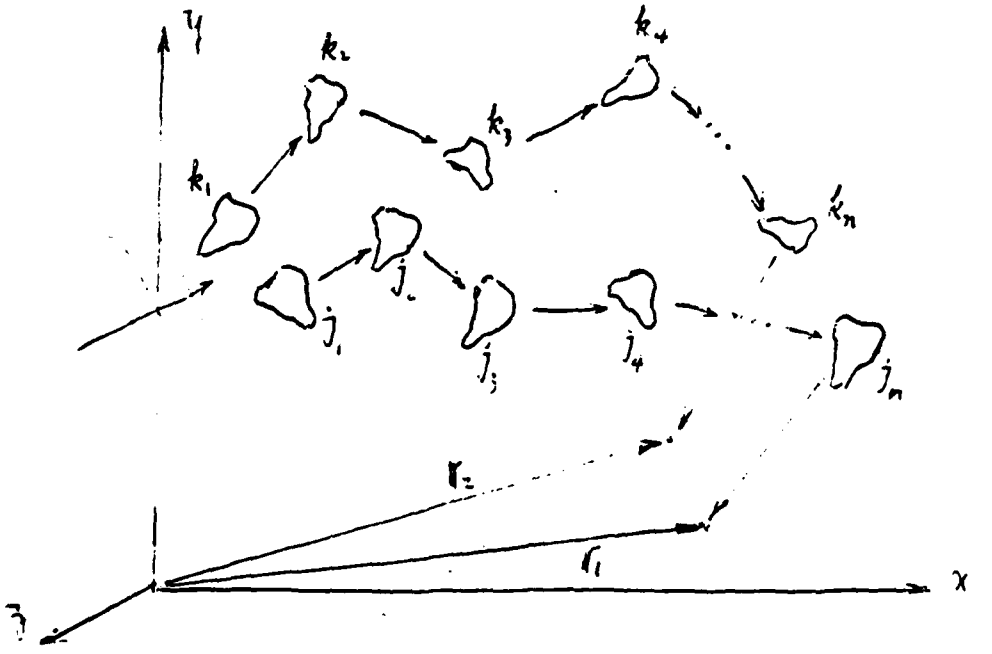

Figure 9. Two ~~sca~~ paths of successive scattering without overlap

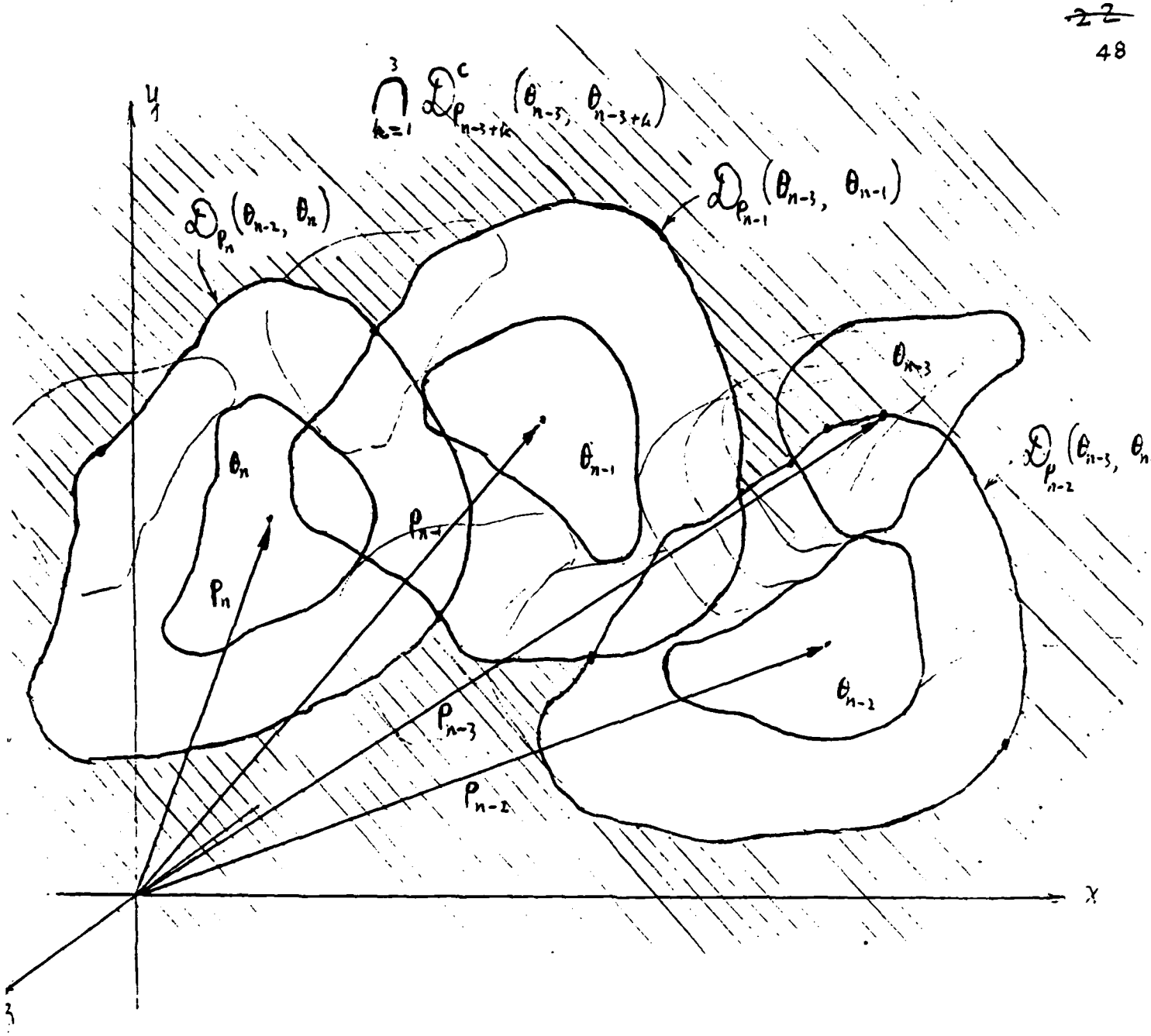

Figure 7

Figure 7. ~~Relation~~ Relative spatial relationship of three scatterers and the formation of $\bigcap_{k=1}^{3} \mathcal{D}^{c}_{\rho_{n-3+k}}(\theta_{n-3}, \theta_{n-3+k})$.

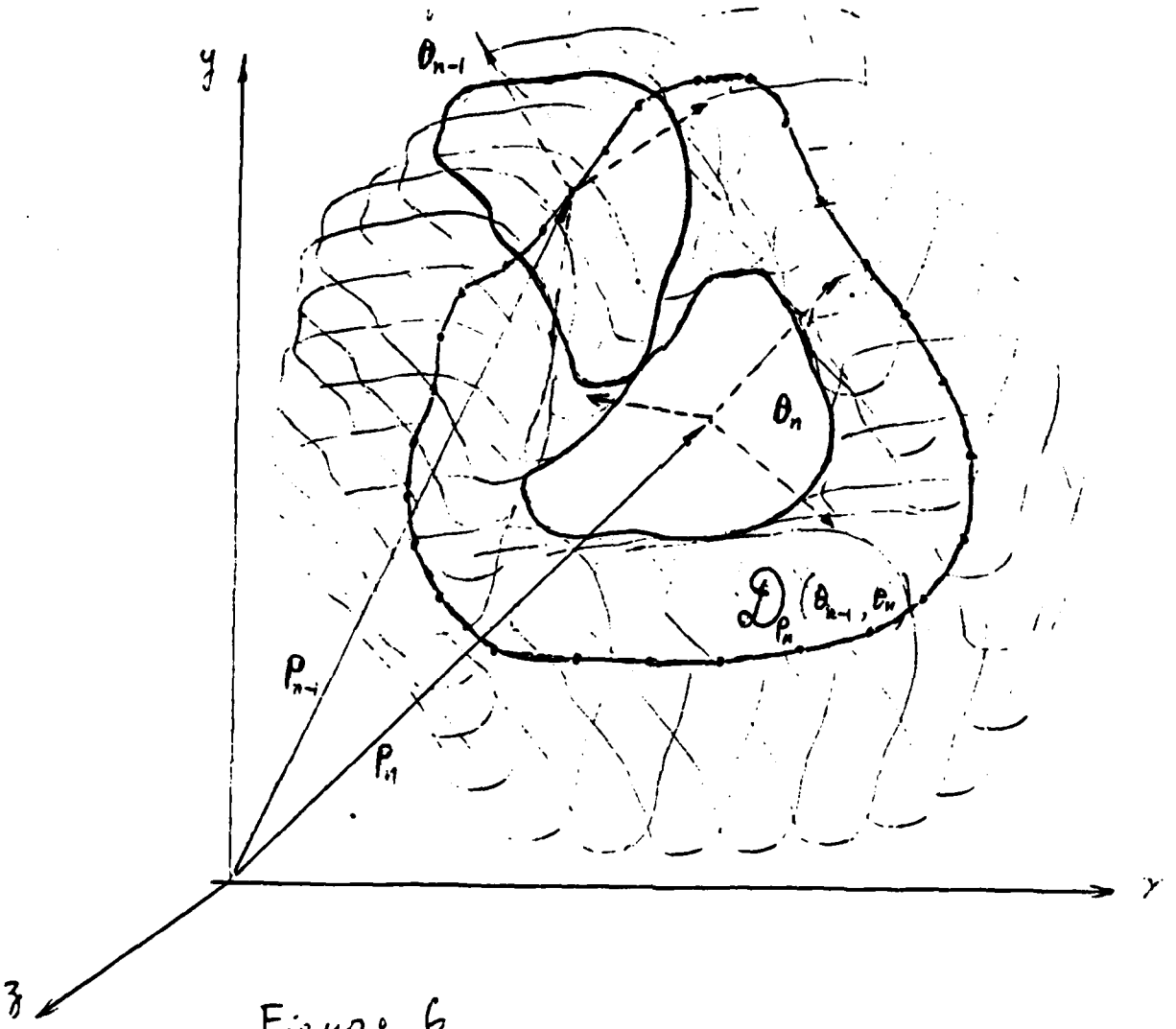

Figure 6

Figure 6. Spatial relative relation between two scatterers and the formation of domain $\mathcal{D}_{\rho_n}(\theta_{n-1}, \theta_n)$

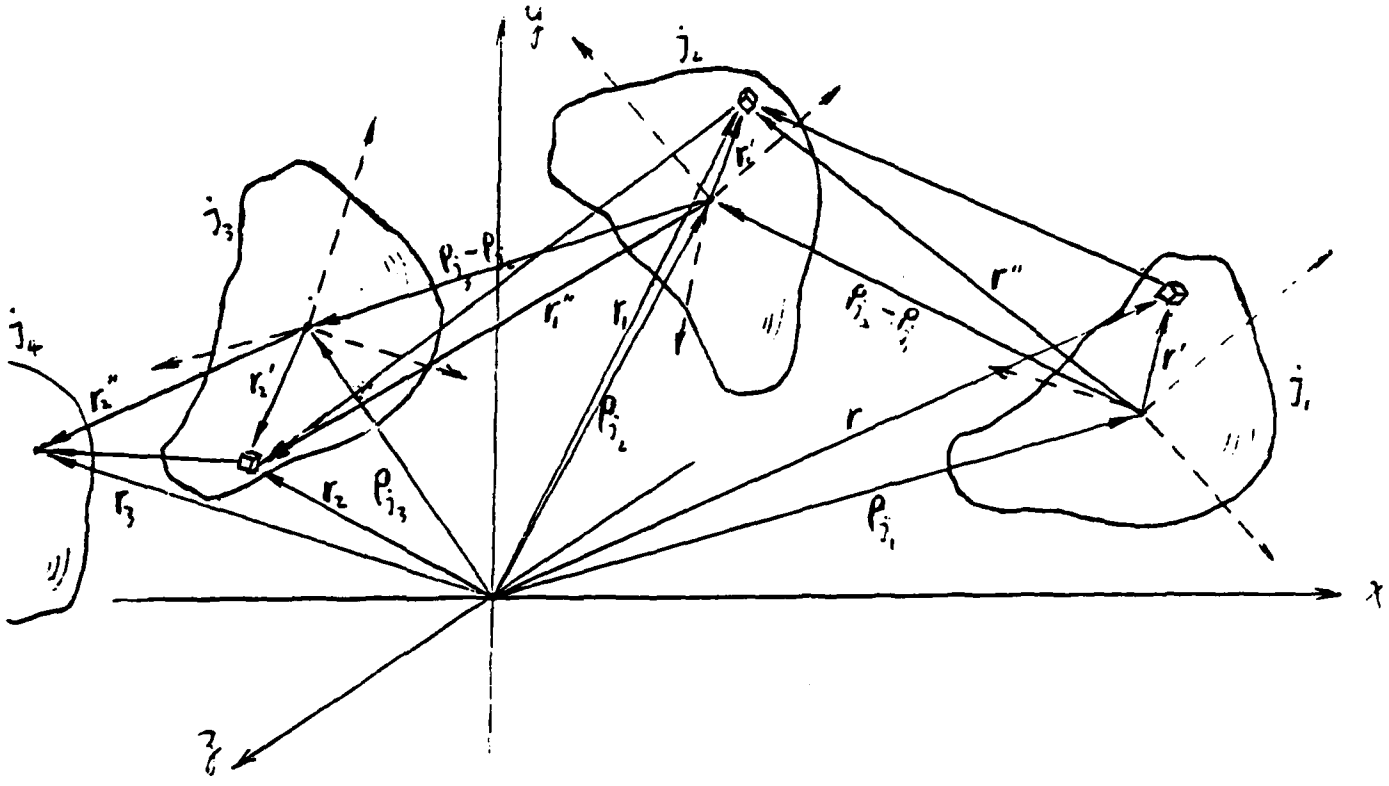

Figure 5. Successive scattering of scatterers and their equivalent systems

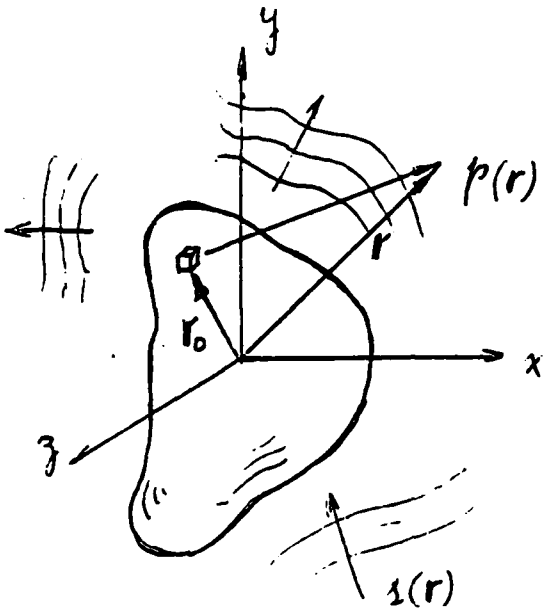

Figure 3. Single scatterer and its equivalent system under arbitrary monochromatic incident wave.

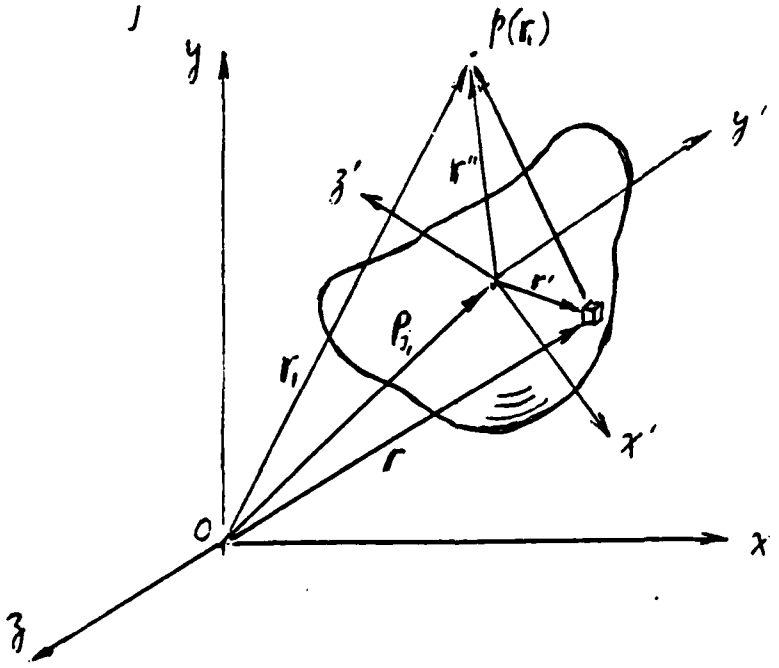

Figure 4. Single scatterer and its equivalent system with arbitrary location and orientation.

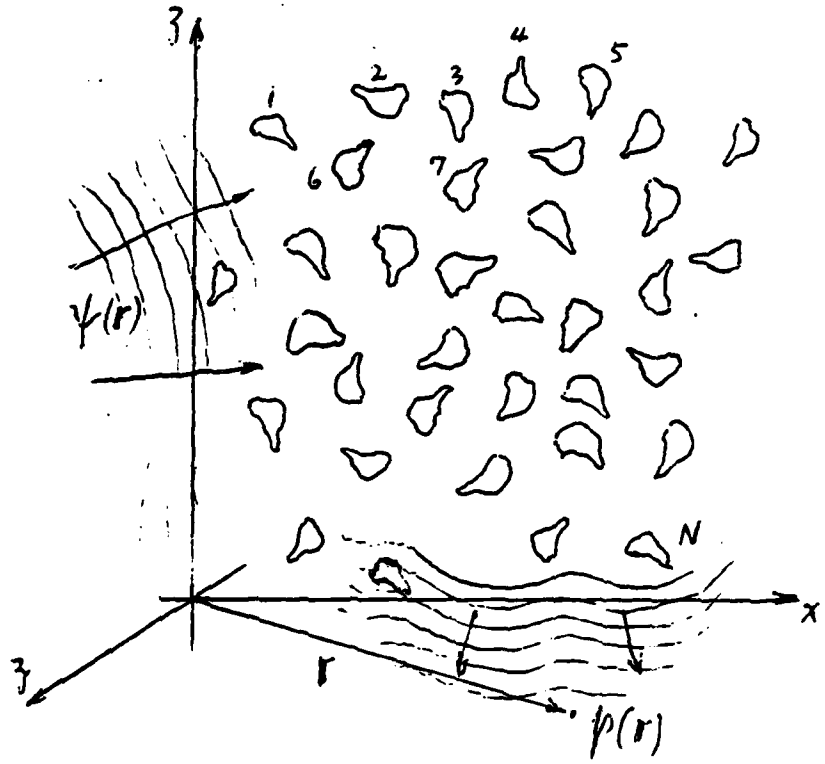

Figure 1. Randomly distributed scatterers with arbitrary monochromatic incident wave

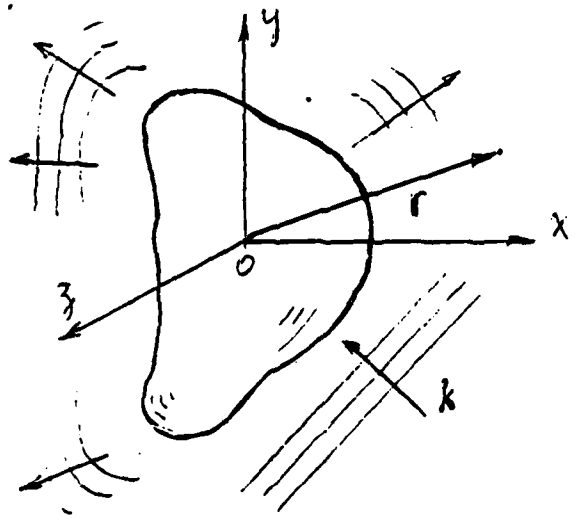

Figure 2. Single scatterer with arbitrary shape ~~and~~ under plane incident wave

9. Twersky, V., "On Scattering of Waves by Random Distributions," I. Free-space scatterer formalism, 1962 Journal of Mathematical Physics 3, 700-715.

10. Twersky, V., "On Scattering of Waves by Random Distributions," II. Two-space Scatterer Formalism, 1962 Journal of Mathematical Physics 3, 724-734.

11. Twersky, V., On Propagation in Random Media of Discrete Scatterers," 1964 in Proceedings of Symposium in Applied Mathematics (Providence, R. I. American Mathematical Society) 16, 84-116.

12. Sibul, L. H., Information Linkage between Applied Mathematics and Industry, 1979 ISBN 0-12-734050-8, Academic Press Inc., 617-631. Stochastic Green's Functions and Scattering Functions.

13. Chow, P. L., Kohler, W. E. and Papanicolaou, G. C., Multiple Scattering and Waves in Random Media, 1981, Amsterdam - New York, Oxford: North-Holland Publishing Company.

REFERENCES

1. Liu, K. C., "Spatial Stochastic Systems Theory and its Application to Fields and Waves in Random Media," 1981 Journal of Sound and Vibration 79, 321-339, I. General Theory.
2. Liu, K. C., "Spatial Stochastic Systems Theory and its Application to Fields and Waves in Random Media," II. Preliminary Application to Scattering and Reverberation, 1982 Journal of Sound and Vibration 80, 473-498.
3. Liu, K. C., "Spatial Stochastic Systems Theory and its Application to Fields and Waves in Random Media," III. Generalized Convolution and System Decomposition.
4. Varadan, V. K. and Varadan, V. V., Acoustic, Electromagnetic and Elastic Wave Scattering - Focus on the T-Matrix Approach, 1980, Pergamon Press.
5. Varadan, V. K., "Scattering of Elastic Waves by Randomly Distributed and Oriented Scatterers," 1979 Journal of the Acoustical Society of America, 65, 655- .
6. Varadan, V. K., Varadan, V. V. and Pao, Y. H., "Multiple Scattering of Elastic Waves by Cylinders of Arbitrary Cross Section," I. SH-waves, 1978 Journal of the Acoustical Society of America 63, 1310.
7. Varatharajulu, V. V. (Varadan) and Vezzetti, D. J., "Approach of the Statistical Theory of Light Scattering to the Phenomenological Theory," 1976 Journal of Mathematical Physics 17, 232.
8. Bringi, V. N., Siliga, T. A., Varadan, V. K. and Varadan, V. V., "Bulk Propagation Characteristics of Discrete Random Media," 1981 in Multiple Scattering and Waves in Random Media (Editors P. L. Chow, W. E. Kohler and G. C. Papanicolaou), Amsterdam, New York. Oxford: North-Holland Publishing Company.

ACKNOWLEDGMENTS

This work was supported by the U.S. Army Research Office under contract No: DAAG29-83-K-0097. The authors are grateful to Dr. R. P. Kanwal and Dr. L. H. Sibul for their suggestions and comments.

contribution of the "scattering cross section and the attenuation) of each single scatterer, and weakly depend on the directivity function Λ (n_1, n, θ) of each scatterer. In other words, the size and density of the scatterers play much more important role than the shape and orientation. This is reasonable from the physical concept.

In this paper, we propose an alternative approach of adopting a contemporary field of mathematics in solving the classical problem of discrete random media. We treat the discrete random media as a random medium with discontinuous property. First, the wave equation with random discontinous coefficient is reduced to a random integral equation of Fredholm type and its solution is obtained in terms of Neumann series. Then, the expressions of the mean value, mean square value and the space correlation function of the scattered field are obtained in terms of the random field $\beta(\vec{r},\omega)$ which depends on the properties, shape, size and concentration of scatterers and the properties of the surrounding medium. For spherical scatterers, the space correlation function is obtained, and the mean square of the scattered field is expressed as a function of concentration of scatterers. The results obtained using this approach are also compared with some available experimental results.

The advantage of the present approach are : a) it is applicable over a wide range of concentration of scatterers (from very low to closest packing), b) the scattering property of a single scatterer is not needed; the discontinuous stochastic field $\beta(\vec{r},\omega)$ and the space correlation function $K_\beta(\vec{r},\omega)$ play important role which depend on the shape and size of each scatterer and the concentration σ of scatterers. For simplicity, we first present the theory only for scalar problem. The vector problem will be studied in our subsequent reports. For general electromagnetic wave scattering problem, we follow the steps outlined in Varadan[9].

2. DISCONTINUOUS STOCHASTIC FIELD $\beta(\vec{r},\omega)$

We consider a random distribution of a large number of identical correlated scatterers embeded with a region R in a homogeneous matrix medium. The wave speeds in the scatterer and the matrix are denoted by c_1 and c_2, respectively. Let S denotes the region occupied by a scatterer. If we define the random field $c(\vec{r},\omega), r \in R_3, \omega \in \Omega$ as follows

$$c(\vec{r},\omega) = \begin{cases} c_1 , & \vec{r} \in S \\ c_2 , & \vec{r} \notin S \end{cases} \qquad (1)$$

where R_3 is ordinary 3-dimensional space, Ω is the probability space, then the total wave field $p(\vec{r},\omega,t)$ will satisfy the random wave equation with random coefficient $c(\vec{r},\omega)$:

$$\nabla^2 p(\vec{r},\omega,t) - \frac{1}{c^2(\vec{r},\omega)} \frac{\partial^2}{\partial t^2} p(\vec{r},\omega,t) = 0 \qquad (2)$$

Here, the position vector $\vec{r}$ can either be inside or outside the scatterer.

We assume that the size of R is much larger than the size of each scatterer, and $c(\vec{r},\omega)$ is a homogeneous (stationary) stochastic field in R. The one dimensional probability distribution density $c(\vec{r},\omega)$ may then be given by

$$f_c(x,\vec{r}) = \sigma\delta(x-c_1) + (1-\sigma)\delta(x-c_2) = f_c(x) \qquad (3)$$

where $\delta(\ )$ is the Dirac Delta function and σ is the concentration of scatterers.

Now, we define another discontinuous stochastic field $\beta(\vec{r},\omega)$ as follows

$$\beta(\vec{r},\omega) = \frac{c_0^2}{c^2(\vec{r},\omega)} - 1 \quad , \quad \vec{r} \in R \qquad (4)$$

where c_0 is a constant defined by

$$c_0 = c_1 c_2 / (\sigma c_2^2 + (1-\sigma) c_1^2)^{1/2} \qquad (5)$$

Physically, c_0 is some kind of mean value of $c(\vec{r},\omega)$. Then, it is easy to show that the mean or expected value of $\beta(\vec{r},\omega)$ is zero, i.e.,

$$E_p\{\beta(\vec{r},\omega)\} = 0 \quad , \quad \forall\, \vec{r} \in R \tag{6}$$

and

$$\beta(\vec{r},\omega) = \begin{cases} \beta_1 \ , & \vec{r} \in S \\ \beta_2 \ , & \vec{r} \notin S \end{cases} \tag{7}$$

where

$$\begin{aligned} \beta_1 &= (1-\sigma)(c_2^2 - c_1^2)/(\sigma c_2^2 + (1-\sigma)c_1^2) \\ \beta_2 &= \sigma(c_1^2 - c_2^2)/(\sigma c_2^2 + (1-\sigma)c_1^2) \end{aligned} \tag{8}$$

The one dimensional probability distribution density of $\beta(\vec{r},\omega)$ may be written as

$$f_\beta(x,\sigma) = \sigma\delta(x-\beta_1) + (1-\sigma)\delta(x-\beta_2) = f_\beta(x) \tag{9}$$

3. NEUMANN SERIES SOLUTION OF STOCHASTIC EQUATION

Let $p_0(\vec{r},t)$ denote the solution of the non-random wave equation

$$\nabla^2 p_0(\vec{r},t) = (1/c_0^2)(\partial^2 p(\vec{r},t)/\partial t^2) \tag{10}$$

Then, the Fourier transform of $p_0(\vec{r},t)$

$$p_0(\vec{r},\nu) = \int_{-\infty}^{\infty} p_0(\vec{r},t)e^{-i\nu t}dt \tag{11}$$

satisfies the non-random Helmholtz equation

$$\nabla^2 p_0(\vec{r},\nu) + k^2 p_0(\vec{r},\nu) = 0 \quad ; \quad k = \nu/c_0 \tag{12}$$

We define

$$p_1(\vec{r},t,\omega) = p(\vec{r},t,\omega) - p_0(\vec{r},t) \tag{13}$$

$$p_1(\vec{r},\nu,\omega) = \int_{-\infty}^{\infty} p_1(\vec{r},t,\omega)e^{-i\nu t}dt$$

$$p(\vec{r},\nu,\omega) = \int_{-\infty}^{\infty} p(\vec{r},t,\omega)e^{-i\nu t}dt \tag{14}$$

which yield

$$p(\vec{r},\nu,\omega) = p_0(\vec{r},\nu) + p_1(\vec{r},\nu,\omega) \tag{15}$$

Using these definitions and taking Fourier transform of Eq.(2) with respect to t, we get

$$-(\nabla^2 + k^2)p_1(\vec{r},\nu,\omega) = k^2\beta(\vec{r},\omega)\, p_0(\vec{r},\omega) + p_1(\vec{r},\nu,\omega) \tag{16}$$

the solution of which may be written as

$$\begin{aligned} p_1(\vec{r},\nu,\omega) = &\int_R (e^{-ik|\vec{r}-\vec{r}'|}/4\pi|\vec{r}-\vec{r}'|)k^2\beta(\vec{r}',\omega)p_0(\vec{r}',\nu)d\vec{r}' \\ &+\int_R e^{-ik|\vec{r}-\vec{r}'|}/4\pi|\vec{r}-\vec{r}'|)k^2\beta(\vec{r}',\omega)p_1(\vec{r}',\nu,\omega)d\vec{r}' \end{aligned} \tag{17}$$

This is a stochastic integral equation of Fredholm type[10,11] since it can be written in the form

$$p_1(\vec{r},\nu,\omega) = \psi(\vec{r},\nu,\omega) + \int_R K(\vec{r},\vec{r}',\nu,\omega)p_1(\vec{r}',\nu,\omega)d\vec{r}' \tag{18}$$

where the forcing function $\psi(\vec{r},\nu,\omega)$ and the kernel $K(\vec{r},\vec{r}',\nu,\omega)$ are defined by

$$\Psi(\vec{r},\nu,\omega) = \int_R (e^{-ik|\vec{r}-\vec{r}'|}/4\pi|\vec{r}-\vec{r}'|)k^2\beta(\vec{r},\omega)p_0(\vec{r},\nu)d\vec{r}' \quad (19)$$

$$K(\vec{r},\vec{r}',\nu,\omega) = (e^{-ik|\vec{r}-\vec{r}'|}/4\pi|\vec{r}-\vec{r}'|)k^2\beta(\vec{r}',\omega) \quad (20)$$

The solution of Eq.(20) may be obtained in the form of Neumann series[10] :

$$p_1(\vec{r},\nu,\omega) = \Psi(\vec{r},\nu,\omega) + \sum_{m=1}^{\infty}\int K_m(\vec{r},\vec{r}',\nu,\omega)\Psi(\vec{r},\nu,\omega)d\vec{r}' \quad (21)$$

or

$$p_1(\vec{r},\nu,\omega) = \Psi(\vec{r},\nu,\omega) + \int_R \Gamma(\vec{r},\vec{r}',\nu,\omega)\Psi(\vec{r}',\nu,\omega)d\vec{r}' \quad (22)$$

where $K_m(\vec{r},\vec{r}',\nu,\omega)$, $m = 1,2,\ldots$, are defined by the recurrence formula

$$K_m(\vec{r},\vec{r}',\nu,\omega) = \int_R K(\vec{r},\vec{r}',\nu,\omega)K_{m-1}(\vec{r}'',\vec{r}',\nu,\omega)d\vec{r}'' \; ; \; m = 2,3,4,\ldots \quad (23)$$

and

$$K_1(\vec{r},\vec{r}',\nu,\omega) = K(\vec{r},\vec{r}',\nu,\omega)$$

$$\Gamma(\vec{r},\vec{r}',\nu,\omega) = \sum_{m=1}^{\infty} K_m(\vec{r},\vec{r}',\nu,\omega) \quad (24)$$

The inverse Fourier transform of Eq.(21) gives

$$p_1(\vec{r},t,\omega) = \Psi(\vec{r},t,\omega) + (1/2\pi)\sum_{m=1}^{\infty}\int_R\int_{-\infty}^{\infty} K_m(\vec{r},\vec{r}',\nu,\omega)\Psi(\vec{r},\nu,\omega)e^{i\nu t}d\vec{r}'d\nu \quad (25)$$

or

$$p_1(\vec{r},t,\omega) = \Psi(\vec{r},t,\omega) + (1/2\pi)\int_R\int_{-\infty}^{\infty}(\vec{r},\vec{r}',\nu,\omega)\Psi(\vec{r}',\nu,\omega)e^{i\nu t}d\vec{r}'\,d\nu \quad (26)$$

where the following definition of inverse Fourier transform has been used.

$$\Psi(\vec{r},t,\omega) = (1/2\pi)\int_{-\infty}^{\infty}\Psi(\vec{r},\nu,\omega)e^{i\nu t}\,d\nu \quad (27)$$

4. MEAN VALUE, MEAN SQUARE VALUE AND SPACE CORRELATION FUNCTION OF SCATTERED FIELD

a) Mean value

Let $M_{p_1}(\vec{r},t)$, $M_{\psi}(\vec{r},t)$ denote the mean (expected) value of $p_1(\vec{r},t,\omega)$, $\Psi(\vec{r},t,\omega)$, respectively, i.e.,

$$M_{p_1}(\vec{r},t) = E\{p_1(\vec{r},t,\omega)\} \quad , \quad M_{\psi}(\vec{r},t) = E\{\Psi(\vec{r},t,\omega)\} \tag{28}$$

The expected value of the scattered field $p_1(\vec{r},t,\omega)$ may be written using Eqs.(25) and (28)

$$M_{p_1}(\vec{r},t) = M_{\psi}(\vec{r},t) + (1/2\pi)\sum_{m=1}^{\infty}\int\int_{-\infty}^{\infty} E\{K_m(\vec{r},\vec{r}',\nu,\omega)\Psi(\vec{r},\nu,\omega)e^{i\nu t}d\vec{r}'\,d\nu \tag{29}$$

Since

$$E\{\beta(\vec{r}',\omega)\} = 0 \qquad \forall\ \vec{r} \in R \tag{30}$$

we see that

$$E\{\beta(\vec{r},t,\omega)\} = 0 \tag{31}$$

The first term in the series given by (29) can be expressed as

$$\frac{1}{2\pi}\iiint_{R}^{\infty}\frac{e^{-ik|\vec{r}-\vec{r}'|}}{4\pi|\vec{r}-\vec{r}'|}\,\frac{e^{-ik|\vec{r}'-\vec{r}''|}}{4\pi|\vec{r}'-\vec{r}''|}\,k^4K_{\beta}(\vec{r}'-\vec{r}'')p_0(\vec{r}'',\nu)e^{i\nu t}d\vec{r}'d\vec{r}''d\nu \tag{32}$$

where

$$K_{\beta}(\vec{r}'-\vec{r}'') = E\{\beta(\vec{r}',\omega)\beta(\vec{r}'',\omega)\} \tag{33}$$

is the space correlation function of $\beta(\vec{r},\omega)$. If $\beta(\vec{r},\omega)$ is isotropic, then $K_{\beta}(\vec{r}'-\vec{r}'') = K_{\beta}(|\vec{r}'-\vec{r}''|)$.

b) Space-time correlation function

From Eq.(26), one can get the general expression of the space time correlation function of the scattered field given by

$$\begin{aligned}K_p(\vec{r}_1,\vec{r}_2,t_1,t_2) &= E\{p_1^*(\vec{r}_1,t_1,\omega)p_1(\vec{r}_2,t_2,\omega)\}\\ &= K_{\psi}(\vec{r}_1,\vec{r}_2,t_1,t_2)\\ &+(1/2\pi)\int_R\int_{-\infty}^{\infty} E\{\Psi^*(\vec{r}_1,t_1,\omega)\Gamma(\vec{r}_2,\vec{r}',\nu,\omega)\Psi(\vec{r}',\nu,\omega)e^{i\nu t_2}\,d\vec{r}'d\nu\\ &+(1/2\pi)\int_R\int_{-\infty}^{\infty} E\{\Psi(\vec{r}_2,t_2,\omega)\Gamma^*(\vec{r}_1,\vec{r}',\nu,\omega)\,\Psi^*(\vec{r}',\nu,\omega)e^{-i\nu t_1}d\vec{r}'d\nu\end{aligned}$$

$$+(1/2^2\pi^2)\iint_R\int_{-\infty}^{\infty}\int_{-\infty}^{\infty} E\{\Gamma^*(\vec{r}_1,\vec{r}_1',\nu_1,\omega)\Psi^*(\vec{r}_1',\nu_1,\omega)\Gamma(\vec{r}_2,\vec{r}_2',\nu_2,\omega)$$
$$x\Psi(\vec{r}_2,\nu_2,\omega)\ e^{-i\nu_1 t_1}e^{i\nu_2 t_2}d\vec{r}_1'd\vec{r}_2'd\nu_1 d\nu_2 \tag{34}$$

where

$$K_\psi(\vec{r}_1,\vec{r}_2,t_1,t_2) = E\{\Psi^*(\vec{r}_1,t_1,\omega)\Psi(\vec{r}_2,t_2,\omega)\} \tag{35}$$

and ' ' denotes conjugate. From Eq.(24), one could write

$$E\{\Psi^*(\vec{r}_1,t_1,\omega)\Gamma(\vec{r}_2,\vec{r}',\nu,\omega)\Psi(\vec{r}',\nu,\omega)\}$$
$$= \sum_{m=1}^{\infty} E\{\Psi^*(\vec{r}_1,t_1,\omega)K_m(\vec{r}_2,\vec{r}',\nu,\omega)\Psi(\vec{r}',\nu,\omega) \tag{36}$$

In Eq.(36), the first term (m=1) can be derived using Eq.(19) and (20) as follows

$$E\{\Psi^*(\vec{r}_1,t,\omega)K(\vec{r}_2,\vec{r}',\nu,\omega)\Psi(\vec{r}',\nu,\omega)\}$$
$$= (1/2\pi)\iint_R\int_{-\infty}^{\infty}[e^{i\nu'|\vec{r}_1-\vec{r}'''|/c_0}\ e^{-i\nu|\vec{r}_2-\vec{r}'|/c_0}\ e^{-i\nu|\vec{r}'-\vec{r}'''|/c_0}\ c_0^6$$
$$/(4\pi)^3|\vec{r}_1-\vec{r}'''||\vec{r}_2-\vec{r}'||\vec{r}'-\vec{r}'''|]\nu'^2\nu^4 p^*(\vec{r}'',\nu')p_0(\vec{r}''',\nu)$$
$$E\{\beta(\vec{r}',\omega)\beta(\vec{r}'',\omega)\beta(\vec{r}''',\omega)\}\ e^{-i\nu' t_1}\ d\vec{r}''d\vec{r}'''d\nu' \tag{37}$$

Similarly, other terms in Eq.(36) can be expressed as the integral consisting of higher order moments of stochastic field $\beta(\vec{r},\omega)$.

c) Mean square value

The mean square value of the scattered field $p_1(\vec{r},t,\omega)$

$$M_{p_1}^{(2)}(\vec{r},t) = E\{|p_1(\vec{r},t,\omega)|^2\} \tag{38}$$

can be obtained directly from the space-time correlation function of the scattered field by setting $\vec{r}_1 = \vec{r}_2$ and $t_1 = t_2$, i.e.,

$$M_{p_1}^{(2)}(\vec{r},t) = K_{p_1}(\vec{r},\vec{r},t,t) \tag{39}$$

It is to be noted that the mean value of the scattered field is always much smaller than its root mean square value, and also, in practice, only the mean square value is measured.

5. SCATTERING OF CONTINUOUS INCIDENT WAVE

Obviously, the non-random field $p_0(\vec{r},t)$ may be regarded as the incident wave (or field). When $p_0(\vec{r},t)$ is continuous field, it can be written as

$$p_0(\vec{r},t) = p_0(\vec{r})e^{i\nu_0 t} \tag{40}$$

where $p_0(\vec{r})$ is its complex amplitude, ν_0 is the angular frequency. Then,

$$p_0(\vec{r},\nu) = 2\pi p_0(\vec{r})\delta(\nu-\nu_0) \tag{41}$$

Now, we consider only far field backscattering and the incident wave to be a plane wave propagating in the direction $\hat{n}$ ($\hat{n}$ is a unit vector), see Fig. 1 with amplitude A. Then,

$$p_0(\vec{r},t) = Ae^{-i(\nu_0\hat{n}\cdot\vec{r}/c_0-\nu_0 t)} \tag{42}$$

and

$$p_0(\vec{r},\nu) = 2\pi Ae^{-i\nu_0\hat{n}\cdot\vec{r}/c_0}\,\delta(\nu-\nu_0) \tag{43}$$

Substituting Eq.(43) into Eq.(29), we get

$$\Psi(\vec{r},t,\omega) = A(\nu_0^2/c_0^2)e^{i\nu_0 t}\int_R [e^{-i\nu_0(|\vec{r}-\vec{r}'| + \hat{n}\cdot\vec{r}')}/4\pi|\vec{r}-\vec{r}'|]\beta(\vec{r}',\omega)d\vec{r}' \tag{44}$$

Since $\Psi(\vec{r},t,\omega)$ is also a monochromatic wave field, we write

$$\Psi(\vec{r},t,\omega) = \Psi(\vec{r},\omega)e^{i\nu_0 t} \tag{45}$$

where $\Psi(\vec{r},\omega)$ is its amplitude. By using Eq.(45) in (44), we get

$$\Psi(\vec{r},\omega) = A(\nu_0/c_0)^2\int_R [e^{-i\nu_0(|\vec{r}-\vec{r}'| + \hat{n}\cdot\vec{r})/c_0}/4\pi|\vec{r}-\vec{r}'|]\beta(\vec{r}',\omega)d\vec{r}' \tag{46}$$

Let the correlation function k_ψ as

$$K_\psi(\vec{r}_1,\vec{r}_2) = E\{\Psi(\vec{r}_1,\omega)\Psi(\vec{r},\omega)\} \tag{47}$$

$$K_\psi(\vec{r}_1,\vec{r}_2,t_1,t_2) = K_\psi(\vec{r}_1,\vec{r}_2)e^{i\nu_0(t_2-t_1)} \tag{48}$$

By employing (46) in the above equations, we obtain

$$K_\psi(\vec{r}_1,\vec{r}_2) = (A\nu_0^2/4\pi c_0^2)^2\iint_R [e^{i\nu_0(\hat{n}\cdot\vec{r} + |\vec{r}_1-\vec{r}'|)/c_0}\, e^{-i\nu_0(\hat{n}\cdot\vec{r}'' + |\vec{r}_2-\vec{r}''|)/c_0} /|\vec{r}_1-\vec{r}'||\vec{r}_2-\vec{r}''|]K_\beta(\vec{r}''-\vec{r}')d\vec{r}'d\vec{r}'' \tag{49}$$

Let $\vec{\ell} = \vec{r}_2-\vec{r}_1$ and consider only the case of $|\vec{\ell}| \ll |\vec{r}_1|,\ |\vec{r}_2|$.

Using the following approximations

$$
\begin{aligned}
|\vec{r}_1-\vec{r}'| &= |\vec{r}_1| + |\vec{r}'|\cos\theta_1 \quad , \quad \hat{n}\cdot\vec{r}' = |\vec{r}'|\cos\theta_1 \\
|\vec{r}_2-\vec{r}''| &= |\vec{r}_2| + |\vec{r}''|\cos\theta_2 \quad , \quad \hat{n}\cdot\vec{r}'' = |\vec{r}''|\cos\theta_2 \\
|\vec{r}_2| &= |\vec{r}_1| + |\vec{\ell}|\cos\theta_1 \quad ,
\end{aligned} \tag{50}
$$

letting $\vec{r}_1 = \vec{r}$, $|\vec{r}_1| = |\vec{r}| = r$, $\vec{\rho} = r''-r'$, $|\vec{\ell}| = \ell$, θ_1, θ_2, θ, as shown in Figure 1, and considering that the radius of each scatterer and the correlation radius of $\beta(\vec{r},\omega)$ are much smaller than the size of region R and $E\{\beta(\vec{r},\omega)\} = 0$, we finally get

$$
K'_\psi(\vec{r},\vec{\ell}) = (A\nu_0^2/4\pi c_0^2)^2 \, e^{i\nu_0\vec{\ell}\cdot\hat{n}/c_0} \, V_R K_\beta(2\vec{k}_0)/r^2 \tag{51}
$$

where

$$
K_\beta(2\vec{k}_0) = \int_R K_\beta(\vec{\rho}) e^{-i2\vec{k}_0\cdot\vec{\rho}} \, d\rho \tag{52}
$$

is just the space spectrum density of the stochastic field $\beta(\vec{r},\omega)$, V_R is the volume of R and $\vec{k}_0 = \nu_0\hat{n}/c_0$ is the wave vector of the incident wave. Here, we changed the function form $K_\psi(\vec{r}_1,\vec{r}_2)$ into $K_\psi(\vec{r}_1,\vec{r}_2-\vec{r}_1)$, i.e.,

$$
K'_\psi(\vec{r},\vec{\ell}) = K_\psi(\vec{r},\vec{r}+\vec{\ell}) \tag{53}
$$

If the scatterers in space are distributed non-directional, then the $\beta(\vec{r},\omega)$ will be isotropic implying

$$
K_\beta(\vec{\rho}) = K_\beta(|\vec{\rho}|) = K_\beta(\rho) \tag{54}
$$

Then from Eq.(52), we obtain

$$
K_\beta(2\vec{k}_0) = 2\pi(c_0/\nu_0)\int_0^\infty \rho K_\beta(\rho)\sin(2\nu_0\rho/c_0)d\rho \tag{55}
$$

6. SCATTERING OF IMPULSE INCIDENT WAVE

Consider an impulse monochromatic plane wave with frequency ν_0, propagation direction $\hat{n}$, duration τ and amplitude A

$$p_0(\vec{r},t) = Ae^{-i(\nu_0\hat{n}\cdot\vec{r}/c_0-\nu t)}u(\hat{n}\cdot\vec{r}/c_0 - t) \tag{56}$$

where u(t) is the "rectangular" function defined by

$$u(t) = \begin{cases} 1 & t \in [-\tau/2, \tau/2] \\ 0 & t \notin [-\tau/2, \tau/2] \end{cases} \tag{57}$$

The spectrum (Fourier Transform) of u(t) may be written as

$$u(t) = \int_{-\infty}^{\infty} u(t)e^{-i\nu t}dt = 2\sin(\tau\nu/2)/\nu \tag{58}$$

$P_0(\vec{r},\nu)$ can be expressed as

$$p_0(\vec{r},\nu) = Ae^{-i\nu_0\hat{n}\cdot\vec{r}/c_0}\, 2\sin[\tau(\nu - \nu_0)/2]/(\nu - \nu_0) \tag{59}$$

For narrow band $\tau >> 1/\nu_0$, one can show that

$$\Psi(\vec{r},t,\omega) = A(\nu_0^2/c_0^2)e^{i\nu_0 t}\int_R [e^{-i\nu_0(|\vec{r}-\vec{r}'| + \hat{n}\cdot\vec{r})/c_0}/4\pi|\vec{r}-\vec{r}'|] \times\beta(\vec{r}',\omega)u[t-(|\vec{r}-\vec{r}'| + \hat{n}\cdot\vec{r}')/c]d\vec{r}' \tag{60}$$

We also notice that if u(t) is not a "rectangular" function, but an "arbitrary" function with duration $\tau >> 1/\nu_0$, then the expression(60) still holds.

If the radiation system of incident wave has a narrow directivity, then using the same approximation as (50), we obtain the mean square value of $\Psi(\vec{r},t,\omega)$:

$$M_\psi^{(2)}(\vec{r},t) = (A\nu_0^2/4\pi c_0^2)^2\pi R^2 c_0 K_\beta(2\vec{k}_0)/2r^2 \tag{61}$$

where

$$M_\psi^{(2)}(\vec{r},t) = E\{|\Psi(\vec{r},t,\omega)|^2\} \tag{62}$$

and R is the radius of the illuminated area of scatterer region by the

incident wave. In this derivation, the illuminated area is not necessarily to be a circular one. If we use $\mathcal{A}$ to denote this area, then (61) takes the form

$$M_{\psi}^{(2)}(\vec{r},t) = (A\nu_0^2/4\pi c_0^2)^2 \mathcal{A} c_0 \tau K_{\beta}(2\vec{k}_0)/2r^2 \tag{63}$$

Comparing (63) with the formula for continuous wave

$$M_{\psi}^{(2)}(\vec{r},t) = (A\nu_0^2/4\pi c_0^2)^2 V_R K_{\beta}(2\vec{k}_0)/r^2 \tag{64}$$

which is obtained from Eq.(51) when we let $\vec{\ell} = 0$, we can see that they are completely similar, $\mathcal{A} c_0 \tau/2$ just plays the role of V_R. This seems physically reasonable.

7. SPACE CORRELATION FUNCTION FOR SPHERICAL SCATTERER

From the previous section, we see that the space correlation function $K_\beta(\ell)$ or the space spectrum density $K_\beta(\vec{k})$ plays important role in the calculation of the statistical moments of the scattered field. $K_\beta(\ell)$ depends on the shape and size of each scatterer and the concentration σ of scatterers. The calculation of $K_\beta(\ell)$ or $K_\beta(\vec{k})$ here is based on geometrical probability.

Obviously, the stochastic field $\beta(\vec{r},\omega)$ is ergodic. Therefore, for any sample (realization) $\beta(\vec{r},\omega_i)$, we have

$$K_\beta(\ell) = \lim_{V(D)\to\infty} (1/V(D)) \int_D \beta(\vec{r},\omega_i)\beta(\vec{r}-\vec{\ell},\omega_i)d\vec{r} \qquad (65)$$

where D is a region with any shape in R and V(D) is the volume of D.

Assume that the distance from any sphere to the nearest sphere is the random variable $\xi(\omega)$, see Figure 2, and $\xi(\omega)$ has the exponential probability distribution density

$$f_\xi(x) = e^{-x/\xi_0}/\xi_0 \quad , \qquad x \in [0,\infty) \qquad (66)$$

where ξ_0 is the mean value of $\xi(\omega)$, i.e.,

$$\xi_0 = E\{\xi(\omega)\} \qquad (67)$$

Using Eqs.(9), (65) and (66), from geometry, we get

$$K_\beta(\ell) = \sigma\beta_1^2 [\sigma - 2\sigma^{1/3} + \sigma^{1/3} \sum_{j=0}^{j_0} I(\ell,\sigma,j)]/(1-\sigma)^2 \qquad (68)$$

where

$$j_0 = \text{int}\{\ell/2a - 1\} \qquad (69)$$

$$I(\ell,\sigma,j) = j\xi_0 e^{-(\ell-2ja)/\xi_0} \sum_{k=0}^{j} \frac{1}{k} [e^{2a/\xi_0}(\ell-2(j+1)a)^k/\xi_0^k + e^{-2a/\xi_0}(\ell-2(j-1)a)^k/\xi_0^k - 2(\ell-2ja)^k/\xi_0^k]$$

$$-[\ell-2(j+1)a]e^{-(\ell-2ja)/\xi_0}\sum_{k=0}^{j-1}(1/k!)[e^{2a/\xi_0}\,(\ell-2(j+1)a)^k/\xi_0^k - (\ell-2ja)^k/\xi_0^k]$$

$$+[\ell-2(j-1)a]e^{-(\ell-2ja)/\xi_0}\sum_{k=0}^{j-1}(1/k!)[(\ell-2ja)^k/\xi_0^k - e^{-2a/\xi 0}\,(\ell-2(j-1)a)^k/\xi_0^k],$$

$$j < \ell/2a - 1 \qquad (70)$$

$$I(\ell,\sigma,\,0) = \begin{cases} 2a-\ell & \ell \in [0,2a] \\ 0 & \ell \geq 2a \end{cases} \qquad (71)$$

In Eq.(69), int{ } denotes the integer part of{ }. We may be able to write Eq.(68) in the form

$$K_\beta(\ell\,) = be^{-\gamma\ell}(1 + \cos 2\pi\ell/\ell_0) \qquad (72)$$

On the other hand, for small values of ℓ, ($\ell \leq 2a$), from geometry, we get exact expression of $K_\beta(\ell)$ given by

$$K_\beta(\ell) = \sigma\beta_1^2[(1-\sigma)-3\ell/4\sigma + \ell^3/16a^3]/(1-\sigma)^2\,, \quad \ell \leq 2a \qquad (73)$$

From Eq.(72), we find

$$\left.\frac{dK_\beta(\ell)}{d\ell}\right|_{\ell=0} = -2\gamma b\,, \qquad K_\beta(0) = 2b \qquad (74)$$

while from Eq.(65), we find

$$\left.\frac{dK_\beta(\ell)}{d\ell}\right|_{\ell=0} = -3\sigma\beta_1^2/4(1-\sigma)^2 a\,, \quad K_\beta(0) = \sigma\beta_1^2/(1-\sigma) \qquad (75)$$

Comparing Eqs.(74) and (75), we obtain expressions for b and γ given by

$$b = \sigma\beta_1^2/2(1-\sigma)\;; \qquad \gamma = 3/4(1-\sigma)a \qquad (76)$$

Substituting Eq.(76) into (72), we finally obtain an expression for $K_\beta(\ell)$ as

$$K_\beta(\ell) = (\sigma/2(1-\sigma))\beta_1^2\, e^{-3\ell/4(1-\sigma)a}\,[1 + \cos(\pi\,\sigma^{1/3}\ell\,/a)] \qquad (77)$$

8. RESULTS AND CONCLUSION

In this section, we present the final expression for mean square value $M_{\psi}^{(2)}$ and space spectrum density $K_{\beta}(2\vec{k}_0)$. Substituting Eq.(77) into Eq.(64), integrating the resulting expression and again substituting the result into Eq.(70), we finally obtain for narrow band pulse ($\tau >> 1/\nu_0$)

$$K_{\beta}(2k_0) = (4/3)^3(\pi c_0/\nu_0)a^2\sigma(1-\sigma)^2\,\beta_1^2\{4k_0a + \frac{2k_0a + \pi\sigma^{1/3}}{[1 + (4/3)^2(1-\sigma)^2(2k_0a + \pi\sigma^{1/3})^2]^2} + \frac{2k_0a - \pi\sigma^{1/3}}{[1 + (4/3)^2(1-\sigma)^2(2k_0a - \pi\sigma^{1/3})^2]^2} \tag{78}$$

and

$$M_{\psi}^{(2)}(\vec{r},t) = (2A^2\nu_0^3 R^2 \tau a^2/27r^2)(c_0^2(c_2^2-c_1^2)^2/c_1^4c_2^4)\sigma(1-\sigma)^4\{4k_0a + \frac{2k_0a + \pi\sigma^{1/3}}{[1 + (4/3)^2(1-\sigma)^2(2k_0a + \pi\sigma^{1/3})^2]^2} + \frac{2k_0a - \pi\sigma^{1/3}}{[1 + (4/3)^2(1-\sigma)^2(2k_0a - \pi\sigma^{1/3})^2]^2} \tag{79}$$

To the author's knowledge, extensive experimental results are not available on incoherent intensity from random media, except that of some controlled laboratory experiments in acoustics[13]. In Ref. 13, some backscattering measurements were reported for a random distribution of fluid particles dispersed in another fluid. The wave speeds of the scatterers and of the host medium considered in their experiments are c_1 = 1596 m/sec and c_2 = 1499 m/sec. For such a system, $\beta_1 << 1$, $\beta_2 << 1$ and $\beta(\vec{r},\omega) << 1$ $\forall\ \vec{r} \in R,\ \omega \in \Omega$. This suggets that we could neglect higher order moments (The theory presented, however, is general) resulting in the following

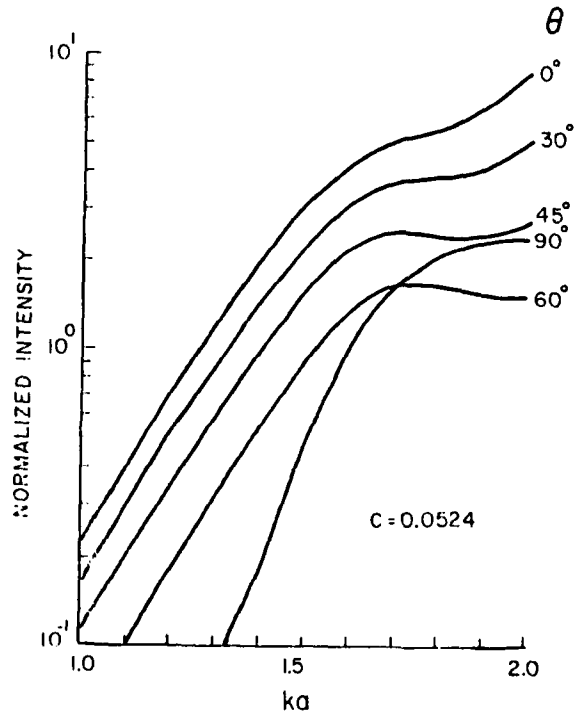

Figure 4b. Expanded version of figure 4a for the range of ka from 1.0 to 2.0.

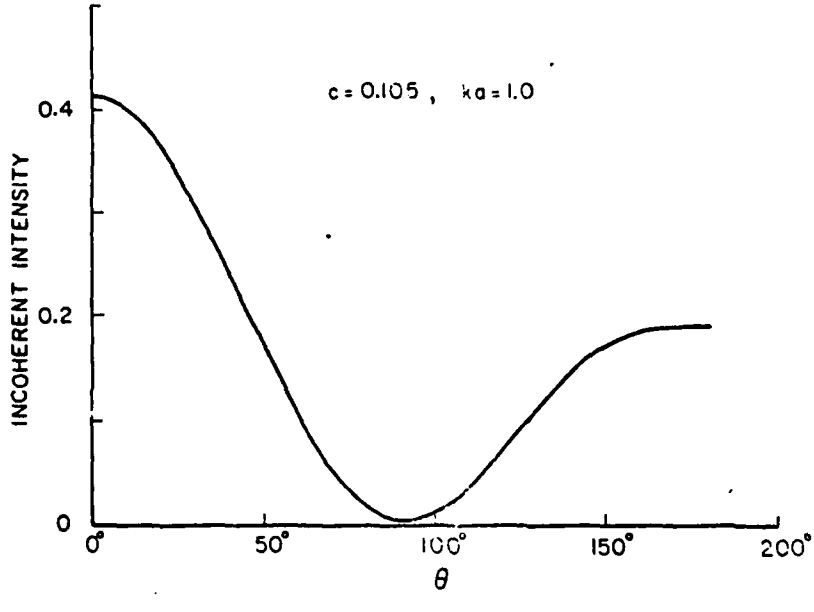

Figure 5. Normalized incoherent intensity as a function of observation angle θ for c = 0.105 and ka = 1.0.

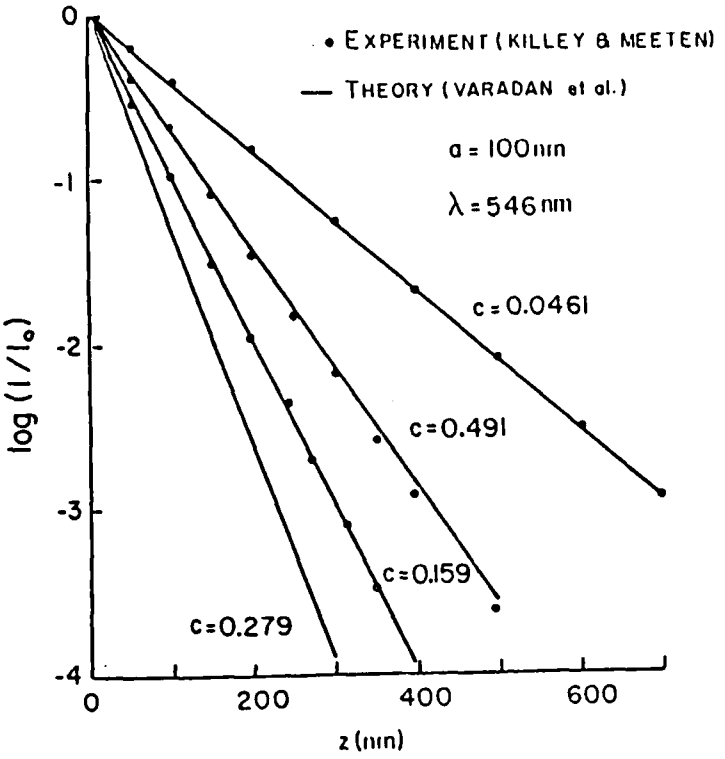

Figure 3. Coherent intensity as a function of depth Z for various values of concentration c and for λ = 546 nm.

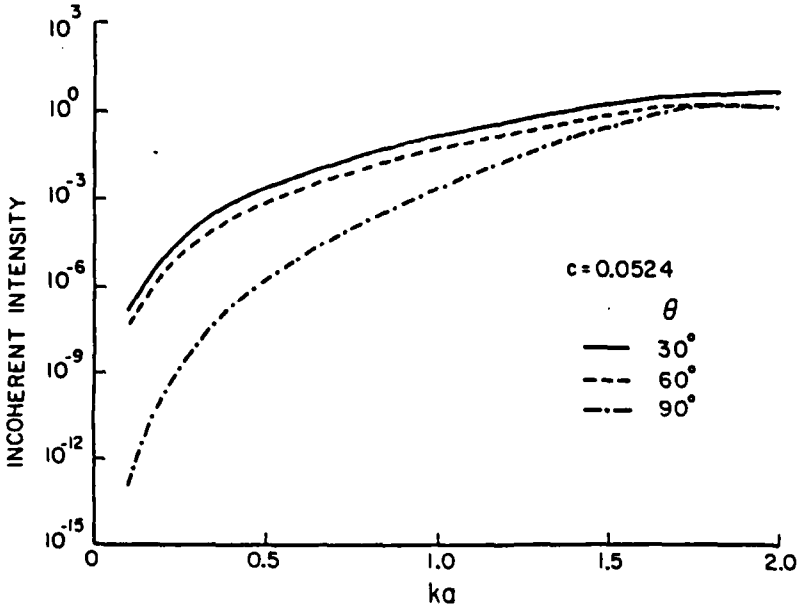

Figure 4a. Normalized incoherent intensity vs. ka for c = 0.0524 and for various angles θ.

5. V.V. Varadan and V.K. Varadan, The quasi-crystalline approximation and multiple scattering of waves in random media, submitted to IEEE Trans. Antennas and Propagation.

6. A. Killey and G.H. Meeten, Optical extinction and refraction of concentrated latex dispersions, J. Chem. Soc., Faraday Trans. 2, 587-599, 1981.

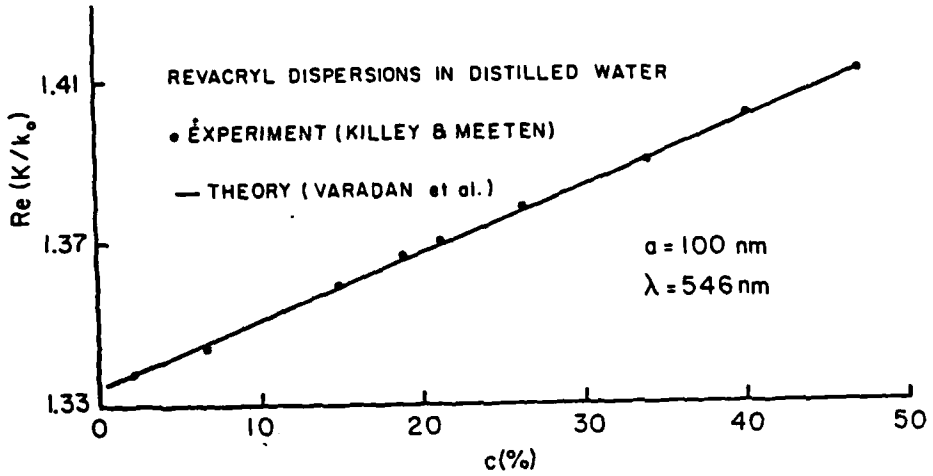

Figure 1. Phase velocity vs. concentration c for λ = 546 nm.

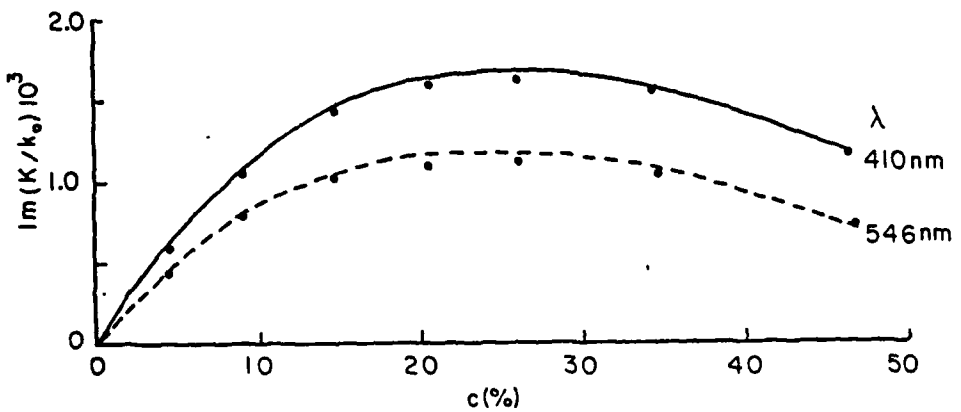

Figure 2. Coherent attenuation vs. concentration c for λ = 410 nm, 546 nm.

The first set of the above diagrams represents a partial summation of QCA type terms incorporating two body correlations while the second set represents the conventional ladder diagrams. In both sets of diagrams, we can use so called "dressed propagators" obtained from Eq. (6) between scatterers instead of "bare propagators". This means that K from (6) can be used as the wave number characterizing the medium between scatterers involved in calculation of the spectral density, i.e., the other scatterers that participate in only one or other of the field lines are averaged over separately and replaced by K.

NUMERICAL RESULTS

The numerical procedure is described in detail in Refs. 3-4, and will not be repeated here. The effective wave number $K(=K_1+K_2)$ is computed for Revacryl spheres in distilled water for a range of frequencies and concentrations of scatterers. The real part K_1 is related to the phase velocity while the imaginary part K_2 is related to coherent attenuation. We have also calculated the coherent and incoherent intensity for electromagnetic wave propagation through ice particles ($\varepsilon_r = 3.168$) in free space using the first term of the two series of diagrams given in Eq. (8).

In Figs. 1 and 2, the real and imaginary parts of the coherent field are compared with the experimental measurements of Killey and Meeten[6]. In Fig. 3, calculations of the coherent intensity for a suspension of Revacryl spheres in distilled water show excellent comparison with measurements of Killey and Meeten[6].

In Fig. 4, the incoherent intensity is plotted as a function of ka for c = 0.0524 and for various angles θ. It is interesting to note that as ka increases, the leading term of the incoherent intensity approaches a constant value for all values of θ. Figure 5 displays the incoherent intensity as a function of the observation angle θ, and the intensity reduces to zero at $\theta = 90°$ as expected.

ACKNOWLEDGEMENTS

This work was supported by the U.S. Army Research Office under contract DAAG29-83-K-0097. Many helpful discussions with Dr. W.A. Flood are gratefully acknowledged.

REFERENCES

1. V. Twersky, Coherent scalar field in pair-correlated random distributions of aligned scatterers, J. Math. Phys., 18, 2468-2486, 1977.

2. V. Twersky, Coherent electromagnetic waves in pair-correlated random distributions of aligned scatterers, J. Math. Phys., 19, 215-230, 1978.

3. V.N. Bringi, V.K. Varadan and V.V. Varadan, Coherent wave attenuation by a random distribution of particles, Radio Sci., 17, 946-952, 1982.

4. V.K. Varadan, V.N. Bringi, V.V. Varadan and A. Ishimaru, Multiple scattering theory for waves in discrete random media and comparison with experiments, Radio Sci., 18, 321-327, 1983.

functions g (given by $p(\vec{r}_j|\vec{r}_1) = \frac{1}{V} g(\vec{r}_{1j})$) which are denoted by $\bar{\sigma}(K)$ and $\bar{g}(K)$, respectively, and using the convolution theorem, we obtain

$$\langle E(\vec{r})\rangle = E^0(\vec{r}) + Ou\ \psi_n(\vec{r}-\vec{r}_1)\ T_{nn'}\ n_o \int [1-n_o\ \bar{\sigma g}\ (K)\ T]^{-1}\ e^{iK\ \cdot\ (\vec{r}_1-\vec{r}_2)}\ a_{n''}^{(2)}\ d\vec{K}\ d\vec{r}_1\ d\vec{r}_2 \qquad (5)$$

This new form of the average field can be interpreted as an incident plane wave propagating through an effective medium of propagation constnat K and *propagator* $[1-n_o\ \overline{\sigma g}\ (K)T]^{-1}$ undergoing scattering from a particle at r_1 and then propagating to the observation point r with the wave number of the host medium. The dispersion equation in the model medium can be obtained by setting the determinant of the propagator equal to zero:

$$|\ 1-n_o\ \overline{\sigma g}(K)\ T\ | = 0 \qquad (6)$$

This equation is identical to the one obtained by us earlier using the self-consistent multiple scattering approach, see Ref. 4.

The field fluctuations $\Delta\vec{E}$ may now be given by

$$\Delta\vec{E} = \vec{E} - \langle\vec{E}\rangle \qquad (7)$$

and can be represented as a multiple scattering series which may be represented by the following diagrams

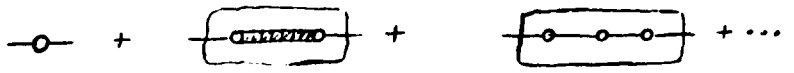

where —— denotes propagation of the field from one point to the other and 0 denotes a scatterer. If two ore more scatterers are enclosed in an area such as 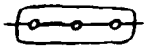 arbitrary multiple scattering any number of times and in any order can go on between scatterers 1, 2 and 3.

Along these lines, we define the incoherent intensity or the spectral density $G_\alpha(\vec{R},\omega)$ at position $\vec{R}$, for field polarization in the direction $\hat{\alpha}$.

$$G_\alpha(\vec{R},\omega) = \frac{1}{4}\langle|\hat{\alpha}\cdot\Delta\vec{E}|^2\rangle \qquad (8)$$

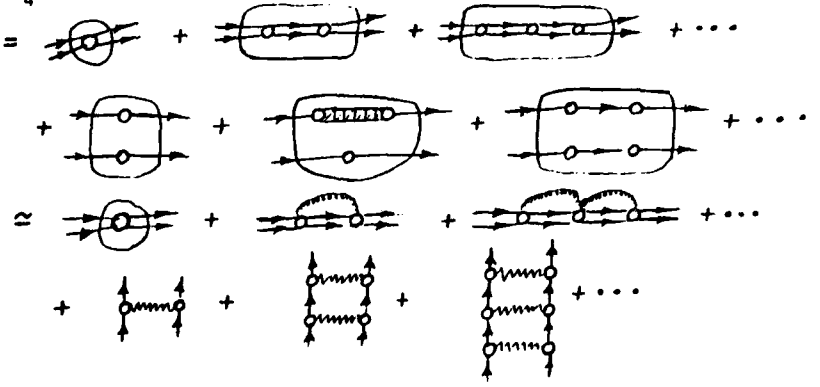

geometries without much difficulty.

FORMULATION

Consider wave propagation in an infinite medium of volume $V \to \infty$ containing a random distribution of N scatterers, $N \to \infty$, such that $n_o = N/V$, the number density of scatterers is finite. Plane harmonic waves of frequency ω propagate in the medium and undergo multiple scattering. Let $\vec{E}$, $\vec{E}^0$, $\vec{E}^e_i$, and $\vec{E}^s_i$ denote respectively the total field, the incident field, the field exciting the i-th scatterer and the field scattered by the i-th scatterer. Then self consistency requires the following relationships between the fields[3,4].

$$\vec{E} = \vec{E}^0 + \sum_{i=1}^{N} \vec{E}^s_i \tag{1}$$

and

$$\vec{E}^e_i = \vec{E}^0 + \sum_{j\neq i}^{N} \vec{E}^s_j \tag{2}$$

The configurational average of the total field results in

$$\langle E(\vec{r})\rangle = E^0(\vec{r}) + \sum_i T_{nn'} \, 0u \, \psi_n(\vec{r}-\vec{r}_i) \, a^i_n \, p(\vec{r}_i) \, d\vec{r}_i$$

$$+ \sum_i \sum_j{}' \, T_{nn'} \, T_{n''n'''} 0u \, \psi_n(\vec{r}-\vec{r}_i) \, \sigma_{n'n''}(\vec{r}_{ij}) \, a^j_{n''} \, p(\vec{r}_i) \, p(\vec{r}_j) \, p(\vec{r}_j|\vec{r}_i) \, d\vec{r}_j \, d\vec{r}_i + \ldots \tag{3}$$

In Eq. (3), $T_{nn'}$, is the T-matrix of an isolated scatterer, a^i_n are the known coefficients of expansion of the incident field at the site of the i-th scatterer, $\sigma_{nn'}(\vec{r}_y)$ is the translation matrix for vector spherical functions and describes the propagation of waves from $\vec{r}_i$ to $\vec{r}_j$. The functions $p(\vec{r}_j)$, $p(\vec{r}_j|\vec{r}_1)$... etc. are the single particle, two particle conditional probabilities distribution functions. We have shown[5] that invoking the QCA implies that the coherent field and the resulting dispersion equation were limited to terms of the form

$\langle E\rangle_{QCA}$ = 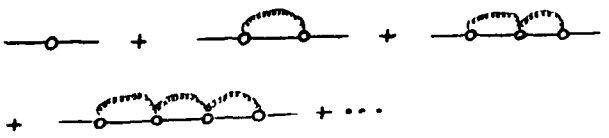 (4)

where  denotes positional correlation between two scatterers and it is clear from the diagrams that each scatterer participates only once in a given term, there is no back and forth scattering and all scattering is sequential and only sequential positional correlations are allowed.

Introducing spatial Fourier transforms of the translation matrix σ and the radial distribution

PROGRESS IN RESEARCH ON WAVE PROPAGATION AND SCATTERING IN DISCRETE RANDOM MEDIA USING MULTIPLE SCATTERING THEORY

V.K. Varadan and V.V. Varadan
Department of Engineering Science and Mechanics
Wave Propagation Laboratory
The Pennsylvania State University
University Park, PA 16802

ABSTRACT

This paper is concerned with a propagator model for multiple scattering and wave propagation in discrete random media. The coherent and incoherent intensity of a time harmonic electromagnetic field in such a medium are calculated and compared with available experimental results showing good agreement. This work has been published and submitted for publication as follows:

V.V. Varadan and V.K. Varadan,"The Quasi-Crystalline Approximation and Multiple Scattering of Waves in Random Media", IEEE Trans. A and P., submitted for publication.

V.K. Varadan and V.V. Varadan, "A Propagator Model for Multiple Scattering and Wave Propagation in Discrete Random Media", Radio Science, submitted for publication.

V.K. Varadan, Y. Ma and V.V. Varadan, "Coherent Electromagnetic Wave Propagation Through Randomly Distributed and Oriented Pair-correlated Scatterers", Radio Science, in press.

V.V. Varadan, Y. Ma and V.K. Varadan, "Frequency Dependence of the Attenuation of Electromagnetic Waves in Media with Anisotropy Induced by Microstructure", IEEE Trans. A and P., submitted.

INTRODUCTION

We consider the propagation of plane coherent electromagnetic waves in an infinite medium containing identical, loss less, randomly distributed particles. Our aim here is to characterize the random medium by an effective complex wave number K (which would be a function of particle concentration, the electrical size, and the statistical description of the random positions of the scatterers), and to study both coherent and incoherent intensities as a function of frequency for various values of concentration c (the fractional volume occupied by the scatterers). Although the formulation is generally valid for non-spherical, aligned or randomly oriented scatterers, initial calculations are confined to spherical scatterers which generally gives us a better picture of the order of magnitude of the different contributions to the intensity without the additional complications of non-spherical geometry and orientation.

Extensive work by Twersky[1-2] has laid the foundation for multiple scattering theory in discrete random media. A related approach using the T-matrix of a single scatterer together with configurational averaging procedures, has been used by the authors to develop a computational method for electromagnetic wave propagation problem in inhomogeneous media[3-4]. Lax's quasi-crystalline approximation (QCA) is used in conjunction with suitable models for the pair-correlation function to obtain an effective wave number $K(=K_1+iK_2)$ which is complex and frequency dependent. The real part K_1 is related to the phase velocity while the imaginary part K_2 is related to coherent attenuation. In this paper, we present a propagator model which is shown to present the same dispersion equation as the one obtained in our previous papers[3-4]. In addition, this model enables us to compute both coherent and incoherent intensities for more realistic

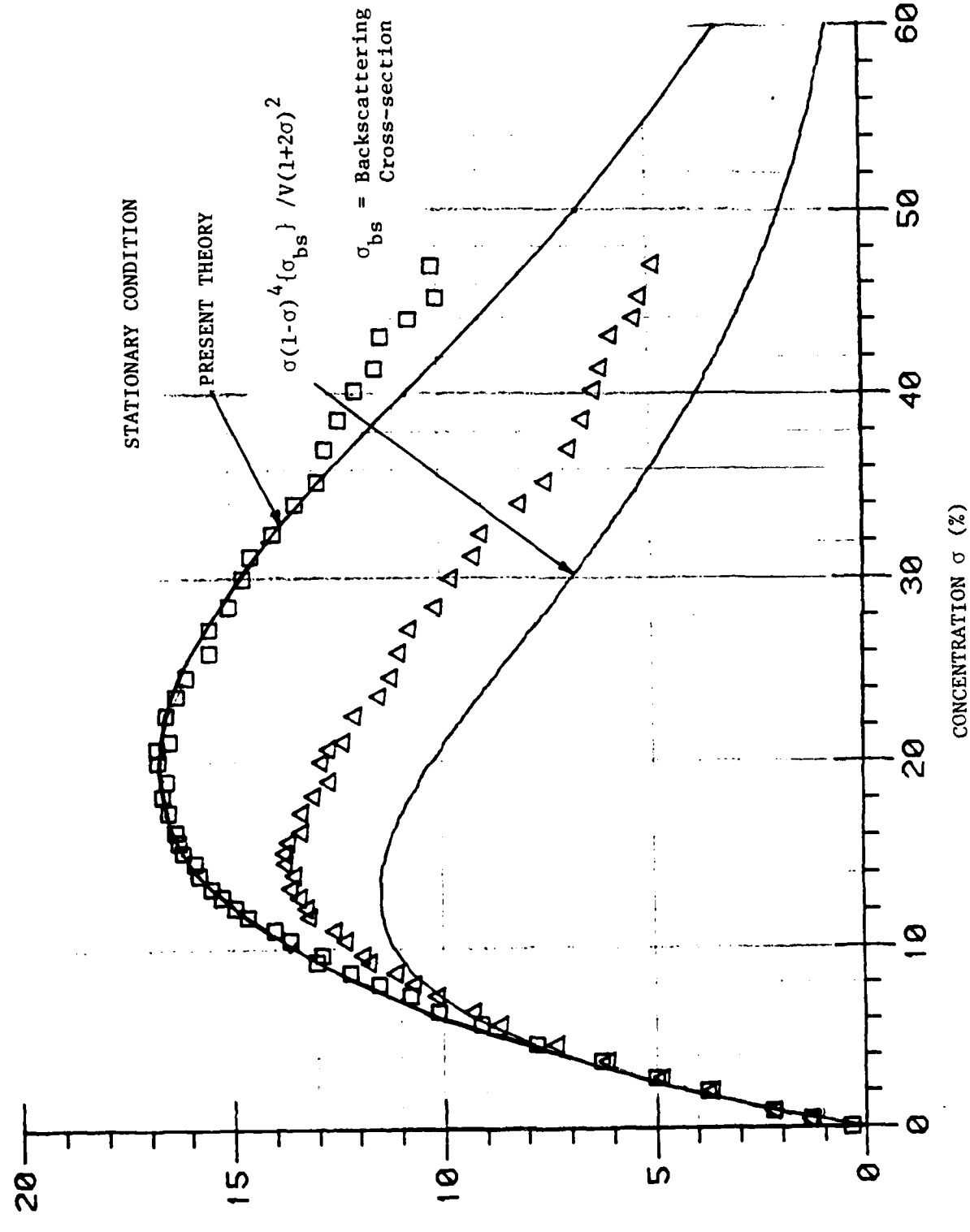

Figure 4. Backscattering coefficient vs. concentration for stationary condition.

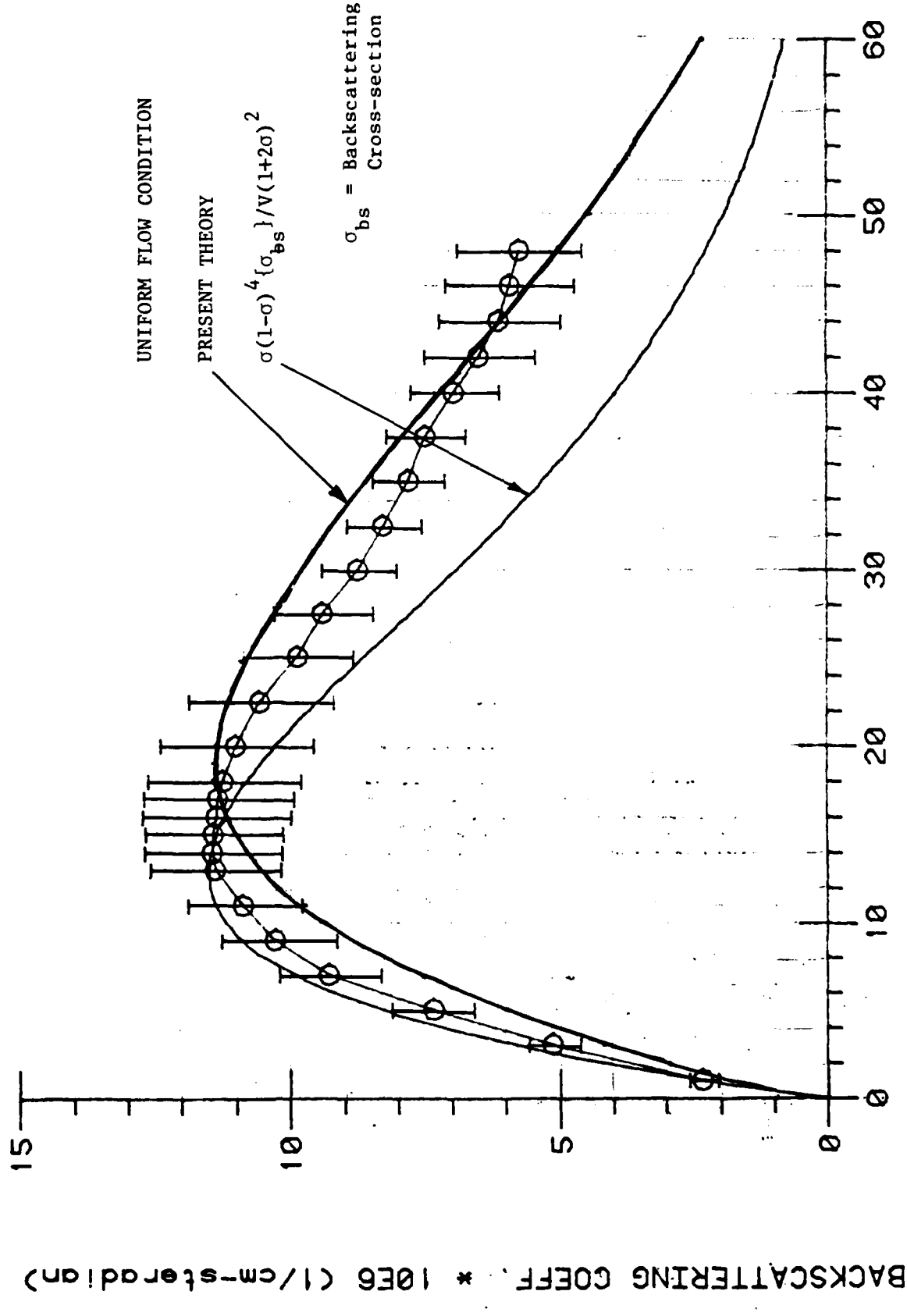

Figure 3. Backscattering coefficient vs. concentration for uniform flow condition.

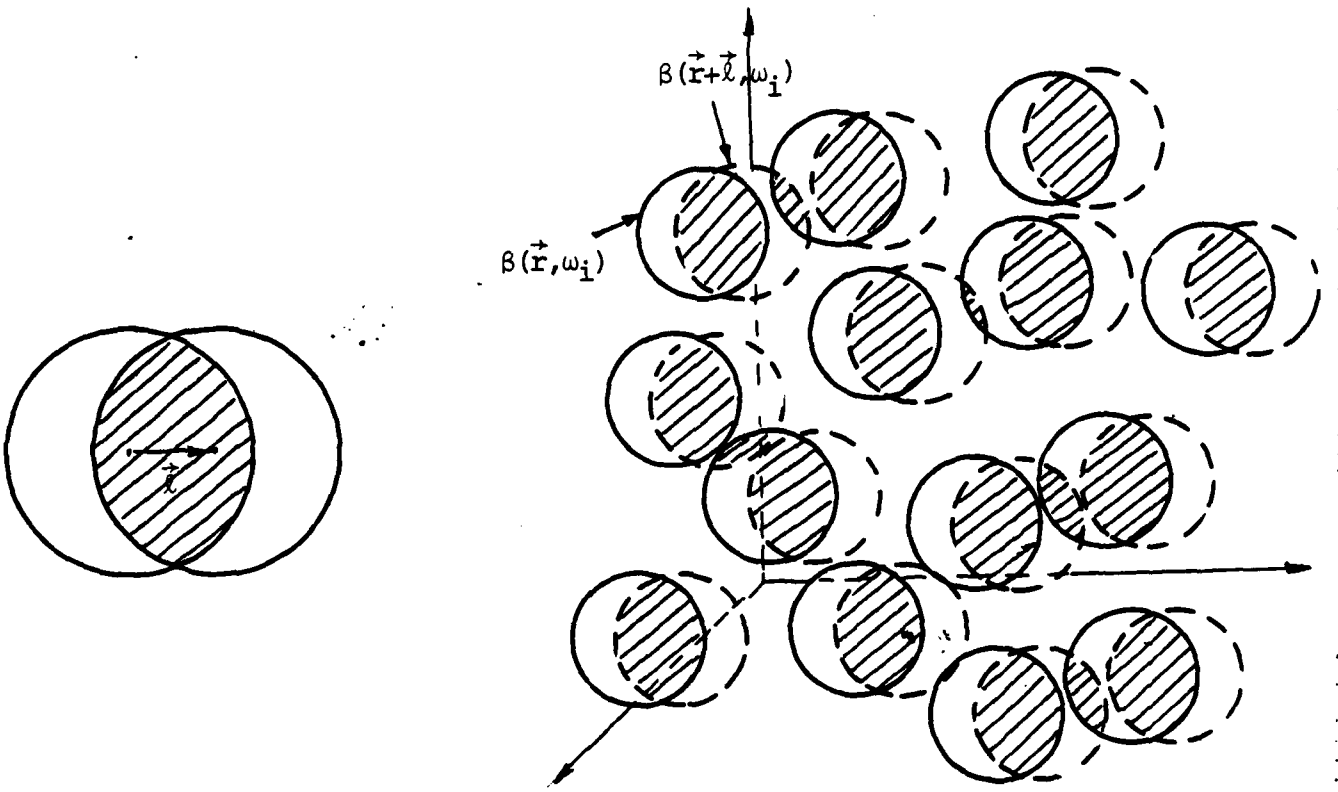

Fig.2a Two different configurations of the random system and and their region of overlap

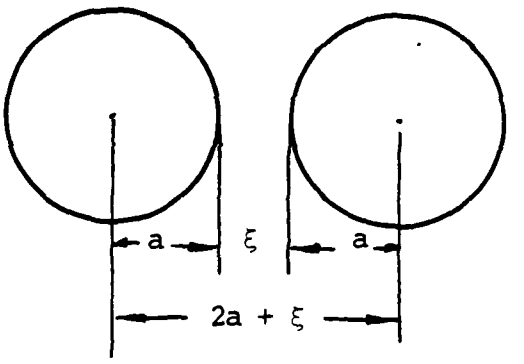

Fig. 2b Nearest neighbours and the random distance ξ+2a between them

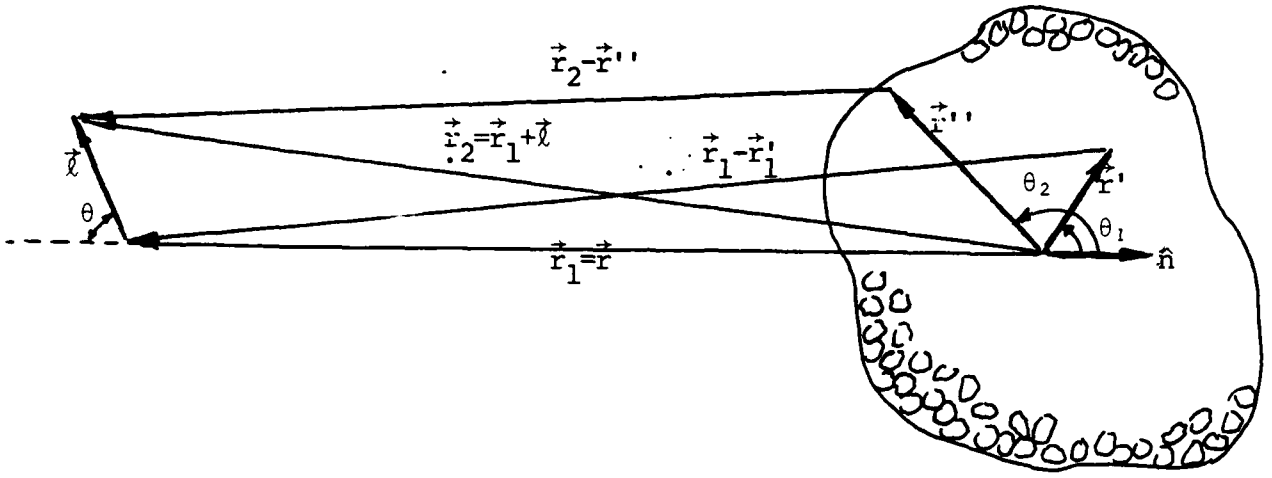

Fig. 1a. Scattering geometry and coordinate system

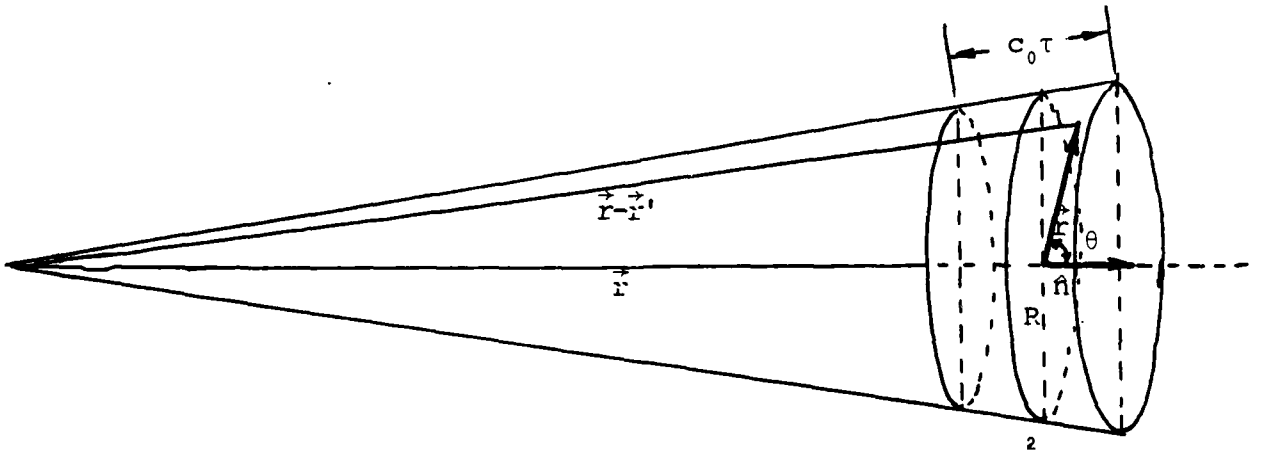

Fig. 1b. Narrow beam incidence and measurement volume $V_R = \pi R^2 c_0 \tau/2$

REFERENCES

1. V. Twersky, J. Math. Phys. 18, 2468 (1977)

2. V. Twersky, J. Math. Phys. 19, 215 (1978)

3. V. Twersky, J. Acous. Soc. Am., 64, 1710 (1978)

4. V. N. Bringi, V. V. Varadan and V. K. Varadan, Radio Sci., 17, 946 (1982)

5. V. K. Varadan, V. N. Bringi, V. V. Varadan and A. Ishimaru, Radio Sci., 18, 321 (1983)

6. V. K. Varadan, Y. Ma and V. V. Varadan, Radio Sci., 19, 1445 (1984)

7. A. Ishimaru, Wave Propagation and Scattering in Random Media, Vols. 1 and 2, Academic Press, New York (1978)

8. V. K. Varadan and V. V. Varadan, Radio Sci., Submitted (1984)

9. V. V. Varadan (Varatharajulu), On the Statistical Theory of the Propagation and Scattering of Light in Simple Fluids, Ph.D. Thesis, University of Illinois, Chicago (1975)

10. A. T. Bharucha-Reid, Random Integral Equations, Academic Press, New York (1972)

11. G. Adomian, Stochastic Systems, Academic Press, New York (1983)

12. L. H. Sibul, Application of Linear Stochastic Operator Theory, Ph. D. Thesis, The Pennsylvania State University (1968)

13. K. K. Shung, Y. W. Yuan, D. Y. Fei and J. M. Jarbell, J. Acoust. Soc. Am., 75, 1265 (1984)

ACKNOWLEDGEMENTS

This work was supported by the U. S. Army Research Office under Contract No: DAAG29-83-K-0097. Many helpful discussions with Dr. Sibul and Professor K. K. Shung are gratefully acknowledged.

observations :

$$K_{p_1}(\vec{r}_1,\vec{r}_2,t_1,t_2) \simeq K_{\psi}(\vec{r}_1,\vec{r}_2,t_1,t_2)$$
$$K_{p}(\vec{r},\vec{\ell}) \simeq K_{\psi}(\vec{r},\vec{\ell}) \qquad (80)$$
$$M^{(2)}_{p_1}(\vec{r},t) \simeq M^{(2)}_{\psi}(\vec{r},t)$$

The mean square value of the scattered field $M^{(2)}_{p_1}(\vec{r},t)$ may then be calculated from Eq. (79). The results are shown in Figs. 3 and 4 wherein the backscattering intensity is plotted as a function of concentration for a fixed frequency of 7.5 MHz. The agreement between theory and experiment is very good.

A PROPAGATOR MODEL FOR MULTIPLE SCATTERING AND WAVE PROPAGATION IN DISCRETE RANDOM MEDIA

by

V. K. Varadan and V. V. Varadan
Wave Propagation Laboratory
Department of Engineering Science and Mechanics
The Pennsylvania State University
University Park, PA 16802

ABSTRACT

A propagator model is presented for studying both coherent and incoherent intensities of the electromagnetic field in a discrete random medium. Lax's quasi-crystalline approximation (QCA) with suitable averaging techniques and the T-matrix of a single scatterer has been emeployed in the analysis. Pair-correlation functions generated by Monte-Carlo simulation have been used in the computation. This model also provides a dispersion equation which is solved for both phase velocity and coherent attenuation as a function of frequency for various values of concentrations of scatterers. Numerical results obtained show excellent agreement with experimental measurements of Killey and Meeten (J. Chem. Soc., Faraday Trans. 2., Vol. 77, pp. 587-599, 1981).

INTRODUCTION

We consider the propagation of plane coherent electromagnetic in an infinite medium containing identical, loss less, randomly distributed particles. Our aim here is to characterize the random medium by an effective complex wave number K (which would be a function of particle concentration, the electrical size, and the statistical description of the random positions of the scatterers), and to study both coherent and incoherent intensities as a function of frequency for various values of concentration c (the fractional volume occupied by the scatterers). Although the formulation is generally valid for non-spherical, aligned or randomly oriented scatterers, initial calculations are confined to spherical scatterers which generally gives us a better picture of the order of magnitude of the different contributions to the intensity without the additional complications of non-spherical geometry and orientation.

Extensive work by Twersky[1-5] has laid the foundation for multiple scattering theory in discrete random media. A related approach using the T-matrix of a single scatterer[6] together with configurational averaging procedures, has been used by the authors to develop a computational method for electromagnetic wave propagation problem in inhomogeneous media[7-9]. Lax's[10] quasi-crystalline approximation (QCA) is used in conjunction with suitable models for the pair-correlation function to obtain an effective wave number $K(=K_1+iK_2)$ which is complex and frequency dependent. The real part K_1 is related to the phase velocity while the imaginary part K_2 is related to coherent attenuation. In this paper, we present a propagator model which is shown to present the same dispersion equation as the one obtained in our previous papers[7-9]. In addition, this model enables us to compute both coherent and incoherent intensities for more realistic geometries without much difficulty.

FORMULATION

Consider wave propagation in an infinite medium of volume $V \to \infty$ containing a random distribution of N scatterers, $N \to \infty$, such that $n_o = N/V$, the number density of scatterers is finite. Plane harmonic waves of frequency ω propagate in the medium and undergo multiple scattering. Let $\vec{E}$, $\vec{E}^0$, $\vec{E}^e_i$, and $\vec{E}^s_i$ denote respectively the total field, the incident field, the field exciting the i-th scatterer and the field scattered by the i-th scatterer. Then self consistency requires the following relationships between the fields[7-9].

$$\vec{E} = \vec{E}^0 + \sum_{i=1}^{N} \vec{E}^s_i \tag{1}$$

and

$$\vec{E}^e_i = \vec{E}^0 + \sum_{j\neq i}^{N} \vec{E}^s_j \tag{2}$$

Let $\underset{\text{Re}}{\text{Ou}}\psi_n$ generally denote outgoing functions (Hankel functions) and functions regular at the origin (Bessel functions). We dispense with vector notation and the abbreviated index may denote $n \to \tau, \ell, m, \sigma$; $\tau = 2,3$; $\ell \in [0,\infty]$; $m \in [0,\ell]$, see Refs. 7-9.

At a field point $\vec{r}$ in the host medium, the incident, scattered and exciting fields are expanded as follows

$$E^0(\vec{r}) = \sum_n a_n \, \text{Re}\, \psi_n(\vec{r}) \tag{3}$$

$$E^e(\vec{r}) = \sum_n \alpha^i_n \, \text{Re}\, \psi_n(\vec{r}-\vec{r}_i) \; ; \; |\vec{r}-\vec{r}_i| < 2a \tag{4}$$

$$E^s(\vec{r}) = \sum_n f^i_n \, \text{Ou}\, \psi_n(\vec{r}-\vec{r}_i) \; ; \; |\vec{r}-\vec{r}_i| > 2a \tag{5}$$

where $\vec{r}_i$ denotes the center of the i-th scatterer, and a is the radius of the sphere circumscribing any scatterer. The coefficients a_n are known while the coefficients f^i_n and α^i_n are unknown but are, however, related through the T-matrix[6]:

$$f^i_n = \sum_{n'} T_{nn'} \alpha^i_{n'} \tag{6}$$

Substituting Eqs. (3)-(6) in (2) and using the translation-addition theorems for spherical wavefunctions and the orthogonality properties of spherical harmonics[6], we obtain

$$\alpha_n^i = a_n^i + \sum_{j\neq i} \sum_{n'} \sum_{n''} \sigma_{nn'} (\vec{r}_j - \vec{r}_i)\, T_{n'n''}\, \alpha_{n''}^j \tag{7}$$

where

$$\text{Ou}\ \psi_n(\vec{r}-\vec{r}_j) = \sum_{n'} \sigma^t_{nn'} (\vec{r}_j - \vec{r}_i)\ \text{Re}\ \psi_{n'}(\vec{r}-\vec{r}_i) \tag{8}$$

and $\sigma_{nn'}$ is the translation matrix for spherical wavefunctions.

If we substitute Eqs. (7) and (5) in (1) and iterate, we obtain

$$E(\vec{r}) = E^0(\vec{r}) + \sum_i \text{Ou}\ \psi_n(\vec{r}-\vec{r}_i)\, T_{nn'} a_{n'}^i + \sum'_{ij} \text{Ou}\ \psi_n(\vec{r}-\vec{r}_i)$$

$$T_{nn'}\, \sigma_{n'n''}(\vec{r}_{ij})\, T_{n''n'''}\, a_{n'''}^j + \sum_i \sum'_j \sum'_k \text{Ou}\ \psi_n(\vec{r}-\vec{r}_i)\, T_{nn'} \ldots + \ldots \tag{9}$$

where $\vec{r}_{ij} = (\vec{r}_j - \vec{r}_i)$.

The first term in Eq. (9) is the incident field reaching the observation point $\vec{r}$ denoted by P in Fig. 1a. The second term of Eq. (9) is a sum of N contributions each of which can be represented by a diagram of the type shown in Fig. 1b. The thin line represents the incident field E^0 and the thick solid line represents the "propagator", $\text{Ou}\ \psi_n(\vec{r}-\vec{r}_i)\, T_{nn'}$, which propagates the field from scatterer i to observation point $\vec{r}$. The sum of all N diagrams of this type is termed single scattering. The third term of Eq. (9) is a sum of N(N-1) contributions, each involving a pair of particles, and is represented by the diagram of Fig. 1c. There are also N(N-1) terms of the form given in Fig. 1d which involve only a pair of particles. There are N(N-1) (N-2) terms of the type shown in Fig. 1e. As seen from Fig. 1, the three body process can include any number of scattering in any order between the three objects.

Equation (9) can be averaged over the positions of the particles to yield

$$\langle E(\vec{r})\rangle = E^0(\vec{r}) + \sum_i T_{nn'}\, Ou\, \psi_n(\vec{r}-\vec{r}_i)\, a_n^i\, p(\vec{r}_i)\, d\vec{r}_i$$

$$+ \sum_i \sum_j{}' T_{nn'}\, T_{n''n'''}\, Ou\, \psi_n(\vec{r}-\vec{r}_i)\, \sigma_{n'n''}(\vec{r}_{ij})\, a_{n''}^j\, p(\vec{r}_i)\, p(\vec{r}_j) \qquad (10)$$

$$p(\vec{r}_j|\vec{r}_i)\, d\vec{r}_j\, d\vec{r}_i + \ldots$$

which involves all orders of joint probability functions, $p(\vec{r}_i)$, $p(\vec{r}_j|\vec{r}_i)$, etc. We have shown[10] that invoking the QCA implies that the coherent field and the resulting dispersion equation were limited to terms of the form

$\langle E\rangle_{QCA}$ =

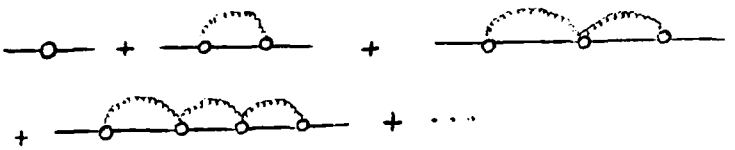

(11)

where  denotes positional correlation between two scatterers and it is clear from the diagrams that each scatterer participates only once in a given term, there is no back and forth scattering and all scattering is sequential and only sequential positional correlations are allowed.

Introducing spatial Fourier transforms of the translation matrix σ and the radial distribution functions g (given by $p(\vec{r}_j|\vec{r}_i) = \frac{1}{V}\, g\,(\vec{r}_{ij})$) which are denoted by $\overline{\sigma}\,(K)$ and $\overline{g}(K)$, respectively, and using the convolution theorem, we obtain

$$\langle E(\vec{r})\rangle = E^0(\vec{r}) + \int Ou\, \psi_n(\vec{r}-\vec{r}_i)\, T_{nn'}\, n_o \int [1-n_o\, \overline{\sigma g}\,(K)\, T]^{-1}$$

$$e^{iK\cdot(\vec{r}_1-\vec{r}_2)}\, a_{n''}^{(2)}\, d\vec{K}\, d\vec{r}_1\, d\vec{r}_2 \qquad (12)$$

This new form of the average field can be interpreted as an incident plane wave propagating through an effective medium of propagation constant K and propagator $[1-n_o\, \overline{\sigma g}(K)T]^{-1}$ undergoing scattering from a particle at r_1 and then propagating to the observation point r with the wave number of the host medium. The dispersion equation in the model medium can be obtained

by setting the determinant of the propagator equal to zero:

$$| 1-n_o \overline{\sigma g}(K)\ T | = 0 \tag{13}$$

This equation is identical to the one obtained by us earlier using the self-consistent multiple scattering approach, see Ref. 9.

The field fluctuations $\Delta\vec{E}$ may now be given by

$$\Delta\vec{E} = \vec{E} - \langle\vec{E}\rangle \tag{14}$$

and can be represented as a multiple scattering series which may be represented by the following diagrams

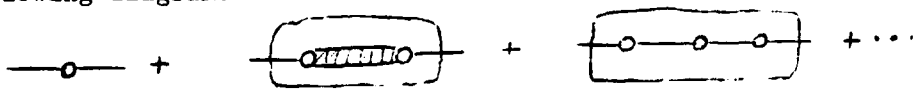

(15)

where — denotes propagation of the field from one point to the other and 0 denotes a scatterer. If two or more scatterers are enclosed in an area such as 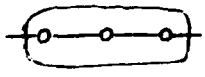 arbitrary multiple scattering any number of times (16) and in any order can go on between scatterers 1, 2 and 3.

Along these lines, we define the incoherent intensity or the spectral density $G_\alpha(\vec{R},\omega)$ at position $\vec{R}$, see Fig. 2 frequency ω for field polarization in the direction as (see Fig. 5 for the definition of $\hat{\alpha}$).

$$G_\alpha(\vec{R},\omega) = \frac{1}{4}\langle|\hat{\alpha}\cdot\Delta\vec{E}|^2\rangle$$

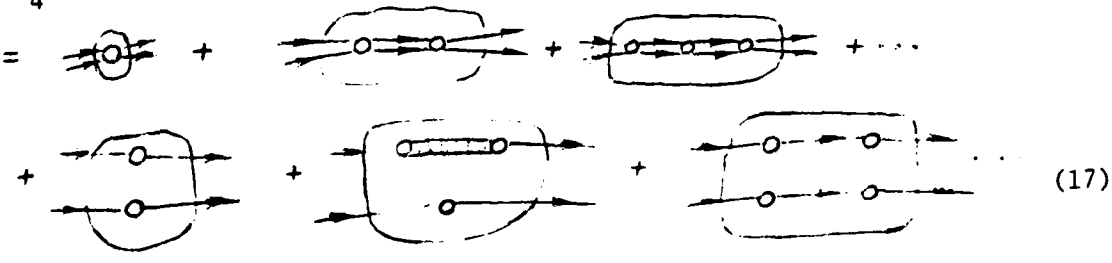

(17)

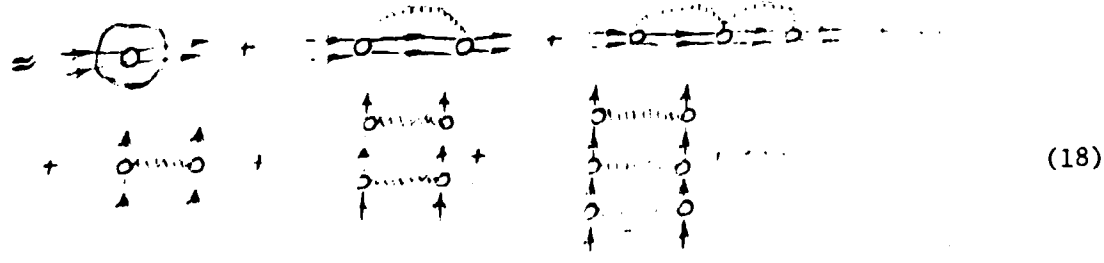

(18)

The first set of the above diagrams represents a partial summation of QCA type terms incorporating two body correlations while the second set represents the conventional ladder diagrams. In both sets of diagrams, we can use so called "dressed propagators" obtained from Eq. (13) between scatterers instead of "bare propagators". This means that K from (13) can be used as the wave number characterizing the medium between scatterers involved in calculation of the spectral density, i.e., the other scatterers that participate in only one or other of the field lines are averaged over separately and replaced by K.

NUMERICAL RESULTS

The numerical procedure is described in detail in Refs. 6-9, and will not be repeated here. The effective wave number $K(=K_1+iK_2)$ is computed for Revacryl spheres in distilled water for a range of frequencies and concentrations of scatterers. The real part K_1, is related to the phase velocity while the imaginary part K_2 is related to coherent attenuation. We have also calculated the coherent and incoherent intensity for electromagnetic wave propagation through ice particles ($\varepsilon_r = 3.168$) in free space using the terms of the two series of diagrams given in Eq. (18) that make up our approximation using the pair correlation functions to the spectral intensity.

In Figs. 2 and 3, the real and imaginary parts of the coherent field are compared with the experimental measurements of Killey and Meeten[11]. In Fig. 4, calculations of the coherent intensity for a suspension of Revacryl spheres in distilled water show excellent comparison with measurements of Killey and Meeten[11]. In Fig. 5, the geometry for the computation of incoherent intensity is given. In Fig. 6, the incoherent intensity is plotted as a function of ka for c = 0.0524 and for various angle θ (see Fig. 5 to see how θ is measured).

In Figs. 7 and 8, similar results are presented for higher concentrations. Figure 9 displays the incoherent intensity as a function of the observation angle θ, and the intensity reduces to zero at $\theta = 90°$ as expected while in Fig. 10, we have plotted the back scattering intensity as a function of ka for a concentration of .0524. There are two minima in the intensity spectrum.

ACKNOWLEDGMENTS

This work was supported by the U.S. Army Research Office under contract DAAG29-83-K-0097. Many helpful discussions with Dr. W.A. Flood are gratefully acknowledged.

REFERENCES

1. V. Twersky, Coherent scalar field in pair-correlated random distributions of aligned scatterers, J. Math. Phys., 18, 2468-2486, 1977.

2. V. Twersky, Coherent electromagnetic waves in pair-correlated random distributions of aligned scatterers, J. Math. Phys., 19, 215-230, 1978.

3. V. Twersky, Multiple scattering of waves by periodic and by random distributions, in Electromagnetic Scattering, edited by P.L.E. Uslenghi, Academic Press, New York, 221,251, 1978.

4. V. Twersky, Acoustic bulk parameters in distribution of pair-correlated scatterers, J. Acoust. Soc. Am., 64, 1710-1719, 1978.

5. V. Twersky, Propagation and attenuation in composite media, Lect. Notes Phys., 154, 258-271, 1982.

6. V. K. Varadan and V. V. Varadan (Eds.) Acoustic, Electromagnetic and Elastic Wave Scattering-Focus on the T-matrix Approach, Pergamon Press, New York, 1980.

7. V. V. Varadan, V. N. Bringi and V. K. Varadan, Frequency dependent dielectric constants of discrete random media, Lect. Notes Phys., 154, 272-284, 1982.

8. V. N. Bringi, V. K. Varadan and V. V. Varadan, Coherent wave attenuation by a random distribution of particles, Radio Sci., 17, 946-952, 1982.

9. V. K. Varadan, V. N. Bringi, V. V. Varadan and A. Ishimaru, Multiple Scattering theory for waves in discrete random media and comparison with experiments, Radio Sci., 18, 321-327, 1983.

0. V. V. Varadan and V. K. Varadan, The quasi-crystalline approximation and multiple scattering of waves in random media, submitted to IEEE Trans. Antennas and Propagation.

1. A. Killey and G. H. Meeten, Optical extinction and refraction of concentrated latex dispersions, J. Chem. Soc., Faraday Trans. 2, 587-599, 1981.

FIGURE CAPTIONS

Fig. 1 A diagramatic representation of multiple scattering processes.

Fig. 2 Phase velocity vs concentration c for Revacryl dispersions in distilled water at λ = 546 nm.

Fig. 3 Coherent attenuation vs concentration c for Revacryl dispersions in distilled water at λ = 410 nm and 546 nm.

Fig. 4 Coherent intensity as a function of propagation depth z for various values of c at λ = 546 nm.

Fig. 5 Scattering geometry.

Fig. 6a Incoherent intensity as a function of ka for c = 0.0524 and for various angles of observation θ.

Fig. 6b Expanded version of Fig. 6a for the frequency range $1.0 < ka < 2.0$.

Fig. 7 Incoherent intensity as a function of ka for different values of c at $\theta = 60°$.

Fig. 8 Incoherent intensity as a function of ka for c = 0.157 at $\theta = 60°$; the dotted line is the contribution due to the ladder diagram only.

Fig. 9 Incoherent intensity as a function of observation angle θ for c = 0.105 and ka = 1.0.

Fig. 10 Backscattering intensity as a function of ka for c = 0.0524.

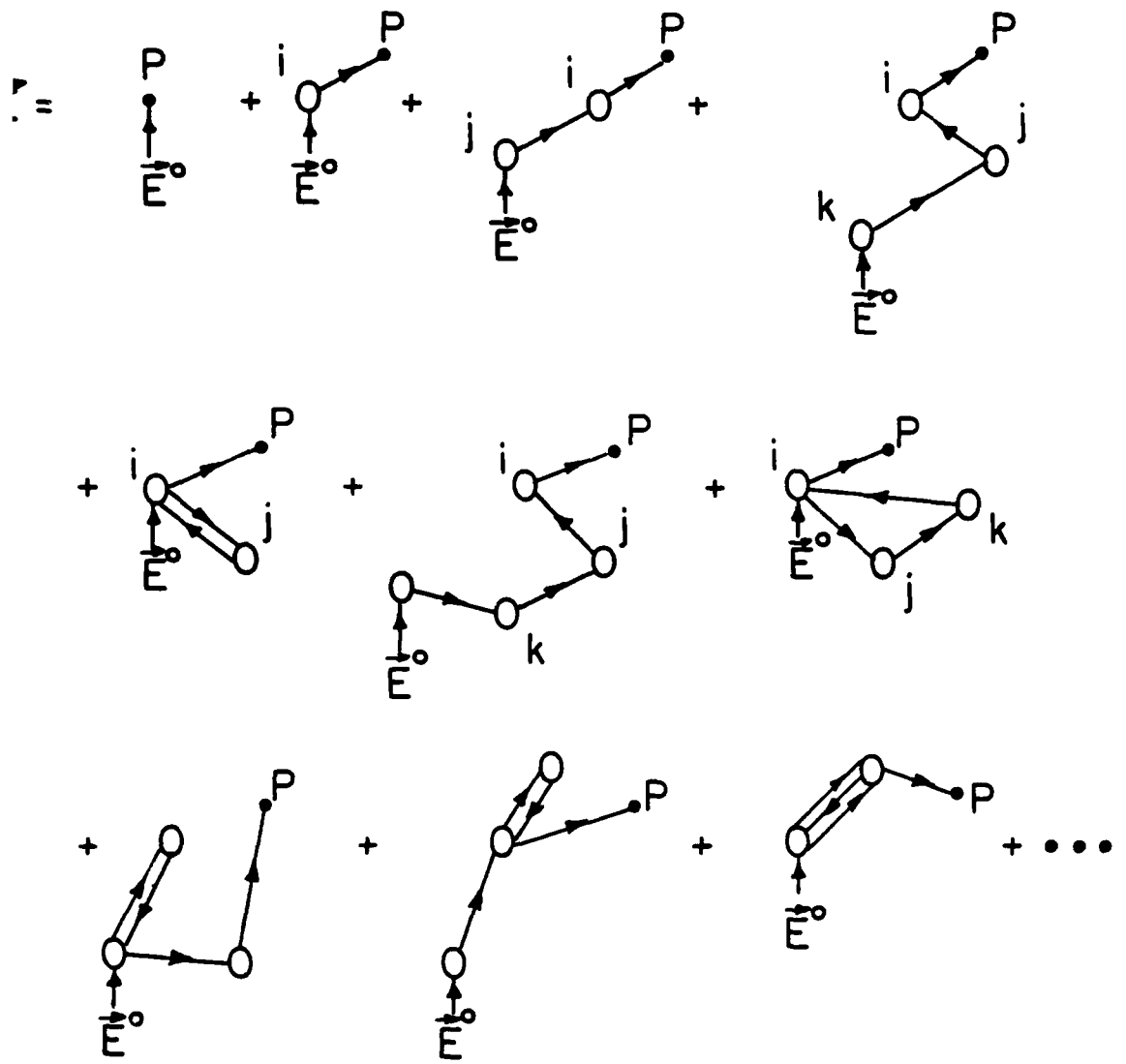

Figure 1

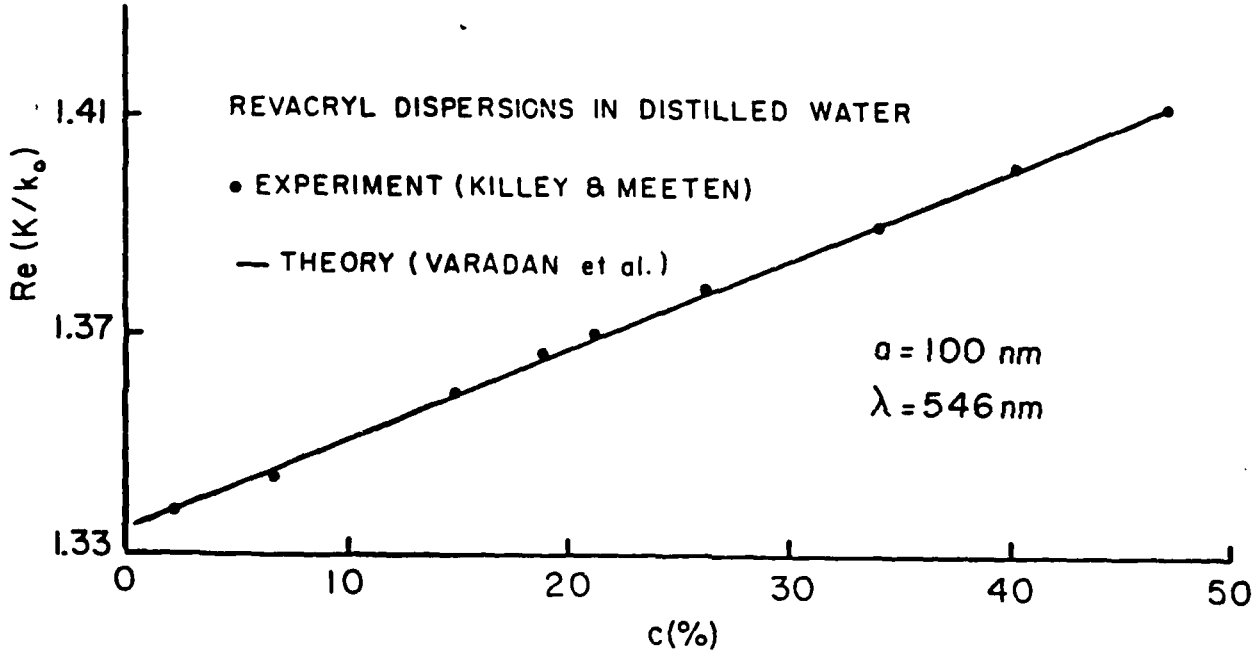
REVACRYL DISPERSIONS IN DISTILLED WATER
• EXPERIMENT (KILLEY & MEETEN)
— THEORY (VARADAN et al.)
a = 100 nm
λ = 546 nm
Re (K/k₀)
1.41
1.37
1.33
0
10
20
30
40
50
c(%)

Figure 2

INTRODUCTION

The intensity measurements are quite common in many physical problems dealing with the wave scattering. In order to compare the field measurements with the theoretical calculations one needs to carefully introduce the incoherent intensity into consideration, which proved to be significant enough as the frequency increases. In this paper the intensity calculation based on the energy principle for nonabsorbing scatterers, which has been well investigated by Twersky (1957), is discussed, and the rule of conservation of energy serves as a guideline to check the numerical accuracy. We shall, however, consider only sparse distribution of scatterers so that higher order scattering can be neglected although the interactions among scatterers are still considered. The incorporation of the multiple scattering theory so as to accomodate denser concentrations of scatterers is explained and the computational scheme involving the pair correlation function is also introduced. In addition, any given size distribution of scatterers can be handled following Ma et al (1983). However, only uniform and Rayleigh size distributions have been used to perform the calculations.

θ	Scattering angle
ω	Angular frequency
Ω	Solid angle
ρ	Area number density
σ	Scattering cross section
∇	Gradient operator
$\cdot$	Denotes scalar multiplication of two vectors
ψ	Wave function
$< >$	Configurational average
$< >_i$	Configurational average holding jth scatterer fixed
$< >_{jk}$	Configurational average holding jth and kth scatterers fixed

SUBSCRIPTS

a	Amplitude
i	Refers to incident wave
m,n	indices (integer)
s	Refers to scattered wave

SUPERSCRIPTS

*	Complex conjugate
$\rightarrow$	vector sign
+	$z > 0$ plane
-	$z < 0$ plane

LIST OF SYMBOLS

a	Size of particle
C^+	Coherent reflection coefficient
C^-	Coherent transmission coefficient
c	Speed of wave propagation
$\hat{e}_r$	Unit radial vector in spherical coordinates
$\hat{e}_z$	Unit vector in the positive z direction in rectangular coordinates
$f(a,\theta)$	Scattering function
H	Distance from receiver
$h_n^{(2)}$	Spherical Hankel function of the 2nd kind
I	Wave intensity (energy flux)
$Im(\ )$	Imaginary part of ( )
i	Imaginary unit ($i^2 = -1$)
$j_n(\ )$	Spherical Bessel function
k	Wave number
N	Total number of scatterers
$O(\ )$	Order of ( )
$P_n(\cos\theta)$	Legendre polynomials
p	Pressure
R	Distance between particle and receiver
$Re(\ )$	Real part of ( )
r	Distance between particle and the reference origin
U	Total scattered field
u	Individual scattered field
$\vec{v}$	Velocity vector
$x,y,z,$	Rectangular coordinates
$y_n(\ )$	Spherical Neumann function

ABSTRACT

In this paper, the configurational averages of the wave function ψ, ψ^2, and the wave energy flux S are derived for planar distributed particles excited by a normally incident plane wave. Although the higher order scattering terms are neglected for sparse distributions of particles, the interactions among them are still considered, using the multiple scattering theory, to perform the numerical calculations. Both the reflection and transmission coefficients for the rough plane are investigated. Relations between the coherent and incoherent energy flux are obtained using the principle of conservation of energy. Computations of the intensity are presented as a function of frequency for different concentrations of particles with uniform and Rayleigh size distributions.

MULTIPLE SCATTERING OF WAVES FROM PLANAR DISTRIBUTED PARTICLES

by

Y. Ma, V. K. Varadan and V. V. Varadan

Wave Propagation Lab
Department of Engineering Science and Mechanics
The Pennsylvania State University, University Park, PA 16802

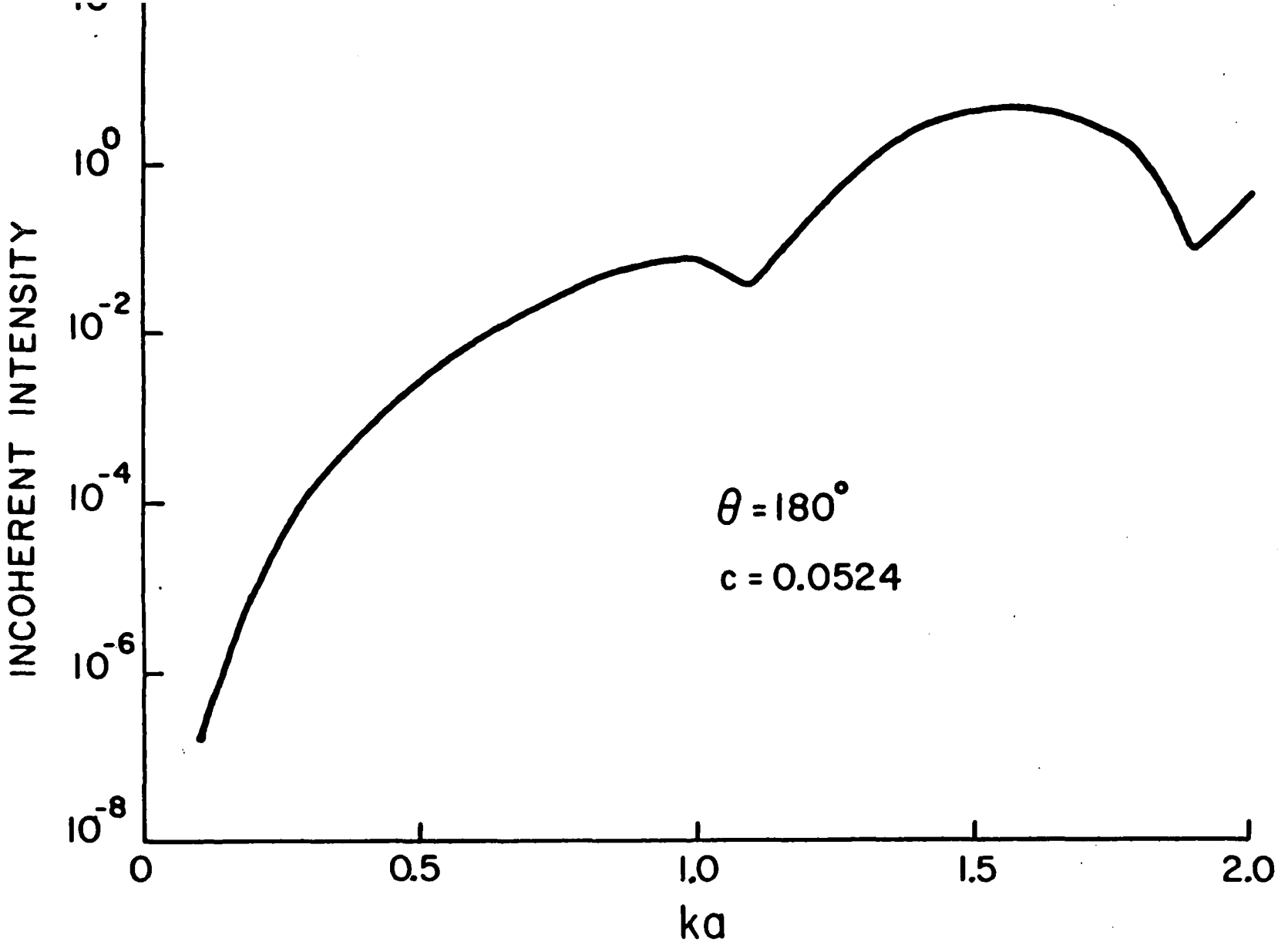
INCOHERENT INTENSITY
10^{0}
10^{-2}
10^{-4}
10^{-6}
10^{-8}
0
0.5
1.0
1.5
2.0
ka
$\theta = 180^{\circ}$
c = 0.0524

Figure 10

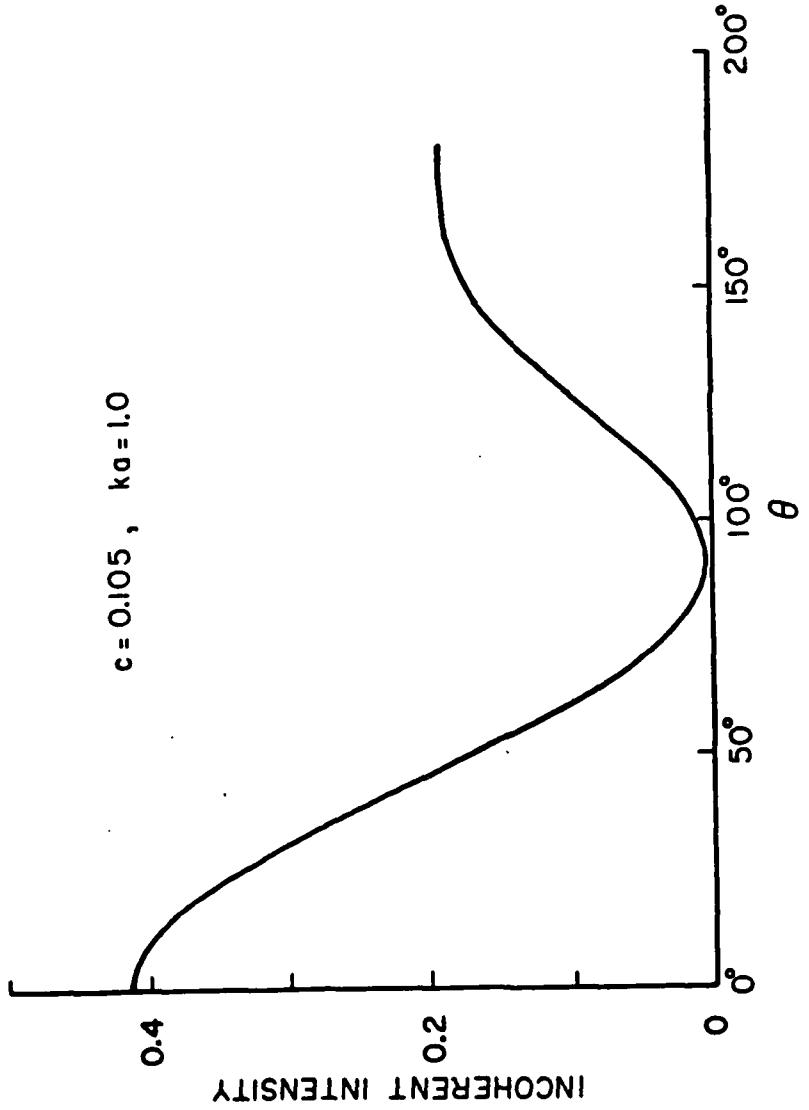

Figure 9

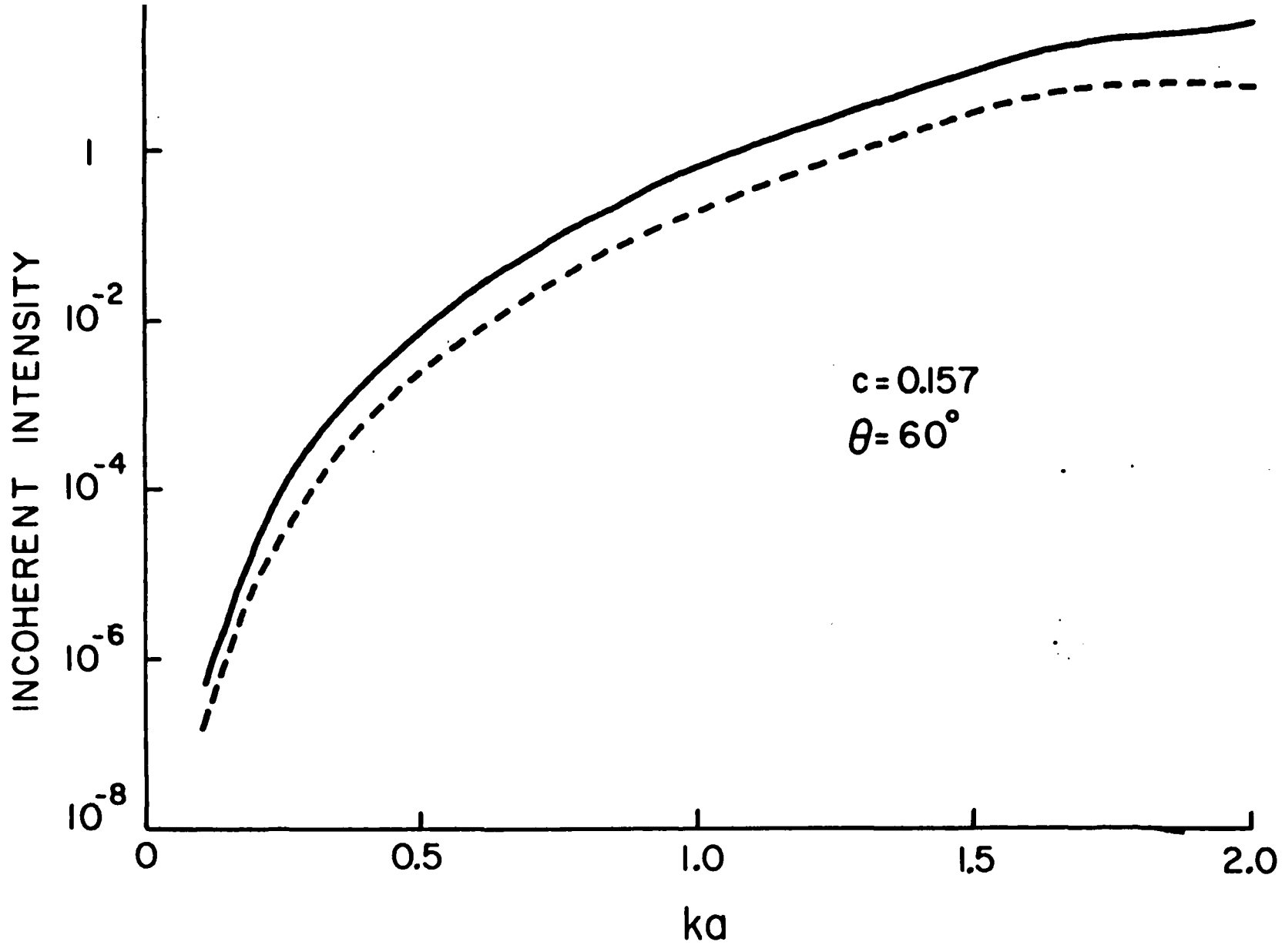
INCOHERENT INTENSITY
1
10^{-2}
10^{-4}
10^{-6}
10^{-8}
0
0.5
1.0
1.5
2.0
ka
c = 0.157
$\theta = 60^{\circ}$

Figure 8

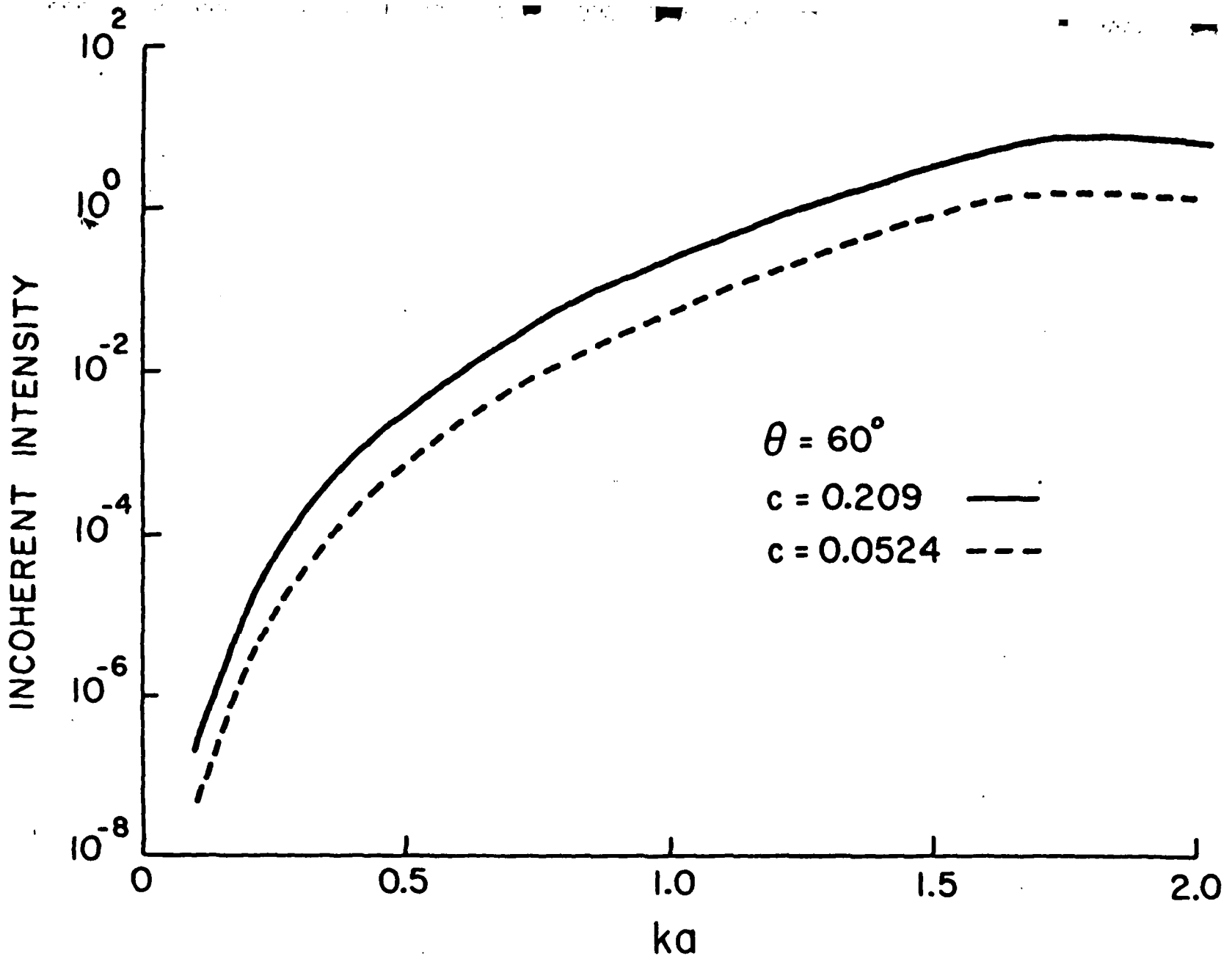
INCOHERENT INTENSITY
10^{2}
10^{0}
10^{-2}
10^{-4}
10^{-6}
10^{-8}
0
0.5
1.0
1.5
2.0
ka
θ = 60°
c = 0.209
c = 0.0524

Figure 7

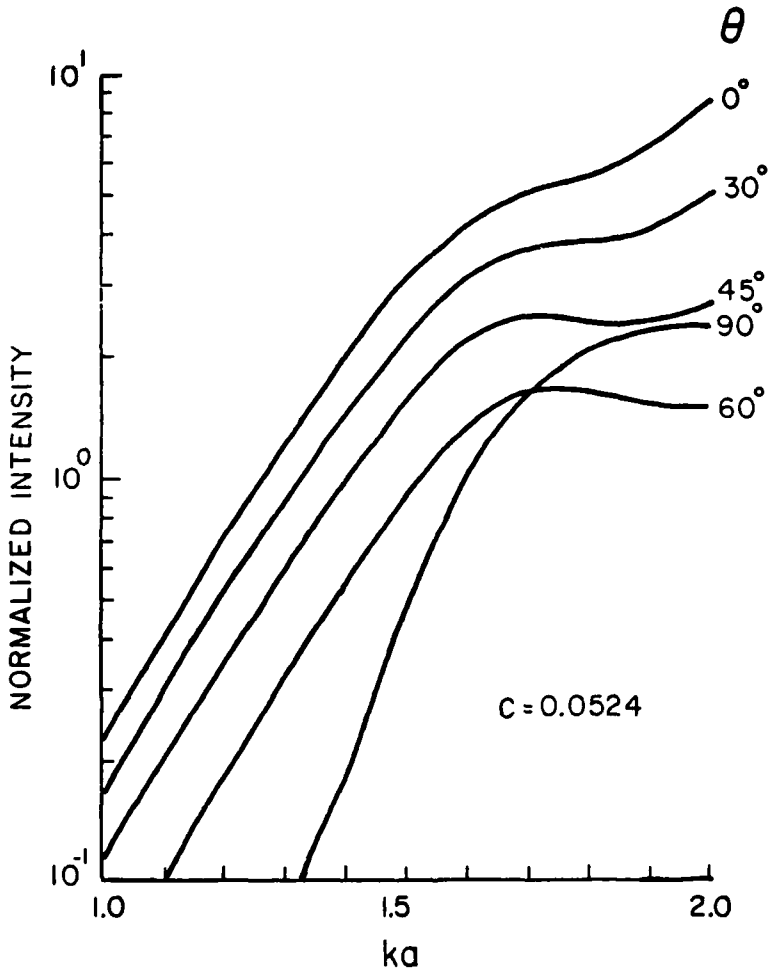
θ
0°
30°
45°
90°
60°
C = 0.0524
NORMALIZED INTENSITY
10^1
10^0
10^-1
1.0
1.5
2.0
ka

Figure 6b

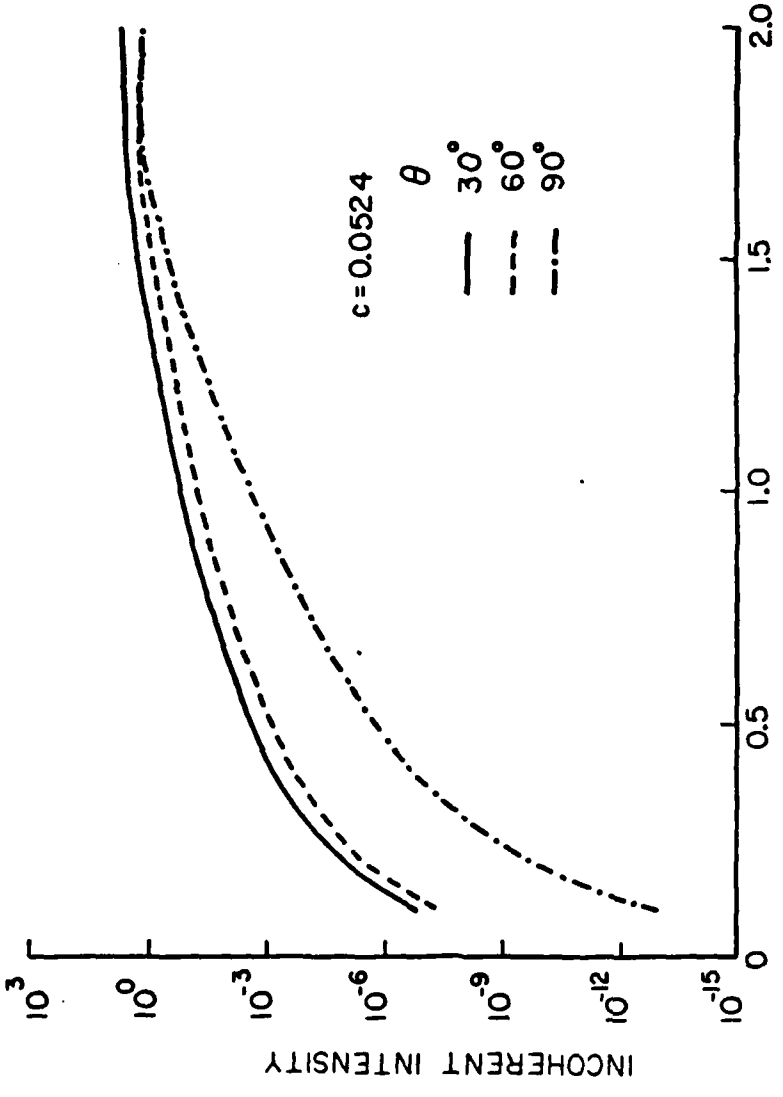
INCOHERENT INTENSITY
10^{3}
10^{0}
10^{-3}
10^{-6}
10^{-9}
10^{-12}
10^{-15}
0
0.5
1.0
1.5
2.0
ka
c=0.0524
θ
30°
60°
90°

Figure 6a

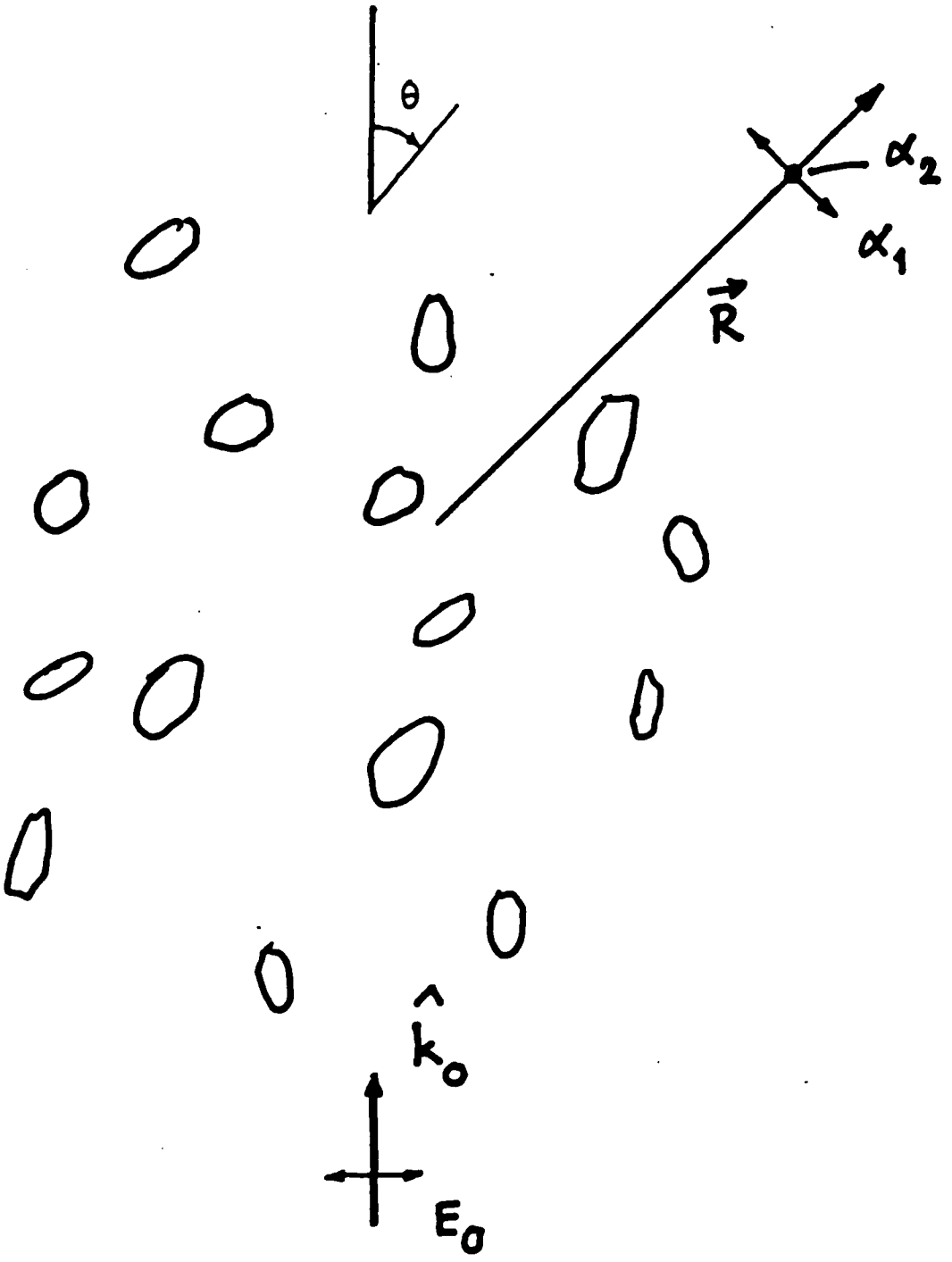

Figure 5

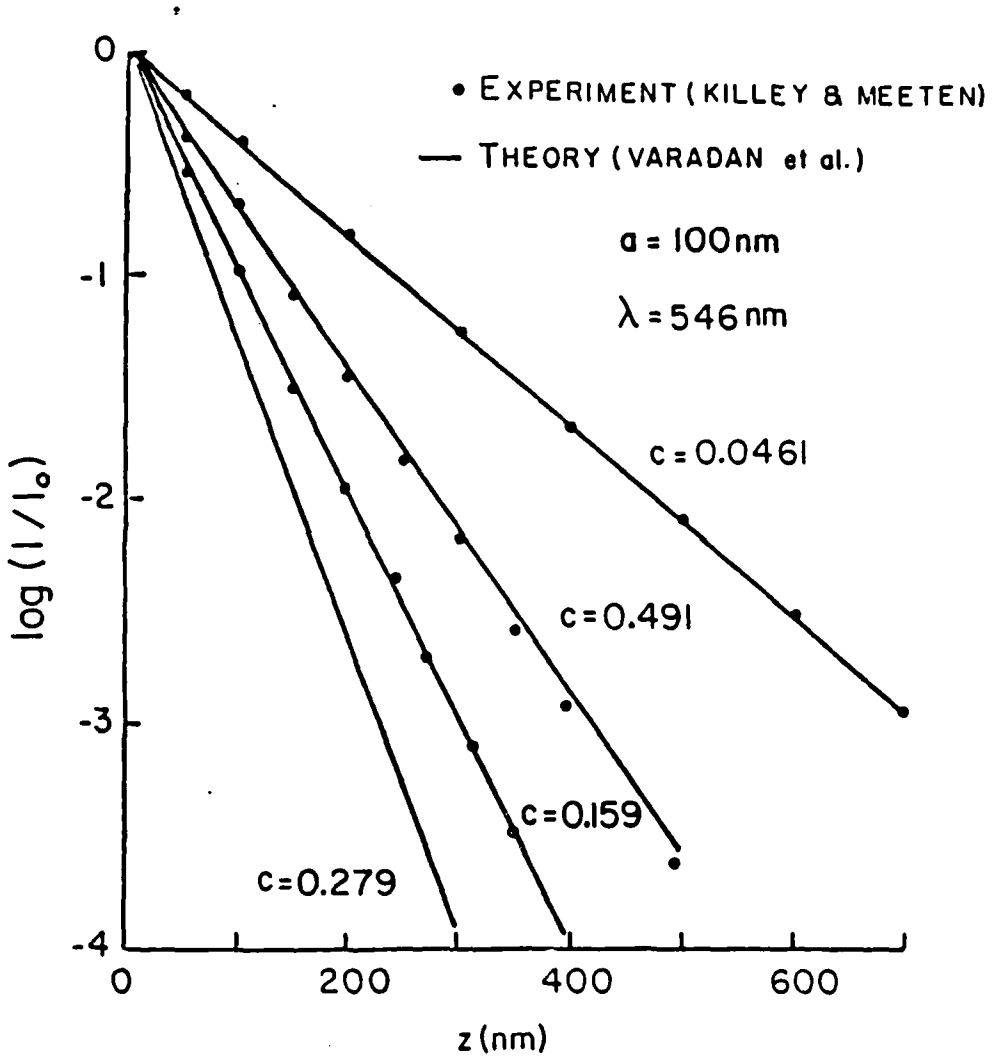
• EXPERIMENT (KILLEY & MEETEN)
— THEORY (VARADAN et al.)
a = 100nm
λ = 546 nm
c = 0.0461
c = 0.491
c = 0.159
c = 0.279
log (I/I₀)
0
-1
-2
-3
-4
0
200
400
600
z (nm)

Figure 4

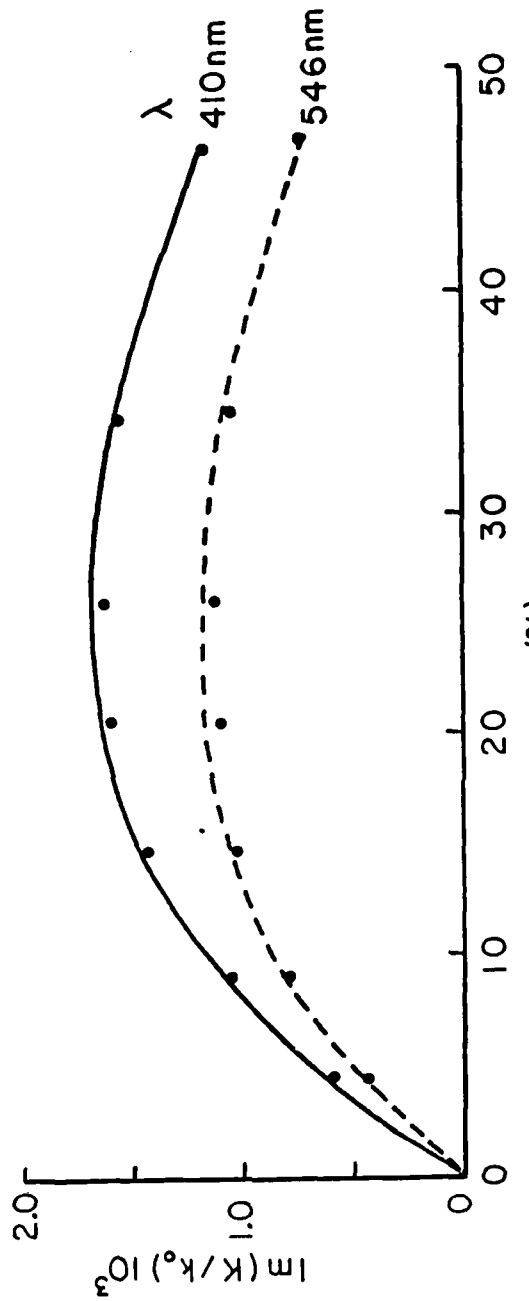

Figure 3

THE CONFIGURATIONAL AVERAGE OF THE WAVE FUNCTION, $\langle\psi\rangle$

Consider a plane wave normally incident upon a plane covered by particles (see Figure 1). The total coherent field is then given by

$$\langle\psi\rangle = \langle\psi_i\rangle + \langle\sum_{j=1}^{N} u_j\rangle$$

$$= \psi_a e^{ikz} + \langle U\rangle \ , \tag{1}$$

where ψ_i and U are the incident and total scattered field, respectively, and ψ_a is the amplitude of the incident wave. The average scattered field $\langle U\rangle$ is defined to be, following Foldy (1945),

$$\langle U\rangle = \rho\int\overline{\langle F(a_j,\theta_j)}\ \psi\ (\vec{r}_j)\rangle d\vec{r}_j, \tag{2}$$

where $$F(a_j,\theta_j) = (1/k)\sum_{n=0}^{\infty}[(2n+1)/(1+iC_n)]i^n h_n^{(2)}\ (k|\vec{R}-\vec{r}_j|)P_n(\cos\theta_j)$$

$$\overline{F(a_j,\theta_j)} = \int_0^{\infty} F(a_j,\theta_j)q(a)da$$

$q(a)$ = the size distribution function

and C_n is related to the T-matrix of the scatterer.

Physically speaking, the average scattered field can be expressed as a combination of a reflected wave and a transmitted wave due to the plane wave excitation (Twersky, 1957). Therefore, for the present case (normal incidence), $\langle U\rangle$ may be expressed as

$$\langle U\rangle\big|_{z>0} = \langle U\rangle^{+} = C^{+}\psi_a e^{-ikz}$$

$$\langle U\rangle\big|_{z<0} = \langle U\rangle^{-} = C^{-}\psi_a e^{ikz} \tag{3}$$

or $$\langle U\rangle^{\pm} = C^{\pm}\psi_a e^{ik|z|}, \quad z\neq 0 \ ,$$

where $\langle U\rangle^{+}$ and $\langle U\rangle^{-}$ are the normally upward and downward going plane

waves characterized by the coherent reflection coefficient C^+ and the transmission coefficient C^-.

However, the coherent field $\langle\psi\rangle$ on the bottom plane, i.e. z = 0, is constant attributed to both halves of the upward and downward going waves (including the incident wave) and can be reasonably written following Twersky (1957)

$$\langle\psi\rangle(\vec{r}_j)\rangle\big|_{z=0} = \langle\psi_i\rangle\big|_{(x_j,y_j,0)} + [(\langle U\rangle^+ + \langle U\rangle^-)/2]_{(x_j,y_j,0)}$$
$$= \psi_a + (C^+ + C^-)\,\psi_a/2 \,. \tag{4}$$

Substituting Eq. (4) into Eq. (2) yields

$$\langle U\rangle = \rho\psi_a \int \overline{F(a_j,\theta_j)}[\,1 + (C^+ + C^-)/2\,]\, d\vec{r}_j. \tag{5}$$

At large distance from nodules ($k|\vec{R}-\vec{r}_j|>>1$) and using the polar coordinates for integration, the far-field expression for Eq. (5) becomes

$$\langle U\rangle = 2\pi\rho\psi_a \int_0^\infty \exp\,(-ik|\vec{R}-\vec{r}_j|\,/|\vec{R}-\vec{r}_j|)\;\overline{f(a_j,\theta_j)}[1+(C^+ + C^-)/2]\; r_j dr_j, \tag{6}$$

where

$$f(a_j,\theta_j) = (1/k)\sum_{n=0}^{\infty}[(2n+1)i/(1+iC_n)](-1)^n P_n(\cos\theta_j)$$

and $|\vec{R}-\vec{r}_j| = H/\cos\theta_j$ (see Figure 2). We can rewrite Eq. (6) in terms of the integration as

$$\langle U\rangle = 2\pi\rho\psi_a \int_0^\pi ([1+C^-/2]\overline{f(a_j,\theta_j)}+(C^-/2)\overline{f(a_j,\pi-\theta_j)})e^{-ikH/\cos\theta_j}$$
$$\times\; (H\tan\theta_j/\cos\theta_j)d\theta_j$$
$$= (2\pi\rho\psi_a i/k)\int_0^\pi [(1+C^-/2)\overline{f(a_j,\Lambda)}+(C^+/2)\overline{f(a_j,\Lambda)}e^{-\Lambda}]d\Lambda, \tag{7}$$

where $\Lambda = -ikH/\cos\theta_j$.

In order to solve Eq. (7) for kH>> 1, the principle of stationary

phase (Lamb, 1932) is used. The solution can thus be written in terms of the stationary phase angle γ as

$$\langle U\rangle = (2\pi\rho i\psi_a[1+C^-/2)\overline{f(a_j,\gamma)}+(C^-/2)\overline{f(a_j,\pi-\gamma)}]e^{-ikH/\cos\gamma})/k. \quad (8)$$

The stationary phase angle γ is obtained by solving

$$d\Lambda/d\theta_j = -ikH\tan\theta_j/\cos\theta_j = 0$$

and found to be $\gamma = n\pi$ ($n = 0, 1, 2, \ldots$) for this case.

One sees from the geometry (Figure 1) that $\langle U\rangle^+$ can be solved, by integrating θ_j from 0 to $\pi/2$ (θ_j is the so-called meridian angle in the spherical coordinates and is defined as $0 \leq \theta_j < \pi/2$ for $z>0$) using Eq. (7). The only appropriate phase angle in this region is zero, so $\langle U\rangle^+$ is found by using Eqs. (1) and (3) at $z = H$,

$$\langle U\rangle^+ = 2\pi\rho i\psi_a[(1+C^-/2)\overline{f(a_j,0)}+(C^+/2)\overline{f(a_j,\pi)}]e^{-ikH}/k = C^+\psi_a e^{-ikH}. \quad (9)$$

Similarly,

$$\langle U\rangle^- = 2\pi\rho i\psi_a[(1+C^-/2)\overline{f(a_j,\pi)}+(C^+/2)\overline{f(a_j,0)}]e^{ikH}/k = C^-\psi_a e^{ikH}. \quad (10)$$

The two unknowns C^+ and C^- can now be solved simultaneously from the above two equations using Cramer's rule:

$$C^+ = \beta_0 \,/\, [\, 1 - \beta_\pi + (\beta_\pi^2 + \beta_0^2)/4\,] \quad (11)$$

$$C^- = (\,\beta_\pi - [(\,\beta_\pi^2 + \beta_0^2\,)/2])/[\,1 - \beta_\pi + (\beta_\pi^2 + \beta_0^2\,)/4], \quad (12)$$

where,

$$\beta_0 = 2\pi\rho i\overline{f(a_j,0)}/k$$

$$\beta_\pi = 2\pi\rho i\overline{f(a_j,\pi)}/k.$$

Substituting the expressions for C^+ and C^- into Eqs. (9) and (10) respectively, we obtain

$$\langle U\rangle^{+} = [\ \beta_0 + \beta_0\beta_\pi + 0(\beta_0^3)]\psi_a e^{-ikz},\ z>0 \tag{13}$$

$$\langle U\rangle^{-} = [\beta_\pi + (\beta_\pi^2 + \beta_0^2\ )/2 + 0(\beta_\pi^3)]\psi_a e^{ikz},\ z<0 \tag{14}$$

The first terms on the RHS's of Eqs.(13) and (14) are due to the single scattering whose excitation is the incident plane wave ψ_i only. This can be obtained simply by substituting ψ_i (z=0) for $\langle\psi(\vec{r}_j)\rangle$ in Eq. (2). The second term is obtained using the self-consistent approach which is essentially Picard's process of successive approximation in the present case. Foldy (1945) introduced this method to explain the orders of scattering since the higher order scattering is approximated by iteration using the previous one (i.e. lower order scattering). The idea is that the average scattered field $\langle U\rangle^{+}$ (or $\langle U\rangle^{-}$) can be obtained from a Neumann series which is, in this case

$$\langle U(\vec{R})\rangle = u_1^{\pm} + \sum_{m=2}^{\infty} u_m^{\pm}\ , \tag{15}$$

where

$$u_m^{\pm} = \rho\int \overline{f(a_j,\theta_j)}[u_{m-1}^{+}(\vec{r}_j) + u_{m-1}^{-}(\vec{r}_j))/2][e^{-ik|\vec{R}-\vec{r}_j|}/|\vec{R}-\vec{r}_j|]d\vec{r}_j$$

and $\quad u_1^{+} = \beta_0\psi_a e^{-ikz},\ z>0$

$$u_1^{-} = \beta_\pi\psi_a e^{ikz},\quad z<0\ .$$

One sees from Eq. (15) that m = 1, 2, and 3 correspond to single, double and triple scattering respectively.

Generally speaking, in Eqs. (13) and (14) the successive terms are smaller compared to the previous terms for a sparse distribution of particles. Therefore, the higher order scattering can be neglected in the approximation of the average scattered field <U> for a loosely packed planar area.

CONFIGURATIONAL AVERAGE OF $\langle\psi^2\rangle$

Since particles are randomly distributed, the scattered field U is not constant. This is because scatterers make an otherwise homogeneous medium inhomogeneous. The magnitude and phase of U will fluctuate in a random manner. Thus the total field at $\vec{R}$, i.e. $\psi(\vec{R})$, is also a random function and can usually be divided into average field $\langle\psi\rangle$ and the fluctuating field ψ'.

The square of the magnitude of the coherent field $|\langle\psi\rangle|^2$ is the coherent component and the average of the square of the magnitude of the incoherent field is the incoherent component. The sum of the coherent and incoherent components is the average of the square of the magnitude of the acoustic field, i.e.

$$\langle|\psi|^2\rangle = |\langle\psi\rangle|^2 + \langle|\psi'|^2\rangle \quad , \tag{16}$$

where ψ' is related to U as $\psi' = U - \langle U\rangle$

or

$$\langle|\psi'|^2\rangle = \langle|U|\rangle^2 - |\langle U\rangle|^2 \quad . \tag{17}$$

The coherent component $|\langle\psi\rangle|^2$ can be obatined directly from the coherent field $\langle\psi\rangle$ which is known (Eq. (4)). It is of interest to find here the incoherent component $\langle|\psi'|^2\rangle$ only. Substituting the expression for U (i.e. $U = \sum_{j=1}^{N} u_j$) into Eq. (17) yields

$$\langle|\psi'|^2\rangle = \langle\Sigma u_j^* \Sigma u_k\rangle - \Sigma\langle u_j\rangle^* \Sigma\langle u_k\rangle \tag{18}$$

$$= \sum_{j\neq k} \sum_{k} \langle u_j^* u_k\rangle + \sum_{j} \langle|u_j|^2\rangle - \sum_{j} \sum_{k} \langle u_j\rangle^* \langle u_k\rangle$$

The above equation can also be written in the following form

$$\langle|\psi'|^2\rangle = \rho^2\iint[(N-1)\,\langle u_j^* u_k\rangle_{jk}/N - \langle u_j\rangle_j^* \langle u_k\rangle_k]d\vec{r}_j d\vec{r}_k$$

$$+\rho^2\int\langle|u_j|^2\rangle_j d\vec{r}_j \ , \tag{19}$$

by using the definition of the configurational average (see Varadan and Varadan (1980)). In order to calculate the incoherent component $\langle|\psi'|^2\rangle$ in Eq. (19) two approximations were also introduced. First, (N-1)/N is replaced by unity which is certainly valid for large N. Secondly, we use

$$\langle u_j^* u_k\rangle_{jk} \sim \langle u_j\rangle_j^* \langle u_k\rangle_k \tag{20}$$

as suggested by Twersky (1957). Eq. (20) may be interpreted physically as neglecting contributions to the excitations of a scatterer arising from the fluctuations of the average radiation scattered by the other scatterers.

It should be noted from Eqs. (18) and (19) that actually $\sum_{j\neq k}\langle u_j^* u_k\rangle$ can be approximated using $|\langle U\rangle|^2$. This implies that $\sum_{j\neq k}\sum_k \langle u_j(\nabla/-ik)u_k\rangle$, i.e. the average of the jth scattered field multiplied by the gradient of the kth scattered field can be estimated as

$$\sum_{j\neq k}\sum_k \langle u_j^* \frac{\nabla}{-ik} u_k\rangle^+ \sim |\langle U\rangle^+|^2\,\hat{e}_z \ , \quad z>0 \tag{21}$$

$$\sum_{j\neq k}\sum_k \langle u_j^* \frac{\nabla}{-ik} u_k\rangle^- \sim |\langle U\rangle^-|^2\,\hat{e}_z \ , \quad z<0 \tag{22}$$

where $\hat{e}_z$ is the unit vector in the positive z direction. Although, the gradient of u_j gives a radial direction, the average direction should be in the z direction as expected from the symmetry of the problem (energy flux is cancelled out along x and y directions). Both Eqs. (21) and (22) are, thus, important approximations in considering the energy conservation.

THE CONFIGURATIONAL AVERAGE OF ENERGY FLUX, $\langle\vec{S}\rangle$

The energy flux (intensity) is defined as (Morse and Ingard, 1968),

$$\vec{S} = (p^{*}\vec{v} + p\,\vec{v}^{*})/2 \tag{23}$$

which is an important quantity in wave propagation theory for considering energy conservation. Since we define

$$\vec{v} = \nabla\psi \tag{24}$$

from potential theory and thus we obtain

$$p = i\omega\rho_0\psi \tag{25}$$

from linearized momentum equation. Therefore the energy flux can be expressed in terms of ψ as:

$$\vec{S} = i\omega\rho_0(\psi^{*}\nabla\psi - \psi\nabla\psi^{*})/2. \tag{26}$$

The configurational average of the energy flux becomes

$$\langle\vec{S}\rangle = i\omega\rho_0[\langle\psi^{*}\nabla\psi\rangle - \langle\psi\nabla\psi^{*}\rangle]/2 \tag{27}$$

and it contains, now, both coherent and incoherent components.

Since $\psi = \psi_i + U$, then substituting it into Eq. (27) gives, taking the real part for magnitude,

$$\langle\vec{S}\rangle = \omega\rho_0 k\,\mathrm{Re}\left[\frac{\psi_i^{*}\nabla\psi_i}{-ik} + \frac{\psi_i^{*}}{-ik}\nabla\langle U\rangle + \frac{\langle U\rangle^{*}\nabla\psi_i}{-ik} + \frac{\langle U^{*}\nabla U\rangle}{-ik}\right], \tag{28}$$

in which the following relationship (Foldy, 1945)

$$\langle\nabla U\rangle = \nabla\langle U\rangle \tag{29}$$

has been employed.

One expects $\langle\vec{S}\rangle$ for scattered waves to be going outward away from the plane on which particles lie. Since the scattering characteristics are

different in the positive and negative z directions, it is necessary to separate $\langle\vec{S}\rangle$ into two parts for consideration. Let, therefore,

$$\langle\vec{S}\rangle = \langle\vec{S}\rangle^{+}, \quad z>0 \tag{30}$$

$$\langle\vec{S}\rangle = \langle\vec{S}\rangle^{-}, \quad z<0 \tag{31}$$

where the expressions for $\langle\vec{S}\rangle^{+}$ and $\langle\vec{S}\rangle^{-}$ are as follows,

$$\langle\vec{S}\rangle^{+} = \omega\rho_0 k\,\mathrm{Re}\left[\frac{\psi_i^{*}\psi_i}{-ik} + \frac{\psi_i^{*}}{-ik}\nabla\langle U\rangle^{+} + \frac{\langle U\rangle^{+*}\nabla\psi_i}{-ik} + \frac{\langle U^{*}\nabla U\rangle^{+}}{-ik}\right] \tag{32}$$

$$\langle\vec{S}\rangle^{-} = \omega\rho_0 k\,\mathrm{Re}\left[\frac{\psi_i^{*}\psi_i}{-ik} + \frac{\psi_i^{*}}{-ik}\nabla\langle U\rangle^{-} + \frac{\langle U\rangle^{-*}\nabla\psi_i}{-ik} + \frac{\langle U^{*}\nabla U\rangle^{-}}{-ik}\right] \tag{33}$$

On substituting the expressions for ψ_i, $\langle U\rangle^{+}$ and $\langle U\rangle^{-}$ into Eqs. (32) and (33) one obtains

$$\langle\vec{S}\rangle^{+} = \omega\rho_0 k\,\left[-\psi_a^2\,\hat{e}_z + \mathrm{Re}\left(\frac{\langle U^{*}\nabla U\rangle^{+}}{-ik}\right)\right] \tag{34}$$

$$\langle\vec{S}\rangle^{-} = \omega\rho_0 k\,\left[-\psi_a^2\,\hat{e}_z - (C^{-}+C^{-*})\psi_a^2\,\hat{e}_z + \mathrm{Re}\left(\frac{\langle U^{*}\nabla U\rangle^{-}}{-ik}\right)\right]. \tag{35}$$

The second term on the RHS of Eq. (34) (or the third term on the RHS of Eq. (35)) can be further separated into two parts. Thus,

$$\frac{\langle U^{*}\nabla U\rangle^{\pm}}{-ik} = \sum_{j\neq k}\sum_{k}\left\langle u_j\frac{\nabla}{-ik}u_k\right\rangle^{\pm} + \sum_{j}\left\langle u_j\frac{\nabla}{-ik}u_j\right\rangle^{\pm}. \tag{36}$$

Using Eqs. (36), (21) and (22), the average energy flux $\langle\vec{S}\rangle^{\pm}$ become

$$\langle\vec{S}\rangle^{+} = \omega\rho_0 k\,\left[\psi_a^2(-\hat{e}_z) + \psi_a^2(|\langle U\rangle^{+}|^2)\hat{e}_z + \vec{I}^{+}\right] \tag{37}$$

$$\langle\vec{S}\rangle^{-} = \omega\rho_0 k\,\left[\psi_a^2(-\hat{e}_z) + \psi_a^2\,(C^{-}+C^{-*})(-\hat{e}_z) + \psi_a^2(|\langle U\rangle^{-}|^2\,(-\hat{e}_z) + \vec{I}^{-}\right] \tag{38}$$

where

$$\vec{I}^{+} = \mathrm{Re}\left(\sum_j\left\langle u_j\,\frac{\nabla}{-ik}\,u_j\right\rangle^{+}\right) = \mathrm{Re}\left(\frac{\rho}{-ik}\left\langle u_j^{*}\,\nabla\,u_j\right\rangle_j^{+}\,d\vec{r}_j\right) \tag{39}$$

$$\vec{I}^{-} = \mathrm{Re}\left(\sum_j\left\langle u_j^{*}\,\frac{\nabla}{-ik}\,u_j\right\rangle^{-}\right) = \mathrm{Re}\left(\frac{\rho}{-ik}\left\langle u_j^{*}\,\nabla\,u_j\right\rangle_j^{-}\,d\vec{r}_j\right) \tag{40}$$

The energy principle simply states that the mean energy outflow for nondissipative scatterers, from any enclosed volume vanishes (Twersky, 1957)

$$\int \langle \vec{S} \rangle \cdot d\vec{A} = 0 \tag{41}$$

In order to verify this a simple control volume is assumed (see Figure 3). For the upper half plane (z>0), we have

$$\int \langle \vec{S} \rangle^{+} \cdot d\vec{A} = \omega \rho_0 k \psi_a^2 \left[(-\hat{e}_z) + (|\langle U \rangle^{+}|^2) \hat{e}_z \right] \cdot \hat{e}_z + \omega \rho_0 k \int \vec{\vec{I}}^{+} \cdot d\vec{A} \tag{42}$$

while for the lower half plane (z<0), we have

$$\int \langle \vec{S} \rangle^{-} \cdot d\vec{A} = \omega \rho_0 k \psi_a^2 \left[(-\hat{e}_z) + (C^{-} + C^{-*})(-\hat{e}_z) + (|\langle U \rangle^{-}|^2) \hat{e}_z \right] \cdot (\hat{e}_z) + \omega \rho_0 k \int \vec{\vec{I}}^{-} \cdot d\vec{A} \tag{43}$$

Actually one sees from Figure 3 that the total average energy flux has two separate parts. One is the coherent energy flux which has components either in positive or negative z direction but not in x and y directions. The other is the power scattered into all directions (specified by $\hat{e}_r$) and called the incoherent energy flux, i.e. $\vec{\vec{I}}^{+}$ and $\vec{\vec{I}}^{-}$. After adding Eq. (43) to (42) it gives

$$\int \langle \vec{S} \rangle \cdot d\vec{A} = \omega \rho_0 k \psi_a^2 \left[(C^{-} + C^{-*}) + (|\langle U \rangle^{+}|^2 + |\langle U \rangle^{-}|^2 \right] + \omega \rho_0 k \int \vec{\vec{I}} \cdot d\vec{A}. \tag{44}$$

The term $u_j^* \frac{\nabla}{-ik} u_j$ appearing in $\vec{\vec{I}}^{+}$ and $\vec{\vec{I}}^{-}$ in the $p_s p_s^*$ term is related to the scattering cross section σ (see Appendix), and one can show that

$$\int \vec{\vec{I}}^{+} \cdot d\vec{A} = \rho \bar{\sigma}^{+} \psi_a^2$$
$$\int \vec{\vec{I}}^{-} \cdot d\vec{A} = \rho \bar{\sigma}^{-} \psi_a^2 \tag{45}$$

and $$\int \vec{I} \cdot d\vec{A} = \rho(\bar{\sigma}^{+} + \bar{\sigma}^{-})\psi_a^2 = \rho\bar{\sigma}\psi_a^2$$

where $$\bar{\sigma} = \int \sigma\, q(a)da.$$

After dividing Eq. (44) by $\psi_a^2\, \omega\rho_0 k$ and neglecting the terms $|\langle U\rangle^{+}|^2$ and $|\langle U\rangle^{-}|^2$ (of order $|C^{\pm}|^2$ which are small compared with $|C^{\pm}|$), we obtain

$$\int \langle\vec{S}\rangle \cdot dA = (C^{-} + C^{-*}) + \rho\bar{\sigma} \tag{46}$$

The first term on the RHS of Eq. (46), using Eq. (12), then becomes

$$(C^{-} + C^{-*}) = -4\pi\rho\, \mathrm{Im}(\overline{f(a,\pi)})/k. \tag{47}$$

Substituting Eq. (47) back into (46) one sees, using the forward scattering theorem (Morse and Ingard , 1968)

$$\int \langle\vec{S}\rangle \cdot dA = \rho[\bar{\sigma} - 4\pi\mathrm{Im}\overline{f(a,\pi)})/k] = 0 \tag{48}$$

Eq. (48) states that the energy flux coherently transmitted is cancelled out by that incoherently scattered which verifies the energy principle for nonabsorbing scatterers as mentioned by Twersky (1957).

RESULTS AND DISCUSSIONS

In Figures 4 and 5 we present the computed values of the intensity, which has been normalized by $\omega^2\rho_0\psi_a^2/c$, versus the nondimensional frequency ka for sparse distributions of particles. One sees from Figures 4 and 5 that the contribution of the coherent intensity toward the total back-scattered intensity is quite small; therefore, it can be neglected for high values of ka. As expected, the coherent intensity is hundred times larger when the concentration changes from 0.002 to 0.02 while the total intensity is only ten times bigger. The size distribution seems to affect the intensity little which may be due to the reason that it is a Rayleigh distribution and the cutoff size is limited in our case. However, this should be investigated further for an even denser distribution. Moreover, the randomness in shape can also be included in the configurational average consideration through the T-matrix for arbitrary scatterer if it is required.

The present study takes into account the interactions among scatterers but the higher order scattering terms are ignored due to the sparse distribution and low concentration of scatterers. For high concentrations of scatterers, the complete introduction of the higher order scattering terms plus the appropriate distribution function are required to analyze the problem using the multiple scattering theory and it is discussed in the Appendix.

ACKNOWLEDGEMENTS

This work was supported by the U.S.Army Research Office under Contract NO: DAAG29-83-K-0097.

REFERENCES

Foldy, L. L., 1945, The multiple scattering of waves : Physical Review, V. 67, pp. 107-119.

Lamb, H., 1932, Hydrodynamics, New York, Dover Publications, Inc.

Ma, Y., Varadan, V. K., Varadan, V. V., and Bedford, K. W., 1983, Multifrequency remote acoustic sensing of suspended materials in water: J. Acoust. Soc. Am., V. 74, pp. 581-585.

Morse, P. M., and Ingard, K. U., 1968, Theoretical Acoustics: New York, McGraw-Hill Book Co., Inc.

Twersky, V., 1957, On scattering and reflection of sound by rough surfaces: J. Acoust. Soc. Am., V. 29, pp. 208-225.

Twersky, V., 1983, Multiple scattering of sound by correlated monolayers: J. Acoust. Soc. Am., V. 73, pp. 68-84.

Steele, W. A., 1975, Theory of monolayer physical adsorption. I. Flat surface : J. Chem. Physics, V. 65, pp. 5256-5266.

Varadan, V. K., and Varadan, V. V., 1980, Acoustic, Electromagnetic and Elastic Wave Scattering - Focus on the T-matrix Approach, New York, Pergamon Press.

APPENDIX

The configurational average of ψ^2 presented in this paper is for sparsely distributed scatterers on a plane. In other words, the intensity calculation based on Eqns. (16-19) is valid only for a moderate concentration of particles. As can be seen in Varadans' previous work, in order to accurately compute the scattering response from a dense distribution of scatterers, the pair correlation function which is a necessary description of the relative position of one scatterer to the other must be taken into account in the multiple scattering theory. The introduction of the pair correlation function not only enables us to physically explain the results but also compare the results quite well with the available experimental measurements. In fact, the single scattering theory or several modified multiple scattering estimation without considering the pair correlation function yields unphysical numerical results which inevitably exist when plotting against either frequency or concentration.

To describe the positions of the scatterers in a monolayer, a two dimensional distribution function specified by $p(|\vec{R}|)$ for randomly distributed impenetrable disks is to be introduced here for the intensity calculation for high concentration of particles. Since the top view of the scatterers on a plane is essentially that disks distributed in a monolayer, we may assume that the cross section of each scatterer which can be arbitrary in shape is enclosed by a circular disk lying on a plane. To this end, hard disk pair correlation functions $p(|\vec{R}|)$ are obtained for ρd^2 up to 0.7 ('d' is the diameter of the disk) by solving Percus-Yevick equations in two dimensions.

The modification of equations for the intensity calculation for high

concentrations of scatterers is only through Eq.(19) by introducing the two dimensional pair correlation function $p(|\vec{R}|)$. One should notice that R is now a planar vector connecting centers of two circular disks of the same size. The pair correlation function for non-circular hard disks as well as a size distribution of circular disks can also be implemented in the intensity calculation for monolayer scatterers, however, they are beyond the scope of this paper. The modified equation using Eq.(19), after some manipulation, for ψ'^2 is thus written as

$$\langle|\psi'|^2\rangle = \rho^2\iint[\langle u_j^* u_k\rangle_{jk}\, p(\vec{R}_{jk}) - \langle u_j\rangle_j^* \langle u_k\rangle_k]\, d\vec{r}_j d\vec{r}_k + \rho\int\langle|u_j|^2\rangle_j d\vec{r}_j, \quad \text{(A1)}$$

which can be found its equivalent form in Twersky's work [1983]. The remaining part is then to carry out the integral numerically on the computer to obtain the incoherent intensity for the interested concentrations and frequencies. The procedures involved are explained in the main text and will not be repeated here.

There are a number of approximate integral equations as well as quasi-exact approaches to obtain the pair correlation for hard spheres and the details can be founf elsewhere. However, for hard disks, a published table of pair correlation function for various concentrations is incomplete, at least to our interest. In order to obtain a table of pair correlation function $p(|\vec{R}|)$ for a wide range of concention, we used the following procedures as mentioned in Steele's paper [1975]. For hard disks,

$$p(|\vec{R}|) = \exp[\, -u(|\vec{R}|)/kT\,]\, y(|\vec{R}|), \quad \text{(A2)}$$

where $u(|\vec{R}|)$ is the inter-scatterer potential, k is the Boltzmann constant, T is the temperature and $y(|\vec{R}|)$ is generated using the two dimensional

AD-A151 766 MULTIPLE SCATTERING OF ELECTROMAGNETIC WAVES IN DISCRETE RANDOM MEDIA..(U) PENNSYLVANIA STATE UNIV UNIVERSITY PARK WAVE PROPAGATION LAB.. 3/3

UNCLASSIFIED V K VARADAN ET AL. 31 DEC 84 F/G 20/14 NL

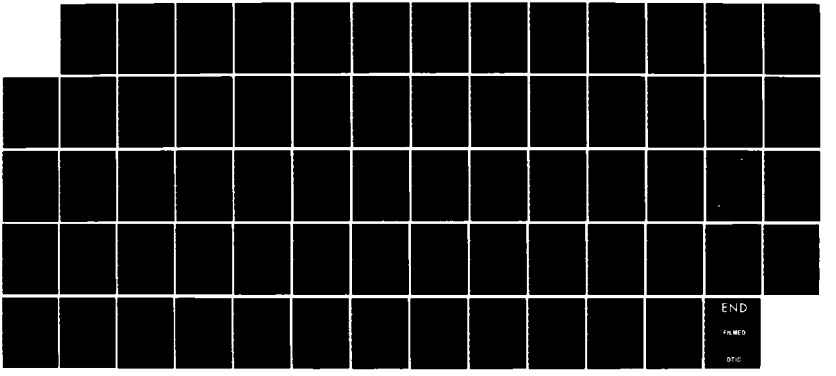

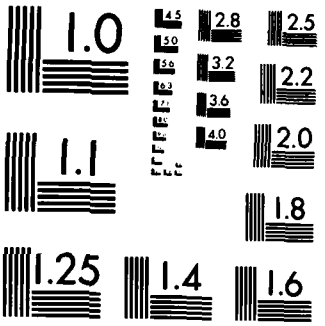

Percus-Yevick equation which can be written as

$$y(|\vec{R}_{ij}|) = 1 + 2\rho\int_0^d\int_0^\pi y(|\vec{R}_{ik}|)[y(|\vec{R}_{jk}|)H(|\vec{R}_{jk}| - d) - 1]d\alpha d\vec{r}_{jk}d\vec{r}_{ik}, \quad (A3)$$

where α is the angle between $\vec{R}_{ik}$ and $\vec{R}_{jk}$ and H(x) is the Heavyside function equal to zero for $x < 0$ and unity for $x > 0$.

The pair correlation function can thus be obtained using Eq.(A2) through the direct numerical iteration for $y(|\vec{R}|)$ in Eq.(A3). Several sets of the pair correlation function $p(|\vec{R}|)$ for different concentrations as a function of the separation distance between disks are presented in Tables I-VII and graphically in Figure 6.

APPENDIX

(1) $$\sigma = 2\pi \int_0^{\pi} |p_s|^2 R^2 \sin\theta d\theta / |p_i|^2 \text{ , for spherical coordinates}$$

(2) $$\sigma^- = 2\pi \int_{\frac{\pi}{2}}^{\pi} |p_s|^2 R^2 \sin\theta d\theta / |p_i|^2$$

(3) $$\sigma^+ = 2\pi \int_0^{\frac{\pi}{2}} |p_s|^2 R^2 \sin\theta d\theta / |p_i|^2$$

(4) $$\sigma = \sigma^+ + \sigma^- = (4\pi/k^2) \sum_{n=0}^{\infty} (2n+1)/(1+C_n^2)$$

(5) $$q(a) = (2a^3/0.74\bar{a}^4)\exp(-a^4/1.48\bar{a}^4)$$

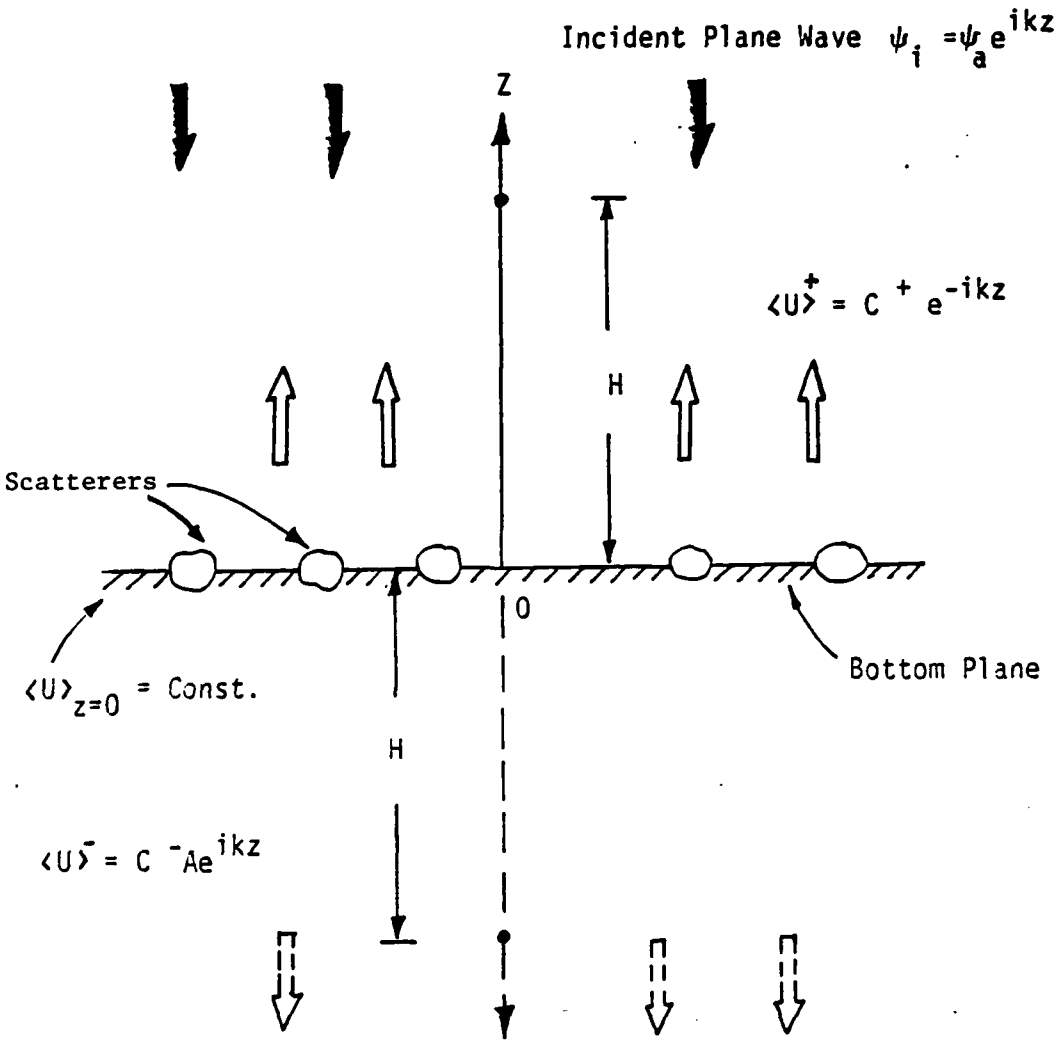

Figure 1. The Average Scattered Field Excited by a Normally Incident Plane Wave.

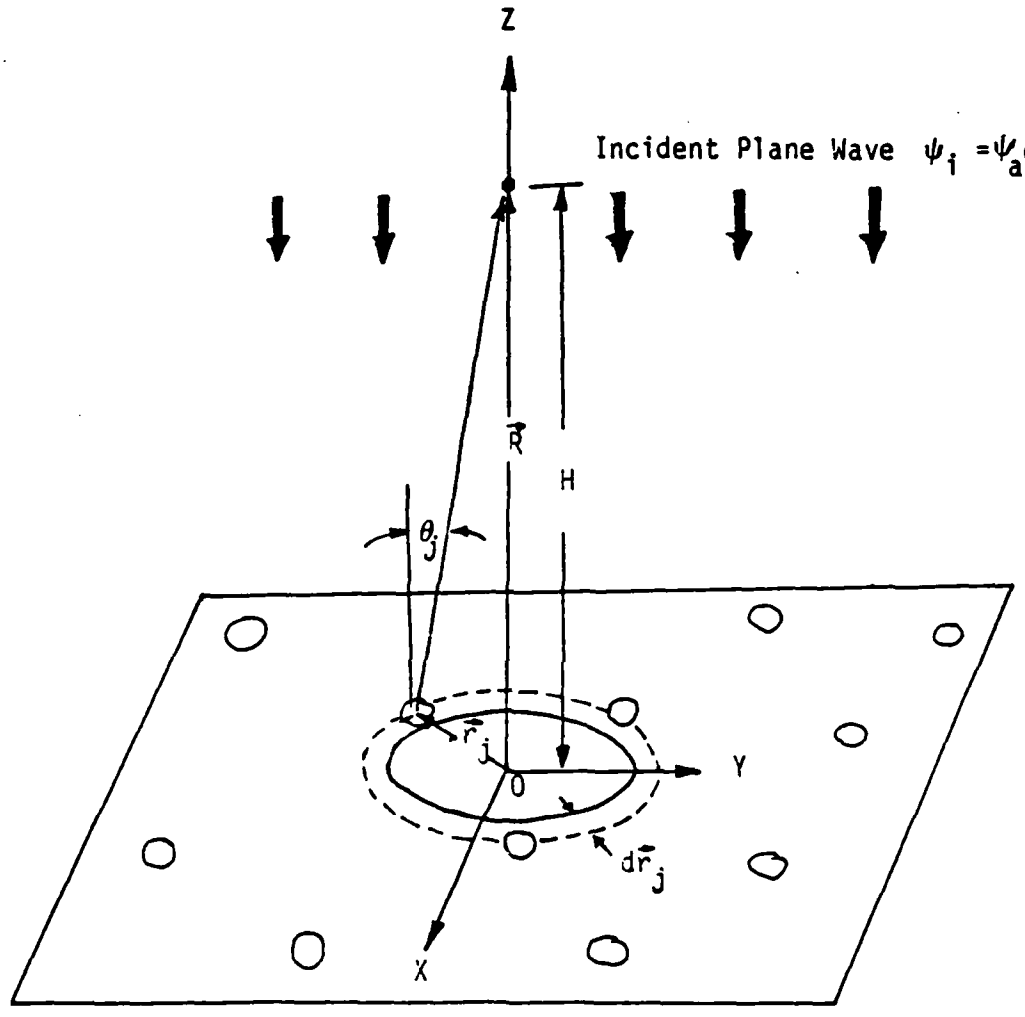

Figure 2. Scattering from particles.

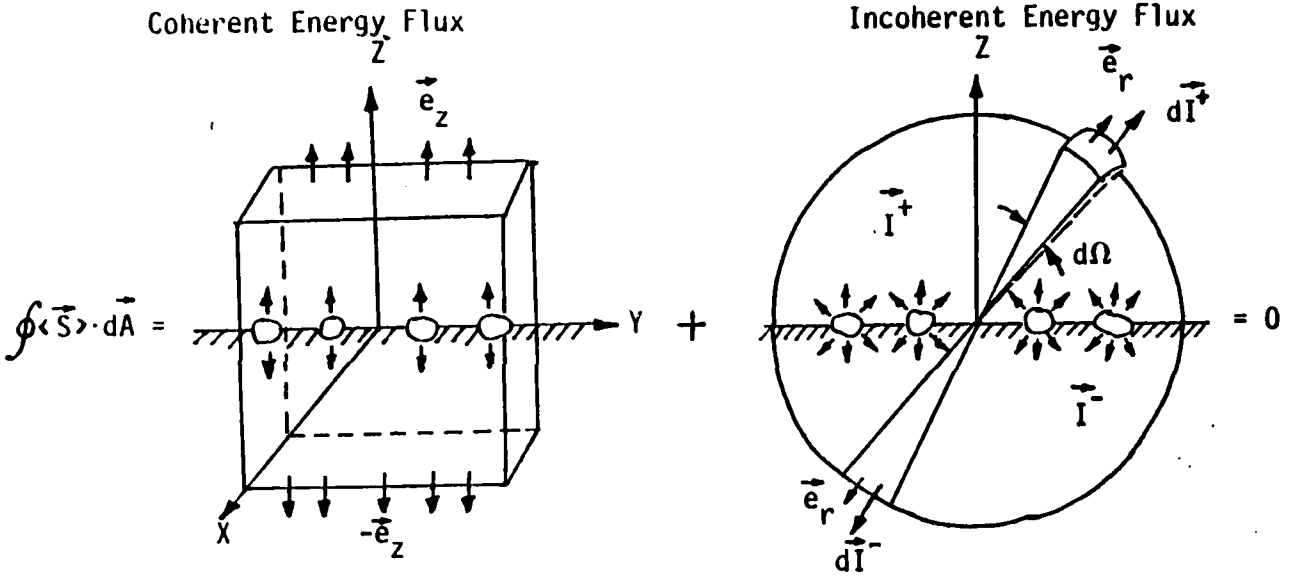

Figure 3. Control Volume for Energy Flux Consideration.

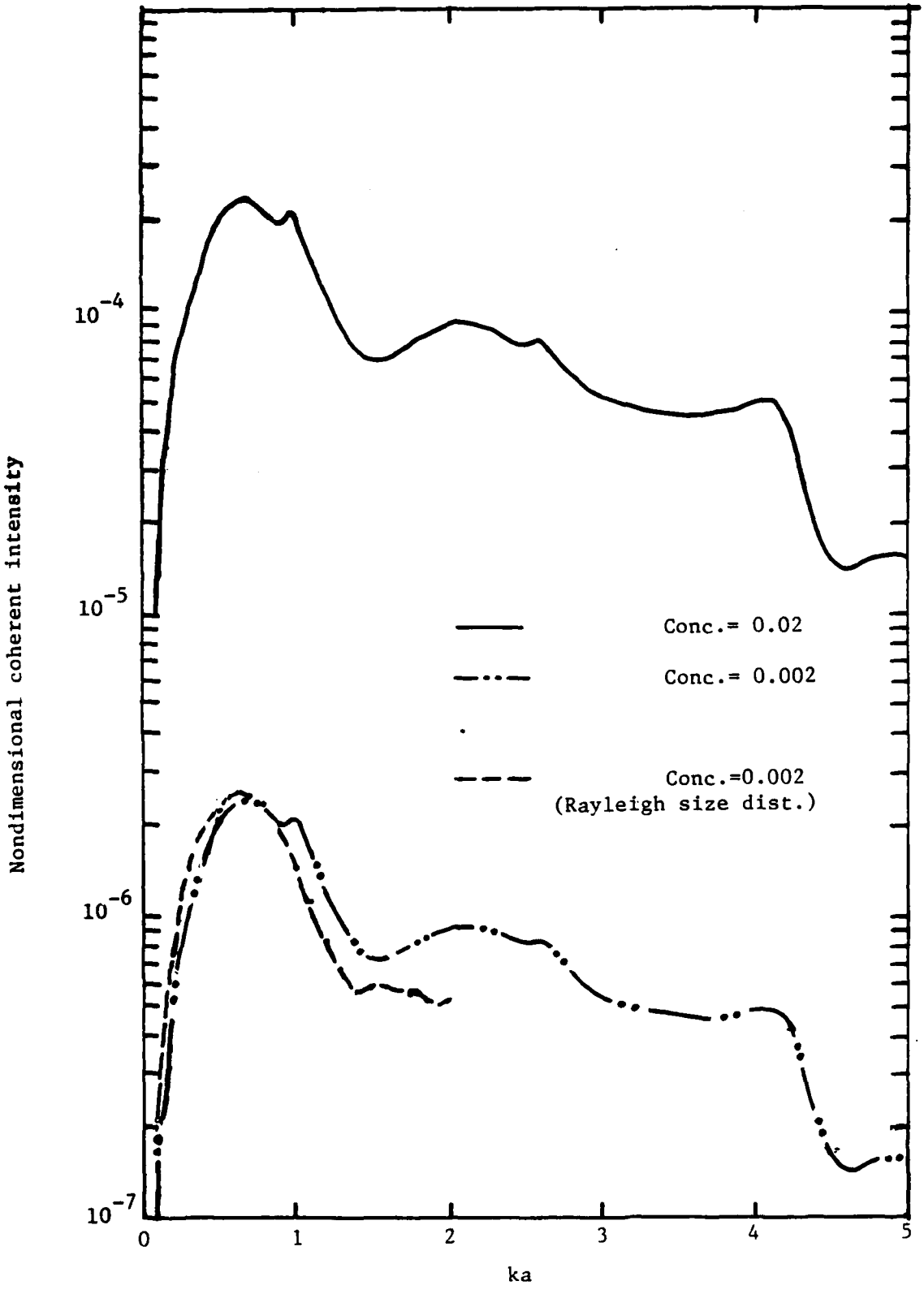

Figure 4. Nondimensional coherent intensity versus nondimensional frequency

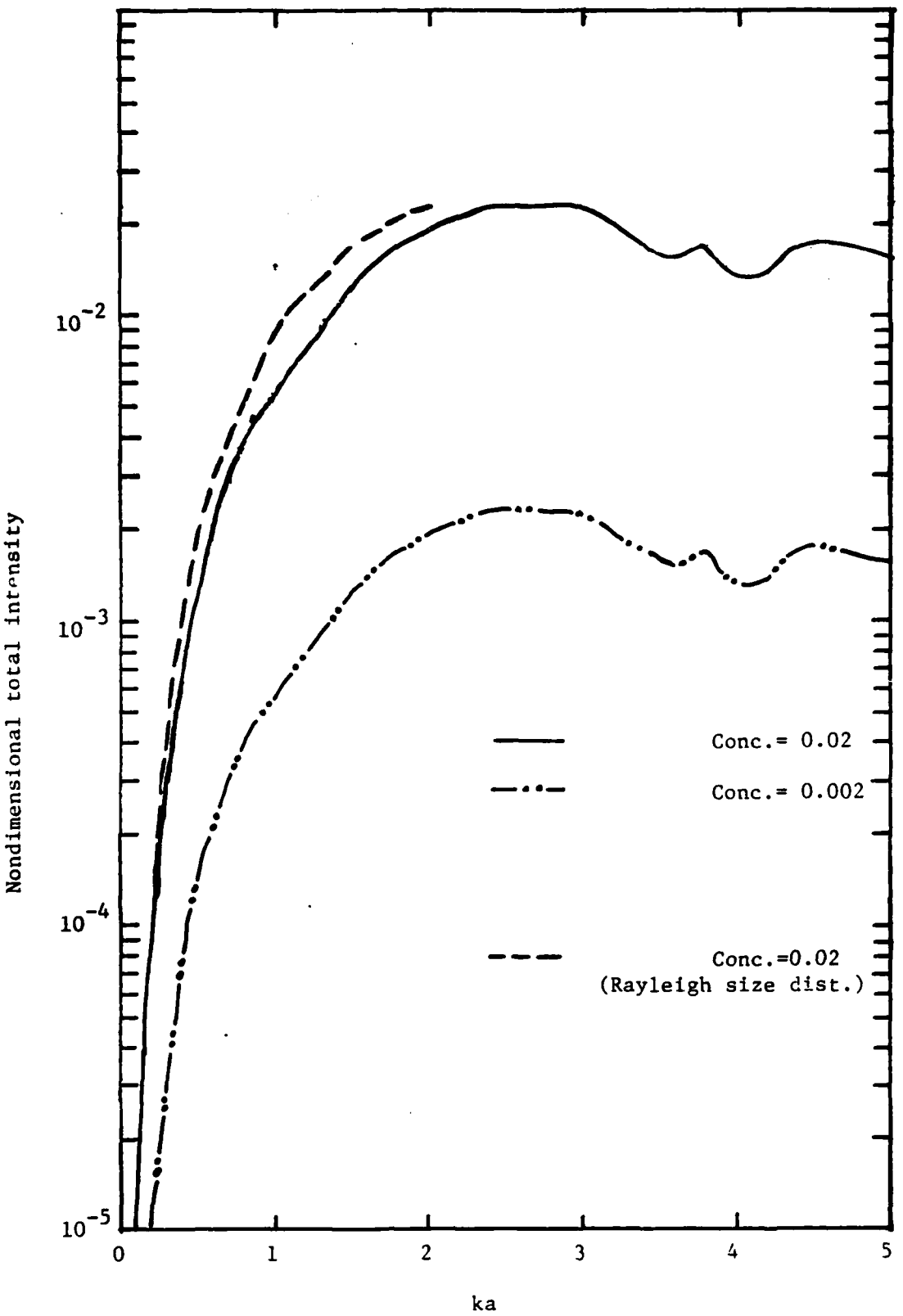

Figure 5. Nondimensional total intensity versus nondimensional frequency

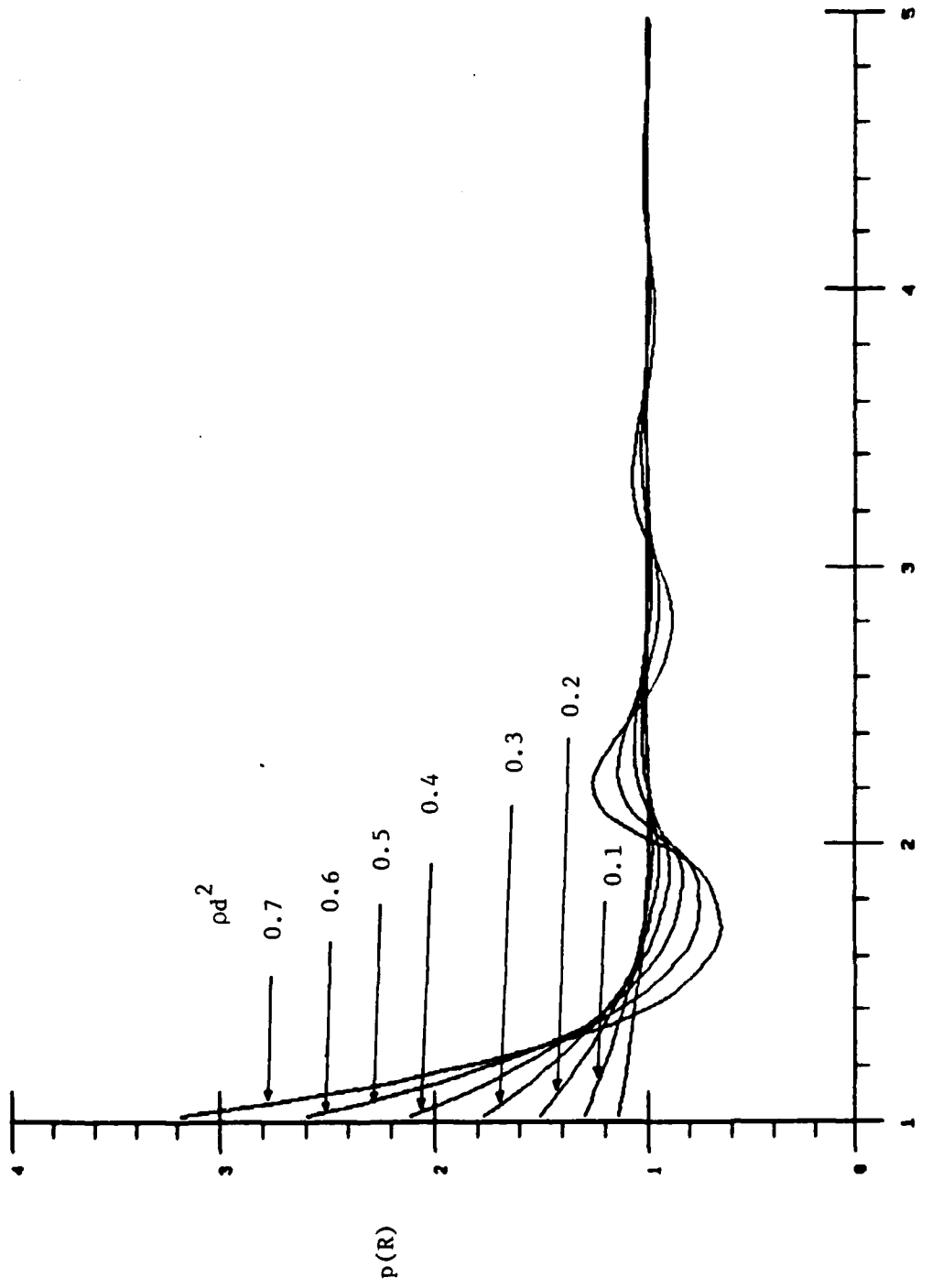

Figure 6. Hard disk pair correlation function p(R) vs. R/d

TABLE I. Pair correlation function p(R) for $\rho d^2 = 0.1$

R/d	p(R)	R/d	p(R)
1.02	1.13220	1.04	1.12775
1.06	1.12351	1.08	1.11935
1.10	1.11503	1.12	1.11093
1.14	1.10674	1.16	1.10282
1.18	1.09908	1.20	1.09524
1.22	1.09126	1.24	1.08769
1.26	1.08351	1.28	1.07968
1.30	1.07647	1.32	1.07283
1.34	1.06848	1.36	1.06532
1.38	1.06208	1.40	1.05864
1.42	1.05509	1.44	1.05199
1.46	1.04878	1.48	1.04569
1.50	1.04248	1.52	1.03981
1.54	1.03701	1.56	1.03424
1.58	1.03114	1.60	1.02847
1.62	1.02561	1.64	1.02297
1.66	1.02059	1.68	1.01824
1.70	1.01569	1.72	1.01362
1.74	1.01150	1.76	1.00955
1.78	1.00735	1.80	1.00553
1.82	1.00391	1.84	1.00215
1.86	1.00048	1.88	0.99903
1.90	0.99778	1.92	0.99668
1.94	0.99569	1.96	0.99506
1.98	0.99462	2.00	0.99469
2.02	0.99494	2.04	0.99525
2.06	0.99557	2.08	0.99589
2.10	0.99619	2.12	0.99649
2.14	0.99677	2.16	0.99703
2.18	0.99728	2.20	0.99752
2.22	0.99775	2.24	0.99796
2.26	0.99816	2.28	0.99835
2.30	0.99853	2.32	0.99870
2.34	0.99885	2.36	0.99900
2.38	0.99913	2.40	0.99926
2.42	0.99937	2.44	0.99948
2.46	0.99958	2.48	0.99967
2.50	0.99975	2.52	0.99982
2.54	0.99988	2.56	0.99994
2.58	0.99999	2.60	1.00004
2.62	1.00007	2.64	1.00011
2.66	1.00013	2.68	1.00016
2.70	1.00017	2.72	1.00019
2.74	1.00019	2.76	1.00020
2.78	1.00020	2.80	1.00020
2.82	1.00019	2.84	1.00019
2.86	1.00018	2.88	1.00017
2.90	1.00016	2.92	1.00014
2.94	1.00013	2.96	1.00012
2.98	1.00010	3.00	1.00007

TABLE II. Pair correlation function p(R) for $\rho d^2 = 0.2$

R/d	p(R)	R/d	p(R)
1.02	1.29095	1.04	1.27949
1.06	1.26944	1.08	1.25876
1.10	1.24888	1.12	1.23853
1.14	1.22793	1.16	1.21872
1.18	1.20935	1.20	1.19986
1.22	1.19033	1.24	1.18011
1.26	1.17152	1.28	1.16310
1.30	1.15373	1.32	1.14629
1.34	1.13745	1.36	1.12885
1.38	1.12067	1.40	1.11269
1.42	1.10561	1.44	1.09781
1.46	1.09068	1.48	1.08384
1.50	1.07634	1.52	1.06903
1.54	1.06278	1.56	1.05628
1.58	1.05053	1.60	1.04441
1.62	1.03855	1.64	1.03308
1.66	1.02712	1.68	1.02210
1.70	1.01686	1.72	1.01272
1.74	1.00824	1.76	1.00342
1.78	0.99988	1.80	0.99615
1.82	0.99259	1.84	0.98888
1.86	0.98631	1.88	0.98427
1.90	0.98173	1.92	0.97950
1.94	0.97831	1.96	0.97760
1.98	0.97739	2.00	0.97814
2.02	0.97970	2.04	0.98142
2.06	0.98310	2.08	0.98464
2.10	0.98604	2.12	0.98740
2.14	0.98862	2.16	0.98986
2.18	0.99093	2.20	0.99200
2.22	0.99299	2.24	0.99380
2.26	0.99470	2.28	0.99544
2.30	0.99621	2.32	0.99690
2.34	0.99751	2.36	0.99809
2.38	0.99858	2.40	0.99908
2.42	0.99946	2.44	0.99982
2.46	1.00013	2.48	1.00037
2.50	1.00067	2.52	1.00088
2.54	1.00103	2.56	1.00116
2.58	1.00127	2.60	1.00136
2.62	1.00141	2.64	1.00144
2.66	1.00149	2.68	1.00147
2.70	1.00145	2.72	1.00139
2.74	1.00133	2.76	1.00126
2.78	1.00118	2.80	1.00109

TABLE II. ---continue

R/d	p(R)	R/d	p(R)
2.82	1.00099	2.84	1.00088
2.86	1.00077	2.88	1.00066
2.90	1.00055	2.92	1.00045
2.94	1.00035	2.96	1.00025
2.98	1.00017	3.00	1.00009
3.02	1.00002	3.04	0.99996
3.06	0.99991	3.08	0.99986
3.10	0.99982	3.12	0.99979
3.14	0.99976	3.16	0.99974
3.18	0.99972	3.20	0.99971
3.22	0.99970	3.24	0.99970
3.26	0.99969	3.28	0.99969
3.30	0.99970	3.32	0.99970
3.34	0.99971	3.36	0.99972
3.38	0.99973	3.40	0.99974
3.42	0.99975	3.44	0.99977
3.46	0.99978	3.48	0.99979
3.50	0.99981	3.52	0.99982
3.54	0.99984	3.56	0.99985
3.58	0.99986	3.60	0.99988
3.62	0.99989	3.64	0.99990
3.66	0.99991	3.68	0.99992
3.70	0.99993	3.72	0.99994
3.74	0.99995	3.76	0.99996
3.78	0.99997	3.80	0.99997
3.82	0.99998	3.84	0.99999
3.86	0.99999	3.88	0.99999
3.90	1.00000	3.92	1.00000
3.94	1.00000	3.96	1.00000
3.98	1.00001	4.00	1.00001

TABLE III. Pair correlation function p(R) for $\rho d^2 = 0.3$

R/d	p(R)	R/d	p(R)
1.02	1.50077	1.04	1.47856
1.06	1.45764	1.08	1.43728
1.10	1.41595	1.12	1.39604
1.14	1.37613	1.16	1.35800
1.18	1.34087	1.20	1.32312
1.22	1.30466	1.24	1.28858
1.26	1.26908	1.28	1.25196
1.30	1.23820	1.32	1.22204
1.34	1.20216	1.36	1.18897
1.38	1.17537	1.40	1.16095
1.42	1.14610	1.44	1.13362
1.46	1.12055	1.48	1.10848
1.50	1.09578	1.52	1.08604
1.54	1.07560	1.56	1.06532
1.58	1.05314	1.60	1.04323
1.62	1.03232	1.64	1.02283
1.66	1.01476	1.68	1.00682
1.70	0.99786	1.72	0.99158
1.74	0.98496	1.76	0.97916
1.78	0.97199	1.80	0.96681
1.82	0.96261	1.84	0.95763
1.86	0.95304	1.88	0.94960
1.90	0.94710	1.92	0.94539
1.94	0.94421	1.96	0.94481
1.98	0.94636	2.00	0.95034
2.02	0.95502	2.04	0.95980
2.06	0.96438	2.08	0.96875
2.10	0.97284	2.12	0.97664
2.14	0.98017	2.16	0.98346
2.18	0.98649	2.20	0.98930
2.22	0.99185	2.24	0.99419
2.26	0.99630	2.28	0.99823
2.30	0.99994	2.32	1.00148
2.34	1.00283	2.36	1.00402
2.38	1.00505	2.40	1.00592
2.42	1.00666	2.44	1.00726
2.46	1.00773	2.48	1.00809
2.50	1.00833	2.52	1.00849
2.54	1.00854	2.56	1.00852
2.58	1.00840	2.60	1.00821
2.62	1.00796	2.64	1.00764
2.66	1.00727	2.68	1.00687
2.70	1.00642	2.72	1.00595
2.74	1.00544	2.76	1.00493
2.78	1.00440	2.80	1.00386
2.82	1.00332	2.84	1.00278
2.86	1.00225	2.88	1.00174
2.90	1.00125	2.92	1.00079

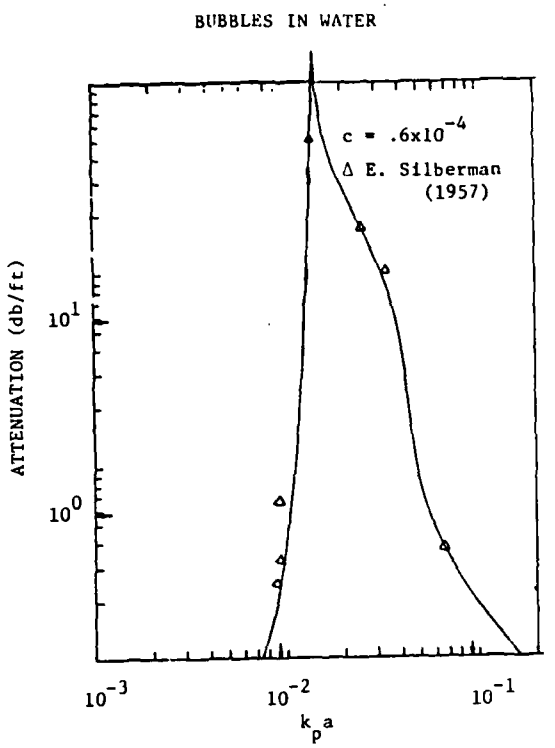

Fig. 2 Coherent attenuation vs compressional wave number for bubbles in water. Experimental data points are from Ref. [29].

We now present some results for electromagnetic ave propagation through a composite media consisting f Revacryl spheres dispersed in distilled water. The efractive index of the scatterers is 1.48 while that f the distilled water is 1.334. Figure (3) shows an xpamle of the behavior of real part of refractive index, ' (which is related to the phase velocity) as a function f volume fraction occupied by the scatterers(c), while igure (4) shows the variation of the imaginary part of efractive index n" (which is related to the coherent ttenuation) as a function of concentration c of the catterers for two different wavelengths λ = 410nm and 46nm. The agreement between our theory and the experient of Killey and Meeten[31] is excellent even for the ense system. Figure (5) shows again an excellent agreeent between theory and experiment for coherent intensity or various values of concentration for wavelength = 546nm. To show that the theory presented here is alid even for very high frequencies we have plotted the esults of coherent attenuation versus concentration c or latex spheres in water even for $k_s a$ = 83.352 where k_s is the wavenumber of the electromagnetic wave in water, ee Figure 6. The attenuation is normalized with respect o single scattering approximation and is denoted by γ. he agreement between our theory and the experiment easurements of Ishimaru and Kuga[32] is quite good. For ther dielectric-dielectric composite media with spherial and non-spherical inclusions, we have shown excellent greement between our theory and experiments of Ishimaru nd Kuga[17].

For the study of wave propagation in elastic compoite media, we have taken a model of a particulate omposite containing a random distribution of lead pheres in EPON 828-Z.

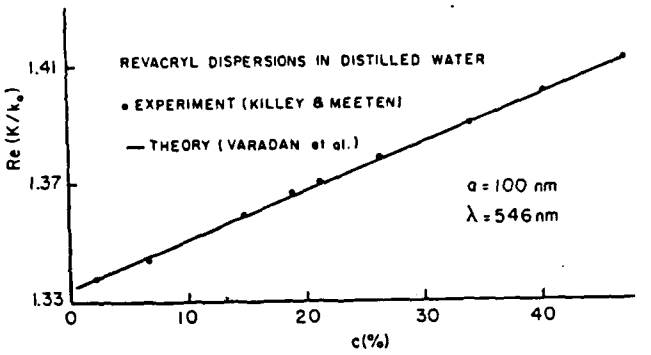

Fig. 3 Phase velocity vs concentration for electromagnetic wave propagation through Revacryl dispersions in distilled water. Experimental data points are from Ref. [31].

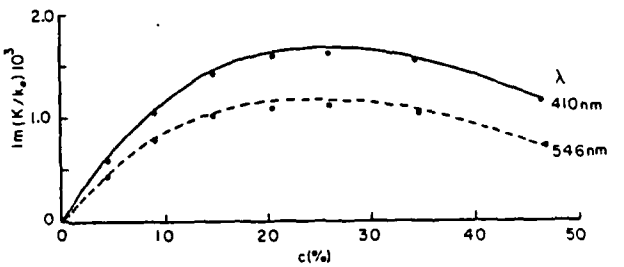

Fig. 4 Coherent attenuation vs concentration for the case given in Fig. 3.

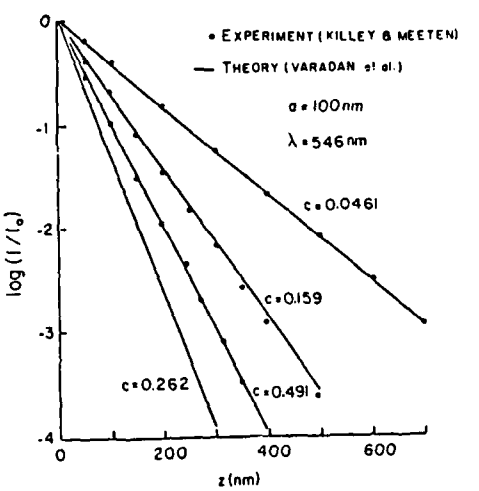

Fig. 5 Coherent intensity vs propagation depth z. Experimental data points are from Ref. [31]

ariables but K, the determinantal equation can be olved numerically to yield the value of the effective ropagation constant.

Equation (27) can be written in its expanded form s follows:

$$X_{1n}^{\ell} = \sum_{q=|n_1-m|}^{|n_1+m|} \sum_{m=0}^{\infty} \sum_{p=-m}^{m} \sum_{n_1=0}^{\infty} \sum_{m_1=-n_1}^{n_1} (-1)^p (-i)^q$$

$$i^{m_1+m+q-n_1} \delta_{m_1 p} \Big\{ I_q^p X_{1n_1}^{m_1} (T^{11})_{nm}^{\ell p} a(m_1,n_1|-p,m|q)$$

$$+ I_q^s \Big\{ X_{2n_1}^{m_1} [(T^{12})_{nm}^{\ell p} a(n_1,m,q) a(m_1,n_1|-p,m|q) - (T^{13})_{nm}^{\ell p}$$

$$b(n_1,m,q) a(m_1,n_1|-p,m|q,q-1)] + X_{3n_1}^{m_1} [(T^{13})_{nm}^{\ell p} \quad (28a)$$

$$a(n_1,m,q) a(m_1,n_1|-p,m|q) - (T^{12})_{nm}^{\ell p} b(n_1,m,q)$$

$$a(m_1,n_1|-p,m|q,q-1)] \Big\} \Big\}$$

$$X_{2n}^{\ell} = \ldots . \quad (28b)$$

$$X_{3n}^{\ell} = \ldots . \quad (28c)$$

quation (28b) can be obtained from (28a) by replacing T^{11}, T^{12}, T^{13}, by T^{21}, T^{22}, T^{23}, while (28c) can be btained by replacing T^{11}, T^{12}, T^{13} by T^{31}, T^{32}, and T^{33}.

In equations (28a,b,c), the contributions due to air-correlation functions are given by the expression $I_q^{\tau}(\tau=1,2)$ as follows:

$$I_q(K,k_\tau,c) = \frac{6c}{(k_\tau a)^2-(Ka)^2} [2k_\tau a\, j_q(2Ka) h_q'(2k_\tau a) -$$

$$2Ka\, h_q(2k_\tau a) j_q(2Ka)] + 24c \int_{x=1}^{\infty} x^2 [g(x)-1] h_q(k_\tau x) \quad (29)$$

$$j_q(Kx)dx$$

For acoustic wave problem, we get uncoupled equation for X_{1n}^{ℓ}; for electromagnetic problem, we get coupled equations in terms of X_{2n}^{ℓ} and X_{3n}^{ℓ}; for elastic wave problem, we obtain coupled equations in terms of X_{1n}^{ℓ}, X_{2n}^{ℓ} and X_{3n}^{ℓ}. Equation (28) is a system of simultaneous linear homogeneous equations for the unknown amplitudes $X_{\tau n}$. For a nontrivial solution, we require that the determinant of the truncated coefficient matrix vanishes, which yields an equation for the effective wave number K in terms of k_τ and the T-matrix of the scatterer. This is the dispersion relation for the scatterer filled medium. Equation (28) is a general expression valid for any arbitrary shaped scatterer, since the T-matrix is the only factor that contains information about the exact shape and boundary conditions at the scatterer. Thus the formalism presented here is valid for all the three wave fields. The effective wave number K obtained in the analysis is a complex quantity, the real part of which relates to the phase velocity, while the imaginary part relates to attenuation of coherent waves in the medium.

RESULTS AND CONCLUSION

Using the theory outlined in previous sections, we present some numerical results for a variety of three-dimensional problems in all three wave fields and compare them with some laboratory experimental measurements to show the broad applicability of our multiple scattering approach.

In the Rayleigh or low frequency limit, the size of the scatterers is considered to be small when compared to the incident wavelength. It is then sufficient to take only the lowest order coefficient in the expansion of the fields. At resonance and higher frequencies, we must in general consider higher powers in $k_\tau a$ which implies that a larger number of terms $(X_{\tau n})^{\tau}$ must be kept in the expansion of the average field. Numerical procedure is outlined in detail in our previous papers and hence will not be repeated here.

In Figures 1 and 2, we have plotted the phase velocity and attenuation coefficients for bubbles in water. The dots in these figures are the experimental measurements by Silberman[29]. The agreement between our theory and experiment is extremely good. For this composite media, "breathing mode" resonances of the bubbles and the associated marked variation of coherent attenuation and phase velocity occur. The curve of phase velocity versus wavenumber in water (matrix medium) shows an oscillating behavior in the resonance region. The oscillations in the phase velocity occur even for such low concentration between the "acoustic" and "optical" branches as evidenced in Figure 1. It is interesting to note that the coherent attenuation reaches a maximum value at the "breathing mode" resonance in the "acoustic" branch. However, there is not any evidence of the location of the "optical branch" in the attenuation versus the wavenumber plot, see Figure 2. It is to be noted that the imaginary part K_2 of the effective wavenumber becomes greater than the real part K_1. This causes the propagating wave in the composite media to be damped out over a distance smaller than a wavelength. This so called "superviscous" propagation has also been noted by Chaban[30] and Varadan et al[20] for voids in rubber-like materials. It is worth mentioning at this state that the Kuster and Toksöz model even with the giant monopole resonance included does not present satisfactory results in the "optical branch".

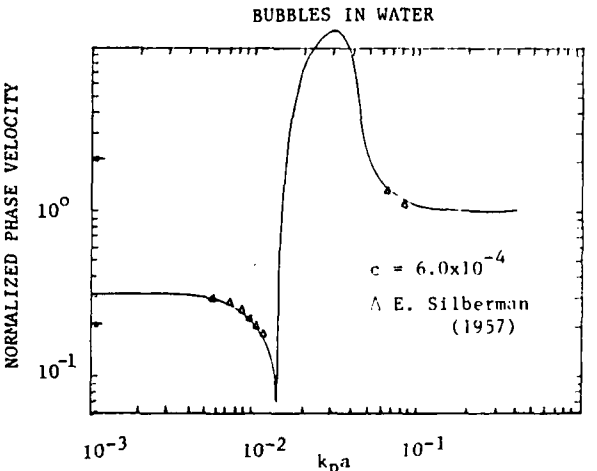

Fig. 1 Phase velocity vs compressional wave number for bubbles in water. Experimental data points are from Ref. [29].

we obtain

$$\langle\alpha_n^i\rangle = a_n^i + n_o T_{n'n''} \int_{V-v} \sigma_{nn'}(\vec{r}_{ij}) \langle\alpha_{n''}^j\rangle_j \, g(|\vec{r}_{ij}|) d\vec{r}_j \tag{19}$$

In equation (18), g(x) is the radial distribution function assuming spherically symmetric statistics even for non spherical particles, i.e. the exclusion volume of the impenetrable particles is assumed to be spherical. In equation (19), the summation convention is used, and if the particles are identical $\Sigma_j^! = N-1 \simeq N$ when N is large and v is the exclusion volume equal to $4\pi(2a)^3/3$.

The joint probability density is defined as

$$p(\vec{r}_j|\vec{r}_i) = \begin{cases} \frac{1}{V} g(|\vec{r}_j - \vec{r}_i|); & |\vec{r}_j - \vec{r}_i| \geq 2a \\ 0 & ; |\vec{r}_j - \vec{r}_i| > 2a \end{cases} \tag{20}$$

Equation (20) implies that the particles do not interpenetrate and the excluded volume is a sphere of radius 2a although the particles themselves may be non-spherical. A suitable non-spherical statistics may also be included through Monte-Carlo calculation especially for non-spherical scatterers. The function $g(|\vec{r}_j - \vec{r}_i|)$ is called the pair correlation function and depends only on $|\vec{r}_j - \vec{r}_i|$ due to translational invariance of the system under consideration.

Several models of g(x) are available. For uncorrelated impenetrable particles

$$g(x) = \begin{cases} 1/(1-c), & x>1 \\ 0, & x<1 \end{cases} \tag{21}$$

This approximation for g(x) known as the well-stirred approximation (WSA) is expected to be valid for low values of concentration c, and as discussed by Bringi et al[17], fails at c>0.125. Twersky[12] has used a virial expansion to obtain g(x) shown as

$$g(x) = \begin{cases} 0, & x<1 \\ 1+8c(1-\frac{3}{4}x+\frac{1}{16}x^3), & 1<x<2 \\ 1, & x>2 \end{cases} \tag{22}$$

which is valid at low concentrations.

Improved models of the pair correlation function valid for concentrations up to 40% are the Percus-Yevick approximation (PYA) and the Hypernetted-Chain approximation (HNC). The Percus-Yevick model[24] has been solved analytically by Wertheim[25] for the case of hard impenetrable particles. It is expected to be somewhat better than the HNC[26]. One of the defects of the PYA is that the two equations that can be derived for the pressure P in a fluid containing "hard" particles lead to different answers when the PYA for g(x) are substituted in them. Rowlinson[27] remedied this by assuming that the direct correlation function which is the short range part of the correlation function is a linear combination of the ones resulting from the PYA and HNC models. They were combined with an adjustable parameter ϕ and the two pressure equations were solved simultaneously for P and ϕ. This is called the self-consistent approximation (SCA) and it is valid for higher concentrations than the PYA and HNC models. Twersky[28] has considered non-spherical statistics for spheroidal scatterers in the sparse concentration limit. Extending this model to dense systems and numerically implementing it for high frequencies will be a problem of interest to the research community. Pair-correlation functions by Monte-Carlo simulation were used in our numerical computations.

PROPAGATION CHARACTERISTICS OF THE AVERAGE WAVES IN THE MEDIUM

To solve the integral equations given by (19), we now assume that the average field in the medium is a plane wave propagating in the direction $\hat{k}_o$ of the original plane wave in the host medium, however, the average field propagates in an effective or average medium which is homogeneous and characterized by an effective propagation constant $K = K_1 + iK_2$ which is complex and frequency dependent. Thus

$$\langle\alpha_n^i\rangle = X_n e^{iK\hat{k}_o \cdot \vec{r}_i} \tag{23}$$

and equation (13) can hence be written as

$$X_n e^{iK\hat{k}_o \cdot \vec{r}_i} = A_n e^{ik\hat{k}_o \cdot \vec{r}_i} + n_o T_{n'n''} X_{n''} e^{iK\hat{k}_o \cdot \vec{r}_i} \left\{ \int_{V-v} \sigma_{nn'}(\vec{r}_{ij}) e^{iK\hat{k}_o \cdot \vec{r}_{ji}} d\vec{r}_j + \int_{V-v} \sigma_{nn'}(\vec{r}_{ij}) e^{iK\hat{k}_o \cdot \vec{r}_{ji}} [g(|\vec{r}_{ij}|)-1] d\vec{r}_j \right\} \tag{24}$$

The second term on the RHS of equation (24) can be converted into a surface integral using the divergence theorem and surface integral on S_∞, which defines the boundary of the system, cancels the incident wave term on the RHS of equation (24). Thus equation (24) simplifies to

$$X_n = n_o T_{n'n''} X_{n''} \sum_{\lambda=|\ell-\ell'|}^{\ell+\ell'} D_{nn'}(\lambda) \left\{ [2ka j_\lambda(2Ka) h'_\lambda (2ka) - 2Ka j'_\lambda(2Ka) h_\lambda(2ka)] + \int_{V-v} [g(x)-1] j_\lambda (Kx) h_\lambda (kx) x^2 dx \right\} \tag{25}$$

where $D_{nn'}(\lambda)$ is the vestige of the translation matrix after the spatial and angular parts have been absorbed in the integration. Different expressions result depending on whether we are discussing acoustic, electromagnetic or elastic wave propagation. Equation (25) can be rewritten as

$$(\delta_{nn'} - M_{nn'}) X_{n'} = 0 \tag{26}$$

The dispersion equation for the effective medium is then simply

$$|\delta_{nn'} - M_{nn'}|(k, K, n_o, v, T, g) = 0 \tag{27}$$

which depends on $k = \omega/c$, the effective wavenumber K, the number density n_o, the exclusion volume v, the T-matrix or the scatterer characteristics and a model for the radial distribution function. By assuming values for all

$$= \sqrt{\lambda_f/\rho_f} \qquad \text{(acoustic waves in fluids)} \quad (4)$$

$$c_s = \sqrt{\mu/\rho} \qquad \text{(elastic waves)} \quad (5)$$

$$= C/\sqrt{\mu_r \varepsilon_r} \qquad \text{(electromagnetic waves)} \quad (6)$$

In equations (3) - (6), c_p and c_s refer to compressional and transverse wave velocities, respectively. In equation (6), C refers to the velocity of light in free space. The corresponding quantities inside the scatterers are differentiated by subscript 1. For brevity, we use the notation k_τ for the wave numbers; $\tau = 1$ corresponds to compressional wave while $\tau = 2,3$ corresponds to shear wave.

The total field at any point in the matrix (outside the scatterers) is the sum of the incident field and the fields scatterered by all the scatterers. This is written as

$$\vec{u}(\vec{r}) = \vec{u}^o(\vec{r}) + \sum_{i=1}^{N} \vec{u}_i^s(\vec{r}-\vec{r}_i) \quad (7)$$

where $\vec{u}_i^s(\vec{r}-\vec{r}_i)$ is the field scattered by the i-th scatterer to the point of observation $\vec{r}$. This expression by itself does not provide a complete formulation of the multiple scattering problem[22]. In order to complete the formulation, we require an expression for u_i^s which in turn depends on the field actually exciting on the i-th scatterer. The exciting field on the i-th scatterer is the incident field $\vec{u}^o$ plus the sum of the fields scattered by all the other scatterers:

$$\vec{u}_i^e(\vec{r}) = \vec{u}^o(\vec{r}) + \sum_{j\neq i}^{N} \vec{u}_j^s(\vec{r}-\vec{r}_j), \quad a \leq |\vec{r}-\vec{r}_i| \leq 2a \quad (8)$$

where 'a' is the radius of the imaginary sphere circumscribing a scatterer. In this analysis, we have assumed that there is no interpenetration of the imaginary spheres of radius 'a' which circumscribe each scatterer. The system of equation (7) and (8) provide one of the standard formulations of the multiple scattering problem.

Although a general dispersion equation can be derived as in Twersky[10], in order to obtain explicit results for particular shapes of scatterers, one has to expand the exciting and scattered fields in a convenient set of basis functions, such as spherical wave functions. Let $\underset{Re}{Ou}\ \psi_n$ generally denote outgoing functions (Hankel functions) and functions regular at the origin (Bessel functions). We dispense with vector notation and the abbreviated index may denote $n \to \tau, \ell, m, \sigma$; $\tau = 1, 2, 3$, $\ell \in [o,\infty]$; $m \in [o, \ell]$. Thus the present discussion can apply equally well to acoustic ($\tau=1$ only), electromagnetic ($\tau=2, 3$ only) or elastic ($\tau=1,2,3$) wave propagation.

At a field point $\vec{r}$ in the host medium, the incident, scattered and exciting fields are expanded as follows,

$$u^o(\vec{r}) = \sum a_n \underset{Re}{} \psi_n(\vec{r}) \quad (9)$$

with for example

$$a_n = i^{-\ell} Y_{\ell m\sigma}(\hat{k}_o) \quad (10)$$

for plane acoustic waves propagating along $\hat{k}_o$ and $Y_{\ell m\sigma}$ are spherical harmonics:

$$u_i^e(\vec{r}) = \sum_n a_n^i \underset{Re}{} \psi_n(\vec{r}-\vec{r}_i); |\vec{r}-\vec{r}_i| < 2a \quad (11)$$

and

$$u_i^s(\vec{r}) = \sum_n f_n^i \underset{ou}{} \psi_n(\vec{r}-\vec{r}_i); |\vec{r}-\vec{r}_i| > 2a \quad (12)$$

where $\vec{r}_i$ denotes the center of the i-th scatterer, and 'a' is the radius of the sphere circumscribing any scatterer. The coefficients f_n^i and α_n^i are unknown but are, however, related via the T-matrix, which can be numerically calculated for scatterers of arbitrary shape using Waterman's extended boundary condition method[23]. Thus,

$$f_n^i = \sum_{n'} T_{nn'} \alpha_{n'}^i \quad (13)$$

where we have assumed that all scatterers are identical.

Substituting equations (11) - (13) in (8) and using the translation-addition theorems for spherical wavefunctions and the orthogonality properties of spherical harmonics[23], we obtain

$$\alpha_n^i = a_n^i + \sum_{j\neq i} \sum_{n'} \sum_{n''} \sigma_{nn'}(\vec{r}_j-\vec{r}_i) T_{n'n''} \alpha_{n''}^j \quad (14)$$

where

$$\underset{ou}{} \psi_n(\vec{r}-\vec{r}_j) = \sum_{n'} \sigma_{nn'}^t(\vec{r}_j-\vec{r}_i) \underset{Re}{} \psi_{n'}(\vec{r}-\vec{r}_i) \quad (15)$$

and $\sigma_{nn'}$ is the translation matrix for spherical wavefunctions[23].

Equation (14) is averaged over the positions of the scatterers to yield an equation of the form

$$\langle \alpha_n^i \rangle_i = a_n^i + \sum_{j\neq i} \sum_{n'} \sum_{n''} T_{n'n''} \sigma_{nn'}(\vec{r}_j-\vec{r}_i) \langle \alpha_{n''}^j \rangle_{ij} p(\vec{r}_j|\vec{r}_i) d\vec{r}_j \quad (16)$$

where

$$a_n^i = a_n e^{ik\hat{k}_o \cdot \vec{r}_i},$$

$p(\vec{r}_j|\vec{r}_i)$ is the conditional probability distribution and $\langle \alpha_{n''}^j \rangle_{ij}$ is the conditional average of $\alpha_{n''}^j$ with the positions of both the i-th and j-th scatterers held fixed.

It is obvious that equation (16) results in an infinite heirarchy because $\langle \alpha_{n''}^j \rangle_{ij}$ is related to $\langle \alpha_n^k \rangle_{ijk}$ and so on. The QCA first invoked by Lax[3,4] and also independently by Twersky[7] simply states that

$$\langle \alpha_{n''}^j \rangle_{ij} \approx \langle \alpha_{n''}^j \rangle_j \quad (17)$$

i.e., the conditional expectation of α_n^j is independent of the position of the i-th scatterer. This would be an exact statement if the system was perfectly crystalline, because, in this case the position of every scatterer in the system is fixed and the neighborhood of every scatterer is the same. The QCA required only a knowledge of two body correlations.

Substituting equation (17) in (16) and noting that

$$p(\vec{r}_j|\vec{r}_i) = \begin{cases} 0; |\vec{r}_j-\vec{r}_i| < 2a \\ \frac{1}{V} g(|\vec{r}_{ij}|); |\vec{r}_j-\vec{r}_i| = |\vec{r}_{ij}| \geq 2a \end{cases} \quad (18)$$

WAVE PROPAGATION IN COMPOSITE MEDIA

By

V. K. Varadan, V. V. Varadan and Y. Ma
Wave Propagation Laboratory
Department of Engineering Science and Mechanics
The Pennsylvania State University
University Park, PA 16802

ABSTRACT

A unified theory for acoustic, electromagnetic and elastic wave propagation in composite media is presented. The theory is based on multiple scattering formalism developed by the authors which involves the T-matrix of a single scatterer, pair-correlation functions to account for the interaction between scatterers and a suitable configurational averaging procedures. Results are presented for acoustic, electromagnetic and elastic wave cases and are compared with experimental measurements.

INTRODUCTION

In this paper, the term "composite media" is used to define a two phase system consisting of a continuous phase, said to be the matrix (host) phase, with discrete inclusions (scatterers) of general shape. When a wave is incident in such composite media, it undergoes multiple scattering thus reducing the amplitude of the coherent wave, and one is interested in studying the dynamic behavior of the composite media via the phase velocity, coherent attenuation, effective elastic or dielectric properties, etc.

The study of wave propagation and scattering in composite media is growing at a rapid rate resulting in many theoretical developments and experimental measurements. As with any rapidly expanding field, the contributions are often diverse and sometimes fragmentary; some theories are based on solid theoretical foundations while others are based on no more than empirical fits to limited sets of data. Except for quasi-static case, most of the available results by various theories differ widely that any clear interpretation of the dynamic behavior of composite media can not be achieved over a range of frequency. The aim of this work is to present a unified theory for all three wave fields, namely acoustic, electromagnetic and elastic cases and a computational scheme for obtaining such frequency dependent parameters including comparison with some experimental measurements.

Lord Rayleigh[1] first addressed the problem using the single scattering approach neglecting multiple scattering or interaction between scatterers. A multiple scattering formalism was introduced by Foldy[2] where he had obtained a closed form expression for the effective wavenumber of the coherent wave for the case of point scatterers. A quasicrystalline approximation was developed by Lax[3,4] which involves two particle correlation function. In a series of papers, Twersky[5-14] presented a thorough analysis giving various orders of multiple scattering using various forms of pair-correlation functions. Recently, Varadan et al and Bringi et al [15-21] have presented a rigorous multiple scattering approach which lends itself to a numerical computations for a range of frequencies and concentrations and for more realistic geometries of the scatterers. Pair-correlation functions are used in these analyses using Percus-Yevick Approximation (P-YA), Self-Consistent Approximation (SCA) and "exact" Monte Carlo computations.

FORMULATION BASED ON SCATTERING THEORY

We consider N number of three-dimensional arbitrary shaped scatterers randomly distributed in an elastic (matrix) medium. The orientation of the scatterers may be quite general. We describe the medium and the scatterers for all three wave fields. For an acoustic problem, we consider fluid scatterers immersed in another fluid, bubbles in a fluid, elastic or viscoelastic scatterers immersed in a fluid, etc. For an electromagnetic scattering problem, we consider dielectric scatterers in free space, dielectric scatterers embedded in a different dielectric medium, etc. For an elastic wave scattering problem, we consider elastic or viscoelastic inclusions embedded in another elastic or viscoelastic material, stress free or fluid filled cavities and cracks in an elastic or viscoelastic material, etc. The properties of the medium and the scatterers are given in terms of Lame' constants λ,μ and density ρ for an elastic material, compressibility λ_f and density ρ_f for non-viscous fluids and relative dielectric constant ϵ_r and permeability μ_r with respect to free space describing dielectric medium. We use subscript 1 to denote these qualities inside the scatterers.

A time harmonic plane wave of unit amplitude and frequency ω is incident on the medium such that the direction of propagation of the incident waves is along the z-axis. The incident wave field may then be represented by

$$\vec{u}^{o} = e^{i(k_p z - \omega t)}\hat{z} + e^{i(k_s z - \omega t)}\hat{x} \qquad (1)$$

where k_p and k_s are compressional (longitudinal) and transverse (shear) wave numbers, respectively, and t is the time. The acoustic waves are purely compressional type and thus, the second term of equation (1) is set equal to zero; for electromagnetic waves which are transverse type, the first term on the right hand side of (1) is zero; for elastic waves which contain both compressional and transverse types, all the term of (1) are present. For acoustic and elastic wave problems, $\vec{u}^{o}$ refers to the incident displacement field vector, while for electromagnetic case, it refers to the incident electric field vector. In equation (1), we use the superscript (o) to indicate an incident wave. The wave numbers k_p and k_s are given by

$$k_p = \omega/c_p \; ; \; k_s = \omega/c_s \; , \qquad (2)$$

respectively, where

$$c_p = \sqrt{(\lambda + 2\mu)/\rho} \qquad \text{(elastic waves)} \qquad (3)$$

TABLE VII. ---continue

R/d	p(R)	R/d	p(R)
2.94	0 91460	2.96	0.92345
2.98	0.93330	3.00	0.94401
3.02	0.95538	3.04	0.96717
3.06	0.97910	3.08	0.99094
3.10	1.00244	3.12	1.01338
3.14	1.02362	3.16	1.03302
3.18	1.04147	3.20	1.04887
3.22	1.05516	3.24	1.06031
3.26	1.06432	3.28	1.06719
3.30	1.06895	3.32	1.06965
3.34	1.06934	3.36	1.06809
3.38	1.06600	3.40	1.06314
3.42	1.05961	3.44	1.05548
3.46	1.05085	3.48	1.04581
3.50	1.04044	3.52	1.03483
3.54	1.02905	3.56	1.02319
3.58	1.01733	3.60	1.01153
3.62	1.00586	3.64	1.00038
3.66	0.99515	3.68	0.99021
3.70	0.98562	3.72	0.98141
3.74	0.97762	3.76	0.97429
3.78	0.97143	3.80	0.96907
3.82	0.96722	3.84	0.96588
3.86	0.96506	3.88	0.96474
3.90	0.96493	3.92	0.96560
3.94	0.96673	3.96	0.96827
3.98	0.97019	4.00	0.97241
4.02	0.97489	4.04	0.97760
4.06	0.98049	4.08	0.98353
4.10	0.98666	4.12	0.98984
4.14	0.99302	4.16	0.99616
4.18	0.99919	4.20	1.00212
4.22	1.00485	4.24	1.00741
4.26	1.00976	4.28	1.01189
4.30	1.01375	4.32	1.01532
4.34	1.01662	4.36	1.01763
4.38	1.01833	4.40	1.01875
4.42	1.01887	4.44	1.01873
4.46	1.01834	4.48	1.01773
4.50	1.01690	4.52	1.01590
4.54	1.01470	4.56	1.01334
4.58	1.01187	4.60	1.01033
4.62	1.00865	4.64	1.00694
4.66	1.00522	4.68	1.00348
4.70	1.00170	4.72	0.99996
4.74	0.99826	4.76	0.99668
4.78	0.99518	4.80	0.99380
4.82	0.99253	4.84	0.99140
4.86	0.99042	4.88	0.98967
4.90	0.98910	4.92	0.98876
4.94	0.98882	4.96	0.98972
4.98	0.99174	5.00	0.99444

TABLE VII. Pair correlation function p(R) for $\rho d^2 = 0.7$

R/d	p(R)	R/d	p(R)
1.02	3.18014	1.04	2.99172
1.06	2.81434	1.08	2.64612
1.10	2.47818	1.12	2.32789
1.14	2.19006	1.16	2.06993
1.18	1.95757	1.20	1.84489
1.22	1.73154	1.24	1.63373
1.26	1.52250	1.28	1.42857
1.30	1.35086	1.32	1.26750
1.34	1.17413	1.36	1.11397
1.38	1.05541	1.40	1.00031
1.42	0.94899	1.44	0.90819
1.46	0.86892	1.48	0.84083
1.50	0.81197	1.52	0.79580
1.54	0.77486	1.56	0.75438
1.58	0.72450	1.60	0.70315
1.62	0.67933	1.64	0.66582
1.66	0.66002	1.68	0.65606
1.70	0.64983	1.72	0.65584
1.74	0.65980	1.76	0.66709
1.78	0.66865	1.80	0.67782
1.82	0.68994	1.84	0.69967
1.86	0.71072	1.88	0.72816
1.90	0.75058	1.92	0.77849
1.94	0.81110	1.96	0.85256
1.98	0.89990	2.00	0.95574
2.02	1.01229	2.04	1.06555
2.06	1.11279	2.08	1.15341
2.10	1.18663	2.12	1.21284
2.14	1.23246	2.16	1.24624
2.18	1.25441	2.20	1.25775
2.22	1.25644	2.24	1.25124
2.26	1.24253	2.28	1.23106
2.30	1.21714	2.32	1.20136
2.34	1.18393	2.36	1.16551
2.38	1.14626	2.40	1.12666
2.42	1.10689	2.44	1.08726
2.46	1.06786	2.48	1.04908
2.50	1.03089	2.52	1.01356
2.54	0.99702	2.56	0.98134
2.58	0.96650	2.60	0.95271
2.62	0.93996	2.64	0.92844
2.66	0.91821	2.68	0.90936
2.70	0.90185	2.72	0.89576
2.74	0.89104	2.76	0.88772
2.78	0.88573	2.80	0.88504
2.82	0.88562	2.84	0.88744
2.86	0.89049	2.88	0.89476
2.90	0.90021	2.92	0.90685

TABLE VI. ---continue

R/d	p(R)	R/d	p(R)
2.94	0.94625	2.96	0.94855
2.98	0.95154	3.00	0.95519
3.02	0.95941	3.04	0.96407
3.06	0.96905	3.08	0.97424
3.10	0.97951	3.12	0.98477
3.14	0.98993	3.16	0.99492
3.18	0.99967	3.20	1.00415
3.22	1.00829	3.24	1.01206
3.26	1.01544	3.28	1.01842
3.30	1.02098	3.32	1.02312
3.34	1.02484	3.36	1.02614
3.38	1.02705	3.40	1.02759
3.42	1.02776	3.44	1.02760
3.46	1.02712	3.48	1.02635
3.50	1.02532	3.52	1.02406
3.54	1.02259	3.56	1.02095
3.58	1.01916	3.60	1.01724
3.62	1.01524	3.64	1.01318
3.66	1.01109	3.68	1.00898
3.70	1.00689	3.72	1.00484
3.74	1.00285	3.76	1.00094
3.78	0.99913	3.80	0.99744
3.82	0.99588	3.84	0.99448
3.86	0.99323	3.88	0.99215
3.90	0.99125	3.92	0.99054
3.94	0.99001	3.96	0.98967
3.98	0.98950	4.00	0.98949
4.02	0.98962	4.04	0.98990
4.06	0.99029	4.08	0.99080
4.10	0.99140	4.12	0.99210
4.14	0.99286	4.16	0.99368
4.18	0.99454	4.20	0.99543
4.22	0.99633	4.24	0.99724
4.26	0.99814	4.28	0.99902
4.30	0.99986	4.32	1.00066
4.34	1.00142	4.36	1.00211
4.38	1.00273	4.40	1.00329
4.42	1.00378	4.44	1.00419
4.46	1.00452	4.48	1.00478
4.50	1.00496	4.52	1.00508
4.54	1.00512	4.56	1.00509
4.58	1.00499	4.60	1.00485
4.62	1.00463	4.64	1.00437
4.66	1.00407	4.68	1.00374
4.70	1.00335	4.72	1.00294
4.74	1.00251	4.76	1.00207
4.78	1.00162	4.80	1.00117
4.82	1.00072	4.84	1.00028
4.86	0.99985	4.88	0.99944
4.90	0.99906	4.92	0.99871
4.94	0.99842	4.96	0.99826
4.98	0.99824	5.00	0.99831

TABLE VI. Pair correlation function p(R) for $\rho d^2 = 0.6$

R/d	p(R)	R/d	p(R)
1.02	2.59123	1.04	2.47586
1.06	2.36728	1.08	2.26336
1.10	2.15679	1.12	2.06050
1.14	1.96996	1.16	1.89062
1.18	1.81600	1.20	1.73972
1.22	1.66165	1.24	1.59500
1.26	1.51582	1.28	1.44916
1.30	1.39524	1.32	1.33444
1.34	1.26279	1.36	1.21779
1.38	1.17245	1.40	1.12741
1.42	1.08350	1.44	1.04772
1.46	1.01157	1.48	0.98286
1.50	0.95278	1.52	0.93374
1.54	0.91126	1.56	0.88943
1.58	0.85999	1.60	0.83831
1.62	0.81392	1.64	0.79714
1.66	0.78632	1.68	0.77651
1.70	0.76402	1.72	0.76178
1.74	0.75792	1.76	0.75699
1.78	0.75111	1.80	0.75211
1.82	0.75595	1.84	0.75737
1.86	0.75977	1.88	0.76707
1.90	0.77795	1.92	0.79249
1.94	0.80989	1.96	0.83406
1.98	0.86248	2.00	0.89853
2.02	0.93586	2.04	0.97163
2.06	1.00404	2.08	1.03293
2.10	1.05774	2.12	1.07874
2.14	1.09613	2.16	1.11038
2.18	1.12145	2.20	1.12982
2.22	1.13542	2.24	1.13870
2.26	1.13972	2.28	1.13895
2.30	1.13643	2.32	1.13252
2.34	1.12723	2.36	1.12096
2.38	1.11371	2.40	1.10578
2.42	1.09724	2.44	1.08829
2.46	1.07892	2.48	1.06945
2.50	1.05982	2.52	1.05029
2.54	1.04078	2.56	1.03139
2.58	1.02211	2.60	1.01312
2.62	1.00439	2.64	0.99609
2.66	0.98826	2.68	0.98101
2.70	0.97428	2.72	0.96820
2.74	0.96275	2.76	0.95798
2.78	0.95389	2.80	0.95047
2.82	0.94773	2.84	0.94569
2.86	0.94434	2.88	0.94373
2.90	0.94383	2.92	0.94468

TABLE V. ---continue

R/d	p(R)	R/d	p(R)
2.82	0.98841	2.84	0.98605
2.86	0.98396	2.88	0.98217
2.90	0.98068	2.92	0.97952
2.94	0.97868	2.96	0.97819
2.98	0.97804	3.00	0.97824
3.02	0.97875	3.04	0.97954
3.06	0.98056	3.08	0.98178
3.10	0.98315	3.12	0.98463
3.14	0.98619	3.16	0.98781
3.18	0.98946	3.20	0.99110
3.22	0.99273	3.24	0.99431
3.26	0.99584	3.28	0.99730
3.30	0.99869	3.32	0.99998
3.34	1.00117	3.36	1.00225
3.38	1.00323	3.40	1.00410
3.42	1.00485	3.44	1.00550
3.46	1.00603	3.48	1.00646
3.50	1.00678	3.52	1.00700
3.54	1.00712	3.56	1.00715
3.58	1.00709	3.60	1.00696
3.62	1.00675	3.64	1.00648
3.66	1.00615	3.68	1.00577
3.70	1.00534	3.72	1.00488
3.74	1.00439	3.76	1.00387
3.78	1.00334	3.80	1.00281
3.82	1.00227	3.84	1.00174
3.86	1.00122	3.88	1.00072
3.90	1.00025	3.92	0.99981
3.94	0.99942	3.96	0.99909
3.98	0.99880	4.00	0.99856
4.02	0.99836	4.04	0.99818
4.06	0.99803	4.08	0.99790
4.10	0.99782	4.12	0.99776
4.14	0.99773	4.16	0.99773
4.18	0.99776	4.20	0.99781
4.22	0.99789	4.24	0.99799
4.26	0.99811	4.28	0.99824
4.30	0.99838	4.32	0.99853
4.34	0.99869	4.36	0.99885
4.38	0.99901	4.40	0.99918
4.42	0.99934	4.44	0.99950
4.46	0.99965	4.48	0.99979
4.50	0.99993	4.52	1.00006
4.54	1.00017	4.56	1.00028
4.58	1.00037	4.60	1.00045
4.62	1.00052	4.64	1.00058
4.66	1.00062	4.68	1.00066
4.70	1.00068	4.72	1.00069
4.74	1.00069	4.76	1.00068
4.78	1.00066	4.80	1.00064
4.82	1.00060	4.84	1.00056
4.86	1.00052	4.88	1.00047
4.90	1.00042	4.92	1.00037
4.94	1.00031	4.96	1.00026
4.98	1.00020	5.00	1.00014

TABLE V. Pair correlation function p(R) for $\rho d^2 = 0.5$

R/d	p(R)	R/d	p(R)
1.02	2.10600	1.04	2.03906
1.06	1.97614	1.08	1.91556
1.10	1.85251	1.12	1.79487
1.14	1.73916	1.16	1.68965
1.18	1.64296	1.20	1.59479
1.22	1.54507	1.24	1.50272
1.26	1.45131	1.28	1.40759
1.30	1.37269	1.32	1.33220
1.34	1.28297	1.36	1.25185
1.38	1.21997	1.40	1.18719
1.42	1.15435	1.44	1.12724
1.46	1.09914	1.48	1.07510
1.50	1.04968	1.52	1.03208
1.54	1.01243	1.56	0.99342
1.58	0.96930	1.60	0.95090
1.62	0.93018	1.64	0.91407
1.66	0.90187	1.68	0.89016
1.70	0.87617	1.72	0.86933
1.74	0.86145	1.76	0.85573
1.78	0.84647	1.80	0.84225
1.82	0.84030	1.84	0.83653
1.86	0.83350	1.88	0.83371
1.90	0.83631	1.92	0.84117
1.94	0.84764	1.96	0.85865
1.98	0.87228	2.00	0.89157
2.02	0.91214	2.04	0.93226
2.06	0.95092	2.08	0.96811
2.10	0.98351	2.12	0.99721
2.14	1.00927	2.16	1.01991
2.18	1.02904	2.20	1.03691
2.22	1.04340	2.24	1.04875
2.26	1.05293	2.28	1.05616
2.30	1.05840	2.32	1.05985
2.34	1.06044	2.36	1.06039
2.38	1.05966	2.40	1.05840
2.42	1.05662	2.44	1.05442
2.46	1.05177	2.48	1.04886
2.50	1.04562	2.52	1.04222
2.54	1.03862	2.56	1.03486
2.58	1.03095	2.60	1.02699
2.62	1.02296	2.64	1.01895
2.66	1.01497	2.68	1.01110
2.70	1.00731	2.72	1.00368
2.74	1.00021	2.76	0.99693
2.78	0.99386	2.80	0.99101

TABLE IV. ---continue

R/d	p(R)	R/d	p(R)
2.82	1.00195	2.84	1.00051
2.86	0.99915	2.88	0.99788
2.90	0.99671	2.92	0.99566
2.94	0.99474	2.96	0.99395
2.98	0.99332	3.00	0.99284
3.02	0.99251	3.04	0.99232
3.06	0.99226	3.08	0.99230
3.10	0.99244	3.12	0.99267
3.14	0.99296	3.16	0.99331
3.18	0.99371	3.20	0.99414
3.22	0.99461	3.24	0.99509
3.26	0.99559	3.28	0.99609
3.30	0.99659	3.32	0.99709
3.34	0.99758	3.36	0.99805
3.38	0.99850	3.40	0.99893
3.42	0.99934	3.44	0.99972
3.46	1.00007	3.48	1.00039
3.50	1.00068	3.52	1.00094
3.54	1.00117	3.56	1.00136
3.58	1.00153	3.60	1.00166
3.62	1.00177	3.64	1.00185
3.66	1.00190	3.68	1.00192
3.70	1.00192	3.72	1.00189
3.74	1.00185	3.76	1.00178
3.78	1.00170	3.80	1.00160
3.82	1.00149	3.84	1.00137
3.86	1.00124	3.88	1.00110
3.90	1.00096	3.92	1.00082
3.94	1.00067	3.96	1.00052
3.98	1.00038	4.00	1.00024

TABLE IV. Pair correlation function p(R) for $\rho d^2 = 0.4$

R/d	p(R)	R/d	p(R)
1.02	1.76705	1.04	1.72725
1.06	1.69007	1.08	1.65417
1.10	1.61613	1.12	1.58131
1.14	1.54679	1.16	1.51608
1.18	1.48731	1.20	1.45729
1.22	1.42577	1.24	1.39944
1.26	1.36588	1.28	1.33725
1.30	1.31525	1.32	1.28878
1.34	1.25488	1.36	1.23445
1.38	1.21303	1.40	1.19023
1.42	1.16671	1.44	1.14763
1.46	1.12739	1.48	1.10963
1.50	1.09041	1.52	1.07702
1.54	1.06195	1.56	1.04728
1.58	1.02857	1.60	1.01439
1.62	0.99813	1.64	0.98483
1.66	0.97425	1.68	0.96387
1.70	0.95131	1.72	0.94403
1.74	0.93582	1.76	0.92926
1.78	0.91976	1.80	0.91405
1.82	0.91011	1.84	0.90453
1.86	0.89942	1.88	0.89653
1.90	0.89524	1.92	0.89534
1.94	0.89623	1.96	0.90033
1.98	0.90596	2.00	0.91592
2.02	0.92690	2.04	0.93780
2.06	0.94803	2.08	0.95764
2.10	0.96642	2.12	0.97446
2.14	0.98176	2.16	0.98844
2.18	0.99442	2.20	0.99984
2.22	1.00459	2.24	1.00881
2.26	1.01243	2.28	1.01559
2.30	1.01823	2.32	1.02047
2.34	1.02223	2.36	1.02367
2.38	1.02469	2.40	1.02541
2.42	1.02581	2.44	1.02595
2.46	1.02579	2.48	1.02543
2.50	1.02483	2.52	1.02409
2.54	1.02316	2.56	1.02208
2.58	1.02084	2.60	1.01949
2.62	1.01802	2.64	1.01648
2.66	1.01488	2.68	1.01326
2.70	1.01159	2.72	1.00992
2.74	1.00826	2.76	1.00662
2.78	1.00502	2.80	1.00346

TABLE III. ---continue

R/d	p(R)	R/d	p(R)
2.94	1.00036	2.96	0.99996
2.98	0.99961	3.00	0.99931
3.02	0.99905	3.04	0.99884
3.06	0.99866	3.08	0.99853
3.10	0.99843	3.12	0.99836
3.14	0.99832	3.16	0.99830
3.18	0.99830	3.20	0.99832
3.22	0.99836	3.24	0.99841
3.26	0.99848	3.28	0.99856
3.30	0.99864	3.32	0.99873
3.34	0.99882	3.36	0.99892
3.38	0.99902	3.40	0.99912
3.42	0.99922	3.44	0.99932
3.46	0.99942	3.48	0.99951
3.50	0.99960	3.52	0.99969
3.54	0.99977	3.56	0.99985
3.58	0.99992	3.60	0.99998
3.62	1.00004	3.64	1.00009
3.66	1.00014	3.68	1.00018
3.70	1.00022	3.72	1.00025
3.74	1.00027	3.76	1.00029
3.78	1.00030	3.80	1.00031
3.82	1.00031	3.84	1.00031
3.86	1.00031	3.88	1.00030
3.90	1.00029	3.92	1.00028
3.94	1.00026	3.96	1.00024
3.98	1.00022	4.00	1.00020

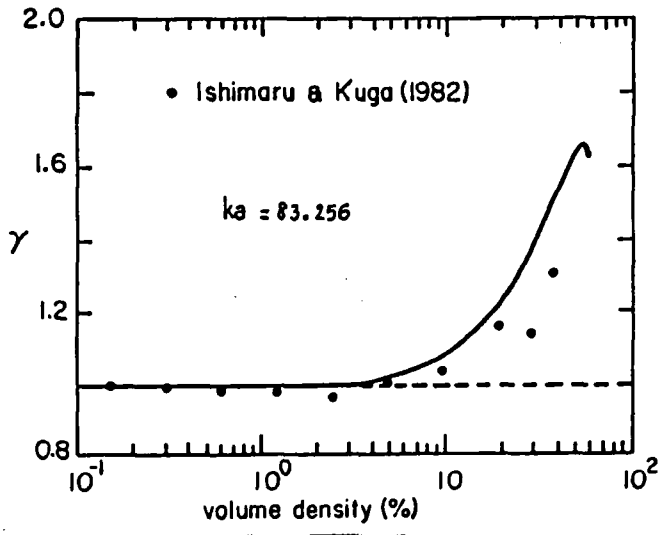

Fig. 6 Coherent attenuation normalized with respect to single scattering approximation vs concentration. Experimental data points are from Ref. [32].

The experimental measurements were reported by Kinra[33] only for the phase velocity as a function of frequency for few values of concentration. In Figure (7), we have shown the comparison of our theoretical results with those of Kinra's experimental measurements. The agreement is extremely good all the way both on "acoustical" and "optical" branches. It should be noted that other theories based on long wavelength approximation, for exmaple that of Datta et al[34] do not predict this anamoly in phase velocity, and the Kuster and Toksöz model even with giant monopole term, does not provide reliable results in the "optical" branch. This drawback of using such simpler theories without multiple scattering and pair-correlation between scatterers has also been realized by Gaunaurd and Überall[35]. In Figure (8), we have plotted the corresponding coherent attenuation as a function of frequency for few values of concentration. Other examples of elastic wave propagation in elastic particulate composite has been studied by us in Reference[21] wherin we had shown excellent agreement between our theory and the experimental results of Kinra and Adler.

In conclusion, we have demonstrated that a rigorour multiple scattering theory with pair-correlation function is absolutely needed to study wave propagation for all wave fields (acoustic, electromagnetic and elastic) in composite media. A unified theory such as the one presented here also provides a basic tool in studying the elastic wave propagation in an elastic composite media containing piezo-electric inclusions wherin elastic and electromagnetic wave coupling plays an important role in attenuation.

ACKNOWLEDGEMENTS

This research was supported in part by the Office of Naval Research under Contract No:N00 173-82-M-T485 and by the U.S. Army Research Office under Contract No: DAAG 29-83-K-0097.

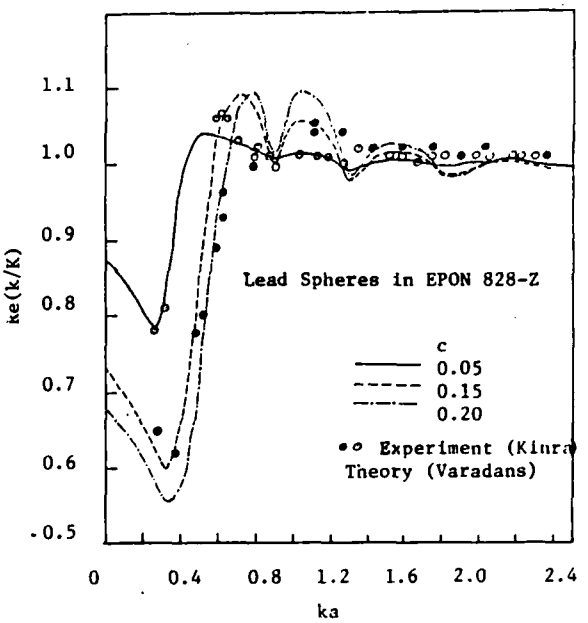

Fig. 7 Phase velocity vs compressional wave number for elastic wave propagation through lead spheres in EPON 828-Z. Experimental data points are from Ref. [33].

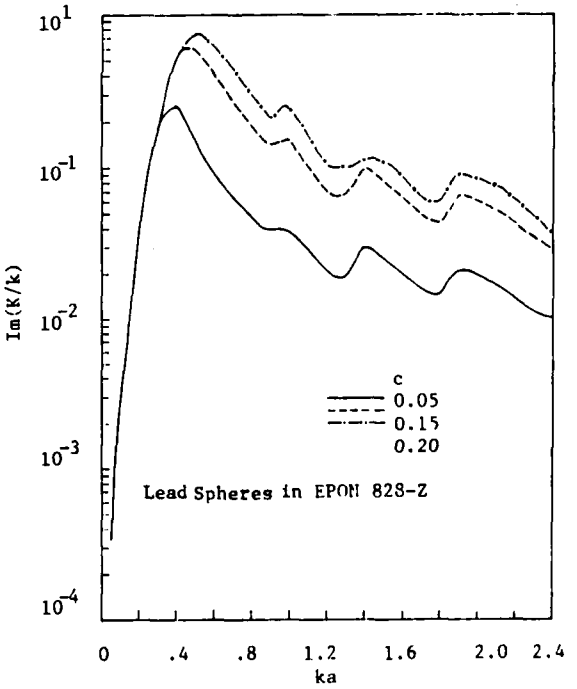

Fig. 8 Coherent attenuation vs compressional wave number for the case given in Fig. 7.

REFERENCES

1. Lord Rayleigh, "On the Transmission of Light Through an Atmosphere Containing Small Particles in Suspension, and on the Origin of the Blue Sky," Philosophical Magazine, Vol. 47, 1899, pp 375-383.
2. Foldy, L.L., "The Multiple Scattering of Waves," Physical Review, Vol. 67, No. 2, 1945, pp 107-119.
3. Lax, M., "Multiple Scattering of Waves," Reviews of Modern Physics, Vol. 23, 1951, pp 287-310.
4. Lax, M., "The Effective Field in Dense Systems," Physical Review, Vol. 88, No. 2, 1952, pp 621-629.
5. Twersky, V., "On the Scattering of Waves by Random Distributions, I.Free-Space Scatterer Formalism," Journal of Mathematical Physics, Vol. 3, 1962, pp 700-715.
6. Twersky, V., "On the Scattering of Waves by Random Distributions, II. Two-Space Scatterer Formalism," Journal of Mathematical Physics, Vol. 3, 1962, pp 724-734.
7. Twersky, V., "On Propagation in Random Media of Discrete Scatterers," Proceedings of the Symposium on Applied Mathematics, Vol. 16, 1964, pp 84-116.
8. Twersky, V., "Multiple Scattering of Waves and Optical Phenomena," Journal of the Optical Society of America, Vol. 52, 1962, pp 145-171.
9. Twersky, V., "Absorption and Multiple Scattering by Biological Suspensions," Journal of the Optical Society of America, Vol. 60, 1970, pp 1084-1093.
10. Twersky, V., "Coherent Scalar Field in Pair-correlated Random Distributions of Aligned Scatterers," Journal of Mathematical Physics, Vol. 18, 1977, pp 2468-2486.
11. Twersky, V., "Coherent Electromagnetic Waves in Pair-correlated Random Distributions of Aligned Scatterers," Journal of Mathematical Physics, Vol. 19, 1978, pp 215-230.
12. Twersky, V., "Acoustic Bulk Parameters in Distributions of Pair-correlated Scatterers," Journal of the Acoustical Society of America, Vol. 64, 1978, pp 1710-1719.
13. Twersky, V., "Scattering Theory and Diagnostic Applications," in Multiple Scattering and Waves in Random Media, Edited by P.L. Chow, W.E. Kohler and G. Papanicolaou, North-Holland Publishing Company, Amsterdam, 1981, pp 267-286.
14. Twersky, V., "Propagation and Attenuation in Composite Media," in Macroscopic Properties of Disordered Media, Edited by R. Burridge, S. Childress and G. Papanicolaou, Springer-Verlag Lecture Notes in Physics, 154, 1982, pp 258-271.
15. Varadan, V.V., Bringi, V.N., and Varadan, V.K., "Frequency Dependent Dielectric Constants of Discrete Random Media," in Macroscopic Properties of Disordered Media, Edited by R. Burridge, S. Childress and G. Papanicolaou, Springer-Verlag Lecture Notes in Physics, 154, 1982, pp 272-284.
16. Bringi, V.N., Varadan, V.V., and Varadan, V.K., "The Effects of Pair Correlation Function on Coherent Wave Attenuation in Discrete Random Media," IEEE Transactions on Antennas and Propagation, AP-30, 1982, pp 805-808.
17. Bringi, V.N., Varadan, V.K., and Varadan, V.V., "Coherent Wave Attenuation by a Random Distribution of Particles," Radio Science, Vol. 17, 1982, p 946-952.
18. Bringi, V.N., Varadan, V.K., and Varadan, V.V., "Average Dielectric Properties of Discrete Random Media Using Multiple Scattering Theory," IEEE Transactions on Antennas and Propagation, AP-31, 1983, pp 371-375.
19. Varadan, V.K., Bringi, V.N., Varadan, V.V., and Ishimaru, A., "Multiple Scattering Theory for Waves in Discrete Random Media and Comparison with Experiments," Radio Science, Vol. 18, 1983.
20. Varadan, V.K., Varadan, V.V., and Ma, Y., "Frequency Dependent Elastic Properties of Rubber-like Materials with a Random Distribution of Voids," Journal of the Acoustical Society of America, Vol. 76, 1984, pp 296-300.
21. Varadan, V.K., Ma, Y., and Varadan, V.V., "A Multiple Scattering Theory for Elastic Wave Propagation in Discrete Random Media," Journal of the Acoustical Society of America, in press.
22. Kuster, G.T., and Toksöz, M.N., "Velocity and Attenuation of Seismic Waves in Two-Phase Media: Part I. Theoretical Formulation," Geophysics, Vol. 39, 1974, pp 587-606.
23. Varadan, V.K., and Varadan, V.V., ed., Acoustic Electromagnetic and Elastic Wave Scattering-Focus on the T-matrix Approach, Pergamon Press, New York, 1980.
24. Percus, J.K., and Yevick, G.J., "Analysis of Classical Statistical Mechanics by Means of Collective Coordinates," Physical Review, Vol. 110, 1950.
25. Wertheim, M.S., "Exact Solution of the Percus-Yevick Integral Equation for Hard Spheres," Physical Review Letters, Vol. 10, 1963, pp. 321-
26. McQuarrie, D.A., Statistical Mechanics, Harper and Row, Inc., New York, 1976.
27. Rowlinson, J.S., "Self-Consistent Approximation for Molecular Distribution Function," Molecular Physics, Vol. 9, 1965, pp 217-
28. Twersky, V., "Multiple Scattering of Sound by Correlated Monolayers," Journal of the Acoustical Society of America, Vol. 73, 1983, pp 68-84.
29. Silberman, E., "Sound Velocity and Attenuation in Bubbly Mixtures Measured in Standing Wave Tubes," Journal of the Acoustical Society of America, Vol. 29, 1957, pp 925-933.
30. Chaban, I.A., "Self Consistent Field Approach to Calculation of the Effective Parameters of Microinhomogeneous Media," Soviet Physics Acoustics, Vol. 10, 1965, pp 298-304.
31. Killey, A., and Meetan, G.H., "Optical Extinction and Refraction of Concentrated Latex Dispersions," Journal of the Chemical Society, Faraday Transactions, Vol. 77, 1981, pp 587-599.
32. Ishimaru, A., and Kuga, Y., "Attenuation Constant of Coherent Field in Dense Distribution of Particles," Journal of the Optical Society of America, Vol. 72, 1982, pp 1317-1320.
33. Kinra, V.K., Ker, E., and Datta, S.K., "Influence of Particle Resonance on Wave Propagation in a Random Particulate Composite," Vol. 9, 198, pp 109-114.
34. Datta, S.K., Ledbetter, H.M., and Kinra, V.K., "Wave Propagation and Elastic Constants in Particulate and Fibrous Composites," in Composite Materials; Mechanics, Mechanical Properties and Fabrication, Edited by K. Kawatz and T. Akasada, Proceedings of the Japan-U.S. Conference, Tokyo, 1981, pp 30-38.
35. Gaunaurd, G.C., and Uberall, "Resonance Theory of the Effective Properties of Peforated Solids," Journal of the Acoustical Society of America, Vol. 71, 1982, pp 282-295.

Iterative extended boundary condition method for scattering by objects of high aspect ratios

Akhlesh Lakhtakia, Vijay K. Varadan, and Vasundara V. Varadan
Department of Engineering Science and Mechanics, The Pennsylvania State University, University Park, Pennsylvania 16802

(Received 6 November 1983; accepted for publication 21 May 1984)

The limitations of the T-matrix procedure or the extended boundary condition method (EBCM) for wave scattering problems, when used for long slender objects, are due to the shrinking volume over which the incident field is extinguished. The resulting ill-conditioning of the matrices involved makes it impossible to invert them. For nondissipative objects only, we observe that the Reinforced Modified Gram–Schmidt (RMGS) orthogonalization procedure works best of all such unitary approaches investigated, but information about the surface and the internal fields is lost in the process. An alternate approach, called the iterative EBCM (IEBCM) is more general in its scope since it provides convergent surface and internal field values and can also work for dissipative targets. This success of the IEBCM results because it extends the interior volume over which the incident field is extinguished.

PACS numbers: 43.20.Fn, 43.20.Bi

INTRODUCTION

The transition matrix (T-matrix) approach or the extended boundary condition method (EBCM) has been extensively utilized to describe acoustic, electromagnetic, and elastic scattering by a variety of nonspherical three-dimensional objects.[1–4] The various field quantities involved are expanded in a suitable set of basis functions, and the integral equations employed in the T-matrix formulation are converted into a finite number of simultaneous equations to be solved by truncating the field expansions appropriately. This procedure is, however, subject to numerical limitations, particularly for objects of high aspect ratios. Therefore, in 1971 Waterman cleverly restructured the T-matrix formalism into a form more tractable for computations by providing explicit symmetry and unitarity constraints on the transition matrix.[4] In addition, by the introduction of the Schmidt orthogonalization technique the computations were further simplified by utilizing the unitary transformations of matrices instead of matrix inversion operations. However, this formulation was limited to acoustic scattering by impenetrable objects, and to electromagnetic scattering by perfectly conducting ones. Recently, Werby and Green have been able to improve upon this formulation and have applied their unitary method[5] to the case of acoustic scattering from elastic shells for which the T-matrix has a much more complicated structure.

Nevertheless, these various formulations have still been limited to objects of only moderately high aspect ratios. For example, the solution of an acoustic problem involving hard spheroids has been tackled for aspect ratios no larger than 2:1.[6] For the more complicated problems involving elastic shells, even Werby and Green have not published results for aspect ratios exceeding 5:3.[5]

Acoustic scattering by prolate spheroids can always, in principle, be solved for by utilizing prolate spheroidal functions, which are the solutions of the wave equation in prolate spheroidal coordinates. However, the generation of these spheroidal functions is very tedious as well as prone to error, and even Senior,[7] who has utilized them extensively, considers only the results for end-on incidence for highly aspherical spheroids.

On the other hand, a new iterative technique applicable for electromagnetic scattering by high-loss dielectric objects has been recently proposed and examined.[8,9] Although published results are available for 6.34:1 spheroids,[8,9] as yet this technique has been successfully used for 8:1 spheroids in the resonance and the post-resonance frequency ranges. For the various features of this new procedure, called the iterative EBCM (IEBCM) the interested reader is referred to Refs. 8 and 9.

Based on the IEBCM, this paper presents another way of solving for the acoustic scattering by impenetrable bodies. We shall restrict ourselves, in presenting the new formulation, to acoustic scattering by sound-hard objects, though similar procedures can easily be applied for acoustic scattering by sound-soft objects and to electromagnetic scattering by perfectly conducting ones. Furthermore, in this initial study, we shall consider only end-on incidence, in order to illustrate the new technique, although there is no restriction on the IEBCM as is clear from Refs. 8 and 9. It will also be shown from the numerical results provided, that the new IEBCM is computationally superior to the T-matrix approach. In contrast with the unitary methods, one strength of the IEBCM lies in its ability to compute convergent values of the fields induced on the surface and inside (if applicable) the scattering target.

I. FORMULATION

Consider a spheroidal scattering volume V (which can be replaced by any axisymmetric, elongated, convex volume for this method) which has a surface S on which Neumann boundary conditions prevail, as shown in Fig. 1. If $\Psi^i(\bar{r})$ is the incident potential at any point $\bar{r}$ indicated with respect to an origin O suitably located inside V, it is easy to show that

 0001-4966/84/090906-07$00.80

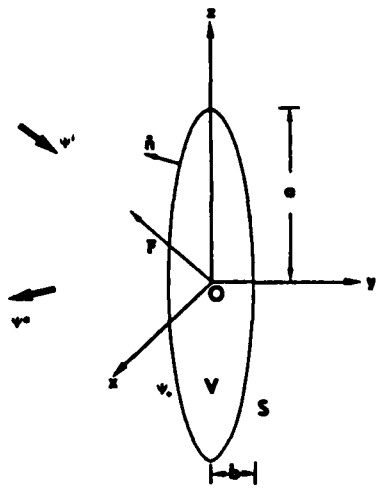

FIG. 1. The geometry of the IEBCM formulation.

the scattered potential $\Psi^s(\bar{r})$ can be calculated in terms of the surface potential $\Psi_+(\bar{r})$[10]:

$$\Psi^s(\bar{r}) = \frac{1}{4\pi}\int_S \hat{n}(\bar{r}')\cdot\Psi_+(\bar{r}') \times\nabla[\exp(ik|\bar{r}-\bar{r}'|)/|\bar{r}-\bar{r}'|]ds', \quad \bar{r}\notin V, \tag{1}$$

where $\Psi_+(\bar{r})$ is itself related to the incident potential by a similar integral equation

$$\Psi^i(\bar{r}) = -\frac{1}{4\pi}\int_S \hat{n}(\bar{r}')\cdot\Psi_+(\bar{r}') \times\nabla[\exp(ik|\bar{r}-\bar{r}'|)/|\bar{r}-\bar{r}'|]ds', \quad \bar{r}\in V. \tag{2}$$

In both of these equations, $k=\omega/c$, $\hat{n}$ is a unit outward normal to S, the ubiquitous expression $\exp(ik|\bar{r}-\bar{r}'|)/|\bar{r}-\bar{r}'|$ is the Green's function, and Eq. (2) is known as the extinction theorem.

The solution of (1) and (2) is usually attempted using the T-matrix approach outlined by Waterman.[10] First, the three potentials involved are expanded in terms of scalar harmonics $\chi_\nu(\bar{x})$:

$$\Psi^i(\bar{r}) = \sum_{\nu=1}^{N} a_\nu \,\mathrm{Re}\,\chi_\nu(k\bar{r}),$$
$$\Psi_+(\bar{r}) = \sum_{\nu=1}^{N} \alpha_\nu \,\mathrm{Re}\,\chi_\nu(k\bar{r}), \tag{3}$$
$$\Psi^s(\bar{r}) = \sum_{\nu=1}^{N} f_\nu \,\mathrm{Ou}\,\chi_\nu(k\bar{r}),$$

where N is some appropriate truncation size, and $\chi_\nu(\bar{x})$ is defined as

$$\left.\begin{matrix}\mathrm{Ou}\\ \mathrm{Re}\end{matrix}\right\}\chi_\nu(\bar{x}) = \epsilon_m\left((2n+1)\frac{(n-m)!}{(n+m)!}\right)^{1/2}\begin{Bmatrix}h_n^{(1)}(x)\\ j_n(x)\end{Bmatrix} \times P_n^m(\cos\theta)\begin{Bmatrix}\cos m\phi\\ \sin m\phi\end{Bmatrix}, \quad \sigma=\begin{Bmatrix}\text{even}\\ \text{odd}\end{Bmatrix}.$$

The index ν is actually a triple index incorporating indices σ, m, n. The index σ can take two values—even and odd, while the indices m and n vary from 0 to ∞. The functions $\mathrm{Ou}\,\chi_\nu(\bar{x})$ and $\mathrm{Re}\,\chi_\nu(\bar{x})$ differ only in the form of the radial functions involved; while $\mathrm{Ou}\,\chi_\nu(\bar{x})$ represents outgoing waves, $\mathrm{Re}\,\chi_\nu(\bar{x})$ is regular at the origin $x=0$. The factor ϵ_m is the Neumann factor.

Finally, the Green's function is also expanded in terms of these scalar harmonics:

$$\frac{e^{ik|\bar{r}-\bar{r}'|}}{|\bar{r}-\bar{r}'|} = ik\sum_{\nu=1}^{\infty}[\mathrm{Ou}\,\chi_\nu(k\bar{r}_>)\mathrm{Re}\,\chi_\nu(k\bar{r}_<)]. \tag{4}$$

On substituting the expansions (3) and (4) into (1) and (2) and on utilizing the orthogonalities of the scalar harmonics over two spheres—one inscribed inside V, and the other circumscribing V—the integral equations (1) and (2) are converted into two sets of N simultaneous equations which can be expressed in matrix notation as[10]

$$\mathbf{a} = -i\mathbf{Q}\boldsymbol{\alpha}, \quad \mathbf{f} = i\,\mathrm{Re}\,\mathbf{Q}\boldsymbol{\alpha}, \tag{5}$$

and which can now be solved using standard matrix procedures[10]:

$$\mathbf{f} = -\mathrm{Re}\,\mathbf{Q}\cdot\mathbf{Q}^{-1}\mathbf{a} = \mathbf{T}\mathbf{a}. \tag{6}$$

For nondissipative objects it can be shown that the matrix $\mathbf{S}=\mathbf{I}+2\mathbf{T}$ satisfies the unitarity constraint

$$(\mathbf{S}^{\mathrm{TR}})^*\mathbf{S} = \mathbf{I},$$

and the symmetry constraint

$$\mathbf{S}^{\mathrm{TR}} = \mathbf{S}.$$

Consequently, if we are interested only in the scattered field we can factorize Q as (see the Appendix)

$$\mathbf{Q} = \hat{\mathbf{Q}}\mathbf{M}, \tag{7}$$

where $\hat{\mathbf{Q}}$ is a unitary matrix and M is an upper triangular matrix. This yields for the S matrix

$$\mathbf{S} = -\hat{\mathbf{Q}}^*(\mathbf{M}^*\mathbf{M}^{-1})(\hat{\mathbf{Q}}^{\mathrm{TR}})^*.$$

Since M is an upper triangular matrix, so is $\mathbf{M}^{-1}$; therefore, $\mathbf{M}^*\mathbf{M}^{-1}$ is also upper triangular. Furthermore, in the limiting case of infinite matrix size, S is symmetric, which requires $\mathbf{M}^*\mathbf{M}^{-1}$ to be so as well. This can happen only if $\mathbf{M}^*\mathbf{M}^{-1}=\mathbf{I}$ (or, M is real) since we also enforce that the diagonal elements of M are real. With this in view, at some truncation size we can obtain

$$\mathbf{f} = -\mathrm{Re}\,\hat{\mathbf{Q}}\cdot(\hat{\mathbf{Q}}^{\mathrm{TR}})^*\mathbf{a} = \mathbf{T}\mathbf{a}, \tag{8}$$

with $(\hat{\mathbf{Q}}^{\mathrm{TR}})^*$ being the conjugate transpose of $\hat{\mathbf{Q}}$.

In spite of this improvement, however, the T-matrix procedure fails to yield convergent expressions for Ψ_+, particularly for scattering volumes of large size parameters and high aspect ratios. It is to be noted that similar problems are also encountered in the implementation of the straightforward T-matrix procedure for the problem of electromagnetic irradiation by lossy dielectric objects.[8,9,11] These stability problems were considerably reduced by solving the integral equations iteratively and by the use of the multiple subregional internal field expansion scheme[8,9]; these two features together lead to the establishment of the IEBCM mentioned in the Introduction.

Based on the IEBCM, we shall now solve (2) iteratively, for which purpose we rewrite it as

$$\Psi^i(\bar{r}) + \frac{1}{4\pi}\int_{S'}\hat{n}(\bar{r}')\cdot\Psi_+^{(l-1)}(\bar{r}')\nabla\left(\frac{e^{ik|\bar{r}-\bar{r}'|}}{|\bar{r}-\bar{r}'|}\right)ds' = -\frac{1}{4\pi}\int_S \hat{n}(\bar{r}')\cdot\Delta\Psi_+^{(l)}(\bar{r}')\nabla\left(\frac{e^{ik|\bar{r}-\bar{r}'|}}{|\bar{r}-\bar{r}'|}\right)ds', \tag{9}$$

where $\Psi_+^{(l-1)}$ is a previous estimate of the surface potential on S' known from the $(l-1)$th iteration, and $\Delta\psi_+^{(l)}$ is an incremental surface potential to be solved for in the lth iteration. S' is the surface of a spheroid of the same acoustic size ka but a smaller aspect ratio than the spheroid under consideration if $l = 1$, but $S' = S$ for subsequent iterations. The iteration process is now described in Secs. I A–C.

A. First iteration: Step 1

We begin the first iteration ($l = 1$) by assuming $\Psi_+^{(l-1)}$ to be known as the exact surface potential on a spheroid V' having the same acoustical size, but a *smaller* aspect ratio than the spheroid V being considered. Since the left-hand side of (9) is known, and with the assumption that the surface potentials for V and V' shall not be very different, we solve (9) for the increment $\Delta\psi_+^{(l)}$ using the regular Waterman procedure[10] mentioned earlier. The use of his method is justified since we effectively compute for an error term $(\Delta\psi_+^{(l)})$ so that the resultant Q matrix from (9) is small in size and does not involve Hankel functions of large orders. It must be mentioned here that the necessity of using large-order Hankel functions in Q forces the matrix to become ill-conditioned and thereby restricts the use of the regular T matrix.

With the calculation of $\Delta\psi_+^{(l)}$ in the $(l-1)$th iteration, we obtain a revised estimate of the surface potential for the volume V:

$$\psi_+^{(l)} = \Psi_+^{(l-1)} + \Delta\psi_+^{(l)}. \tag{10}$$

Ordinarily, for low aspect ratio objects, the surface potential $\Psi_+^{(l)} = \psi_+^{(l)}$ would be obtained here, but for very slender spheroids we can further reform it by using a multiple subsurface re-expansion in the second step of each iteration.

B. First iteration: Step 2

In the second step of each iteration ($l > 1$) the spheroidal surface S is subdivided into a number of subsurfaces S_i centered at points O_i along the major axis of the spheroid, as shown in Fig. 2. On each S_i, the surface potential $\Psi_{+i}^{(l)}$ is expanded in terms of the scalar harmonics centered at O_i. We estimate $\Psi_{+i}^{(l)}$ on each S_i by using a point-matching technique

$$\psi_+^{(l)}(\bar{r}) = \Psi_{+i}^{(l)}(\bar{r}), \quad \bar{r} \in S_i. \tag{11}$$

In addition, the continuity of the surface potential on S is explicitly enforced by satisfying

$$\Psi_{+i}^{(l)}(\bar{r}) = \Psi_{+,i+1}^{(l)}(\bar{r}), \quad \bar{r} \in S_i \cap S_{i+1}, \tag{12}$$

at a suitable number of points in each of the surface overlaps $S_i \cap S_{i+1}$.

The expansions for the various $\Psi_{+i}^{(l)}$ obtained by using (11) and (12) are thus highly convergent, because each of these $\Psi_{+i}^{(l)}$ is used only on the corresponding subsurface S_i. Furthermore, the continuity of these expansions in the surface overlaps is assured because the equations generated by (11) guarantee it to be so. Regarding the number of subsurfaces S_i, we never used more than three for the calculations presented in this paper; more numbers of S_i were required for objects of higher ratios. In addition, the number of points used to enforce (11) and (12) was between six and 12 per subsurface, the larger number being used for subsurfaces having larger curvatures.

In this way, a re-expansion of $\psi_+^{(l)}$ is used to determine an improved representation $\Psi_+^{(l)}$ of the surface potential, which is more stable and computationally tractable than $\psi_+^{(l)}$ itself. Although it is difficult to provide general criteria governing the expansion size for the various Ψ_{+i} it was found that the required number generally depends on both the acoustical size and curvature of the particular subsurface. Larger acoustical sizes and curvatures usually required more numbers of terms to obtain convergent solutions.

C. The iterative procedure

The rest of the iterations ($l > 1$) proceed exactly as the first iteration. The iterative procedure continues until the surface potential satisfies preset error criteria, or, equivalently, until $\Delta\psi_+^{(l)}$ becomes negligibly small.

Once the surface potential has been satisfactorily computed, the scattered potential is easily determined by the application of (1), from which the various scattering parameters can be determined.

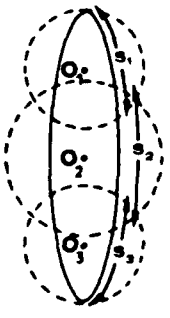

FIG. 2. Multiple subsurface potential expansion scheme employed in step 2 of each iteration in the IEBCM.

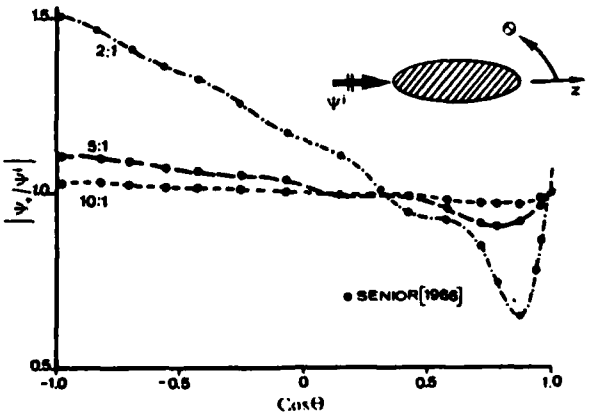

FIG. 3. Surface potential on spheroids of semimajor axis $a = 1.0$ m and aspect ratios $a/b = 2, 5$, and 10 for end-on incidence. The dots represent the values computed by Senior,[7] and the spheroidal parameter $c = k(a^2 - b^2)^{1/2} = 5.0$.

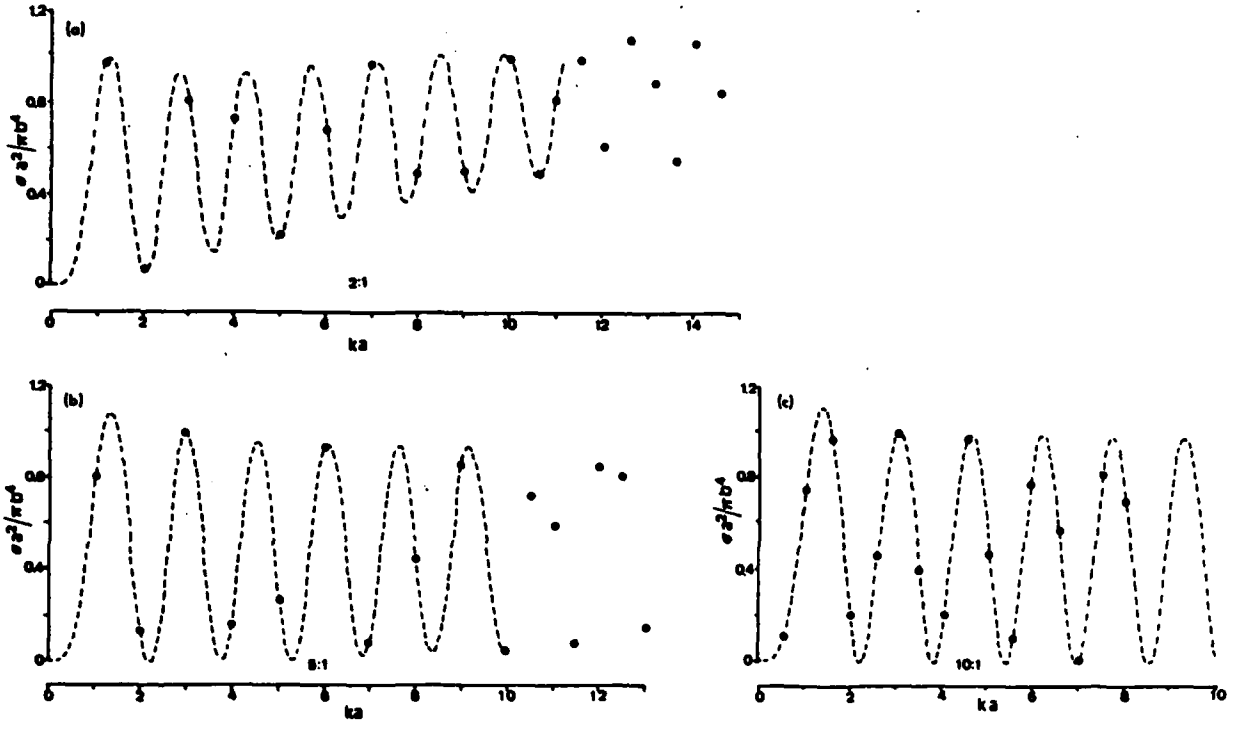

FIG. 4. Backscattering cross section σ for spheroids of semimajor axis $a = 1.0$ m and aspect ratios (a) 2:1, (b) 5:1, and (c) 10:1 for end-on incidence. The backscattering cross section σ is normalized to its geometrical optics value $\pi b^4/a^2$, and is plotted as a function of the size parameter ka. The dots represent the values calculated using the IEBCM, while the dashed curves were computed by Senior.[7]

II. NUMERICAL RESULTS AND DISCUSSION

A computer program to implement the IEBCM on the VAX 11/730 was written and the surface potential and the backscattering cross section were computed for spheroids of unit semimajor axis and varying aspect ratios. Specifically, we considered only the case of end-on incidence so that the only nonvanishing azimuthal mode is $m = 0$.

In Fig. 3, the surface potential Ψ_+ generated on hard spheroids of selected aspect ratios is compared with the values obtained by Senior[7] in 1966. It is to be recalled that while Senior solved the boundary value problem involved in terms of prolate spheroidal functions, the iterative procedure, which is a modification of the T-matrix procedures, uses the spherical harmonics as the basis functions. As can be observed from Fig. 3, the correspondence between the two techniques is excellent.

The backscattering cross section for these spheroids of selected aspect ratios was also computed using the IEBCM as a function of the size parameter ka. In Fig. 4(a)–(c) the calculated backscattering cross-section σ, normalized to its geometrical optics value $\pi b^4/a^2$, is compared with the values computed by Senior.[7] It should be noted that while the IEBCM satisfied the extinction theorem and yielded stable results for 2:1 spheroids up to $ka = 14.5$ and for 5:1 spheroids up to $ka = 13.0$, the iterations *broke down* for 10:1 spheroids after $ka = 8.0$. When compared with the application of the regular T-matrix procedure on the same computer, Fig. 4 reveals a considerable improvement in the solution stability of the IEBCM *vis-à-vis* the T-matrix approach. Its enhanced stability allowed the iterative procedure to handle much more aspherical objects, as is clearly demonstrated by the computation of the surface potential on a 20:1 spheroid in Fig. 5.

Regarding the number of iterations in the calculations discussed so far, the IEBCM actually utilized only two iterations—the first iteration, in which an initial assumption was used, and the second, in which the corrections were applied using the incremental surface potential. We have already mentioned the use of the surface potential on a "fatter" spheroid as an initial assumption for the surface potential on

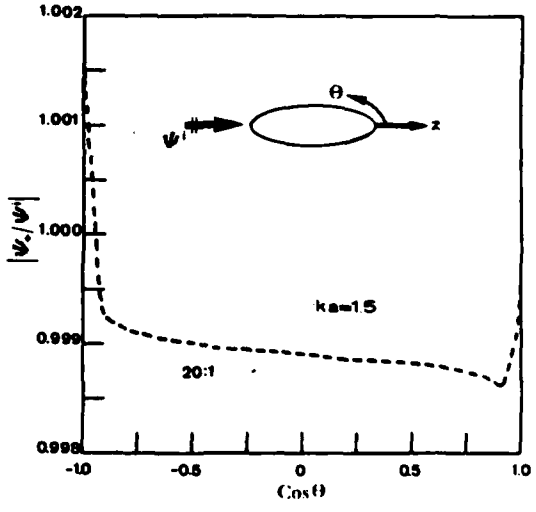

FIG. 5. Surface potential calculated using the IEBCM on a 20:1 spheroid having a size parameter $ka = 1.5$.

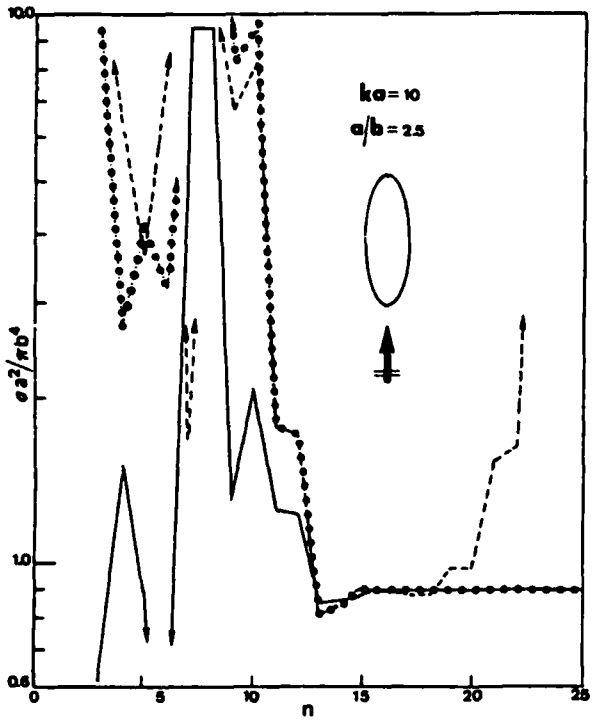

FIG. 6. Comparison of the convergence of the backscattering cross section as a function of n, the number of terms in the series representation of the scattered potential. ——IEBCM, ----regular T-matrix approach, and ····Schmidt's orthogonalization procedure.

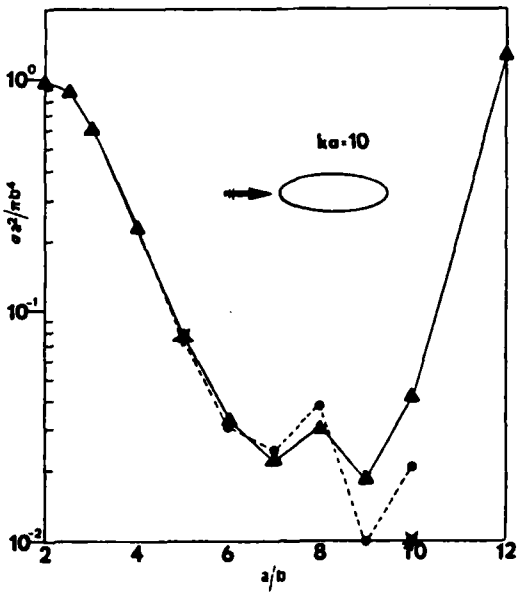

FIG. 7. Backscattering cross section computed using the IEBCM (----) and Schmidt's orthogonalization procedure (——) as a function of a/b for $ka = 10$. The stars represent the values calculated by Senior.[7]

the spheroid being considered. However, the surface potential on the spheroid being considered at a higher or lower frequency can also be, and was actually, employed as an initial assumption to solve the boundary problem at the given frequency of interest. That this second type of an initial assumption has already been employed for dielectric objects should be noted.[9]

With respect to the use of the multiple subsurfaces, not more than two subsurfaces were required to express the surface potential adequately in all of these computations. The number of terms required in the expansion of the surface potential for each subsurface varied from eight to 16, this number being dependent both on the curvature and on the acoustical size of the particular subsurface.

Finally, we also implemented the regular T-matrix procedure, as shown in (6), as well as the Schmidt orthogonalization procedure, as in (8), on the same VAX 11/730 computer and compared them with the IEBCM. In Fig. 6, we compare the backscattering cross section as a function of n, the size of the spherical harmonic expansion of the scattered potential, obtained from these two methods as well as from the IEBCM. It is clear from this figure that while the convergence of the regular T matrix may be somewhat dubious, the orthogonalization procedure as well as the IEBCM have achieved convergence at some comparable value of n.

However, this convergence of the orthogonalization procedure and of the IEBCM may be spurious, as shown in Fig. 7 for spheroids of size parameter $ka = 10$ and of varying aspect ratios. The results obtained from the two methods agree satisfactorily up to $a/b = 7$, but from there on there are sharp differences between the two methods. Indeed, at $a/b = 10$, neither of them is even close to the value computed by Senior.[7] Nevertheless, the redeeming feature of the IEBCM is that it stops at $a/b \cong 10$, but the orthogonalization procedure keeps on "converging" for even higher aspect ratios.

It must be mentioned here that the Q matrix in (6) as well as (8), which is essential to all the three procedures being compared, is, in theory, symmetric.[10] However, computationally it is not so. It is, therefore, of importance to realize that the Q matrix must be artificially symmetrized for the orthogonalization procedure to work; otherwise the orthogonalization of the Q matrix in (8) brings no further improvement in the calculation of the T matrix and is as computationally unstable as the regular T-matrix procedure. It is to be emphasized here that the Schmidt orthogonalization of the Q matrix should satisfy the condition that M is real, otherwise the applicability of (8) is invalid. However, this condition may not always be satisfied,[12] and therefore the use of (8) should never be blindly made. Nevertheless, the "convergence" of (8) is not surprising since the symmetry and the unitarity properties of the T matrix have been built into the orthogonalization procedure. It is, therefore, the authors' view that the orthogonalization of the Q matrix in order to avoid its inversion should not be viewed as a new technique; rather any pertinent factorization of the Q matrix (e.g., the QR factorization) is just another way of handling the inversion of this matrix. Furthermore, we have also observed that if Q has been artificially symmetrized, the regular T-matrix procedure gives results identical to that obtained by using (8).

To examine our contention further, we computed the backscattering cross section when an electromagnetic plane wave is end-on incident on a lossless dielectric spheroid whose size parameter $ka = 1.35$, aspect ratio $a/b = 4.0$, and

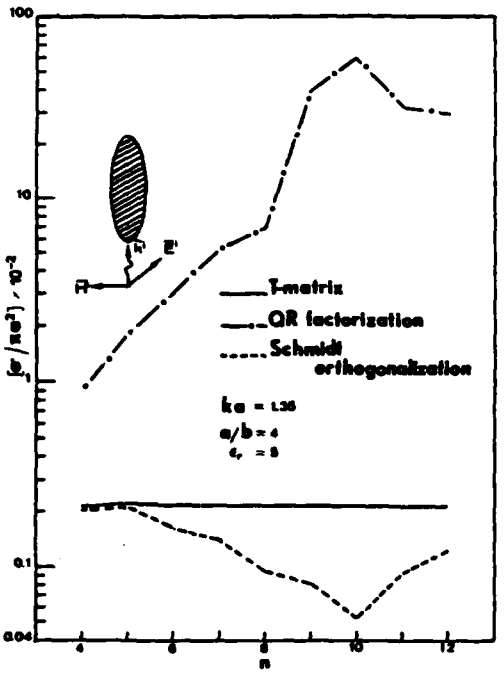

FIG. 8. Backscattering cross section, normalized to πa^2, for a dielectric spheroid ($ka = 1.35$, $a/b = 4$, $\epsilon_r = 5$); an electromagnetic plane wave is end-on incident. Computations are made using (6), and using (8) with QR factorization or Schmidt orthogonalization of the Q matrix.

relative permittivity $\epsilon_r = 5$. The T matrix for this case is identical in form to that given in (6), but the Q matrix is *not* symmetric. The solution was obtained using the regular T-matrix formulation as shown in (6). Furthermore, the matrix Q was first orthogonalized using the Schmidt orthogonalization procedure (see the Appendix) and also it was factorized using a QR transformation.[13] In both of the latter computations, the effect of M was ignored (i.e., M^*M^{-1} was assumed to be a unit matrix) and the solution was attempted using (8). The resulting value of the backscattering cross section σ is plotted against the expansion size in Fig. 8. This plot most eloquently points out the fact that the M matrix cannot be ignored without inspecting whether it is real or not. Furthermore, if this matrix is left in the computation as in (7), the resulting fields are identical to those computed using the regular T-matrix procedure and no further improvement is obtained in terms of either more slender objects or increased size parameters. This would mean that the use of (8) is valid

TABLE I. Extinction and backscattering cross sections for a prolate spheroidal dielectric object of $ka = 1.35$ and $\epsilon_r = 5.0$ obtained using RMGS orthogonalization procedure.

Spheroidal ratio $a:b$	$\sigma_{ext}/\pi a^2$	$\sigma_b/\pi a^2$
4:1	0.5790×10^{-2}	0.2219×10^{-2}
6:1	0.1012×10^{-2}	0.4157×10^{-3}
8:1	0.3042×10^{-3}	0.1283×10^{-3}
10:1	0.1213×10^{-3}	0.5177×10^{-4}
12:1	0.5753×10^{-4}	0.2678×10^{-4}
15:1	0.2321×10^{-4}	0.1021×10^{-4}
20:1	0.7247×10^{-5}	0.3440×10^{-5}

only for very simple problems in which Q is theoretically symmetric.

Finally, in this comparison of procedures we consider a reinforced modified Gram–Schmidt (RMGS) orthogonalization procedure[14] which we have recently found significantly improves the regular T-matrix procedure. Consider a dielectric prolate spheroid whose semimajor dimension $ka = 1.35$ and $\epsilon_r = 5.0$. The T matrix is of the form (6). Here we factorize the nonsymmetric Q matrix as

$$Q = \hat{Q}_1 M_1 = \hat{Q}_2 M_2 M_1 = \cdots,$$

where $\hat{Q}_n = \hat{Q}_{n+1} M_{n+1}$, until we obtain a stable value of $\hat{Q}$. A similar repeated orthogonalization may also be performed, if necessary, on the M matrix thus obtained, and the process is carried out until the final form (7) is obtained and the condition on M being real is satisfied. In Table I the normalized extinction (σ_{ext}) and backscattering (σ_b) cross sections are shown for aspect ratios as high as $a/b = 20.0$. Such a high aspect ratio would not have been possible with a simple Schmidt or QR factorization mentioned earlier.

In summary, it can be stated that the limitations of the regular T-matrix procedure for wave scattering problems, when applied to long slender objects, are due to the shrinking volume over which the incident field is extinguished. The resulting ill-conditioning of the Q matrices involved makes it impossible to invert them. For nondissipative targets only, we have found that the RMGS orthogonalization procedure works best of all such methods investigated in this paper, but all information about the surface and the internal (if applicable) fields is lost in the process. However, the IEBCM is more general in its scope since it provides convergent values of the internal (if applicable) and the surface fields, from which it computes the scattered field. Consequently, it can be, and has been, used for dissipative objects. This success of the IEBCM is due to the fact that it attempts to extend the interior volume over which the incident field is extinguished.

ACKNOWLEDGMENTS

This work was supported in part by the US Army Research Office under Contract no. DAAG 29-83-K0097. The use of the departmental VAX 11/730 minicomputer is gratefully acknowledged. We greatly appreciate the comments provided by one of the reviewers which resulted in the addition of the Appendix.

APPENDIX

There are two distinct orthogonalization procedures, viz.

$$\text{(i) } \hat{Q} = QM^{-1} \text{ (with } M^{-1} \text{ upper triangular)}, \qquad \text{(A1)}$$

and

$$\text{(ii) } Q = M\hat{Q} \text{ (with M upper triangular)}. \qquad \text{(A2)}$$

Waterman,[4] working with the Q^{TR} matrices, used scheme (ii) while we have used scheme (i) throughout this paper. There is a crucial difference between these two schemes: while (i) works with the columns of Q beginning with the first column, (ii) orthogonalizes the row vectors of Q beginning with the last row.

Consequently, the matrix $S = I + 2T$ in these two cases works out to

$$\text{(i) } S = -\hat{Q}^{*}(\hat{Q}^{TR})^{*}, \tag{A3}$$

and

$$\text{(ii) } S = -(\hat{Q}^{TR})^{*}\hat{Q}^{*}. \tag{A4}$$

If, at this point, we constrain Q to be symmetric the two schemes would yield identical results. This, however, would hold only for certain cases, e.g., acoustic scattering by targets which are symmetric about all of the three planes $x = 0$, $y = 0$, and $z = 0$. It must be pointed out that the application of any T-matrix method (including the present IEBCM) for highly aspherical ellipsoidal targets tends to become unwieldy since the various azimuthal modes used in the field expansions then do not decouple. On the other hand, the Rayleigh hypothesis[15] effectively prohibits the current usage of these methods for targets with concavities.

Returning to our discussion on the orthogonalization schemes we observe that the two schemes are not the same if Q is nonsymmetric. Indeed, the validity of either of the schemes would be governed by the satisfaction of two properties: (a) M should tend towards a real matrix, and (b) the individual elements of $\hat{Q}$ should tend to have nonzero final values as the truncation size increases. We have shown in this paper that scheme (i) for symmetric as well as nonsymmetric Q matrices does not always satisfy these conditions. Furthermore, scheme (ii), which is the same as (i) for symmetric Q, suffers similarly, at least, for the cases studied. It appears, however, from our calculations made using (i) for the dielectric case and those made in Ref. 4 using (ii) that the latter scheme is preferable numerically and yields better results.

Insofar as the computational asymmetry of the Q matrix for spheroidal targets and the acoustic case studied is concerned, that can be easily rectified, as noted earlier. It does not, however, follow that for nonspheroidal targets similar numerical errors do not occur or affect the orthogonalization scheme.

Notwithstanding the present discussion, it is our view that the IEBCM presented here and elsewhere[8,9,16] provides the only improvement currently available over the usual T-matrix method for scattering by dissipative or viscoelastic obstacles, and for which purpose any orthogonalization procedure would be in vain.

[1] V. K. Varadan and V. V. Varadan (Eds.), *Acoustic, Electromagnetic and Elastic Wave Scattering—Focus on the T-Matrix Approach* (Pergamon, New York, 1980).
[2] P. C. Waterman, "Matrix Methods in Potential Theory and Electromagnetic Scattering," J. Appl. Phys. 50, 4550–4566 (1979).
[3] P. W. Barber and C. Yeh, "Scattering of Electromagnetic Waves by Arbitrarily-Shaped Dielectric Bodies," Appl. Opt. 14, 2864–2872 (1978).
[4] P. C. Waterman, "Symmetry, Unitarity, and Geometry in Electromagnetic Scattering," Phys. Rev. D 3, 825–839 (1971).
[5] M. F. Werby and L. H. Green, "An Extended Unitary Approach for Acoustical Scattering from Elastic Shells Immersed in a Fluid," J. Acoust. Soc. Am. 74, 625–630 (1983).
[6] V. K. Varadan and V. V. Varadan, "Computation of Rigid Body Scattering by Prolate Spheroids Using the T-matrix Approach," J. Acoust. Soc. Am. 71, 22–25 (1982).
[7] T. B. A. Senior, "The Scattering from Acoustically Hard and Soft Prolate Spheroids for Axial Incidence," Can. J. Phys. 6, 655–667 (1966).
[8] M. F. Iskander, A. Lakhtakia, and C. H. Durney, "A New Procedure for Improving the Solution Stability and Extending the Frequency Range of the EBCM," IEEE Trans. Antennas Propag. 31, 317–324 (1983).
[9] A. Lakhtakia, M. F. Iskander, and C. H. Durney, "An Iterative Extended Boundary Condition Method for Solving the Absorption Characteristics of Lossy Dielectric Objects of Large Aspect Ratios," IEEE Trans. Microwave Theory Tech. 31, 640–647 (1983).
[10] P. C. Waterman, "New Formulation of Acoustic Scattering," J. Acoust. Soc. Am. 45, 1417–1429 (1969).
[11] M. F. Iskander, P. W. Barber, C. H. Durney, and H. Massoudi, "Near-Field Irradiation of Prolate Spheroidal Models of Humans," IEEE Trans. Microwave Theory Tech. 28, 801–807 (1980).
[12] F. Stenger, private communication.
[13] G. Forsythe and C. B. Moler, *Computer Solution of Linear Algebraic Systems* (Prentice-Hall, Englewood Cliffs, NJ, 1967).
[14] J. R. Rice, "Experiments on Gram–Schmidt Orthogonalization," Math. Comput. 20, 325–328 (1966).
[15] P. M. van den Berg and J. T. Fokkema, "The Rayleigh Hypothesis in the Theory of Diffraction by a Cylindrical Obstacle," IEEE Trans. Antennas Propag. 27, 579–583 (1979).
[16] M. F. Iskander and A. Lakhtakia, "Extension of the Iterative EBCM to Calculate Scattering by Low-loss or Lossless Elongated Dielectric Objects," Appl. Opt. 23, 948–953 (1984).

Scattering by lossy dielectric nonspherical objects with nonvanishing magnetic susceptibility

Akhlesh Lakhtakia, Vijay K. Varadan, and Vasundara V. Varadan
Wave Propagation Laboratory, Department of Engineering Science and Mechanics, Pennsylvania State University, University Park, Pennsylvania 16802

(Received 27 February 1984; accepted for publication 25 April 1984)

Using the recently formulated iterative extended boundary condition method (IEBCM) it is shown that the absorption mechanisms in a lossy dielectric object are enhanced by the presence of a nonvanishing magnetic susceptibility. In addition, there is a corresponding reduction in the backscattering cross section. The conditional convergence of the IEBCM algorithm is also proved.

INTRODUCTION

An important development in the last few years in scattering theory has been the T-matrix procedure, which incorporates certain elegant analytical properties and has, therefore, proved to be computationally attractive. Since the T-matrix formulation is fairly general, it has been used for scalar and vector as well as tensor scattering problems, and a unified approach to develop the field equations pertinent to the theories of acoustic, electromagnetic, and elastic scattering is described elsewhere.[1]

However, in applications relating to lossy dielectric spheroids, it was soon recognized that the internal fields induced inside such objects could only be obtained at frequencies below the resonance frequency.[2] The representation of the internal fields by a single vector spherical harmonic expansion, as used in the T-matrix procedure, induces numerical instabilities in the matrix equations.[2] These instabilities become seemingly insurmountable as the frequency approaches the resonance frequency. It hardly needs to be added that these ill-conditioning problems are more pronounced if the object has a large aspect ratio, i.e., if the ratio of the maximum object dimension to the minimum is large.

In order to overcome the convergence-related stability problems in the T-matrix procedure, a new iterative technique called the iterative EBCM (IEBCM) has recently been formulated.[3,4] This method has two main features: firstly, it requires an initial estimate of the tangential fields on the object surface; and secondly, and more importantly, the fields induced inside the object are represented by several overlapping subregional expansions. For highly lossy dielectric objects, the initial estimate may be obtained by replacing the dielectric object by a perfectly conducting one of the same shape and size. The use of the multiple subregional internal field expansion scheme, on the other hand, yields continuous and convergent internal field expansions throughout the interior by a suitable subdivision of the object volume into a number of overlapping subvolumes, in each of which a separate field expansion is assumed. Such a procedure for axisymmetric scatterers is superior to the use of local basis functions utilized in the method of moments[5] in that the internal fields can be obtained on a point-to-point basis rather than in terms of the interpolants commonly used in techniques which call for discretization of the scattering volume.

Since its inception, the IEBCM has largely been used to compute scattering and absorption of homogeneous, lossy dielectric spheroids representing humans and animals, though an extension to lossless dielectric objects has been examined as well.[6] Nothing in the IEBCM formulation, however, restricts its application for a more general problem, i.e., one which involves a scatterer characterized by all of the three constitutive parameters ϵ_r, σ, and μ_r. The scattering properties of such targets have recently come into prominence due to their ability to absorb EM radiation effectively (e.g., Ref. 7). This being the case, in this paper we shall use the IEBCM to examine the plane wave irradiation of penetrable spheroids with nonvanishing conductivities, and possessing dielectric as well as magnetic susceptibilities. We shall, first, prove the conditional convergence of the IEBCM algorithm, though for the details fo the IEBCM algorithm itself, the interested reader is referred to Refs. 3 and 4.

CONVERGENCE OF THE IEBCM

The l th ($l \geq 0$) iteration of the total problem is divided into two problems: (1) an *external* problem, in which the surface fields on a perfectly conducting object of the same shape and size as the actual object are solved, and (2) an *internal* problem, in which the fields inside the actual object are estimated using the results of the external problem previously solved as well as the multiple subregional internal field expansion scheme described in Refs. 3 and 4. These internal fields are then utilized to refine the estimate of the surface fields in the external problem of the next [the $(l+1)$th] iteration. This iterative procedure continues until preset error criteria on the internal fields have been satisfied.

Consider, therefore, a dielectric volume V characterized by a surface S, and described by given ϵ_r, μ_r, and σ, irradiated by a planewave $\{\mathbf{E}^i,\mathbf{H}^i\}$, as shown in Fig. 1. In the external problem of the l th iteration, the equation to be solved is given by Refs. 3 and 4.

$$\{\mathbf{E}^i(k_0\mathbf{r}) + \nabla\times\int_S \hat{n}(\mathbf{r}')\times\mathbf{E}_{\text{int}}^{(l-1)}\cdot\mathcal{G}(k_0\mathbf{r}|k_0\mathbf{r}')ds' - \nabla\times\nabla\times\int_S \frac{1}{j\omega\epsilon_0}\hat{n}(\mathbf{r}')\times\mathbf{H}_{\text{int}}^{(l-1)}\cdot\mathcal{G}(k_0\mathbf{r}|k_0\mathbf{r}')ds'\} = \nabla\times\nabla\times\int_S \frac{1}{j\omega\epsilon_0}\hat{n}(\mathbf{r}')\times\Delta\,\mathbf{H}_{\text{int}}^{(l)}\cdot\mathcal{G}(k_0\mathbf{r}|k_0\mathbf{r}')ds', \quad (1)$$

where $\{\mathbf{E}_{\text{int}}^{(l-1)},\mathbf{H}_{\text{int}}^{(l-1)}\}$ are the estimates of the fields induced

 0021-8979/84/233057-04$02.40

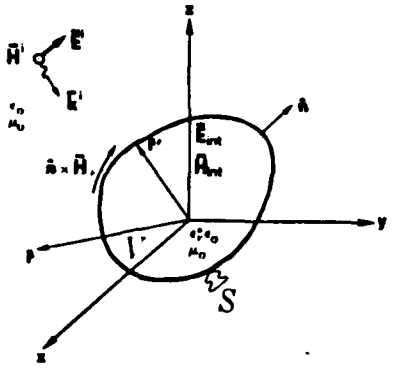

FIG. 1. The geometry of the IEBCM formulation. The various electromagnetic quantities involved are also shown.

inside the dielectric object from the $(l-1)$th iteration, $\hat{n}\times\Delta\mathbf{H}_+^{(l)}$ is an incremental electric current density on the surface of the substitute perfectly conducting object, $\hat{n}$ is a unit outward normal to S, $\mathcal{G}(k_0\mathbf{r}|k_0\mathbf{r}')$ is the freespace transverse dyadic Green's function,[2] $k_0=\omega\sqrt{\mu_0\epsilon_0}$, and $k=k_0\sqrt{(\epsilon_r+j\sigma/\omega\epsilon_0)\mu_r}$. It is obvious that for the zeroth iteration, $\mathbf{E}_{\text{int}}^{(l-1)}$ and $\mathbf{H}_{\text{int}}^{(l-1)}$ are identically zero and that $\hat{n}\times\Delta\mathbf{H}_+^{(0)}=\hat{n}\times\mathbf{H}_+^{(0)}$. The solution of the external problem is $\hat{n}\times\mathbf{H}_+^{(l)}=\hat{n}\times[\mathbf{H}_+^{(l-1)}+\Delta\mathbf{H}_+^{(l)}]$.

In the internal problem, on the other hand, the actual properties of the object are utilized, and fresh estimates of the internal fields $\{\mathbf{E}_{\text{int}}^{(l)},\mathbf{H}_{\text{int}}^{(l)}\}$ are obtained following the procedure described in Secs. II C and II D of Ref. 3. The iterative procedure thus carries on till the incremental surface current density $\hat{n}\times\Delta\mathbf{H}_+^{(l)}$ calculated on the left-hand side of Eq. (1) becomes almost zero, thereby meeting the preset error criterion. In this way the fields induced inside the object can be determined.

Throughout the formulation of the IEBCM, the various field quantities involved, as well as the free-space Green's dyadic, are expressed in a complete set of suitable basis functions $\Psi_\nu(\mathbf{x})$ and $\mathrm{Re}\Psi_\nu(\mathbf{x})$ (Ref. 4). Therefore, the solutions of the external and the internal problems in each iteration are essentially operations involving infinite matrices.[8]

Consider, therefore, the expansion of the incident field $\mathbf{E}^i$ as

$$\mathbf{E}^i(k_0\mathbf{r})=\sum_\nu \alpha_\nu\,\mathrm{Re}\,\Psi_\nu(k_0\mathbf{r}). \tag{2}$$

On solving the external problem in the zeroth iteration, we have a similar expansion for $n\times\mathbf{H}_+^{(0)}$ on the surface of the substitute perfectly conducting object:

$$\hat{n}\times\mathbf{H}_+^{(0)}=\sum_\nu \beta_\nu^{(0)}\,\mathrm{Re}\,\Psi_\nu(k_0\mathbf{r}). \tag{3}$$

In Eq. (3), the superscript on β_ν represents the iteration number. Then, after solving for the internal fields in the internal problem of the zeroth iteration, and calculating the integrodifferential expressions bracketted with $\mathbf{E}^i(k_0\mathbf{r})$ on the right-hand side of Eq. (1) we obtain

$$-\nabla\times\int_S\hat{n}(\mathbf{r}')\times\mathbf{E}_{\text{int}}^{(0)}(k\mathbf{r}')\cdot\mathcal{G}(k_0\mathbf{r}|k_0\mathbf{r}')ds'$$
$$+\nabla\times\nabla\times\int_S\frac{1}{j\omega\epsilon_0}\hat{n}(\mathbf{r}')\times\mathbf{H}_{\text{int}}^{(0)}(k\mathbf{r}')\cdot\mathcal{G}(k_0\mathbf{r}|k_0\mathbf{r}')ds'$$
$$=\sum_\nu\gamma_\nu^{(0)}\,\mathrm{Re}\,\Psi_\nu(k_0\mathbf{r}). \tag{4}$$

In terms of actual matrices Q and R, we can represent the process described in reaching Eq. (4) from Eq. (1) as

$$\beta^{(0)}=Q\alpha,$$
$$\gamma^{(0)}=R\beta^{(0)}=RQ\alpha. \tag{5}$$

Next, in the first iteration, we can similarly write

$$\beta^{(1)}=Q(2\alpha-\gamma^{(0)}), \tag{5a}$$
$$\gamma^{(1)}=RQ(2\mathcal{I}-RQ)\alpha,$$

where $\mathcal{I}$ is the identity matrix. Continuing in this manner, we obtain for the l th iteration:

$$\beta^{(l)}=Q\left((\mathcal{I}+1)\alpha-\sum_{n=0}^{l-1}\gamma^{(n)}\right), \tag{6}$$
$$\gamma^{(l)}=[\mathcal{I}-(\mathcal{I}-RQ)^{l+1}]\alpha,$$

from where, on simplifying the equation for $\beta^{(l)}$ in Eq. (6) we obtain

$$\beta^{(l)}=Q\left(\mathcal{I}+\sum_{n=1}^{l}(\mathcal{I}-RQ)^n\right)\alpha \tag{7}$$

In order to investigate the behavior of the sequences $\{\beta^{(l)}\}_l$ as l increases, Eq. (7) is recast into the following form:

$$\beta^{(l)}=Q\left(\mathcal{I}+(\mathcal{I}-RQ)\sum_{n=0}^{l-1}(\mathcal{I}-RQ)^n\right)\alpha, \tag{8}$$

where the summation over the index n can be easily recognized to be representing a finite Neumann series. It can now be shown[9] that this Neumann series converges to $(RQ)^{-1}$ as l increases, *provided the maximum eigenvalue λ of $(\mathcal{I}-RQ)$ is such that $|\lambda|<1$*; and the sequence $\{\beta^{(l)}\}_l$ therefore converges to β where,

$$\beta=Q[\mathcal{I}+(\mathcal{I}-RQ)(RQ)^{-1}]\alpha$$
$$=R^{-1}\alpha, \tag{9}$$

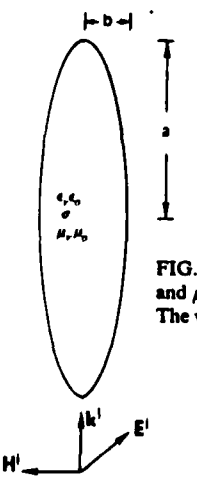

FIG. 2. A prolate spheroid characterized by ϵ_r, σ, and μ_r is exposed to a plane wave incident end on. The vector quantities are in boldface.

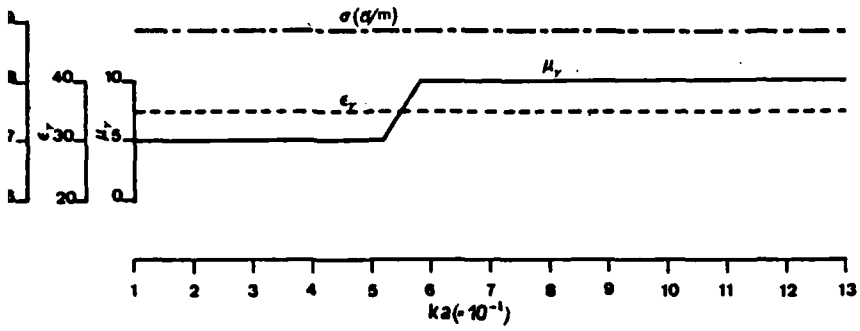

FIG. 3. *Constitutive properties of the spheroid used for the sample IEBCM computations as functions of the size parameter ka.*

the same time the sequence $\{\gamma^{(l)}\}_l$ converges, as expected, r, where

$$\gamma = R\beta = \alpha \tag{10}$$

IMERICAL RESULTS AND DISCUSSION

For our sample computations made using the IEBCM chose a prolate spheroid of semimajor axis $a = 0.2$ m and ving an aspect ratio $a/b = 3.096$, being irradiated by a ane wave $\{\mathbf{E}^i,\mathbf{H}^i\}$ incident end on as shown in Fig. 2. The nstitutive properties of this hypothetical object are plotted Fig. 3 as a function of the frequency. It must be pointed t that for these computations, the conductivity and the ative permittivity were kept independent of the frequency, ıile an idealized variation of the relative permeability was ıumed. This was done in order to explore the effects of ving a nonvanishing magnetic susceptibility vis-a-vis the se when the scatterer does not have any magnetic proper-s. The properties selected, however, do not differ qualita-ely from those experimentally determined for ferrite-im-egnated plastics except that the value of μ_r in these lculations is purely real.[7]

The absorption cross section σ_{abs}, the back scattering oss σ_b, and the total scattering cross section σ_{sca} were computed using the IEBCM for the case of this sample spheroid exposed to a plane wave incident end on. These quantities, non dimensionalized by πa^2, are plotted in Figs. 4–6 as functions of the size parameter. We also used the IEBCM for making similar computations for a spheroid with identical dimensions, relative permittivity, and conductivity but which does not possess any magnetic susceptibility. It is clear from Fig. 4 that the absorption cross section is greatly enhanced when the lossy dielectric object has a nonvanishing magnetic susceptibility as well. This would imply that the presence of magnetic properties enhances the absorption mechanisms in an otherwise lossy dielectric body. Furthermore, there is a corresponding reduction in the backscattering as well. There is, indeed, a slight increase in the total scattering cross section, but this slight increase is com-

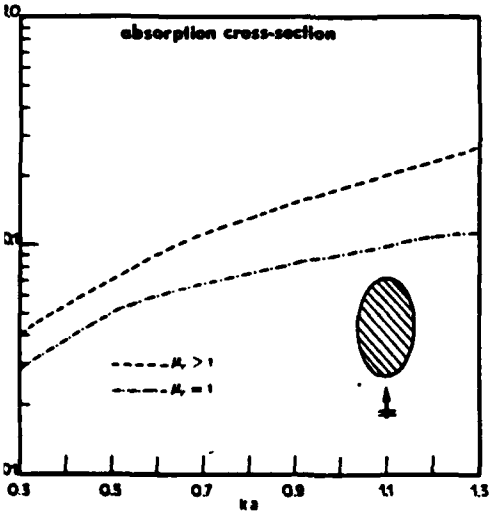

3. 4. Normalized absorption cross section vs size parameter for the ieroid used for the sample IEBCM calculations. The irradiating plane ve is incident end on.

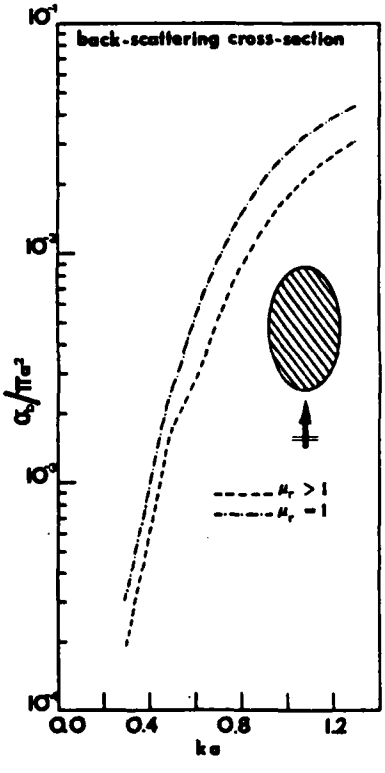

FIG. 5. Normalized backscattering cross section vs size parameter for the spheroid used for the sample IEBCM calculations. The irradiating plane wave is incident end on.

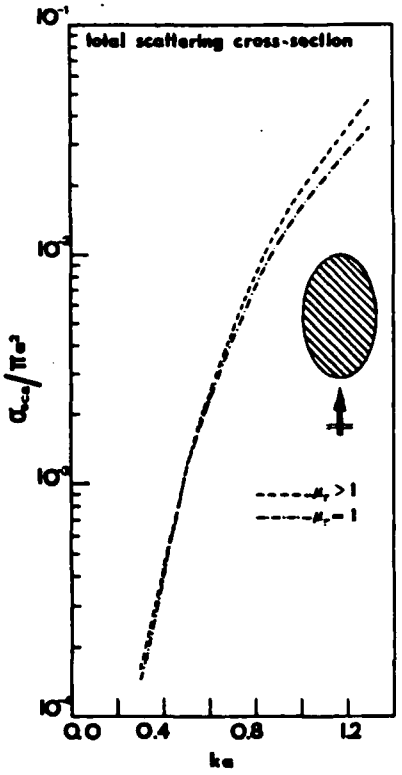

FIG. 6. Normalized total scattering cross section vs size parameter for the spheroid used for the sample IEBCM calculations. The irradiating plane wave is incident end on.

pletely overshadowed by the dramatic increase in the absorption.

In order to understand this enhancement of power dissipation in scatterers possessing $\mu_r > 1$ in addition to their lossy dielectric properties, we computed the electric and the magnetic surface current densities on a spheroid of size parameter $ka = 0.6$ and aspect ratio $a/b = 3.096$. The spheroid is characterized by $\epsilon_r = 35$ and has a conductivity $\sigma = 2.587\ \Omega^{-1}\ m^{-1}$. In the first instance, the scatterer had no magnetic properties (i.e., $\mu_r = 1$), and the current densities are shown in Figs. 7 and 8. Next, the spheroid was assumed to have $\mu_r = 10$ also, and the surface currents are

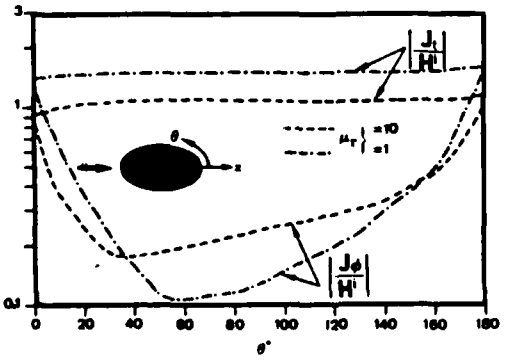

FIG. 7. Surface electric current density J induced on a spheroid ($ka = 0.6$, $a/b = 3.096$, $\epsilon_r = 35$, $\sigma = 2.587\ \Omega^{-1}\ m^{-1}$) computed using IEBCM for (a) $\mu_r = 1$ and (b) $\mu_r = 10$. The irradiating plane wave is incident end on and $\mathbf{J} = J_t \cos\phi\, \hat{t} + J_\phi \sin\phi\, \hat{\phi}$ in a $(\hat{n},\hat{t},\hat{\phi})$ coordinate system.

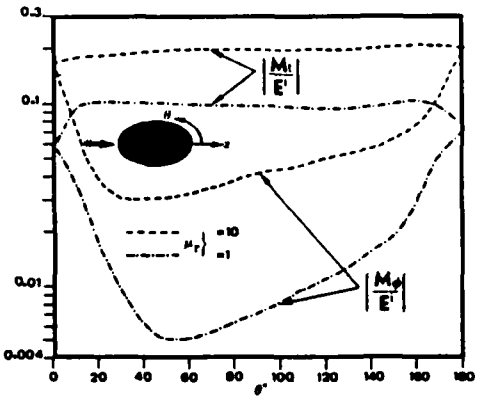

FIG. 8. Surface magnetic current density M induced on a spheroid ($ka = 0.6$, $a/b = 3.096$, $\epsilon_r = 35$, $\sigma = 2.587\ \Omega^{-1}\ m^{-1}$) computed using IEBCM for (a) $\mu_r = 1$ and (b) $\mu_r = 10$. The irradiating plane wave is incident end on and $\mathbf{M} = M_t \sin\phi\, \hat{t} + M_\phi \cos\phi\, \hat{\phi}$ in a $(\hat{n},\hat{t},\hat{\phi})$ coordinate system.

compared in Fig. 7 and 8 with those plotted for the case $\mu_r = 1$. From these two figures, it can be observed that the presence of magnetic susceptibility lowered the surface electric current density J, but it considerably increased the magnetic current density M on the surface of the spheroid. Since $\mathbf{J} = n \times \mathbf{H}_{int}$ and $\mathbf{M} = \mathbf{E}_{int} \times \hat{n}$, where $\hat{n}$ is a unit outward normal to the spheroid surface and $\{\mathbf{E}_{int}, \mathbf{H}_{int}\}$ are the fields computed in the interior of the object, it is obvious that the electric field induced inside the body is increased while the internal magnetic field is lowered by the presence of a magnetic susceptibility. Since the power dissipated inside the lossy spheroid is equal to $1/2\sigma|\mathbf{E}_{int}|^2$, it is not surprising that the absorption is considerably enhanced when $\mu_r > 1$.

It is also inferred from Figs. 7 and 8 that the lowering of the surface electric current due to $\mu_r > 1$ is somewhat overcompensated by an associated increase in the magnetic current density. For this reason, only a slight enhancement in the total scattering cross section is observed as the relative permeability is increased from unity.

ACKNOWLEDGMENT

This work was supported in part by the U. S. Army research office under contract No. DAAG29-83-K-0097.

[1] V. K. Varadan and V. V. Varadan, eds., *Acoustic, Electromagnetic and Elastic Wave Scattering-Focus on the T-matrix Approach* (Pergamon, New York, 1980).
[2] M. F. Iskander, P. W. Barber, C. H. Durney, and H. Massoudi, IEEE Trans. Microwave Theory Tech. 28, 801 (1980).
[3] M. F. Iskander, A. Lakhtakia, and C. H. Durney, IEEE Trans. Antennas Propag. 31, 317 (1983).
[4] A. Lakhtakia, Ph. D. thesis, University of Utah, 1983.
[5] D. E. Livesay and K. M. Chen, IEEE Trans. Microwave Theory Tech. 22, 1273 (1974).
[6] A. Lakhtakia and M. F. Iskander, Appl. Opt. 23, 948 (1984).
[7] R. Ueno, N. Ogasawara, and T. Inui, presented at the Third International Conference on Ferrites, Kyoto, Japan, 1980.
[8] C. C. MacDuffee, *The Theory of Matrices* (Chelsea, New York, 1946).
[9] R. Courant and D. Hilbert, *Methods of Mathematical Physics*, Vol. 1 (Wiley, New York, 1962).

Scattering by highly aspherical targets: EBCM coupled with reinforced orthogonalizations

Akhlesh Lakhtakia, Vijay K. Varadan, and Vasundara V. Varadan

Pennsylvania State University, Wave Propagation Laboratory, University Park, Pennsylvania 16802.
Received 28 April 1984.
0003-6935/84/203502-03$02.00/0.

In a recent paper,[1] Iskander and Lakhtakia have demonstrated the use of the iterative extended boundary condition method (IEBCM) to compute the scattering of EM waves by low-loss or lossless, elongated, axisymmetric dielectric objects. The singular advantage of the IEBCM over the regular EBCM (REBCM)[2] is that it yields numerically stable and convergent fields induced inside and scattered by such elongated objects for which purpose the latter technique is inadequate.[3] This advantage is achieved at the expense of a considerable increase in computation time as well as in programming effort.

If, however, the scattering volume does not absorb energy (i.e., it is either lossless dielectric or perfectly conducting), the *a priori* utilization of the known properties of the T-matrix generated in the REBCM can be used to effect a substantial improvement in the adequacy of the REBCM itself. This improvement comes via certain orthogonalization procedures, but, in the process, all knowledge of the fields induced inside and on the surface of the scatterer is lost. This loss is, however, of little consequence if one is interested only in obtaining the scattered fields. Furthermore, not only elongated needlelike targets can be handled but severely compressed disklike scatterers can be considered with equal ease. This contrasts with the IEBCM whose use is presently constrained to needlelike objects since it utilizes the multiple subregional field expansion scheme to express the internal or the surface fields.[1,4]

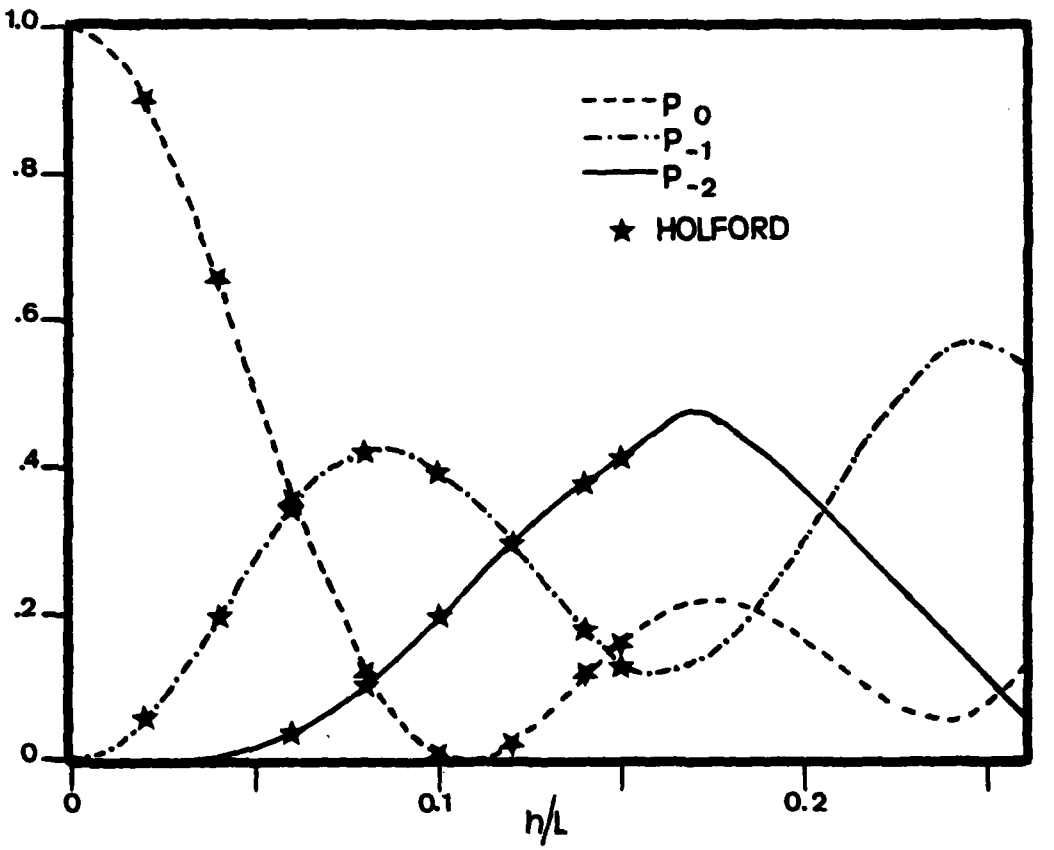

Lakhtakia, et al
Fig 2

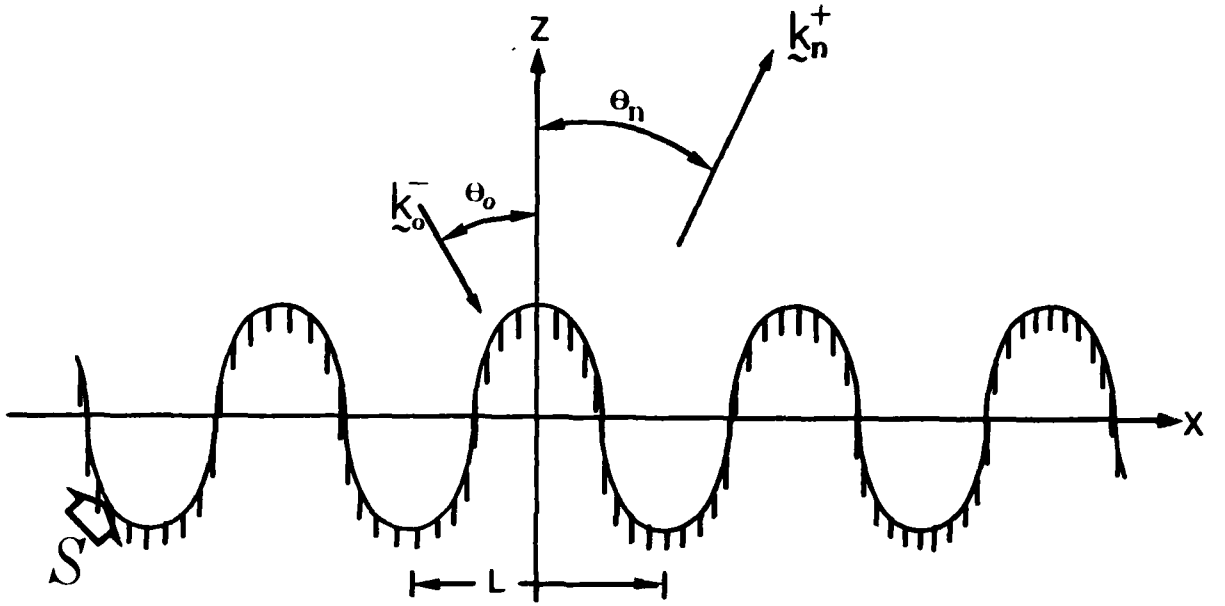

Lakhtakia et al
Fig 1

REFERENCES

1. P. C. Waterman, "Scattering by Periodic Surfaces", J. Acoust. Soc. Am., Vol. 57, pp. 791-802, 1975.

2. J. W. Strutt (Baron Rayleigh), The Theory of Sound, Dover Publication, 1945.

3. R. F. Millar, "The Rayleigh Hypothesis and a Related Least-Squares Solution to Scattering Problems For Periodic Surfaces and Other Scatterers", Radio Science, Vol. 8, pp. 785-796, 1973.

4. J. A. DeSanto, "Scattering From a Sinusoid: Derivation of Linear Equations for the Field Amplitudes", J. Acoust. Soc. Am., Vol. 57, pp. 1195-1197, 1975.

5. R. L. Holford, "Scattering of Sound Waves at a Periodic, Pressure-Release Surface: An Exact Solution", J. Acoust. Soc. Am., Vol. 70, pp. 1116-1128, 1981.

6. R. L. Holford, private communication.

FIGURE CAPTIONS

Fig. 1 Schematic of the problem.

Fig. 2 Power reflection coefficients P_0, P_{-1} and P_{-2} computed using the present approach when a horizontally polarized EM wave strikes a perfectly conducting half-space with a surface defined by $z = h \cos(2\pi x/L)$. $\theta_0=15^\circ$ and $kL=4\pi$. Comparison is made with Holford's computations [5,6] for the acoustic response of an acoustically soft surface.

Fig. 3 Power reflection coefficients P_0, P_{-1} and P_{-2} computed when a vertically polarized EM wave strikes a perfectly conducting half-space with a surface defined by $z=h\cos(2\pi x/L)$. $\theta_0=15^\circ$ and $kL=4\pi$. Comparison is made with Holford's computations [5,6] for the acoustic response of an acoustically hard surface.

upto about 0.2 this time. This is no doubt related to the instabilities of the solution procedure which become more visible when Neumann boundary conditions prevail on S than when Dirchlet boundary conditions do. Again, we have been able to compare very favorably with the acoustic response of an acoustically hard surface supplied to us by Holford [5,6].

In these calculations, as well as in several others made by us, the conservation of energy was satisfied to within ±0.5%. The efficacy of using our surface field expansions, in conclusion, has been very well demonstrated by us using the presented computations. We are currently investigating the use of these expansions in related problems in electromagnetic as well as elastic wave scattering phenomena.

IV. ACKNOWLEDGEMENTS

We gratefully acknowledge the acoustic results supplied to us by Dr. R. L. Holford of AT&T Bell Laboratories. Though yet unpublished, we understand that these results shall be published shortly.

This work was supported in part by the US Army Research Office.

III. NUMERICAL RESULTS

The derivation of the T-matrices in the previous section hold for any arbitrary periodic boundary profile Γ: $z=z(x)$. However, in presenting our numerical results we confine ourselves to the sinusoidal surface $z = h \cos(2\pi x/L)$. These results were calculated on a DEC VAX 11/730 minicomputer.

In Fig. 2 we show the computed values of the power reflection coefficients P_n as functions of the roughness parameter h/L when a horizontally polarized EM wave is incident on S making an angle of 15° with the z-axis, the value of kL being fixed at 4π. The coefficient P_n is defined as

$$P_n = |f_n/a_o|^2 \tag{14}$$

but, in this figure we have suppressed P_1 in the interests of clarity. It is to be noted that while the regular T-matrix procedure [1] would have been restricted by the Rayleigh hypothesis to $h/_L < 1/14$, we have been able to compute upto $h/_L = 0.26$ using the Fourier expansion of the surface field normalized by the incident field. Furthermore, since the problem of scattering is a scalar one we have compared our results with those calculated [6] by Holford for the acoustic response of an acoustically soft surface obtained using a boundary integral equation method [5]. The agreement between the two techniques could not be better.

Finally, in Fig. 3 we have shown P_n computed when a vertically polarized EM field strikes the perfectly conducting rough half space. The parameters for these calculations are otherwise identical to those in Fig. 2. Our previous remarks relating to the regular T-matrix procedure [1] again apply here, though we note we have been able to tackle h/L

and the T-matrix is exactly the same in form as in the equations (10). In obtaining (12a,b), the boundary condition $\hat{n}.\nabla_+ u = 0$ was enforced on S to obtain

$$f_m = -(1/2ikL) \int_\Gamma d\sigma_o \, .\nabla\psi(-\underset{\sim}{k}_m^+ \cdot \underset{\sim}{r}_o) u_+ \qquad (13a)$$

and

$$a_m = (1/2ikL) \int_\Gamma d\sigma_o \, .\nabla\psi(-\underset{\sim}{k}_m^- \cdot \underset{\sim}{r}_o) u_+$$

Substituting (8) in (7a,b) and enforcing $\alpha_0 = 1$ we get

$$f = [\Phi^+]\alpha \quad , \quad a = [\Phi^-]\alpha \tag{8}$$

where the matrices $[\Phi^{\pm}]$ are defined by

$$\Phi^{\pm}_{mn} = \pm (1/L) \int_0^L dx\, \gamma_{mn} \exp\left[-i\,(\underset{\sim}{k}^{\pm}_m - \underset{\sim}{k}^{*}_n) \cdot \underset{\sim}{r}_o\right], \tag{9a}$$

where

$$\gamma_{mn} = -\,(\cos\theta_m \cos\theta_0)^{-1/2}\left[\cos\theta_0 + \sin\theta_n \frac{dz}{dx}\right] \tag{9b}$$

and

$$k^*_n \triangleq k\,(\sin\theta_n\,\hat{x} - \cos\theta_0\,\hat{z}) \tag{9c}$$

We can now obtain a T-matrix such that

$$f = [T]a \tag{10a}$$

with

$$[T] = [\Phi^+]\,[\Phi^-]^{-1} \tag{10b}$$

provided the inverse of $[\Phi^-]$ exists.

For the case of the vertically polarized field i.e. when the electric field is polarized in the x-z plane, and $\overline{H}^o = -\hat{y}u^o$, the problem again reduces to a scalar one, with the exception that the derivative of the total field goes to zero on the surface [1]. The expansion of the surface field u_+ is given by

$$u_+ = 2\sum_n \alpha_n \psi^*_n\,(\underset{\sim}{r}_o), \quad \underset{\sim}{r}_o \in \Gamma \tag{11}$$

where α_0 is again unity; the $[\Phi^{\pm}]$ matrices are now defined by

$$\Phi^{\pm}_{mn} = \pm (1/L) \int_0^L d_x\, \overline{\gamma}^{\pm}_{mn} \exp\left[-i(\underset{\sim}{k}^{\pm}_m - \underset{\sim}{k}^{*}_n) \cdot \underset{\sim}{r}_o\right], \tag{12a}$$

where the $\overline{\gamma}^{\pm}_{mn}$ are given as

$$\overline{\gamma}^{\pm}_{mn} = (\cos\theta_m \cos\theta_0)^{-1/2}\left[-\sin\theta_m \frac{dz}{dx} \pm \cos\theta_m\right]; \tag{12b}$$

$$u^s(\underset{\sim}{r}) = \sum_n f_n \psi(\underset{\sim}{k}_n^+ \cdot \underset{\sim}{r}) \; ; \; \underset{\sim}{r} : \hat{z} \cdot \underset{\sim}{r} < z_{max} \tag{5}$$

with f_n being the unknown coefficients to be determined.

Now, following Waterman [1], we obtain a set of matrix equations for the case of the horizontally polarized fields

$$f_m = (1/2ikL) \int_\Gamma d\underset{\sim}{\sigma}_o \cdot [\psi(-\underset{\sim}{k}_m^+ \cdot \underset{\sim}{r}_o) \nabla_+ u \tag{6a}$$

and

$$a_m = -(1/2ikL) \int_\Gamma d\underset{\sim}{\sigma}_o \cdot [\psi(-\underset{\sim}{k}_m^- \cdot \underset{\sim}{r}_o) \nabla_+ u \tag{6b}$$

where $\nabla_+ u$ refers to the surface field, $d\underset{\sim}{\sigma}_o = \hat{n}\, d\sigma_o = dx(\hat{z} - \hat{x}\frac{dz}{dx})$, $\hat{n}$ is a unit inward normal to the surface and Γ is one period of boundary profile. In deriving these equations Waterman used the Huyghen's principle, followed by the extended boundary condition, specifically, for (6b).

At this point we need a representation for $\hat{n} \cdot \nabla_+ u$ which we obtain as

$$\hat{n} \cdot \nabla_+ \; u = 2 \sum_n \alpha_n \, \hat{n} \cdot \nabla \psi_n^* (\underset{\sim}{r}_o), \; \underset{\sim}{r}_o \; \varepsilon \; \Gamma \tag{7}$$

where the function $\psi_n^* (\underset{\sim}{r}_o)$ is defined as

$$\psi_n^* (\underset{\sim}{r}_o) = \psi(\underset{\sim}{k}_0^- \cdot \underset{\sim}{r}_o) \, e^{\, in2\pi x_o/L} \tag{7a}$$

Equations (7) and (7a) together constitute a Fourier expansion of the surface field normalized by the incident field at the surface S; consequently, $\alpha_0 = 1$ is a reasonable assumption. We note here that by not using $\psi(\underset{\sim}{k}_n^- \cdot \underset{\sim}{r}_o)$ in the expansion (7) we have effectively bypassed the Rayleigh hypothesis. In order now to make (7a) consistent with our basis functions we rewrite it as

$$\psi_n^* (\underset{\sim}{r}_o) = \psi(\underset{\sim}{k}_0 \cdot \underset{\sim}{r}_o) \, e^{ik(\sin\theta_n - \sin\theta_0)x_o} \tag{7b}$$

II. T-MATRIX EQUATIONS FOR A PERIODICALLY CORRUGATED SURFACE

Following the description given by Waterman [1], consider the periodic boundary S described by $z(x)= z(x+L)$, the geometry of which is shown in Fig. 1. First, let the surface be illuminated by an incident plane wave $\underset{\sim}{E}^{o}(x) = \hat{y}\, u^{o}(\underset{\sim}{r})$:

$$u^{o}(\underset{\sim}{r}) = (\cos\theta_0)^{-1/2} \exp(i\, \underset{\sim}{k}_0^{-}\cdot\underset{\sim}{r}) \tag{1}$$

where $\underset{\sim}{k}_0^{-} = k\,(\sin\theta_0\, \hat{x} - \cos\theta_0 \hat{z})$, (2a)

and $\cos\theta_0 = (1 - \sin^2\theta_0)^{1/2}$ (2b)

is a positive real quantity. We begin by introducing a basis of Bloch functions

$$\psi(\pm\underset{\sim}{k}_n^{\pm}\cdot\underset{\sim}{r}) = (\cos\theta_n)^{-1/2} \exp(\pm i\, \underset{\sim}{k}_n^{\pm}\cdot\underset{\sim}{r}),\ n = 0, \pm 1, \ldots, \tag{3a}$$

with $\underset{\sim}{k}_n^{\pm} \triangleq k\,(\sin\theta_n\, \hat{x} \pm \cos\theta_n\, \hat{z})$, (3b)

$$\sin\theta_n = \sin\theta_0 + 2\pi n/kL, \tag{3c}$$

and
$$\cos\theta_n = \begin{cases} (1 - \sin^2\theta_n)^{1/2}, & \sin^2\theta_n \leqslant 1 \quad (3d) \\ +i(\sin^2\theta_n - 1)^{1/2}, & \sin^2\theta_n > 1 \quad (3e) \end{cases}$$

The functions $\psi(\underset{\sim}{k}_n^{+}\cdot\underset{\sim}{r})$ are the outgoing eigenfunctions, to be used to describe the scattered field, while $\psi(\underset{\sim}{k}_n^{-}\cdot\underset{\sim}{r})$ are the incoming eigenfunctions. The equations (3d) and (3e) distinguish propagating and evanescent modes, respectively. We represent formally the incident field (1) as

$$u^{o}(\underset{\sim}{r}) = \sum_n a_n \psi(\underset{\sim}{k}_n^{-}\cdot\underset{\sim}{r}) \tag{4}$$

with $a_n = \delta_{n0}$, $\delta_{nn'}$ being the Kronecker delta function. The scattered field u^{s}, on the other hand, is now represented as

surface field normalized by the incident field on the surface. When compared with Waterman's approach this does not entail any extra numerical effort, but more deeply corrugated surfaces, i.e. those having maximum slopes of the order of 1.5, can now be considered. Our T-matrix approach is also similar to the formulation of acoustic scattering by hard and soft surfaces derived by DeSanto [4] but while we use the extended boundary condition [1] he did not.

In presenting this approach we shall restrict ourselves to the case of a perfectly conducting half-space having a periodically corrugated surface as shown in Fig. 1. Furthermore, we shall describe the derivation for horizontally polarized electromagnetic fields so that the x-z plane is the plane of incidence, $\underset{\sim}{E} = \hat{y}\, u(\underset{\sim}{r})$, $\underset{\sim}{r} = x\hat{x} + z\hat{z}$ and $\hat{y}$ is a unit vector going into the plane of Fig. 1. The analysis for vertically polarized fields proceeds similarly and shall, therefore, be mentioned only in brief. We compare our calculations, made on a DEC VAX 11/730 minicomputer, with those of Holford's integral equation technique [5,6]. We stress, parenthetically, that Holford's method is much harder to implement numerically.

I. INTRODUCTION

The scattering of electromagnetic waves by an infinite rough surface depends very strongly on the roughness of the surface as well as on the angle of incidence. In addition to the specular scattering, which is characteristic of reflexion from a smooth plane, scattering also occurs at many different angles using the nonplaner nature of the surface.

When dealing with the scattering properties of an infinite, periodically corrugated surface it is appropriate to use a planewave spectral representation of the fields of interest, which, for the specific case of a perfectly conducting surface, are the known incident field, and the unknown scattered and surface fields. Two types of plane waves are used for this purpose. The first set of plane waves propagate towards the surface (i.e., in the -z direction as shown in Fig. 1) and are directed symbolically by $\psi\ (\underset{\sim}{k}_n^- \cdot \underset{\sim}{r})$. Obviously, this set of plane waves is best suited to describe the incident field. The scattered field, on the other hand, propagates away from the surface, at least for all points such that $z \geq h$, 2h being the peak-to-peak corrugation depth. These planewaves of the outgoing kind are denoted by $\psi(\underset{\sim}{k}_n^+ \cdot \underset{\sim}{r})$.

It is the surface field whose representation poses a problem. Waterman [1] who originally published a T-matrix to obtain the electromagnetic (EM) response of a perfectly conducting half-space having a periodically rough surface, considered the use of only the $\psi(\underset{\sim}{k}_n^- \cdot \underset{\sim}{r})$ functions to represent the surface field. Incidently, that was also the choice made by Rayleigh [2]. This is, however, a hypothesis that limits the maximum slope of the surface to less than 0.448 [3].

It is our objective in this communication to present a new T-matrix formulation which involves a Fourier exponential representation of the

A T-MATRIX APPROACH FOR EM SCATTERING BY A PERFECTLY CONDUCTING PERIODIC SURFACE

Akhlesh Lakhtakia, Vijay K. Varadan and Vasundara V. Varadan
Department of Engineering Science and Mechanics
The Pennsylvania State University
University Park, PA 16802

ABSTRACT

The novel use of a Fourier exponential representation of the field induced on a perfectly conducting periodic surface is shown to yield a T-matrix which is numerically stable for deeply corrugated surfaces. Whereas the Rayleigh hypothesis limited the maximum slope of the surface to less than 0.448 in Waterman's original T-matrix scheme [1], our T-matrix is applicable even when the maximum slopes are of the order of 1.5.

4. A. Lakhtakia, V. K. Varadan, and V. V. Varadan, "Iterative Extended Boundary Condition Method for Scattering by Objects of High Aspects Ratios," J. Acoust. Soc. Am. 76 (1984).
5. P. C. Waterman, "New Formulation of Acoustic Scattering," J. Acoust. Soc. Am. 45, 1417 (1969).
6. J. R. Rice, "Experiments on Gram-Schmidt Orthogonalization," Math. Comput. 20, 325 (1966).
7. M. F. Werby and L. Green, "An Extended Unitary Approach for Acoustical Scattering from Elastic Shells Immersed in a Fluid," J. Acoust. Soc. Am. 74, 625 (1983).
8. A. Lakhtakia, V. V. Varadan, and V. K. Varadan, "Scattering of Elastic Waves by Smooth and Rough Cracks," Int. J. Wave Motion, submitted (1984).

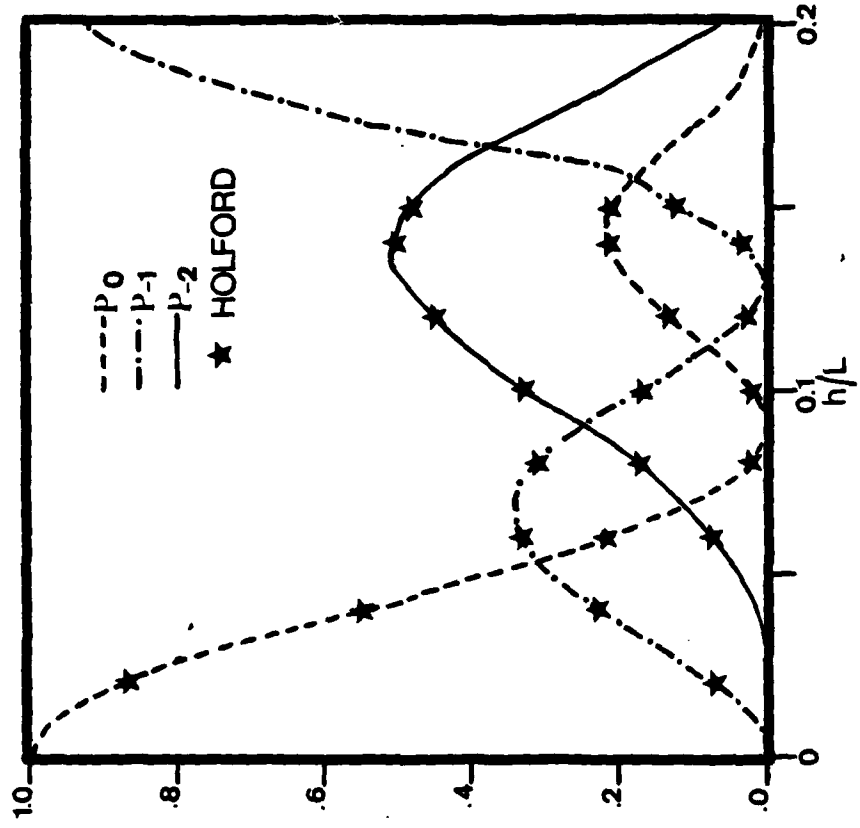

Lakhtakia et al Fig 8

ON AN IMPROVED T-MATRIX APPROACH TO STUDY THE SCALAR SCATTERING RESPONSE OF DOUBLY PERIODIC SURFACES

A. Lakhtakia, V.K. Varadan and V.V. Varadan
Wave Propagation Laboratory
Pennsylvania State University
University Park, PA 16802

ABSTRACT

In investigating the scattering response of a periodic surface, the use of incomplete or inappropriate basis functions for representing the field(s) induced on the scattering surface has given rise to what is now called the Rayleigh Hypothesis (RH). Here we use normalised Fourier bases for this purpose and develop a T-matrix which completely characterises the scalar scattering response of such a surface. The Rayleigh limits are effectively bypassed, and the obtained solutions are seen to obey unitarity as well as reciprocity constraints. We also show that the measurement of the scattered field can lead to two different interpretations of the nature of the scattering surface in inverse shape problems.

INTRODUCTION

The scattering of waves --- be they acoustic, electromagnetic, or elastic, --- by periodic surfaces has been the subject of much investigation ever since Rayleigh studied the scattering response of sinusoidal reflection gratings [1]. He expanded the incident and the scattered fields in terms of relevant incoming and outgoing planewaves, repsectively, and these decompositions are used to this day in such problems. However, he expressed the field(s) generated on the periodic surface in terms of outgoing planewaves alone, a premise, --- now called the Rayleigh Hypothesis (RH), --- which involves an incomplete basis set, and can, therefore, be used for shallow corrugations. In a classic paper, Millar [2] has shown that for 2-D scalar problems involving a surface S^2: $x_3(x_2,x_1) = h \cos(2\pi x_1/L)$ the RH is applicable for $h/L \leq 0.072$. For the corresponding 3-D problems, we believe that Goodman's estimate [3] of $h/L \leq 0.0504$ is correct, the surface S^3: $x_3(x_2,x_1) = h\,[\cos(2\pi x_2/L) + \cos(2\pi x_1/L)]$.

Since then several efforts have been made to bypass the above-mentioned Rayleigh limits on the maximum gradient of periodic surfaces. Most of these methods fall into two categories. Methods of the first kind involve the solution of an integral equation (IE) [4,5]; while the second type are essentially matrix procedures [3, 5-12]. Though the IE methods have been very successful in dealing with highly corrugated S^2, their use for S^3 is extremely cumbersome because of tedious computations. Hence, matrix methods offer the only choice for 3-D problems. In this connection, DeSanto [6] has formulated coupled integral equations which are converted into matrix equations using relevant expansions for the fields of interest. A more elegant approach is due to Waterman [12] who used the 'extinction' theorem to formulate a T-matrix which characterizes the scalar scattering response of periodic S^2. This method, known as the T-matrix procedure, involves an understanding of the scattering problem from first principles using the Huyghen's and the Love's equivalence principles. Recently, this approach has also been extended to elastic scattering problems as well [8,9].

Nevertheless, the expansion of the surface field(s) in terms of only the incoming planewave bases for the T-matrix approach has proved to be a stumbling block in its application for highly corrugated surfaces. Such an expansion is as incomplete as the one used by Rayleigh; consequently, this method has suffered from the same limitations. Recently, however, using a hybrid T-matrix - point-matching technique, wherein the surface field(s) is expressed in terms of both incoming and outgoing planewave bases, the applicability of the method has been increased to higher corrugations than previously possible. We have used this hybrid technique for scalar [13] as well as elastic [9] scattering problems involving S^2 surfaces.

Specifically for scalar problems, Fourier bases have been used for representing the surface field(s) in the T-matrix framework [3] and with success as evinced by the data published in [14]. On the other hand, using these same Fourier bases for computing elastic responses by Chuang and Johnson [8] has not lifted the T-matrix approach from within the Rayleigh limit

on the maximum surface slope. However, the use of normalised Fourier bases of [6,7] has been more promising as shown by our work on the scalar response of S^2 [15].

In this paper we present a T-matrix formalism for computing a stable and accurate T-matrix which characterises the acoustic responses of hard and soft periodic S^3 surfaces. Normalised Fourier bases will be used to express the surface field; and the presented approach will also be valid for electromagnetic problems, where the relevant fields will have to be decomposed into TM-to and TE-to $x_3$fields. The use of these bases for elastic problems is still under investigation and shall not be discussed here. From our results we shall show that the presented T-matrix method is useful .for scalar problems involving surface slopes about 3 to 4 times the Rayleigh limits. We shall also discuss a non-uniqueness in the inverse shape problem when the field scattered by the periodic surface has been determined experimentally.

THEORY

Let $Ox_1x_2x_3$ denote a 3-D Cartesian co-ordinate system. The surface S^3 is given by $x_3 = F(x_1,x_2)$, where F is assumed to be a single-valued, differentiable, periodic function with periodicities L_1 and L_2. This surface, in the mean, should be the flat plane $x_3 = 0$.

The region V above the surface $\{x_3 > F(x_1,x_2)\}$ is occupied by a non-viscous compressible fluid and an incident planewave

$$\psi_i(\underline{x}) = \psi_0 \exp(i\underline{k}_0 \cdot \underline{x}) \tag{1}$$

is incident on S^3 with a temporal variation $\exp(-i\omega t)$. The surface can be either acoustically soft (case S) or hard (case H), and the corresponding boundary conditions on the total field apply. The notation is as follows:

$$\left.\begin{aligned} & k = \omega/c \qquad \underline{k}_0 = k(\alpha_0\underline{u}_1 + \beta_0\underline{u}_2 - \gamma_{00}\underline{u}_3) \\ & \alpha_0 = \sin\theta_0\cos\phi_0 \qquad \beta_0 = \sin\theta_0\sin\phi_0 \\ & \gamma_{00} = \cos\theta_0 \qquad \underline{x} = x_1\underline{u}_1 + x_2\underline{u}_2 + x_3\underline{u}_3 \\ & \psi_0 = \text{constant amplitude.} \end{aligned}\right\} \tag{2}$$

The relevant boundary condition are:

$$\text{Case S:} \quad \psi(\underline{x})\big|_{S^3} = 0 \tag{3}$$

$$\text{Case H:} \quad \underline{\nu} \cdot \nabla\psi(\underline{x})\big|_{S^3} = 0 \tag{4}$$

$$\underline{\nu} = \text{unit vector normal to } S^3 \text{ into the fluid.} \tag{5}$$

The application of the Huyghens' principle, and the use of the free space

Green's function $G(\underline{x}';\underline{x}) = \exp(ik|\underline{x}'-\underline{x}|)/4\pi|\underline{x}'-\underline{x}|$, leads to [12]:

$$H_v(\underline{x}')\psi(\underline{x}') = \psi_i(\underline{x}') + \int_0^{L_1} dx_1 \int_0^{L_2} dx_2 \cdot$$

$$\cdot\{kG(\underline{x}';\underline{x})\, V(\underline{x}) - U(\underline{x})\, \zeta(\underline{x})\, \underline{\nu} \cdot \nabla G(\underline{x}';\underline{x})\}, \tag{6}$$

with $H_v(\underline{x}') = 1$ if $\underline{x}' \in V$, and 0 otherwise; and

$$\left.\begin{aligned} V(\underline{x}) &= k^{-1}\, \zeta(\underline{x})\, \underline{\nu} \cdot \nabla\psi(\underline{x})|_{S^3}\ , \\ U(\underline{x}) &= \psi(\underline{x})|_{S^3}\ , \\ \zeta(\underline{x}) &= \{1 + (\dot{F}_1)^2 + (\dot{F}_2)^2\}^{\frac{1}{2}},\quad \dot{F}_n = \partial F/\partial x_n. \end{aligned}\right\} \tag{7}$$

Equation (6) for $\underline{x}' \notin V$ is the 'extinction theorem' [12], $\psi = \psi_i + \psi_s$.

The free space Green's function can be expanded as

$$G(\underline{x}';\underline{x}) = (i/2kL_1L_2) \sum_{p=-\infty}^{\infty} \sum_{q=-\infty}^{\infty} (1/\gamma_{pq}) \cdot$$

$$\cdot \exp\{ik[\alpha_p(x_1'-x_1) + \beta_q(x_2'-x_2) + \gamma_{pq}|x_3'-x_3|]\}, \tag{8}$$

with

$$\left.\begin{aligned} \alpha_p &= \alpha_0 + 2p\pi/kL_1,\ p = 0, \pm1, \pm2, \ldots. \\ \beta_q &= \beta_0 + 2q\pi/kL_2,\ q = 0, \pm1, \pm2, \ldots. \\ \gamma_{pq} &= [1 - \alpha_p^2 - \beta_q^2]^{\frac{1}{2}},\ \mathrm{Re}(\gamma_{pq}) \geq 0,\ \mathrm{Im}(\gamma_{pq}) \geq 0. \end{aligned}\right\} \tag{9}$$

At this juncture we also define two groups of wave vectors

$$\underline{k}^{\pm}_{pq} = k(\alpha_p \underline{u}_1 + \beta_q \underline{u}_2 \pm \gamma_{pq} \underline{u}_3) \tag{11}$$

with whose help we define the incident and the scattered fields as

$$\psi_{\substack{s\\i}}(\underline{x}) = \sum_{p=-\infty}^{\infty} \sum_{q=-\infty}^{\infty} a^{\pm}_{pq} \exp(i\underline{k}^{\pm}_{pq} \cdot \underline{x}) \tag{12}$$

with $a^{-}_{pq} = \psi_0 \delta_{p0} \delta_{q0}$ and unknown a^{+}_{pq} to be determined.

Let us first consider the case S. The boundary condition (3) would then apply and the Equations (6) would accordingly be modified. On substituting the expansions (12) in the modified (6) we obtain a set of equations:

$$a^{\pm}_{pq} = -\int_0^{L_2} dx_1 \int_0^{L_2} dx_2 \qquad (1/2ikL_1L_2\gamma_{pq}) \cdot$$

$$\cdot \underline{\chi} \cdot \{\exp(-i\underline{k}^{\pm}_{pq}\cdot\underline{x})\ \nabla_+\psi(\underline{x})\}\ , \tag{13}$$

the vector

$$\underline{\chi} = (-\dot{F}_1, -\dot{F}_2, 1).$$

In order to solve the problem all we need now is the surface field representation, which we assume to be [6,15]

$$\underline{\chi}\cdot\nabla_+\psi(\underline{x}) = 2 \sum_{n=-\infty}^{\infty} \sum_{m=-\infty}^{\infty} \alpha_{nm}\, \underline{\chi}\cdot\nabla_+\{\exp(i\underline{k}^{*}_{nm}\cdot\underline{x})\};\ \underline{x}\in S^3 \tag{14}$$

with the wave vectors

$$\underline{k}^{*}_{nm} = k\ (\alpha_n,\ \beta_m,\ -\gamma_{00}); \tag{15}$$

finally, substitution of a truncated (14) in (13) leads to the matrix equations

$$a^{+} = Q^{+}_{d}\cdot(Q^{-}_{d})^{-1}\ a^{-} \tag{16}$$

where the matrices $Q^{\pm}_{d}$ are

$$(Q^{\pm}_{d})_{pq,nm} = \pm \int_0^{L_2} dx_1 \int_0^{L_2} dx_2 [(\gamma_{00} + \alpha_n\dot{F}_1 + \beta_m\dot{F}_2)/\gamma_{pq}L_1L_2]\cdot$$

$$\cdot\exp[-i(\underline{k}^{\pm}_{pq} - \underline{k}^{*}_{nm})\cdot\underline{x}]. \tag{17}$$

At this point we remark that replacing the $\underline{k}^{*}_{nm}$ by either of the $\underline{k}^{\pm}_{nm}$ vectors would completely debilitate the T-matrix procedure and subject it to the Rayleigh limits in its ability to handle deeply corrugated surfaces.

Likewise, for the case H the boundary condition (4) is substituted in (6) as also the assumed surface field expansion

$$\psi_+(\underline{x}) = 2 \sum_{n=-\infty}^{\infty} \sum_{m=-\infty}^{\infty} \alpha_{nm}\exp(i\underline{k}^{\pm}_{nm}\cdot\underline{x});\ \underline{x}\in S^3 \tag{18}$$

which yields the solution

$$a^{+} = Q_n^{+} \cdot (Q_n^{-})^{-1} a^{-}, \tag{19}$$

where

$$(Q_n^{\pm})_{pq,nm} = \pm \int_0^{L_1} dx_1 \int_0^{L_2} dx_2 [(\mp\gamma_{pq} + \alpha_p \dot{F}_1 + \beta_q \dot{F}_2)/\gamma_{pq} L_1 L_2] \cdot$$

$$\cdot \exp[-i(\underline{k}_{pq}^{\pm} - \underline{k}_{nm}^{*}) \cdot \underline{x}]. \tag{20}$$

Defining the energy carried by the (pq)th mode of the scattered field as

$$P_{pq} = (\gamma_{pq}/\gamma_{00}) |a_{pq}^{+}|^2 / |\psi_0|^2, \tag{21}$$

provided, of course that γ_{pq} is positive real, the conservation of energy relation is obtained by

$$E = \sum_p \sum_q P_{pq} = 1. \tag{22}$$

NUMERICAL RESULTS

The system of equations (16) and (19) were programmed on a DEC vax 11/730 minicomputer. The inversion of matrices involved was carried out using a LU decomposition technique [16] via an IMSL subroutine LEQT1C, our numerical procedure being implemented in double precision arithmetic. The Q matrices, themselves, were computed using a two-dimensional Gauss-Legendre quadrature scheme [17], although for special cases of boundary profiles these matrices can be evaluated in closed forms. Convergence of the solution was checked by ensuring that the scattered field coefficients converged to within 0.5%. An additional check was also provided by (22) which had to be satisfied to be within ±0.005 of unity.

The general theory presented in the previous section holds for both S^2 and S^3 surfaces having periodic boundary profiles. However, here we consider surfaces described by $x_3(x_2,x_1) = f(x_2) + f(x_1)$, $f(x) = h\cos(2\pi x/L)$; for S^2, $f(x_2)$ is set to zero. The boundary conditions prevailing on the surface can be either Dirichlet or Neumann.

Consider, first, Fig.1 where we have plotted the scattered powers for a S^2, and have compared our calculations with those of Holford [5]. As is clear from this figure, the improved T-matrix scheme is applicable for much higher values of the parameter h/L than the Rayleigh limit of 0.072.

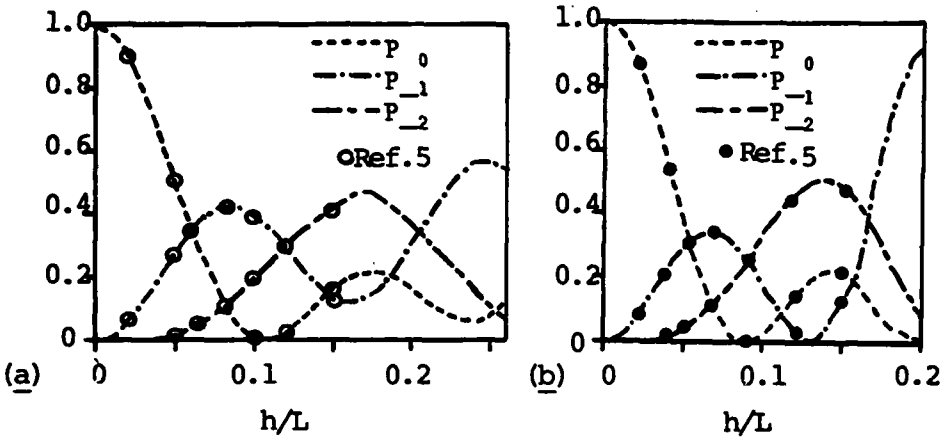

Fig. 1. Reflected mode power P_{pq} computed using the presented approach for a sinusoidal S^2, when a planewave is incident at $\theta_0 = 15°$, $\phi_0 = 0°$; $kL = 4\pi$. Ref. 5 are the IE results. (a) Dirichlet b.c., (b) Neumann b.c.

Similarly, in Table I we consider a doubly sinusoidal S^3 surface, for which case scattering is observed in 9 separate directions. Again, note that h/L = 0.15, which is roughly three times higher than Goodman's conjecture of 0.0504 for the Rayleigh limit. In these calculations, as in others made by us, we have been careful to tolerate only a 0.5% error in the check for the conservation of energy, and this seems to serve adequately as a check on the convergence of the scattered field coefficients as well. Reciprocity of the scattering solution has also been confirmed as is shown by comparing the data in

Table I. Scattering of a normally incident planewave from S^3; h = 0.426, L = 2.84, k = 3.5. Each entry represents P_{pq} of (21).

±p, ±q	Dirichlet b.c.	Neumann b.c.
0,0	0.11534	0.52718
1,0 } 0,1 }	0.03792	0.04348
1,1	0.18407	0.07574
E	1.0033	1.0041

Tables II and III. First, from Table II we see that the scattered power in the direction $\theta = 62.2461°$, $\phi = 0°$ is 0.13240 for the case S and 0.21042 for the case H, when a planewave is incident normally on S^3. Next, in Table III, the exciting planewave is incident at $\theta_0 = 62.2461°$, $\phi_0 = 0°$. For this latter excitation, the scattered power in the normal direction was computed to be 0.13231 for the Dirichlet b.c. and 0.21063 for the Neumann b.c., thus demonstrating the satisfaction of the reciprocity constraints.

Table II. Same as Table I except h = 0.284, L = 2.84, and k = 2.5.

±p, ±q	Case S	Case H
0,0	0.47167	0.15755
1,0 0,1	0.13240	0.21042
E	1.0012	0.9992

Table III. Same as Table II except the incident wave is incident from $\theta_0 = 62.2461°$, $\phi_0 = 0°$.

p, q	Case S	Case H
0,0	0.83265	0.43256
-1,0	0.13231	0.21063
-1,±1	0.01476	0.11957
-2,0	0.00818	0.11768
E	1.0027	1.0000

A NON-UNIQUENESS OF THE INVERSE SHAPE PROBLEM

As has been seen in the preceding sections, a periodic surface scatters an incident planewave in discrete well-defined directions. Some of these directions, for which γ_{pq} is real, have scattered planewaves which go upto $z = \infty$. Others, for which, γ_{pq} is imaginary, represent evanescent planewaves. In the far zone, the reflection coefficients a^+_{pq} can be measured for the propagating planewaves; hence the reflected field can be obtained from measurements as

$$\psi_s(x_3,x_1) = \sum_p a^+_{p0} \exp\{ikr\cos(\theta_p-\theta)\};\quad kx_3 \text{ large} \tag{23}$$

where we have considered, for the sake of brevity, only the 2-D problem; $\theta_p = \arctan(\alpha_p,\gamma_{p0})$; $\theta = \arctan(x_1, x_3)$; and r is the radial distance from the origin to the field point. The summation holds only for the propagating plane-waves. However, in most situations, the scattering surface is finite of total expanse B. Hence, if the surface S^2 were to be illuminated by a finite-aperture field

$$\psi^i(\underline{x}) = \begin{cases} \exp(i\underline{k}_0\cdot\underline{x}), & \underline{x}\in S^2,\ -B/2 \le x \le B/2 \\ 0, & \underline{x}\in S^2,\ |x| > B/2 \end{cases} \tag{24}$$

then, for a sufficiently usual case when the Rayleigh-Wood anomalies are absent, the scattered field has been given by Jordan and Lang [7] to be

$$\psi_s(\underline{x}) = kB\,(2\pi kr)^{-\frac{1}{2}} \exp[i(kr-\pi/4)] \sum_p a^+_{p0} \operatorname{sinc}[kB(\sin\theta_p-\sin\theta)/2]. \tag{25}$$

For (25) to hold, kB must be large; and only the propagating plane waves need be accounted for.

Consider, next, a flat surface of the same expanse B which is illuminated also by the field (24). This flat surface has a periodic reflectivity profile ρ of period L, the reflectivity function being dependent on the frequency. The scattered field field can be easily set down as

$$\psi^1(x_3, x_1) = \int_{-\frac{1}{2}B}^{\frac{1}{2}B} dx'_1\ \rho(x'_1)\exp(ikx'_1\sin\theta_0)\cdot \cdot \exp[ik\{x_3^2 + (x_1-x'_1)^2\}^{\frac{1}{2}}]\ \{x_3^2 + (x_1-x'_1)^2\}^{-\frac{1}{2}} \tag{26}$$

where $\theta_0 = \arcsin(\alpha_0)$. Because of the periodic nature of ρ, this can be reduced to

$$\rho(x) = \sum_p \rho_p \exp(ip2\pi x/L) \tag{27a}$$

$$\psi^1(x_3,x_1) = \sum_p \rho_p \sum_{\ell=-N}^{N} \exp(-ik\ell L\sin\theta_0) \int_{-\frac{1}{2}L}^{\frac{1}{2}L} dx'_1\ \{x_3^2 + (x_1-x'_1+\ell L)^2\}^{-\frac{1}{2}}\cdot \cdot\exp(ikx'_1\sin\theta_p)\exp[ik\{x_3^2 + (x_1-x'_1+\ell L)^2\}^{\frac{1}{2}}], \tag{27b}$$

and which, by approximating,

$$[x_3^2+ (x_1 - x'_1+\ell L)^2]^{\frac{1}{2}} \simeq [x_3^2 + (x_1+\ell L)^2]^{\frac{1}{2}} - - x'_1\ (x_1+\ell L)\ [x_3^2+ (x_1+\ell L)^2]^{-\frac{1}{2}}, \tag{27c}$$

further reduces to

$$\psi^1(x_3,x_1) = \sum_p \rho_p \sum_{\ell=-N}^{N} \exp(-ik\ell L\sin\theta_0)\exp ik\{x_3^2+ (x_1+\ell L)^2\}^{\frac{1}{2}}\ \ r^{-\frac{1}{2}}\cdot \cdot\operatorname{sinc}\{(kL/2)(\sin\theta_p - (x_1+\ell L)[x_3^2+(x_1+\ell L)^2]^{-\frac{1}{2}})\} \tag{28}$$

with sinc(z) = sin(z)/z, and the ratio B/L = 2N+1 is considered integral. The factor $\sqrt{r}$ is introduced since the measurements are made in the far zone. Furthermore, by realizing that $x_1 = x_3 \tan\theta$, and on focussing our attention on the argument of the sinc function, we observe that this function reduces to

$$\text{sinc}\{(kL/2)\ (\sin\theta_p - \sin\theta)\}, \tag{29a}$$

while the second exponential in (28) becomes

$$\exp[ik\ell L(\sin\theta - \sin\theta_0)]. \tag{29b}$$

Since these two are Fresnel-type approximations, ℓ must not assume high enough values so as to render them invalid. Therefore, the somewhat restrictive assumptions that the ratio $B/L \gtrsim 10$ while $NL \ll x_1$ are necessary. However, the product kB can be arbitrarily large. In effect, thus, this is also a high - frequency analysis.

Noting, however, that

$$\sum_{\ell=-N}^{N} \exp(i\ell\xi) = \text{sinc}[(N+\tfrac{1}{2})\xi](2N+1)/\text{sinc}(\tfrac{1}{2}\xi) \tag{30}$$

further simplifies (28) to

$$\psi^1(x_3, x_1) = (2N+1)\ (-)^{2N+1}\ r^{-\frac{1}{2}} \exp(ikr) \cdot \cdot \sum_p \rho_p\ \text{sinc}\{kB(\sin\theta_p - \sin\theta)/2\} \tag{31}$$

after some manipulation of the various sinc functions involved.

Formally, the scattered field ψ^1 is indistinguishable from ψ_s of (25). Furthermore, the Fourier components ρ_p of the reflectivity ρ may be obtained through a least-squares estimation procedure applied to repeated measurements of the scattered field for different angles of incidence. Thus, experimental measurements of the far scattered field for the purpose of determining the surface profile can lead to two different interpretations:

(a) the surface is periodically undulating, and

(b) the surface is flat with a periodic reflectivity profile.

CONCLUSIONS

We have described a scalar T-matrix formalism which is applicable for highly corrugated periodic surfaces and have shown that the solutions obtained obey unitarity as well as reciprocity constraints. We have also shown that the measurement of the scattered field (which exists only in discrete well-defined directions) can give rise to two different interpretations of the nature of the scattering surface. Further work on extending the presented approach for bimaterial interfaces as well as for elastic scattering problems is in progress.

REFERENCES

1. Lord Rayleigh, *The Theory of Sound*, Dover, New york (1945).
2. R.F. Millar, *Rad. Sci.*, *8*, 785 (1973).
3. F.O. Goodman, *J. Chem. Phys.*, *66*, 976 (1977).
4. J.T. Fokkema and P.M. van den Berg, *J. Acoust. Soc. Am.*, *62*, 1095 (1977).
5. R.L. Holford, *ibid*, *70*, 1116 (1981).
6. J.A. DeSanto, *ibid*, *57*, 1195 (1975).
7. A.K. Jordan and R.H. Lang, *Rad. Sci.*, *14*, 1077 (1979).
8. S.L. Chuang and R.R. Johnson, *J. Acoust. Soc. Am.*, *71*, 1368 (1982).
9. A. Lakhtakia, V.K. Varadan, V.V. Varadan and D.J.N. Wall, 'The T-matrix approach for scattering by a traction-free periodic rough surface,' *J. Acoust. Soc. Am.*, in press (1984).
10. A. Wirgin, *J. Acoust. Soc. Am.*, *75*, 345 (1984).
11. R.I. Masel, R.P. Merrill and W.H. Miller, *Phys. Rev. B*, *12*, 5545 (1975).
12. P.C. Waterman, *J. Acoust. Soc. Am.*, *57*, 791 (1975).
13. A. Lakhtakia, V.K. Varadan and V.V. Varadan, 'On the acoustic response of a deeply-corrugated periodic surface - A hybrid T-matrix approach,' *J. Acoust. Soc. Am.*, (submitted) (1984).
14. S.L. Chuang and J.A. Kong, *Proc. IEEE*, *69*, 1132 (1981).
15. A. Lakhtakia, V.K. Varadan and V.V. Varadan, 'The T-matrix approach for EM scattering by perfectly conducting periodic surfaces,' *Proc. IEEE*, in press (1984).
16. G. Forsythe and C.B. Moler, *Computer Solution of Linear Algebraic Problems*, Prentice-Hall, New Jersey (1967).
17. M. Abramowitz and I.A. Stegun, *Handbook of Mathematical Functions*, Dover, New York (1965).

END

FILMED

4-85

DTIC